Emanuele Ambu
Roberto Ghiretti
Riccardo Laziosi

3D Radiology in Dentistry

DIAGNOSIS
PRE-OPERATIVE PLANNING
FOLLOW-UP

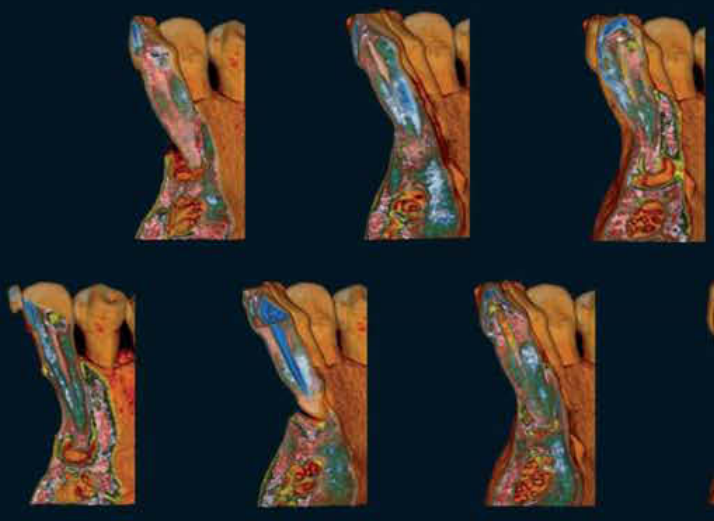

Emanuele Ambu
Roberto Ghiretti
Riccardo Laziosi

3D Radiology in Dentistry

DIAGNOSIS
PRE-OPERATIVE PLANNING
FOLLOW-UP

Traduzione dei capitoli dall'italiano all'inglese a cura di
Roberta Penna - Bologna (Italy)

ELSEVIER

Publishing Director: Valeria Brancolini
Books Publishing Manager & eContent Publisher (Medicine): Tiziano Strambini
Development Editor: Paola Leschiera

Operations Director: Antonio Boezio
Books Team Manager: Paola Sammaritano
Creative Director: Giorgio Gandolfo

Redazione e impaginazione: F.lli Sala snc, Seregno (MB)

ISBN 978-88-214-2971-2
eISBN 978-88-214-3405-1

ELSEVIER

Elsevier Srl
Via Paleocapa 7, 20121 Milano
Tel. 02.88.184.1
www.elsevier.it

Printed in Italy
Finito di stampare nel mese di gennaio 2013 presso "Printer Trento" S.r.l., Trento

Preface

The 3D world is an amusement park where you can run through and catch the most refined details leading to the discovery of a universe which is disclosing itself more and more interesting and surprising day after day.
Loving one's own job is a blessing for Riccardo, Emanuele and me. It is not so usual.
I have known Riccardo for a long time. He works in a company of professional skill and kindness. His "84-tooth smile" is shining in a very skilled and talented information department.
No long introduction is necessary to describe Emanuele "Lele" Ambu: he is perhaps the most important "speleologist" of endodontic "ravines" that the Italian dental world has to offer to the international scientific community. He is the man with the most ruffled hair and beard I have ever met, but with the most precious hands that I have ever seen to operate.
Together we have devoted ourselves with great enthusiasm to this work. We hope it will be helpful to face our dental world in different way. In our world it is often very hard to understand the diseases our patients are suffering from and we often feel uncertain. The 3D analysis can be really effective in most cases.
I would also like to thank the following people.
Firstly, thanks to Antoine Rosset, the inventor of OsiriX, a wonderful software devoted to radiologists that has allowed me to create the 3D volume renderings shown throughout this book. He has also opened my mind to new interpretations in the field of radiological diagnosis.
Secondly, thanks to my wife, Graziella, who has put up with my endless absences when I was stubbornly struggling with OsiriX and my creativity.
And finally sincere thanks to Riccardo Pradella and his Carestream team. Without them this book would have not have been possible. Carestream is an important company in the world of CBCT systems and its 9000 3D that we have used to analyze most cases dealt with in this book is a landmark in the field. It supplies detailed analysis with a very low radiation dose to patients.

I wish you all good luck in 3D.

Porto Mantovano (Mn), December 2, 2012 **Roberto Ghiretti**

Authors and contributors

Authors

Emanuele Ambu, MD, DDS
Active Member SIE (Italian Society of Endodontics); Certified Member ESE (European Society of Endodontology), Private Practice limited to Endodontics and Oral Surgery in Bologna, Italy.

Roberto Ghiretti, MD
Specialist in Maxillo-Facial Surgery
Private Practice in Mantova, Italy.

Riccardo Laziosi, MEng. (electronic)
Dental imaging software and digital systems R&D Manager, Dental Trey s.r.l., Italy.

Contributors

Alberto Bianchi, MD, DMD, FEBOMFS
Oral and Maxillofacial Surgery Unit
S. Orsola-Malpighi University Hospital of Bologna, Italy.

Antonino Cacioppo, DDS, PhD in Oral Science
Co-researcher MIUR in University of Palermo. Member of Editorial Staff of IJCD (International Journal of Clinical Dentistry-NY,USA). Active Member of GIC (Gymnasium Interdisciplinare CadCam). Member of MGA (Model Guide Academy). Private Practice with particular interest in Guided Implantology, Cad/Cam restorative dentistry and prosthetics, in Palermo, Italy.

Daniele Cardaropoli, DDS
Active Member SIDP (Italian Society of Periodontology), EFP (European Federation of Periodontology) and SIO (Italian Society of Osseointegrated Implantology). Scientific Director PROED - Professional Education in Dentistry, Turin (Italy). Private Practice limited to Periodontology and Oral Implantology in Turin, Italy.

Elisa Cuppini, DDS
Aggregate Member of SIE (Italian Society of Endodontics). Private Practice in Bologna, Italy.

Matteo Di Lorenzo
Master in Oral Surgery
Private Practice in Bologna, Italy.

Vittorio Ferri, MD, DDS
Active Member AIE (Italian Academy Endodontics)
Private Practice limited to Oral Surgery in Modena, Italy

Massimo Frosecchi, DDS
Fellow ITI (International Team for Implantology), Active member International Piezosurgery Academy.
Private Practice in Florence, Italy.

Marcos Gribel
Member of Academia Brasileira de Fisiopatologia Crânio-oro-cervical and Sociedade Paulista de Ortodontia e Ortopedia Funcional dos Maxilares, Editor scientífico e colunista da Revista Internacional de Ortopedia Funcional dos Maxilares da Dental Tribune International. Private practice in Bello Orizonte Brasil.

Bruno Frazão Gribel
Mestre em Ortodontia, Pontifícia Universidade Católica de Minas Gerais. Postdoctoral Scholar Orthodontics and Pediatric Dentistry University of Michigan. Private practice in Bello Orizonte Brasil.

Claudio Marchetti, MD
Chief of Oral and Maxillofacial Surgery Unit, S. Orsola-Malpighi University Hospital of Bologna.
Professor of Maxillofacial Surgery at Alma Mater Studiorum University of Bologna, Italy.

Andrea Nakhleh
Member of SIDO (Italian Orthodontics Society)
Private Practice in Mantova, Italy.

Santiago Isaza Penco
Member of SIDO (Italian Orthodontics Society) and SCO (Sociedad Colombiana de Ortopedia).
Editor review of PIO (Progress in Ortodontics).
Private Practice limited to Orthodontics and Orthopedics in Bologna, Italy.

Caterina Sanna, DDS
Private Practice in Bologna, Italy.

Achille Tarsitano, MD
Oral and Maxillofacial Surgery Unit, S. Orsola-Malpighi University Hospital of Bologna. Active Member of SICMF (Italian Society of Maxillofacial Surgery), EACMFS (European Association for Cranio-Maxillo-Facial Surgery), ESTRO. Founding member of AIOCC (Associazione Italiana di Oncologia Cervico-Cefalica).

Marco Vigna, MD, DDS
Ordinary Member SIE (Italian Society of Endodontics)
Private Practice limited to Endodontics and Conservative in Villa Verucchio, Rimini, Italy.

Presentation

In writing this preface I was reminded of a quote from Albert Einstein: "Everyone knows that something is impossible, until it reaches a fool who does not know and invents."
In fact, the CBCT is an outstanding breakthrough for dentistry. It opens a new frontier and allows us to make precise diagnosis where traditional tools were insufficient. In daily practice we are often faced with situations where the X-ray scans and our patient's symptoms do not concur, or may even lead us to multiple scenarios with differential diagnoses. When I look at a traditional radiograph, I always think, in fact, that it is a two-dimensional image of something that actually has three dimensions. At last, thanks to CBCT we have the missing dimension, which amplifies our knowledge exponentially.
Reading the text we can see the enthusiasm and the passion with which the authors have produced this book. Each chapter is a font of information, every detail has been carefully examined, and each clinical case has been extensively reported.
The introductory chapters provide the reader with the knowledge and basic tools to understand CBCT.
Everything else is a highly enjoyable atlas which includes the use of CBCT in both clinical and surgical dentistry, and describes in detail not only the diagnostic phase but also the operational use to plan individual cases and control the future outcome.
This book is intended to be consulted many times, every day, because it is extremely useful for those who approach this new dimension of dentistry and require a guide. Moreover, the authors explain, in a very simple way, concepts that are not at all simple, thus demonstrating their expertise and deep knowledge of the subject.
Again quoting Einstein: "You do not really understand something until you are able to explain it to your grandmother." I'm sure that by reading this exceptional text, even my grandmother would understand CBCT!
I wish the authors all the success they deserve, and to the readers ... happy reading!

Simone Grandini DDS M.Sc. Ph.D.
Chair of Endodontics and Restorative Dentistry
Head of Department of Endodontics and Restorative Dentistry
Dean of the School of Dental Hygienists
Tuscan School of Dental Medicine
University of Siena, Italy

Preface

I have been working with the operative microscope in my daily practice since 1995. Since then, I have focused my work almost exclusively on endodontics. I absolutely believe that I should improve my capacity to investigate inside the root canal system in order to reach better results. The microscope has been a real winning means, although its performance can be hindered by anatomical problems, like canal curves. As soon as I realized that I could not "see" so well what lies around the root or the very structure of the tooth, I felt increasingly frustrated. All conventional radiological systems (always the most important aid to endodontists) were not so helpful in the most important steps of diagnosis and treatment planning, especially in more complex cases. When I was suggested to test a 3D radiological system with a small field of view, I was immediately fascinated. From the very beginning, I had become an enthusiastic user because of its advantages: low radiation dose to patients, high definition with very small voxels, the possibility to see the tooth and the surrounding structures in three different planes, overcoming any anatomical overlapping.

While I was exploring the features of this system, I got to know an engineer, Riccardo Laziosi, whose profession is dental information engineering. We started travelling all over Italy together, showing my colleagues the features of these new devices with new viewing systems and their advantages in daily clinical practice.

This good acquaintance has made me better understand how these systems work and which features they should be equipped with. Almost three years ago, I got to know Roberto Ghiretti at a conference on 3D radiology. He was about to purchase a system similar to mine and he desired to get more information about its advantages in his daily clinical practice.

His experience as an oral surgeon and his daily practice as a dentist have urged me to study further the use of these systems in different fields of surgery. We soon became good friends, and started a profitable professional cooperation. You will see some cases executed by both of us shown in this book.

Our enthusiasm increased more and more: from material collection to case discussion and to the analysis of different uses of this device, the idea of this book grew in our minds.

Other colleagues have joined Riccardo, Roberto and me. They have willingly and invaluably contributed to the drawing of this hard work. I would like to thank them all herein.

I hope that our work will meet our aim: to show the advantages of the use of CBCT systems. This use should be careful and follow the principles of "optimization and justification" and always respect the patient, from the very moment in which we make our choice of purchase.

Lastly, my greatest thanks are to my wife, Roberta, who supported my work, translating from Italian and checking all the scientific contributions that you will find in this book.

Bologna, December 2, 2012 **Emanuele Ambu**

Preface

I have been working for fifteen years on software and digital systems for dental diagnostic imaging.
This period of time can be compared to other 150-year periods in terms of technological changes, innovations, and revolutions. It is sufficient to think about our everyday life and how it has changed thanks to ever advancing computers, cellular phones, and the Internet.
In dentistry, after slow progress in the 1990s, a real explosion of digital two-dimensional radiology occurred in the early 2000s, especially in the sector of intra-oral systems (sensors and phosphor systems) but also in the sector of extra-oral systems (panoramic units). Lower costs and better performance and quality have led to this revolution, which is also thanks to our capacity to use information technology in our everyday life.
All these factors, as well as other innovative ideas, have done something more in these last few years: they have offered to any dental office (even those with one operator) a new extraordinary diagnostic procedure by means of 3D radiological systems.
The challenge to the end user (dentists) and to those who, like me, have chosen to work to supply instruments, services, and application knowledge to use digital technology has been huge. We all had to learn and face absolutely new problems, put forward ideas and intuitions and fight against prejudice and well-established stances—that means hard work.
Satisfaction and gratification have been great, especially in finding how helpful this technology can be in diagnosis, clinical planning, and communication with patients. Sharing all this with professional people and friends like Emanuele and Roberto has been crucial. Without their help, skill, and cooperation, everything would have been much more difficult and much less profitable. To them, my sincere thanks because they have let me live this experience giving way to the idea of this book. I think that all of us—me for sure—developed this idea with the basic belief that in complex and multidisciplinary fields, like the 3D radiological sector, the winning option is teamwork among people with different skills.
Finally, many thanks to those who have contributed to make this idea come true and to the publisher of this book.

Fiumana (FC), December 2, 2012 **Riccardo Laziosi**

Table of Contents

From the discovery of X-rays to the advent of digital tomography

Emanuele Ambu, Caterina Sanna

The entirely accidental discovery of X-rays by Wilhelm Conrad Röntgen in December of 1895 was a true turning point in medical diagnostics. Taking a radiograph, as Röntgen had done of his wife's hand (Fig. 1.1), a doctor could "explore" the human body from the outside without surgical intervention. Periapical radiographs were performed in the first few weeks following Röntgen's discovery. Extra-oral imaging as well as the cephalometric radiograph would be performed soon after. Subsequently, the introduction of orthopantomography in the 1960s and its widespread diffusion in the 1970s and 1980s allowed considerable progress in dental diagnostics, giving dentists a comprehensive image of dental arches and the maxillofacial complex. However, in the years following the discovery of X-rays, a large number of studies and research were carried out in the radiodiagnostics sector in order to achieve three-dimensional images. The studies started by Kieffer in Norwick, in 1929, led to the publication of the first geometric study of single-direction axial stratigraphy in 1938 (Kieffer 1938); they were continued by Amisano, who performed the first axial tomograph in 1944, and by Frain and Lacroix, who carried out the "Radiotome" (Frain and Lacroix 1948). However, Alessandro Vallebona, who developed his first tomograph in 1930, was the scientist that first introduced the use of this system on human beings, with transverse axial stratigraphy. His axial stratigraph (Fig. 1.2) worked with an X-ray tube and required both the patient and film to rotate along relative vertical axes. The stratigraphic plane was chosen by lifting or lowering the patient's stool (Lelli 2009).

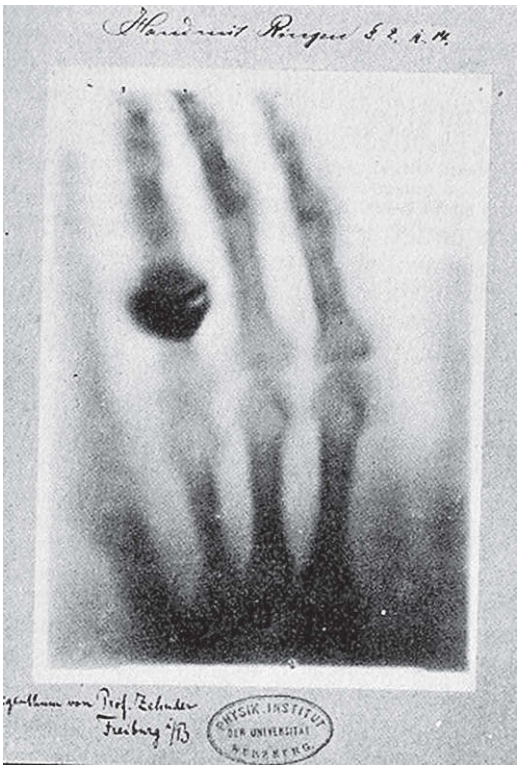

Fig. 1.1 The first X-ray: Anna Bertha Ludwig's hand.

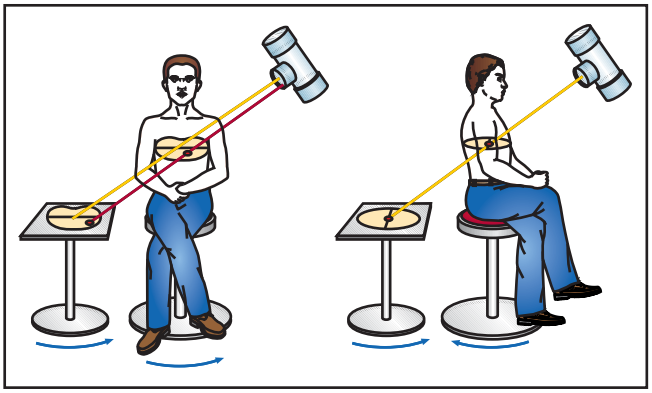

Fig. 1.2 Operating mode of Vallebona's axial stratigraph.

The studies were carried on thanks to Stevenson's, Gebauer's, and Takahashi's contributions in 1949, and to Frain's in 1950.

Only with the introduction of the first electronic processors was it possible to develop computerized axial tomography. In 1967, starting with one of the first devices for computer image recognition, the South African radiologist Alan Cormack and the English engineer Godfrey Hounsfiled (recipients of the Nobel for Medicine in 1979) managed, separetely, to develop a system which was able to reproduce a three-dimensional image of the biological tissues examined. The financing necessary to continue with its development was granted by EMI, after receiving substantial revenues from the Beatles' success and thanks to Paul McCartney's immediate interest (Zannos 2003). Once several technical problems had been resolved, like lengthy data acquisition and processing procedures, the first model, called "EMI CT 1000" (Fig. 1.3), was introduced, in 1972, in Chicago. Computed tomography (CT) was thus born, allowing two-dimensional imaging to give way to three-dimensional.

Today, radiology plays an essential role in dental practice. Almost every dentist's office is equipped with an X-ray system to perform diagnostic exams. However, any intra- and extra-oral procedures, both single and combined, have the same intrinsic limitations as all two-dimensional projections. Like all stratigraphic images, they transform three-dimensional anatomical structures into two-dimensional images.

The recent introduction of CBCT technology (which stands for cone beam computed tomography) has opened up new horizons in dental diagnostic imaging. It is now possible to perform exams in our office which can provide a three-dimensional view of the facial area and structure, thus overcoming the limitations of two-dimensional radiology.

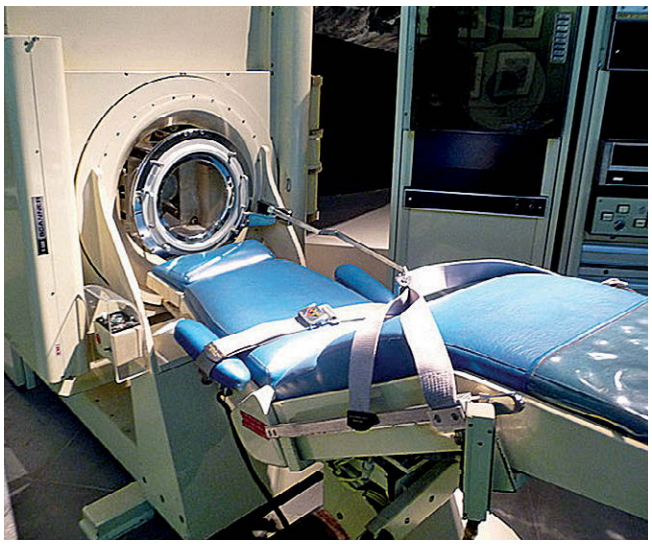

Fig. 1.3 The EMI CT 1000. (Photo by Robin Van Mourik).

Principles of 3D radiology

Riccardo Laziosi

In order to fully understand three-dimensional radiological imaging, it is necessary to have a clear understanding of a number of concepts regarding every radiological activity and the developments which lead up to it. We summarize them below.

Traditional radiological technique and its digital form

At the end of the 19th century, the German physicist Wilhelm Röntgen first detected, by chance, an unknown radiation form while he was experimenting with vacuum tubes. He named this kind of radiation "X". Soon after this discovery, he took the first radiograph, reproducing an image of his wife's left hand on a plate. This happened on 22 December 1895. He was then awarded the Nobel Prize in 1901 as a result of this achievement.

Soon afterwards, radiological diagnostics started to be used in medicine, and remained almost unchanged up until the 1970s. At that time, developments made in electronics and information technology had encouraged the gradual introduction of digital radiological diagnostics, in laboratory experiments at first, and then in clinical practice.

In order to better understand the various features and differences between conventional radiology and digital radiology, it is important to summarize what a radiological image is and how it is formed as a two-dimensional image.

Two-dimensional radiological images

The basic concept of traditional radiological imaging, the same type as that obtained by Röntgen, is almost trivial: measure the reduction rate in a steady beam of X-rays after it has passed though an object. We will try to explain this better, avoiding overly complicated physical and mathematical concepts.

It is commonly known that any radiation, and electromagnetic radiation in particular, carries energy. Simply think about how much the sun's rays heat things when you take a walk in the summertime. We can easily understand that there is a strict relationship between radiation and matter: the radiation releases part of its energy and heats us. We know that, depending on the characteristics of a type of matter, many things may happen: we can see through a window, but we can't see through a wall; we get tanned when lying in the sun, but we do not when sitting by a fireplace. In all cases, the energy carried by radiation is released to matter and weakens. However, this occurs in different ways, according to the features of the radiation and the matter. Electromagnetic radiation consists of an electromagnetic field that periodically varies with time. The variation frequency strictly depends on the energy carried by the radiation and highly affects the mechanism of energy-matter exchange. This mechanism, in turn, affects the attenuation trend. Of course, the physical and chemical characteristics of the matter highly affect this mechanism as well.

It is, however, clear that with appropriate radiation and knowing the intensity, it is theoretically possible to make radiation pass through matter and to measure the intensity of the radiation once it has come out. The more energy absorbed by the matter, the lower the intensity level. If we repeat measurements along other directions, we will be able to see that the radio-absorption capacity of this sample material varies greatly because of other factors (i.e. density). This is the goal of every conventional radiological unit.

The radiation's characteristics should, of course, be suitable for the "sample material" to be examined: too deep radiation may "break through" our sample, passing it with such a low degree of attenuation that it is not possible to detect any significant variations along any directions; on the contrary, poor penetration can lead to complete absorption. "X"-radiation, discovered by Röntgen, is so important because it has proved to have suitable features for examining the internal structures of matter, especially in the fields of medicine and industry. X-radiation is electromagnetic radiation with a frequency ranging from 3×10^{16} Hz to 3×10^{20} Hz (Fig. 2.1). Visible light and radio waves are also electromagnetic radiation, but their frequency value is lower (between 428×10^{12} Hz and 749×10^{12} Hz, and below 3×10^{9} Hz, respectively). The vector particles of electromagnetic interactions are photons; the energy connected to the photons of electromagnetic radiation with a set frequency is connected to that radiation according to the ratio E = hf (E stands for energy, f for frequency, h for Planck's constant).

Since high-frequency electromagnetic radiation interacts with matter especially in compliance with some mechanisms (photo-electric effect, Compton effect, Auger effect) that cause the orbital electrons to move away from the atoms and make them electrically charged, it is usually known as ionizing radiation. X-rays belong to this group; visible light does not.

The amount and mechanisms of the radiant energy released to the object are particularly crucial in medicine, where living beings are observed. Special attention, therefore, must be paid to evaluating any potential or real biological damage that may result from radiation.

After theoretical, experimental, and statistical studies, the notion of "dose" and "effective dose" has been developed over time. These studies are essential to establishing suitable clinical operative protocols and radiation protection procedures. This is a very important matter and will be explained further, but for now it is sufficient to be aware of the notion of a "dose" as a basic parameter in radiology.

It should now be clear that radiology allows us to indirectly explore the internal structures of an object without damaging it. This is possible by measuring the attenuation rate of a radiation beam that is initially steady and composed of ideally parallel rays.

But how is it possible to record and store this information? Traditionally, special photochemical films have been used which follow the same principles as those of conventional photography. These films are arranged at right angles to the beam's direction. As a result, the

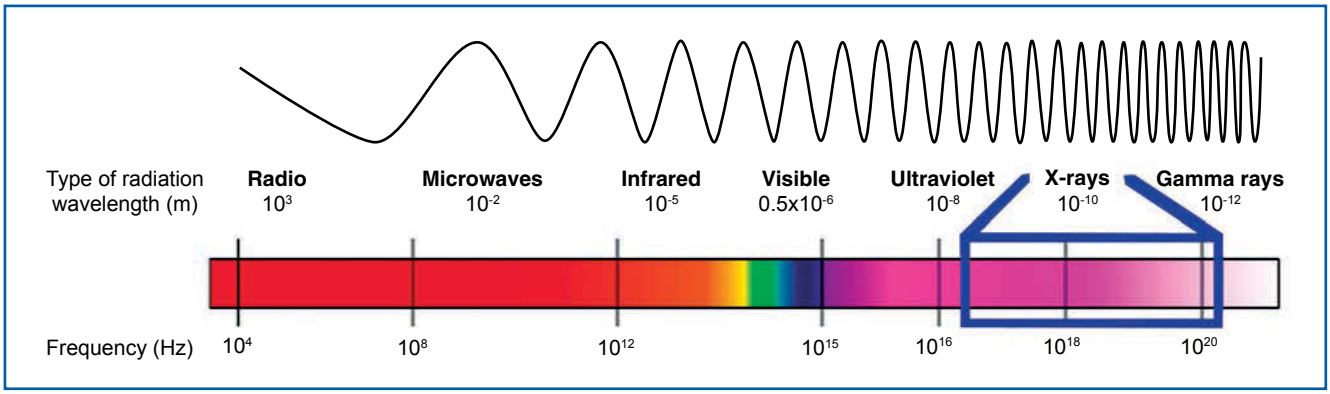

Fig. 2.1 The electromagnetic spectrum.

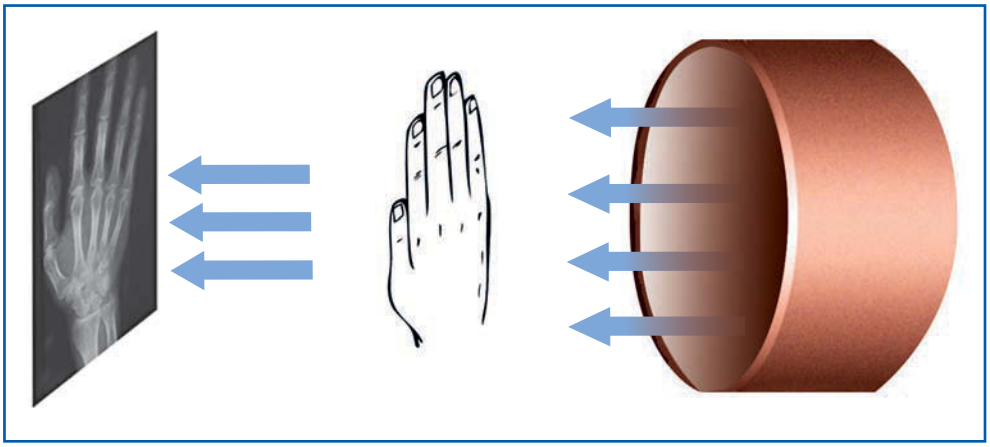

Fig. 2.2 Two-dimensional radiography.

incident radiation causes a chemical reaction in the photographic film—the more intense the radiation, the more powerful the reaction. Consequently, silver crystals form during the subsequent developing phases and the areas struck by stronger rays turn black.
As a result, if a beam strikes not very dense structures during its path, it will release little energy and it will exit with high energy, and will noticeably blacken the area of the film that has been struck. On the contrary, if it strikes dense structures, the amount of energy released will be higher, and the emerging beam will be less intense, making the plate area less dark (Fig. 2.2).
Our radiographic exam recording consists of all the points of the plate, each one recording the information about the attenuation rate of the initial beam according to the structures it has passed through traveling inside the object to be examined.
Thus, it is possible to get information about a three-dimensional object without damaging it. It is also clear that any piece of information obtained is two-dimensional (the plate). We record the sum of all absorption rates of all the structures along the ray's path, but we lose the information about any specific point of the path. If we imagine that we have replaced our three-dimensional object with a two-dimensional one, in which every point is as dense as the sum of the real density rates of the three-dimensional object along the given beam path, we would get the same result.

The imaging chain in conventional radiology

In the previous section, we generically examined the basic concepts of conventional radiology. We will now try to describe how these principles are put to use and what problems may occur.
Apart from the object being examined (the patient, in medicine), radiological systems consist of three elements: the generator, the receptor, and the viewer. In conventional radiology, the receptor is the photographic plate, and the viewer is the negatoscope. The generator produces the amount of X-rays necessary to perform the exam desired.
Generators used in dental radiological units are made of electron, or "vacuum", tubes—glass cruets with a cathode and an anode undergoing an electric potential difference (the anode has a higher potential than the cathode). The cathode is a metal thread heated by an electric charge running down it and heating it so much that it releases negatively-charged particles known as electrons (thermo-ionic effect). These easy-moving particles run within the electric field created by the cathode and the anode. This field makes them accelerate towards the anode and they gain an average energy amount (due to the potential difference between the cathode and the anode) when they hit the anode. The anode is made of a suitable material (usually tungsten) which is resistant to stress and capable of converting part of the energy of the incident electrons into X photons, i.e. into electromagnetic radiation within the field of X-rays.

The frequency of this radiation depends on the energy of the "cutting" electron and on the physical and chemical properties of the anode material. The anode and the cathode are usually dipped in an insulating oil bath so that the heat generated by the X-radiation can easily be disposed of (the percentage of the amount of energy generated that turns into X-rays is very small, the rest will be disposed of).

Since every electron is different in its accelerating and hitting path with the anode (causing different collisions and interactions with the anode), the energy transferred and the frequency of the resulting X photons have no specific values but only average ones. That is to say, the emission is polychromatic (those that we perceive as different colors in the spectrum of visible light are merely different frequency ranges of the radiations of the spectrum). We talk about "soft" rays when referring to lower frequencies and "hard" rays when referring to higher ones.

By adjusting the potential difference (volt) of the anode and the cathode, the distribution curve frequency of the X photons is adjusted (and that of the average value, as well); that is to say, it is possible to adjust the hardness of the resulting rays.

By adjusting the heating current of the cathode (ampere), it is possible to vary the number of electrons and therefore the very number of photons emitted; the ray's intensity is thus set.

In practice, it is possible to vary these two parameters in order to set the amount of radiation generated and make it suitable for every specific exam (in medicine, the optimization principle is the rule: the lowest radiation amount sufficient for obtaining the necessary diagnostic result).

As a rule, the potential difference accounts for some thousand volts and the anodic currents account for few fractions of an ampere. For the sake of simplicity, the voltage value is expressed in KV and the current in mA.

Since too soft X-radiation is useless for diagnosis but it would inevitably damage the biological structures, the tubes are usually shielded with a material which is able to absorb this radiation (aluminum filters). Moreover, radiation is usually emitted from a very small area of the tube and with a narrow angle, with respect to a given direction (collimation), by shielding the surrounding areas with insulating materials (such as lead) or by means of anodes and electrons of a given shape.

The active area of the anode is the part that emits the radiation going out of the unit and is used to irradiate the object to be studied. The graphical projection of this area onto a planar surface perpendicular to the emission direction is the so-called "focal spot" of the generator (Fig. 2.3). The smaller the focal spot, the more in focus the final image will be on the receptor. This can be explained by taking into account that every point of the focal spot is a source of rays; two points at the opposing ends of the focal spot create two different images of the object to be studied. The blurring effect increases as these points move farther away from each other, that is, as the focal spot becomes larger.

It is easy to understand that since the electrical parameters of the generator are essential (especially the field between the anode and the cathode that establishes the emission frequency), it is necessary that these be steady and stable. A decrease in voltage would cause a higher emission of soft (useless and harmless) radiation, to the detriment of harder and useful ones. For the same reason, it is necessary to avoid supplying the tube with alternating (variable) voltage that could have too low values or too long transition periods (i.e. the time necessary for the supplying voltage to reach the regular working value starting from zero). Nowadays, modern generators (often called "high-frequency" or "continuous") work in such a way as to limit these behaviors as much as possible or even to avoid them.

It is also essential for generators to check exactly the exposure time, that is, the duration of the radiation. Varying the exposure time means varying the number of X photons emitted. As we have already seen, the cathode heating current increases the number of photons emitted. That is why the X emission is commonly expressed as mAs.

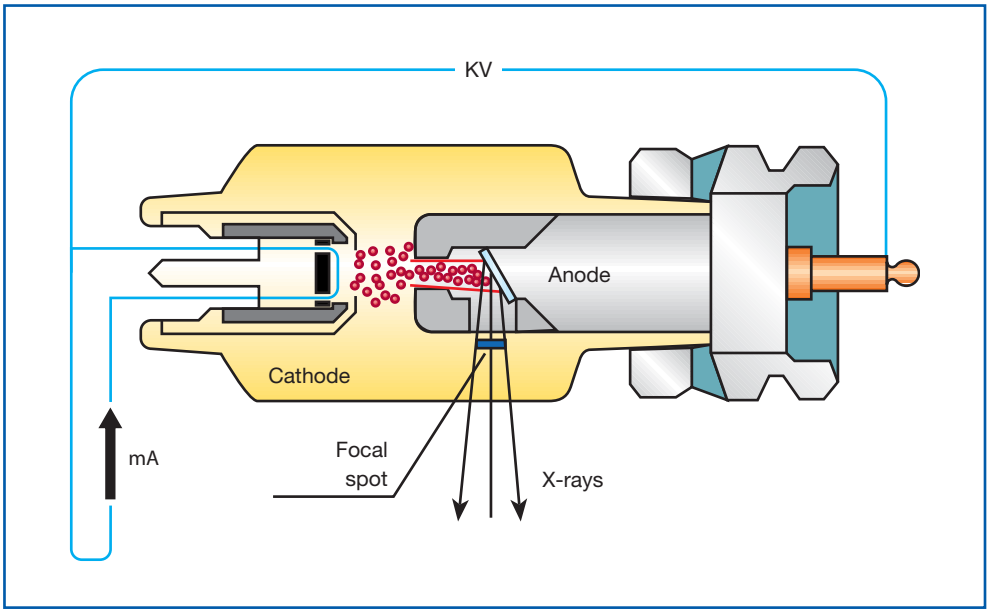

Fig. 2.3 Diagram of a generator.

The receptor is what receives and records the radiation coming out after passing through the object to be studied, and it determines the information available. It is therefore absolutely essential to use the receptor as best as we can, trying to operate in the most suitable conditions, so that all necessary information is completely recorded. As with conventional photochemical receptors—that is, the image they record—the basic concepts to underline are: contrast, density, and resolution.

Contrast indicates the ratio between the brightness of lighter colors and that of darker colors. When we have two images of the same original subject and take homologous points, the image with more contrast will be that with a higher brightness difference among its points. Increasing contrast means increasing the brightness differences. An increase in brightness means, on the other hand, that every single point of the image gets steadily brighter: differences, that is to say, the contrast, remain the same.

Density indicates the value of plate blackening, which is the ratio between the intensity of the light radiation on the plate (the light of the negatoscope) and the intensity of the one coming out of it.

Resolution is the value of the size of the smallest details that can be recorded by the receptor under the best conditions. It should be noted that the receptor's ideal resolution can differ greatly from the actual resolution obtained in the final image, because of other disturbing effects present in the image production process (the focal spot of the generator, the movements of the subject and/or the generator during irradiation, scattered radiation, etc.). This is why the actual resolution to be achieved by a radiological unit is expressed in terms of pairs of lines per mm. A trial can be done by irradiating an object made of line pairs comprising a radiopaque line alternating with a radiotransparent one that get thinner and thinner. When we talk about a resolution of 10 line pairs/mm, we mean that the size of a pair of thinner lines (with a distinct opaque and a transparent line) in the resulting image is such that one millimeter can contain ten of them.

Contrast, density, and resolution affect the final quality of the image, and if the quality is good, we can get the information desired. Contrast and density especially affect the density of structures; resolution affects their morphology. Since contrast and density exclusively depend on how the receptor reacts to radiation, they are used to assess the receptor by means of the so-called "characteristic curve" that connects these parameters to one another (Fig. 2.4). In particular, a very useful datum is the so-called "exposure latitude", which

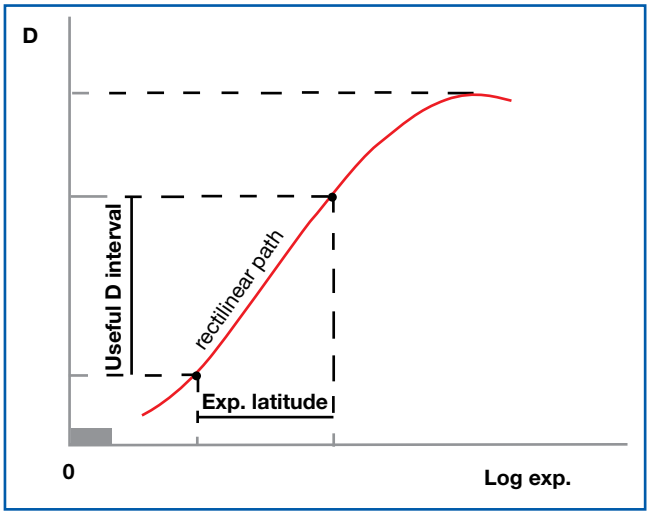

Fig. 2.4 Characteristic curve.

indicates the working exposure field of the receptor, that is, the range where to operate by adjusting the radiation parameters (KV, mAs).

The characteristic curve actually isolates the factors depending on the receptor, because its parameters are those connected to such processes as irradiation and development, in traditional radiology.

It should be taken into account that the irradiation density is connected to mAs: by increasing the current and exposure time, blackening increases. Increasing the exposure time causes problems (such as movements of the patient or the generator).

Contrast is more strictly linked to KV: by increasing KV, the image contrast decreases. This decrease makes the structures less visible. Actually, the reduced contrast is due to a higher number of gray shades, that is, a larger quantity of information (this information is useful if you have to evaluate structures with similar density rates; it is disadvantageous if you have to distinguish structures with very different density rates, such as hard and soft tissues, but it is not necessary to have more precise evaluations of either one).

With conventional photochemical receptors, the characteristic curve and the resulting film after a given exposure time exclusively depend on the conditions of the whole photochemical process: reagent storage, temperatures and working times, environmental conditions, etc. It is easy, then, to understand how difficult and how essential it is to have accurate protocols in order to guarantee satisfactory and reproducible results, as well as reasonable costs.

The final factor to be considered is the viewer, the device that enables us to have all the recorded information available. In conventional radiology, this is made of a suitably processed receptor (the developed plate) together with a proper illuminating device (a negatoscope or diaphanoscope), whose aim is to supply a uniformly lighted area on which to put the plate and underline the different density rates recorded. The light should be at a suitable temperature (from 4,500 °K to 6,500 °K), bright enough (between 1,700 and 3,000 cd/m^2 in the center, usually the brightest area), and as homogeneous as possible (as specifically required, the value in the corners should never be below 70% of the maximum value in the center). Every point is then lighted with the same incoming intensity and with an outgoing intensity depending on the density recorded on the plate in that point. Environmental lighting conditions are essential too: lighting should be low, but not so much as to risk dazzling by negatoscope. (In general, it is recommended to have 50-lux lights in working conditions).

It should be noted that if the negatoscope is not working properly and is not bright enough, the resolution capacity of the whole radiological imaging chain may sharply drop.

From conventional to digital radiology

In the last sixty years, the development of electronic and information technologies has made it possible to have new and more effective measuring and recording units in several sectors. These make information more easily handled, thanks to the high calculating capacity of information systems used to process, communicate, and store data.
Besides their high performance and reasonable costs—which may be enough to justify the decision to give up conventional technologies—these new systems can be applied to a much larger extent than the older ones.
Since any data should be expressed in numbers in order to be processed by these electronic and information systems, when we refer to instruments that supply information we use the adjective "digital".
Radiology, too, has changed likewise.

Digital radiology: structures, characteristics, quality

Compared to that of traditional techiniques, the imaging chain of digital radiology is composed of completely different parts: receptors, memory supports, and storage, as well as viewers. However, the general principle is always the same: a generator produces X-radiation. Its intensity, which is reduced after passing through the subject to be examined, is recorded by a two-dimensional receptor, similar to the conventional photographic plate.
The action of the outgoing radiation is, on the contrary, completely different when the receptor receives and processes this information to be stored. In computed electronics, information is digital; it is made of a number sequence. Computers work with a binary number system; any digit is expressed with only two symbols (instead of ten, the digits from 0 to 9, as we are accustomed to with the decimal number system). Any number is expressed as a sequence of 0 and 1 (the only two digits in the binary system); their position is important and follows the power of 2 (instead of 10). For example, the number that in the decimal system is expressed by 97 (the expression of $10^1 \times 9 + 10^0 \times 7$) is expressed in the binary system by the equivalent sequence 1100001 (the expression of $1 \times 2^6 + 1 \times 2^5 + 0 \times 2^5 + 0 \times 2^4 + 0 \times 2^3 + 0 \times 2^1 + 1 \times 2^0$).
By digital radiological system, we mean that part of the imaging chain that receives radiation and supplies useful information in a digital format. For convenience, the information will always be expressed with an image. This image is now a digital one; its information is stored within a system in the form of number sequences. The first thing to understand is what a digital image is, that is to say, how the information traditionally contained in a radiological image can be changed into a sequence of numbers.
To this end, we virtually divide our traditional photographic plate into rows and columns at steady intervals. The image will virtually appear in small basic elements of the same size. We call them pixels (picture elements). Each element contains a part of the image and therefore several gray shades corresponding to the numberless points of the image the element contains.
Since it is impossible to talk about infinite points, we can simplify as follows: we fill each element with a uniform gray shade that is equal to the average value of the gray shades actually contained in it. In this case, too, there is still an infinite variety of this average value of gray. We can simplify further: we establish a palette with a definite number of gray shades. We replace the previous average value with the gray shade in the palette that most approaches that value. If we label the palette's gray shades with identification numbers, the information of the initial image is a sequence of numbers that detect the gray to use in our palette, pixel after pixel. This structure of ordered numeric values representing the image is known as a bitmap (bit = binary digit; the numbers are expressed in binary code, as sequences of 1 and 0).

The information obtained is actually approximate, but by increasing the number of lines and columns (thus reducing the pixel size) and/or the number of the palette shades, we can reduce this approximation almost to zero. But it will be enough to reduce it to values that are sufficient for reaching our goals.

The pixel size and the number of gray shades are connected to the resolution and gray depth (or color depth, in the case of color images), which determine the quality of the digital image (Fig. 2.5). Digital radiological systems work in such a way as to lead the radiation intensity on the receptor to a bitmap of the image that would have been acquired with traditional systems. As we have already said, with digital images the most approximate reproductions of the object are achieved with the highest resolution and gray depth. Of course, this implies a problem: the quantity of information, that is, the memory space and the performance of the information systems. Within an information system, every binary digit of a bitmap corresponds to a subsystem (electronic, magnetic, optical, etc.) which is able to take either number (either 0 or 1) that the binary digit can take; the more digits to process, the higher the number of these subsystems representing the bitmap. The unit of measurement to represent the amount of memory occupied by data is the byte; it is made of a group of eight bits.

If an image occupies 3 megabytes (MB), it means that this image is made of 24 million bits. It is now clear that working with images of adequate size optimizes the available resources (space occupied and response speed) of the information storing and processing system.

When compared to the traditional imaging chain, digital radiological systems are the equivalent of the traditional plate and the development process put together, while the digital image is the equivalent of the plate produced as the final result of the development process.

The information system supplies a variety of new functions, as compared to the traditional one, and is also useful for storing and visualizing information.

The monitors displaying the digital image also work as negatoscopes. The screen can be imagined as a grid of tiny bulbs arranged in rows and columns that are turned on in order and with such gray shades as to reproduce the information stored in the bitmap.

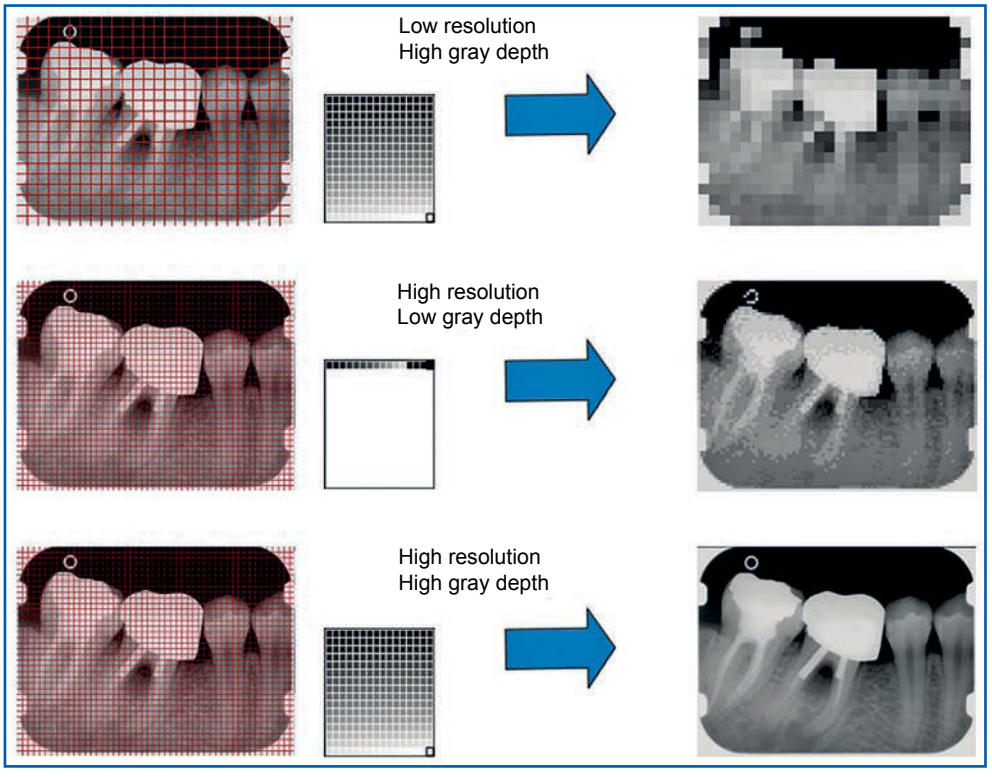

Fig. 2.5 Bitmap: pixel and gray shades.

As with a negatoscope, the quality and performance of monitors play an important role in getting a good reading of the data stored in the bitmap. If the shades coloring the points (the "tiny bulbs") of the monitor are fewer than those in the bitmap, this information will be lost. Furthermore, the monitor's points very often happen to be larger than the area of the receptor referring to a pixel of the digital image. In these cases, when a given point is referred to a pixel, the digital image will appear much larger than the actual object (that of the receptor). Technically speaking, it is said that we are working with "100% magnification".

If we have two digital images of the same object with 100% magnification but different resolutions, the image at a higher resolution will appear larger on the monitor because its bitmap is made up of a larger number of rows and columns, the pixel being smaller.

Thanks to information systems, it is possible to vary magnification electronically and simply: if we light up several points on the screen per pixel, we get a larger (magnified) image. If, on the contrary, we make a point on the screen be referred to several pixels, we get a smaller (reduced) image. In spite of any sophisticated techniques used to calculate the exceeding points when magnifying images or to calculate the points after removing the exceeding ones when reducing images, the image displayed can never be the actual one. This means that the only definitely correct way to visualize an image is to use a 100% magnification factor.

Like with magnification, the digital image can be modified by the information system so as to improve the visibility of some information or to delete other information. This is a distinctive capability of the digital world and there is nothing similar in the traditional one.

Digital receptors have larger characteristic curves than traditional photographic films; this feature, along with digital processing, makes it possible to correct overexposed or underexposed images by varying the gray shades associated to pixels and to optimize the visibility of bone density (varying the gray shades referring to it). To this end, it is very important in X-ray applications to know the gray histogram of digital images. Its gray shades establish the palette of a defined number of gray shades for the bitmap pixels, ranging from a maximum value (white) to a minimum one (black). The gray histogram is that obtained by associating every possible gray shade of the palette to a number of pixels in the bitmap with the same gray shade.

This histogram indicates if the image is overexposed or underexposed and helps us choose and check the effect of any processing aimed at optimizing the visibility of specific structures. If

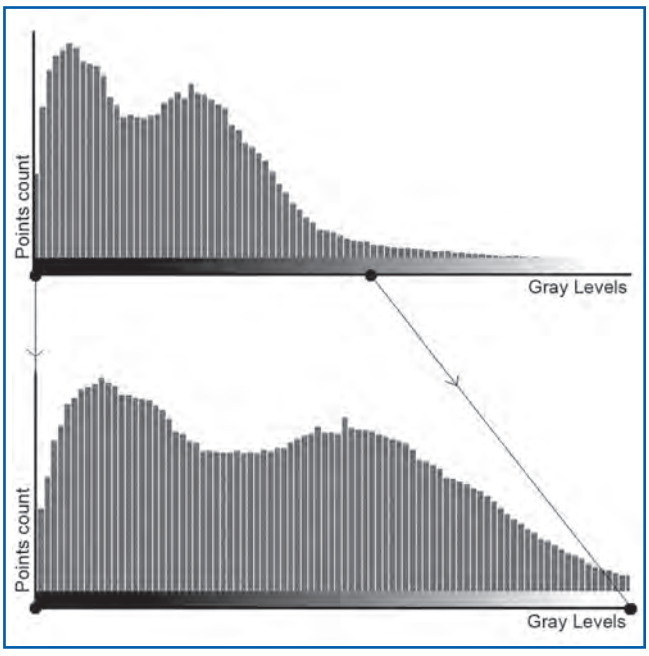

Fig. 2.6 Gray histogram and exposure optimization.

the histogram occupies only a portion of these values, it can be changed without losing any information, so as to make it occupy the entire possible interval. This means it is possible to space the gray levels of various pixels so that they are more easily perceived by the user. The same happens when optimizing the exposure—the best exposure will cause the histogram to occupy the entire field available (Fig. 2.6).

There are also more complex processings that can optimize the visibility of structures, besides the color shades.

They are very useful, but always make sure that you know the original data exactly, otherwise you risk changing them completely. The digital world is extremely simple and accurate for storing, duplicating, and transferring data. This is one of its main advantages.

Technologies for digital radiology

Digital radiology systems and technologies are divided into two main groups: direct and indirect systems. With direct systems, the radiation recording and the digital image reproduction are performed at the same time as the irradiation. With indirect systems, the irradiation and the processing of the digital image are carried out at different times.

The receptor in direct systems is usually a solid state electronic sensor. It is made of a given area (known as "useful area") of tiny basic cells arranged one next to the other and in rows and columns, exactly as in the matrix pattern shown to explain the concept of a bitmap on pages 9-10 (Fig. 2.5). The radiation intensity of these cells is processed in such a way as to produce an electrical charge proportional to the intensity rate. This electrical charge is subsequently measured by the electronic processing system and transformed in a gray shade corresponding to each cell. All cells are then joined together in one bitmap. This bitmap displays the intensity rate in various points of the receptor's useful area. Direct systems usually work together with an information system. As soon as the image is generated, it is immediately stored inside.

Intra-oral sensors, digital pans, and volumetric radiology units are direct digital radiology systems employed in dentistry (Fig. 2.7).

With indirect systems, the receptor is exposed and captures information. Subsequently, a scanner processes the information into digital images and downloads them into the information system. The best-known system is the PSP (based on phosphor plates): the receptor consists of a special plate which can be reused several times; its surface is covered with a

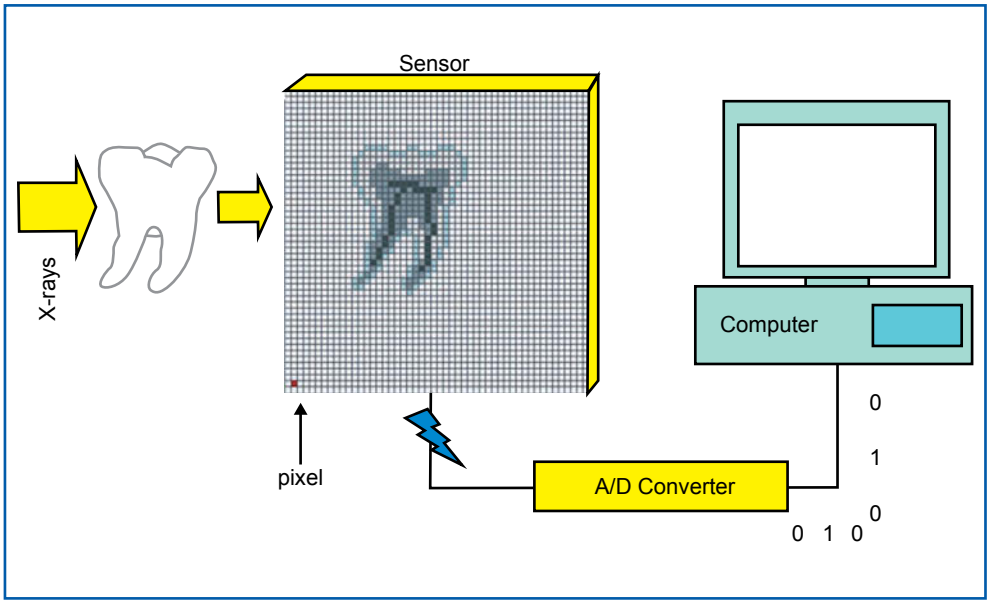

Fig. 2.7 Receptor structure in direct systems.

phosphor film that stores the incident radiation energy during exposure. Afterwards, the plate is stimulated and scanned by a laser beam with a suitable wavelength. The energy stored is released gradually. It is released in the form of a blue light with a proportional intensity rate, as detected by a suitable device (photomultiplier), and transformed into an electric signal. The electronic system reads these values and is able to build the relative bitmap, as already seen in direct systems. This scanning process is not supposed to extract the entire amount of energy stored in the film. In order to use the film for a second exposure, no residual of previous exposure cycles should be left. This is possible because exposing film to visible light means extracting energy, too. After reading, leave the film exposed to intense light for a proper time lapse and any information will be deleted. If you use the same film on different patients, you are required to guarantee sterilization by changing all external protections. This will avoid any contamination due to radiology instruments. In intra-oral use, disposable and waterproof protections are required and a specific operating protocol should be followed.

Thanks to developments in radiology, current digital systems have higher performances than traditional ones. They are simpler (no darkroom, no processing or development liquids, no disposal of special waste). Information systems can process their data (this was impossible with traditional systems). Furthermore, their resolution is now as high as that of traditional photographic plates. In some cases, it should be noted, they use lower radiation doses than the traditional systems (especially when operating with direct systems). With modern intra-oral sensors it is possible to achieve very good results with exposure times that are seventy percent lower than those of traditional photographic films.

Photographic and digital receptors are evaluated by comparing their generic characteristic curves. It can be noted that with the lowest slope and the highest exposure latitude (the highest for indirect receptors), more tolerance to exposure errors and more recordable information are achieved.

The resulting lower contrast is not really a problem; the software can easily amend it. On the other hand, more information can help us give a more accurate diagnosis (Fig. 2.8).

It should be taken into account that digital radiology units require properly developed generators in order to guarantee lower exposure times and therefore lower dose levels.

Direct systems allow us to have digital photographic images immediately at the end of exposure. This improves efficiency and is the basis of the volumetric radiology systems we will discuss further.

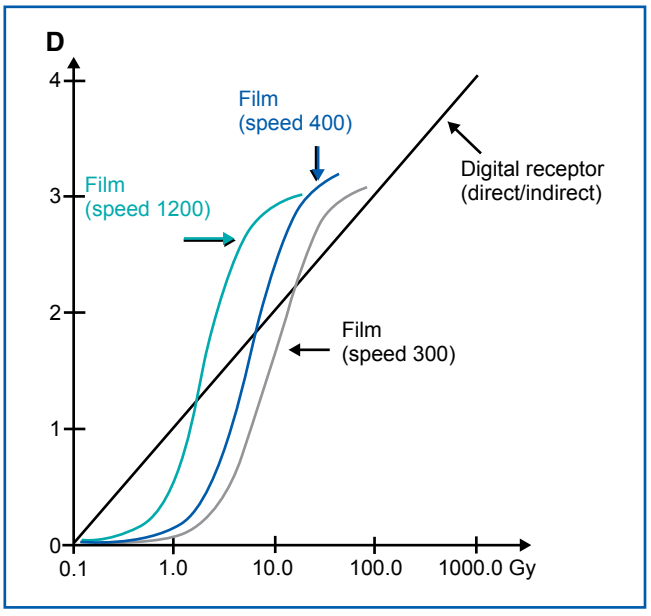

Fig. 2.8 Characteristic curves of digital receptors.

Limitations of two-dimensional radiological images

The concept of the two-dimensional (either traditional or digital) image has been previously and thoroughly explained. We have seen that the image of a three-dimensional object is obtained with a projection onto the flat surface of receptors. Replacing X-rays with the lighting beams of a bulb, we could approximately but effectively compare the object to the bulb's shadow projected onto a wall. In this case, the limits of traditional radiography are more apparent. As is the case with the shadow, in radiography all the information concerning the third direction of the rays is lost. Since the practitioner knows the human anatomy, he can usually perform his diagnosis, interpreting and mentally building the three-dimensional aspects of the structure seen in the film. This process, of course, cannot be completely accurate, even if the clinician's ability and knowledge are excellent. There are several structures along the beam path, some of them are extremely dense and conceal others. Consequently, any information about these structures is absolutely unknown. Furthermore, clinicians sometimes happen to find structures whose three-dimensional position cannot be imagined with two-dimensional film. In this case, there is no sense in measuring a structure since its size in a projection along the direction of the ray is unknown.

For the same reason, it is very difficult or even impossible to establish the density of a structure, because it could be overlapped or be different along the direction of the ray.

It is thus clear that two-dimensional radiology is not accurate in evaluating quality or quantity. To perform a precise diagnosis, other instruments are required. As we will see, volumetric radiology systems can overcome all these limits, even though they share the same starting point as two-dimensional radiology (Fig. 2.9).

Three-dimensional radiology: basic theoretical principles

In the previous section, we examined the basic concepts of two-dimensional radiology, from traditional radiology to the new digital systems. We have also underlined that these are not revolutionary instruments, in spite of their higher performance and efficiency. Two-dimensional radiology has continued to improve, but its operative and diagnostic systems have remained almost the same.

New technologies, however, have encouraged a new diagnostic approach (unanticipated in the past) which ensures remarkably better results: so-called three-dimensional radiology.

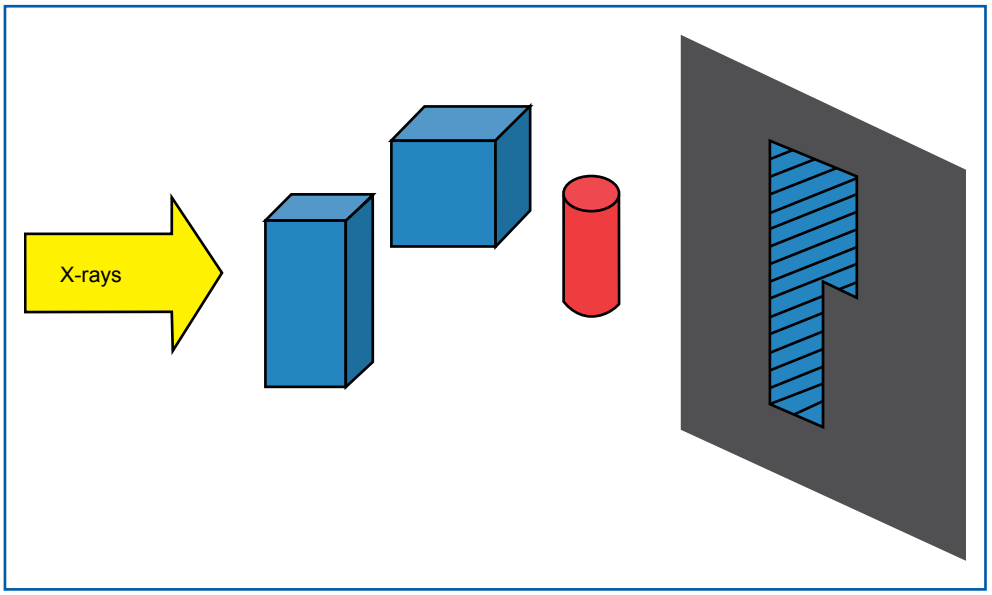

Fig. 2.9 Limitations of 2D radiology.

General objectives of three-dimensional radiology

As already mentioned, the aim of a radiological exam is to examine the internal structure and morphology of an object while keeping it intact. To do this, we take advantage of the matter's capacity to absorb X-radiation, knowing its initial (uniform) intensity. The absorption capacity of the matter depends on the physical properties of its basic parts (atoms).
In medicine, the object is a patient, a three-dimensional structure, and the aim of a radiological exam is to diagnose any diseases; we can get real and accurate information only if we can reproduce the patient's characteristics in a three-dimensional image.

Three-dimensional radiological characterization

With two-dimensional radiology, every single ray reaches the patient with a given initial intensity (I_0), passes through him, and releases some of its energy; and when it comes out of the object, its intensity (I_1) is lower (attenuated).
The greater the loss in intensity is (when all other factors are constant, it depends on the matter's density), the more radio-opaque the matter will appear.
When working with matter with a uniform density and a steady radiation frequency, we know that the physical ratio of I_0 and I_1 is fixed by the ratio $I_1 = I_0 \cdot e^{-\mu \cdot s}$, where s is the thickness the beam penetrates and μ is the specific attenuation coefficient.
When we examine a patient, density is only locally uniform, because the beam passes through several tissues with different specific attenuation coefficients. If we imagine n parts which are uniform along the beam direction, we can describe what is happening according to the following formula:

$$I = I_0 \cdot e^{-m \cdot s} \cdot = \alpha \cdot I_0 \cdot e^{-\mu 1 \cdot s1} \cdot e^{-\mu 2 \cdot s2} \cdot \cdots\cdots e^{-\mu n \cdot sn} = \alpha \cdot I_0$$

Where m is the weighted mean of all coefficients.
If we reduce the size of the parts to the most extreme case, when each part is equal to a point, we will have infinite, different coefficients, but things will not change.
With two-dimensional film, we can register the information about I. Knowing I means that we can only know the whole attenuation value α or the mean value m. This is the two-dimensional radiological characterization of our object along the given direction, but we cannot get the information about the local details, that is to say, the $\mu_1, \mu_2, \ldots, \mu_n$ values.
Only if we know these values, can we have a three-dimensional radiological characterization along the direction of the beam. If we repeat the procedure with every beam passing through the patient, we will get a complete characterization; the goal of three-dimensional radiology is to collect this amount of information (Fig. 2.10).

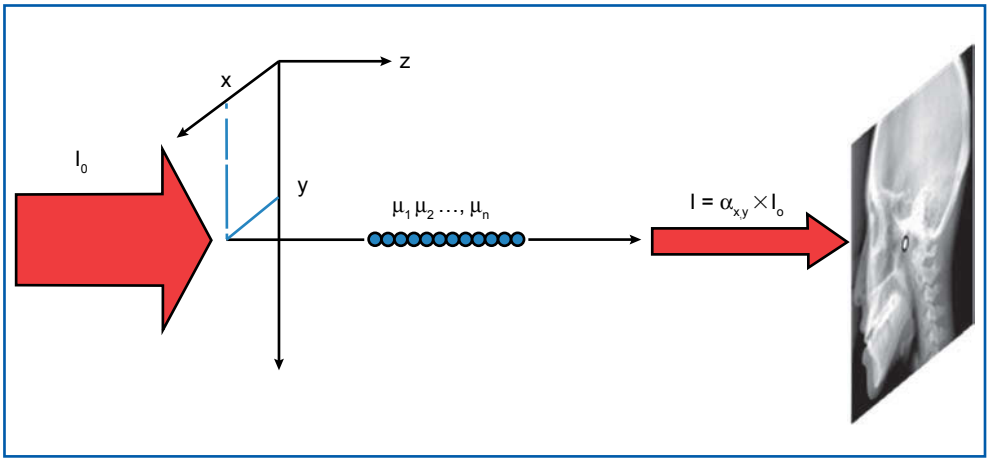

Fig. 2.10 Three-dimensional characterization of radiodensity.

Approach to three-dimensional radiology

Since we now know what three-dimensional radiological characterization means, it is necessary to learn how to operate. Because (of course!) the patient should be kept intact, we have to follow a non-invasive procedure, as in two-dimensional radiology, that is to say, to irradiate with a known radiation intensity and measure the attenuation of the emerging beam.

As we have already pointed out, with this approach we get a sort of mean value of tissues' density instead of the precise specific values we would like to find. What can we do, then? Before trying to explain a little further, we can first try to understand instinctively how we can restore the information that appears no longer accessible. To do so, we can use the following practical example.

Suppose we light some three-dimensional bodies with a direct lamp according to a given direction, as in Figure 2.11, and that behind these bodies there is a wall on which their shadows are projected. As we can see, we get just little information about the bodies and we cannot know how many they are and how they stand or lay. Once again, the projection conceals the information along a dimension of space.

Nevertheless, if we also examine the shadows that these bodies project on another wall, when lighted from another direction, we can have more information about them. In this example, we can see three bodies, the ones in the first shadow are cubes or cylinders with a round base; we can establish how they are arranged, etc.

If we have two-dimensional information taken from two different directions, we can get a much more accurate three-dimensional description. We can intuitively understand that the more projections from different angles we have, the more accurate the 3D description will be. We now have to establish whether it is possible to get a 3D radiological characterization of a patient starting from 2D characterizations from different directions.

Solution to 3D problem: further observations

According to the intuitive concepts mentioned in the previous section, it seems clear that we can get a three-dimensional characterization of a patient using a number of two-dimensional characterizations from different directions. It is useful to point out that all this is also confirmed by theoretical mathematical demonstrations: given a set of specific conditions, it is possible to calculate the three-dimensional attenuation characterization from a set of two-dimensional attenuation characterizations for different directions of irradiation.

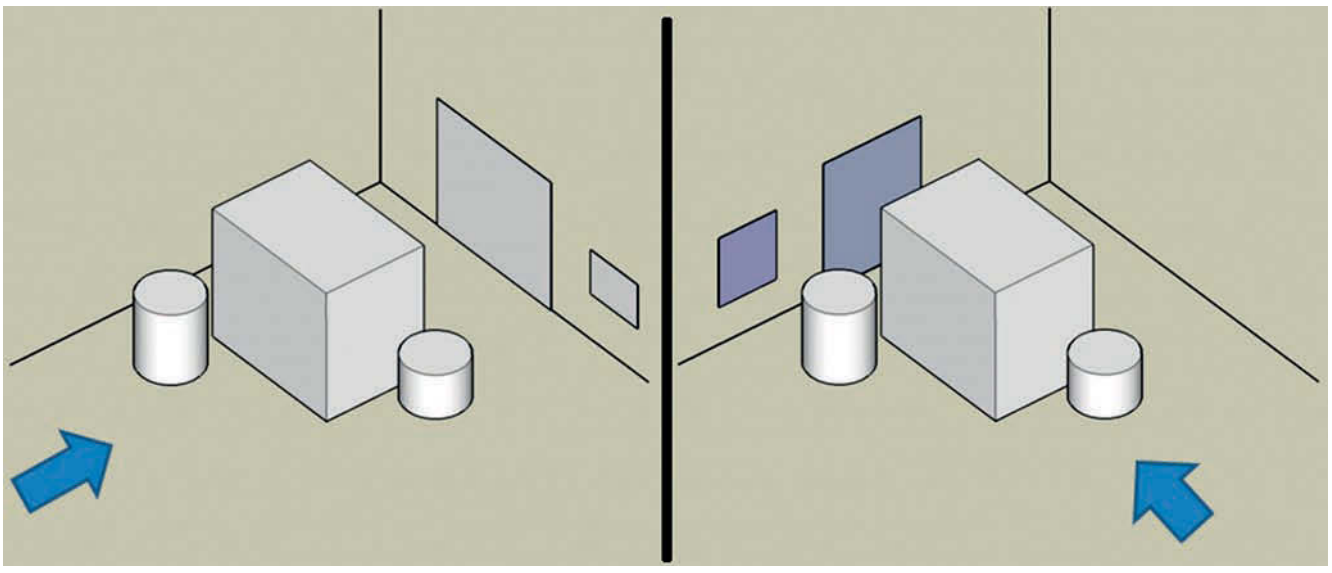

Fig. 2.11 Shadows of three-dimensional bodies projected on two walls.

In other words, we can have a three-dimensional radiological characterization (the specific attenuation in A) of the patient's point A (in the three-dimensional space) according to a mathematical procedure, starting from the average values measured by the passing beam in the two-dimensional characterizations from different directions (Fig. 2.12).
Since we have to extract values (3D) from other values that are actually available (2D), we will refer to 3D data as reconstructed values and we will refer to 2D data as raw ones.
We must take into account the following: the optimal reconstruction of three-dimensional values from two-dimensional data is possible under ideal conditions (i.e. countless irradiation directions around the patient, absence of any disturbances or mistakes, etc.). In real life, it is almost impossible to find these conditions; however, there are no conceptual obstacles to getting close to them, and it is always possible to measure the difference between the real and the theoretical results. Furthermore, the aforementioned mathematical procedure is simply a necessary processing or calculation of the values measured in two-dimensional radiological characterizations, which are their radiological images. Since there are so many points and the calculations are complex, it is easy to understand that the complete three-dimensional reconstruction requires a huge calculating capacity. The larger this is, the lesser the tolerated approximation is. It is therefore necessary in three-dimensional radiology to have technologies and systems that are capable of supplying this calculating capacity. Although the mathematical concepts it is based upon had already been developed and well known for a long time, three-dimensional radiology could not be carried out until the early 1970s, when the first electronics and computer technology that could meet these requirements became available.
Since information processing systems can only work with digital information, it is easier to have digital raw two-dimensional data (digital two-dimensional radiological images) in the case of a three-dimensional reconstruction.
After all these considerations, it should be easy to understand that the more advanced the technical and technological solution is, the smaller the difference between the ideal mathematical conditions and the real ones will be. This will guarantee more accurate results in the reconstruction of the values of a 3D radiological characterization.
In the last thirty years, the development of the electronics and computer industry has been so great that medium- and high-quality computers now have the necessary calculating capacity to implement the required algorithms, at a reasonable price for any user. This is why small or medium-sized three-dimensional radiological systems that are able to supply the raw digital data necessary to reconstruct the corresponding volume are now accessible even to small professional medical practices.

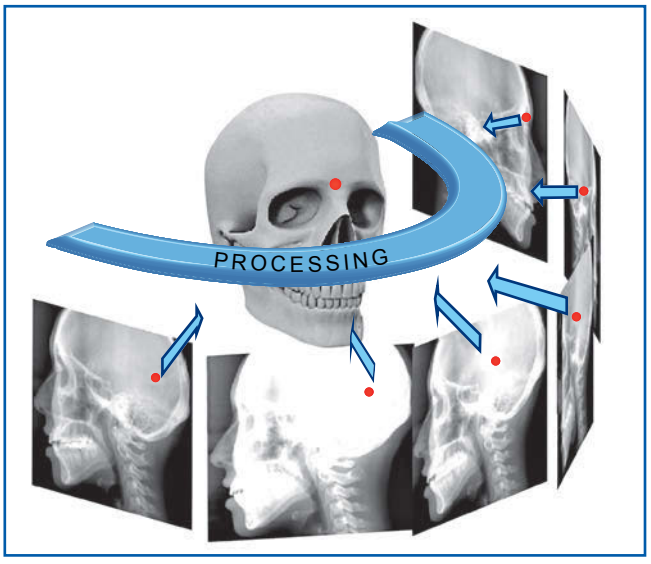

Fig. 2.12 Radiological reconstruction of 3D points from raw 2D data.

Practical 3D radiology: exclusively digital technique

We can summarize all the previous concepts as follows. We get a 3D radiological characterization of a patient after processing the data of his 2D characterizations (the traditional radiological images) obtained irradiating from different directions. The necessary processing capacity for reconstruction is only possible with digital information systems. This is why it would be convenient to start from digital two-dimensional radiological images (bitmaps).
Since it is necessary to have several images obtained from precise and regular positions, it is clear that we must choose direct digital radiological systems because they have higher performances.
After the calculating or reconstruction procedures, the information about the three-dimensional characterization will be inside the computer system and saved in a file. The user will have access to these data by means of a computer, in particular through a screen and a printer. How can this three-dimensional information (volume) be displayed on a screen or a printout that is two-dimensional? And how is it possible to access them? We will face these problems later. Now, we have to underline that the problem of how to use these data is at least as important as that of how to obtain them. The three-dimensional radiological information can be processed using software and computer programs which allow the user to navigate, extract, highlight, and modify these data properly.
It is evident, then, that the 3D radiological activity is inherently a part of the digital world; outside of it, it cannot exist. Since the reconstruction, storage, and usage procedures and techniques are based upon software instruments, these will be essential for obtaining the required performance and results.
In order to better understand how these instruments should work and their aims, we must fully understand the structure and features of the digital data that represent the digital volume. We have to know the result of the 3D radiological characterization starting from the raw data.

What is a (digital) radiological volume?

At the end of the process of reconstructing raw data, we get some values that represent the local radiological characteristics of all the points of the object to be examined, in three dimensions. As we have already explained, all this is only done with digital systems that use and generate numeric data.
As is the case with two-dimensional images, it is necessary to understand fully the connection existing between the three-dimensional data and the physical reality they represent. This is the only way to understand the potential and limitations of three-dimensional radiological techniques in order to use them properly.

From pixel to voxel

When we explained the ideas and principles on which the reconstruction of three-dimensional radiological data is based, we also talked about the possibility of calculating the specific attenuation rates of the points forming the volume of the object to be examined, starting from the average values measured in the homologous points of all two-dimensional images (raw data).
When, in practice, we use systems that supply these raw data in the form of a bitmap, we accomplish what we have already underlined, but it is worthwhile to point out once again: we get rid of the useful but dangerous concept of something infinitely small enclosed in a point, and we take on the concept of a small but finite area, that is, the pixel.
As a result, when we face the process of three-dimensional reconstruction, the concept of point-by-point radiological characterization becomes the concept of local characterization,

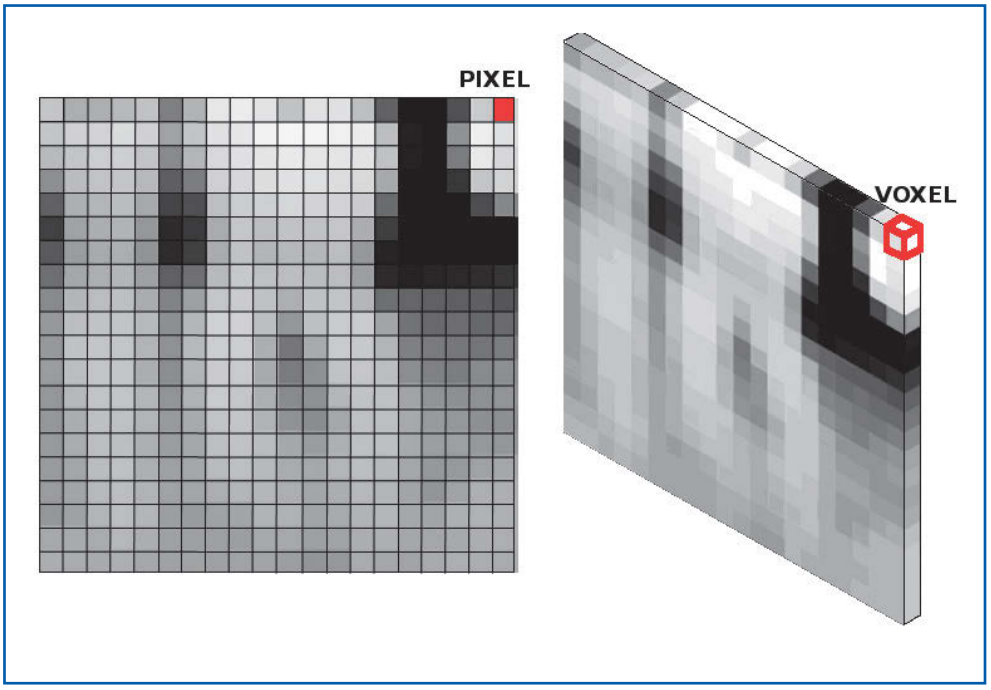

Fig. 2.13 From pixel to voxel.

made up of the small but finite parts of a volume. As was the case with the pixel in the two-dimensional reconstruction, we introduce the concept of a basic, finite part (technically known as a "voxel", or volume picture element) in the three-dimensional reconstruction as well (Fig. 2.13).

The volume reconstruction performed by a digital system starts from raw data which are bit-maps, two-dimensional radiological characterizations obtained by means of two-dimensional grids of pixels, and leads to a three-dimensional grid made of voxels.

The corresponding specific attenuation rate of each voxel will be calculated: similarly to what occurred with pixels, we will take that value of each voxel as homogeneous and constant in the entire volume enclosed.

This is of course an approximation, according to which all the actual structures composing the real subject inside the volume enclosed by the voxel appear to be replaced by a homogenous substance as dense as their average value.

As is the case with pixels in images, all the smaller details of the voxels fade in a uniform value and then are lost or incorrectly represented (Fig. 2.14).

It is easily understood that the information about a planar section of the grid (one-voxel thick) is the same as that of the bitmap obtained associating to each voxel one pixel with the same value (since the information along the thickness of one voxel does not change in the slice, no information will be lost). This idea is demonstrated clearly in figure 2.13.

It is evident that if the voxel is small enough to provide the necessary diagnosis, this is not a problem. But, while the available two-dimensional digital radiological systems have such high performances that this is never a problem, with three-dimensional systems, things are very different. It often happens that, due to technological, financial, or dose restriction problems, three-dimensional radiological systems work with quite large voxels. It is then necessary to make sure that the volumetric radiological system chosen is equipped with the proper features in terms of performance for diagnosis.

Voxels are called "isotropic" when their size is uniform in all three directions. With isotropic voxels, the space resolution of the available information is the same in all directions and there are no problems with object alignment. This is a great advantage.

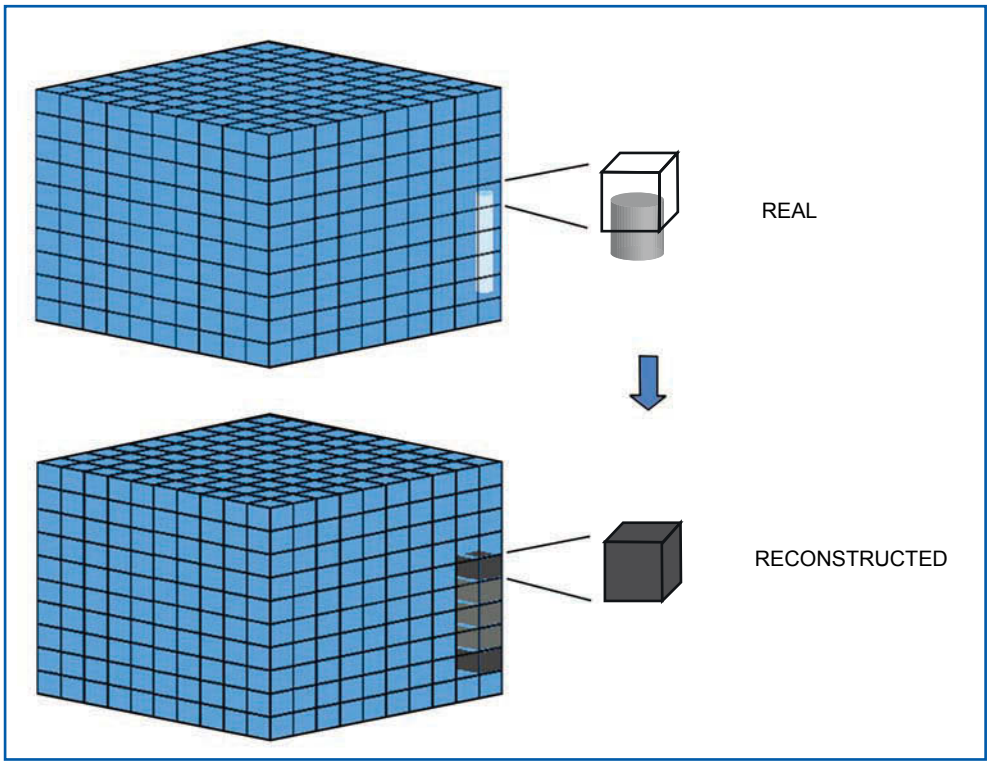

Fig. 2.14 Representation of a voxel matrix and detail of a voxel. Smaller real structures will get lost in the reconstruction process, which uses an average value of homogenous density for each voxel.

Data representation and storage

As with all digital data, with three-dimensional ones we have to face the problems of their storage, transfer, and use.

Storing on reliable and non-volatile supports (that is to say, supports which store information even when computers are off) is done by storing them in the form of a file, a collection of organized information. The specifications defining the structure and organization of files and of the information contained are usually referred to as the "file format".

Any software will recover the information on files if it knows the file format—just as a foreigner will exchange information if he knows the language.

If it is possible to determine a common language (a standard one), any file created in that language can be used by almost anyone. In medicine, they have developed a standard system of information and digital devices known as DICOM (Digital Imaging and Communications in Medicine). This was created and developed in the United States, and it has been used by other national and international authorities (in Europe, the Committee for Standardization has called it MEDICOM). This system is run by an international committee made up of experts and suppliers of medical items. It is updated to meet any new requirements and is frequently upgraded. For easy transfer and use of volumetric radiological data, DICOM is the universal format of the systems that are currently available; any clinician who has a DICOM reader can have access to data generated by any other system.

DICOM is a very complex standard, covering a huge number of different applications. It controls the method of storing data, as well as their transfer to other systems which correspond to the standard. As a rule, it is based on an object paradigm where a specific entity of the real world (hospital admission, patient, image, etc.) is defined and shaped as a precise object with a specific series of attributes. This standard will then establish some services that can be carried out on some specific objects. It is therefore possible to identify the so-called Service Object Pair, known as "SOP" by DICOM, a group made up of an object and all possible ap-

plications. For further information, refer to the relevant literature (on the website medical.nema.org). The standard has been changed over time; the current version available is 3.0.
Each section of the grid of the radiological volume with one-voxel thickness contains information that can be stored with no losses into a bitmap, that is, a digital two-dimensional image. Digital data are usually saved on a disk considering a given direction (usually the axial one, submentovertex) and producing DICOM files of all the images corresponding to the sections of one-voxel thickness making the three-dimensional grid along the chosen direction.
It is clear that the resolution of these images, which defines the pixel size, depends on the three-dimensional volume resolution, that is, the voxel size. The smaller the voxel size, the larger the number of these images and the corresponding files. In short, as the definition increases and the voxel size decreases, the amount of data generated and memory space used in digital systems will greatly increase. In two-dimensional images, this number will increase by the squared value of the resolution; in three-dimensional images, it will increase by the cubic value of the resolution. It is therefore no surprise if even small volumes reconstructed in high resolution occupy a much larger space than large volumes with low resolution.
In order to better understand this idea, we can think that in modern volumetric systems for dental applications, covering a volume with a side of 50 mm could take about 250 MB (approximately two billion binary digits, because B stands for byte, a group of eight binary digits, and M stands for "mega", equal to the multiplying prefix 10^6; other commonly used prefixes are G for "giga" or 10^9, and T for "tera" or 10^{12}).
It should also be taken into account that we can confront these problems using advanced mass memory devices. Hard disks with a capacity of 500 GB or 1 TB are now widely available at prices of around 15 cents per GB for the end-user. This means that, in the case of a volume like that above, on a modern hard disk we can think of storing some 2,000 volumetric exams, with a storage cost of less than 4 cents per exam.
We should always take into account that we require this memory space when supplying a backup device for our information system and when delivering data to a third person. In order to give the patient the data of such an exam, we can use a strong, safe support, like a CD (max. capacity 700 MB) or a DVD (max. capacity 4.7 GB).
Management programs of three-dimensional radiological systems usually have specific functions for transferring data to these supports, and also allow the possibility of copying, at the same time, the software to read DICOM three-dimensional radiological data onto the same support (CD, DVD, etc.). It is therefore possible for anybody to access and display the information contained, with a compatible PC and the support containing the exam.

Practical applications of 3D radiological data

At the end of the reconstruction operations, the information system contains the radiological characterization of the volume examined in terms of the attenuation of every voxel that forms the volume. We now need to know how we can access this information.
At first, we could try to display these data so as to use them for our diagnosis and operate in the same way as with traditional two-dimensional images. However, since the amount of information is so large—and we know that this is a problem when we have to store it—it is difficult to display. It is, of course, not advisable as standard procedure to print all data (as is the case with two-dimensional images). We must then think of proper practical and cost-saving strategies in order to perform the data evaluation phase. In the next sections, we will establish how this is possible. For now, we can say that we can display the information best when using information systems with adequate processing capacity.
These devices offer huge advantages because they are accurate planning and clinical simulation systems.

The volumetric data with isotropic voxels, in particular, allow us to perform real measurements with no distortions of structures and anatomical relations, which would be impossible with two-dimensional techniques.
Yet, these are not the only possibilities. By means of suitable supports with radio-opaque landmarks and adequate operation protocols, the data available can be used to perform, with CAD/CAM techniques, ancillary devices of surgical clinical activities, like masks for guided implantation surgical procedures. With the terms CAD (computer-aided design) and CAM (computer-aided manufacturing), we mean those methods based on information systems that allow us to produce adequate digital data that is useful for implementing auxiliary devices, like surgical guides, by means of numerical control equipment. This is possible after a phase of simulation and clinical planning, during the course of which the clinician will have planned the insertion of one or more implants, verifying with real measurements if the anatomy is adequate and the critical distances are respected.
This is only one of the possible applications. Another one is the use of volumetric data to make, with fast prototyping CAM techniques, a model which completely corresponds to the real anatomical bone structure concerned; this is useful when we have to implement bone grafts. The possibility of modeling the bone from bone banks on a sample and then preparing it adequately before surgery, allows us to work with no unexpected events and very short surgical times, dramatically reducing the risk of contamination and infection.
The use of volumetric data is, however, not limited to clinical aspects. These data used with proper display tools become a very powerful means of communication and persuasion with patients that is much more effective than any traditional radiological image.
Finally, we should take into account the medical-legal aspects of these exams. They demonstrate the state of the art in diagnostics, as has widely been reported in literature, and in the event of charges or legal action, they can really make a difference and guarantee proper and careful conduct, starting from patient information up to diagnosis and clinical activity.

Structure and features of 3D radiological systems

Without the basic theoretical information described in the previous sections, we would not be able to more thoroughly examine actual three-dimensional radiological systems. We will try to underline their main components and characteristics, as well as the problems concerning quality and interpretation of data.

Work cycle and basic components of three-dimensional radiological systems

It should now be clear that every three-dimensional radiological system works following three main phases: acquisition, reconstruction, and display.
These phases are strictly connected to three well-defined and usually separate parts.
The acquisition subsystem is definitely the most expensive part of the system, because it includes all the mechanical and electromechanical components that are necessary to run and position the X-radiation generator and the electronic receptor, the receptor and all electronic supply and control components. Furthermore, it should be equipped with the necessary electronic components to connect and exchange data with the other parts and with the outside world. Its task is to generate and supply the raw data from which the volume will be reconstructed.
The features and quality of the acquisition system will determine the quality and availability of the information supplied by the 3D system.

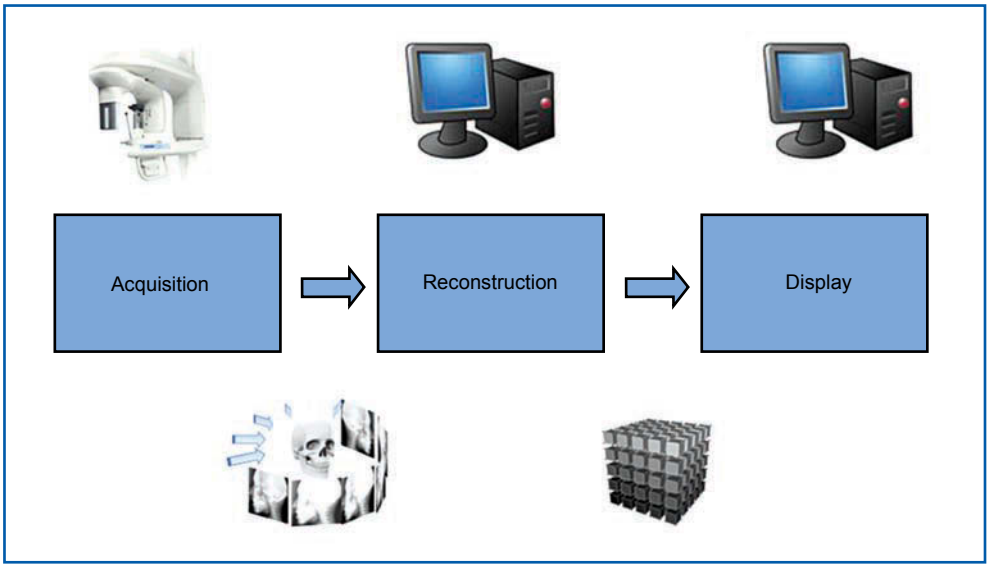

Fig. 2.15 General diagram of a 3D system.

The second essential part that will determine the quality of the data is the reconstruction subsystem. It is basically a data processing system. It communicates and receives raw data from the acquisition system; it processes them according to the algorithms and strategies it has, and then generates the data corresponding to the voxel matrix, that is, the three-dimensional characterization of the volume scanned.

It is usually composed of specific software that can be installed either in a devoted workstation (a computer dedicated exclusively to that function) or in a server (a computer performing several functions, among which the processing necessary for reconstruction). This kind of system is usually equipped with specific and excellent graphic and numeric capabilities. It is often also equipped with an acquisition system. When it is not, the manufacturer will give precise information about the necessary requirements.

The data generated by reconstruction are usually transmitted to the computers of the structure (hospital, clinic, radiological practice, dental practice, etc.) where the 3D radiological system is installed. This structure should be provided with all necessary information instruments in order to display those data. They should have a suitable computer with proper features and software capable of reading digital volumetric data.

Understanding how these systems work, what they enable us to do, and how they should be used, is probably the most important thing for clinicians when performing diagnoses and treatments. Therefore we are absolutely required to learn all these aspects (Fig. 2.15).

In the following sections, we will further examine each one of these three phases of three-dimensional imaging and all the technologies connected to it.

Acquisition

As we have already seen, the core system is the equipment necessary to acquire the raw data from which the three-dimensional image will be reconstructed.

The quality of the volumetric data depends on the quality of the raw data. Regardless of each specific strategy and technology, every volumetric acquisition system is supplied with an X-radiation source which rotates along with a digital receptor—the patient will be positioned between these two.

While working, the source will emit radiation, rotating together with the receptor, which captures the radiation portion left over after passing through the patient's body. He will be positioned with his body, or part of it, along the rotation axis. This axis together with a pair

of other perpendicular axes will form the three main scanning directions of the system. They are the reference directions of the coordinates of the points of the volume scanned. In maxillofacial and dental applications, the patient's head is the scanning volume and the reference axes usually indicate the submentovertex (z-axis) direction, the forward-backward (y-axis) direction, and the condyle-condyle (x-axis) direction.
While rotating, irradiation pulses are emitted from different angles. Detected by a sensor, they produce a series of conventional radiological data of the same object, but from different points of view—this is raw data.
At present there are two available acquisition strategies that lead to two different systems: the so-called CT and CBCT.

CT systems

CT systems (computed tomography) are based on a radiation system with a "fan beam". The X-ray source sends a radiation beam in the form of a fan, which is very narrow in one direction (collimation) and open at a large angle in the other. If we imagine that this beam is so thin as to lie on a plane, we can understand why the sensor able to receive it can be thought of as linear, with a geometric extension along one direction only.
Rotating such a source-receptor pair around the object to be examined, it will detect the raw data concerning a plane portion of the object (actually, a slice as thick as the beam's width). In order to scan a volume with these systems, it will be necessary to shift the patient along the rotation axis and perform several rotations; the combination of rotation and motion will result in a spiral scanning of the patient through the beam (Fig. 2.16).
These systems are shaped so as to scan large volumes because the size along the translation direction is obtained increasing the very translation (at the same rate of speed). With an ideal planar source and receptor, we can see that spiral motions usually prevent scanning any planar portion of the patient from all directions (this would only be possible if we had no translation at all). This is why it is often required to complete raw data, interpolating them. To avoid this problem, special techniques are applied (multiple sensors, enlarged beam) which improve the quality of images, but they generate high radiation doses. On the

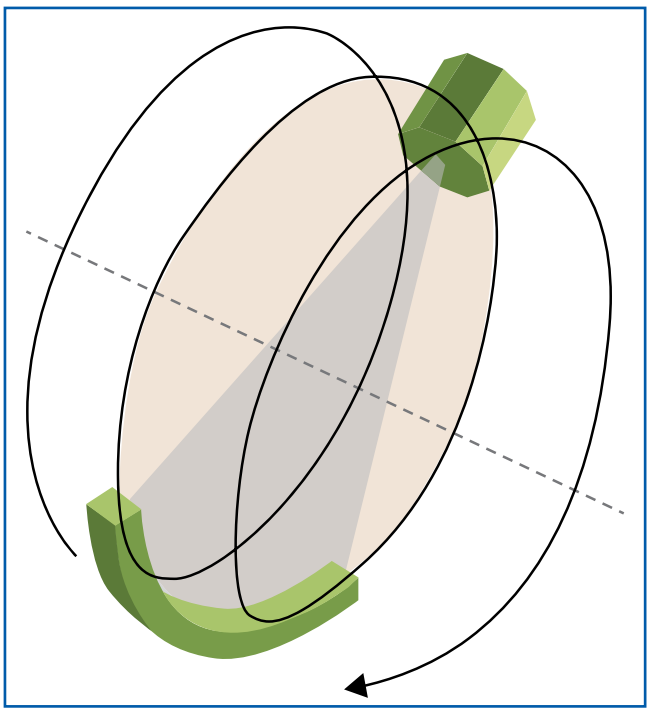

Fig. 2.16 Diagram of a fan beam (CT).

one hand, this increases damage to patients; on the other hand, it allows us to work with a high contrast-to-noise ratio. As will be better explained later, this value is the capacity of the system to differentiate between and recognize tissues with very similar density rates; this is essential for early recognition of tumors. The sensor cells are also affected by the contrast-to-noise ratio; the bigger they are, the higher the ratio.

Large volume systems are also equipped with other important though expensive characteristics, but their costs can generally be justified because they guarantee high-quality imaging, though at high doses. Such systems are usually employed in hospital medical equipment, because they allow us to examine medium-large volumes with high-quality imaging, though with high doses and low resolution. They are mainly employed for surgical, orthopedic, and oncological purposes; they are equipped with a table (translating along the rotation axis of the generator-receptor pair), upon which the patient lies. This table is controlled so as to generate the raw data of the area to be examined.

In these systems the voxel sizes of the reconstructed volume depend on two factors: the sizes of the receptor's single cells and the translation speed. It is clear that while the translation speed will establish the voxel size along the translation direction (conventionally known as the z-axis), the cell sizes will establish the voxel size in axial sections (perpendicular to the translation direction). Only under specific conditions are they the same, or, as we commonly say, is the voxel "isotropic". This condition is essential for measuring the distances of the reconstructed three-dimensional data; only if voxels are isotropic, is it guaranteed that all measurements are always real (wherever they are oriented in the space), unless there is a known scale factor.

It is, of course, always permitted to use these systems, as often happens, for dental applications as well. However, it is essential to carefully evaluate and make sure that the rules of justification and optimization are observed. In the dental sector, there are only few cases (i.e. implantology) where these rules are observed. Furthermore, only CT systems were available until a few years ago, and this is the reason why it is commonly thought that three-dimensional imaging in dentistry is necessary only for implantology. Now, this is no longer the case. New technologies have led to systems with quality, dose, and costs that appear to be suitable for general dental diagnosis: CBCT systems.

Cone beam systems (CBCT)

Cone beam computed tomography systems are equipped with a generator that sends a non-collimated beam, much the same as with CT systems but the beam is conical, that is to say, it opens at a given angle in all directions of the space along a central axis. As a receptor, these systems employ a rectangular panel made according to the usual two-dimensional matrix of pixels, as seen several times in direct digital (two-dimensional) radiological systems.

The generator and receptor are installed at a given distance from each other and fastened together in such a way as to detect raw data by having the patient positioned between them and rotating. In this case, however, we can see that thanks to the cone shape, we can acquire all the raw data with just one rotation of the generator-receptor pair—if the volume to be examined is small enough to fall within the portion hit by the radiation cone. In this case, the data are made of two-dimensional radiological images of the scanned volume, taken from several directions (Fig. 2.17).

Since the maximum volume sizes are small and there is only one rotation with these systems, they are smaller and simpler, and therefore cheaper. Since we obtain all the raw data with one rotation (with no interpolation), these systems are preferrable to CT ones, with regard to the effective dose of radiation given to the patient.

Their imaging quality, on the other hand, is lower. It is easy enough to understand that the contrast-to-noise ratio is negatively affected by scattering and/or secondary radiation, because

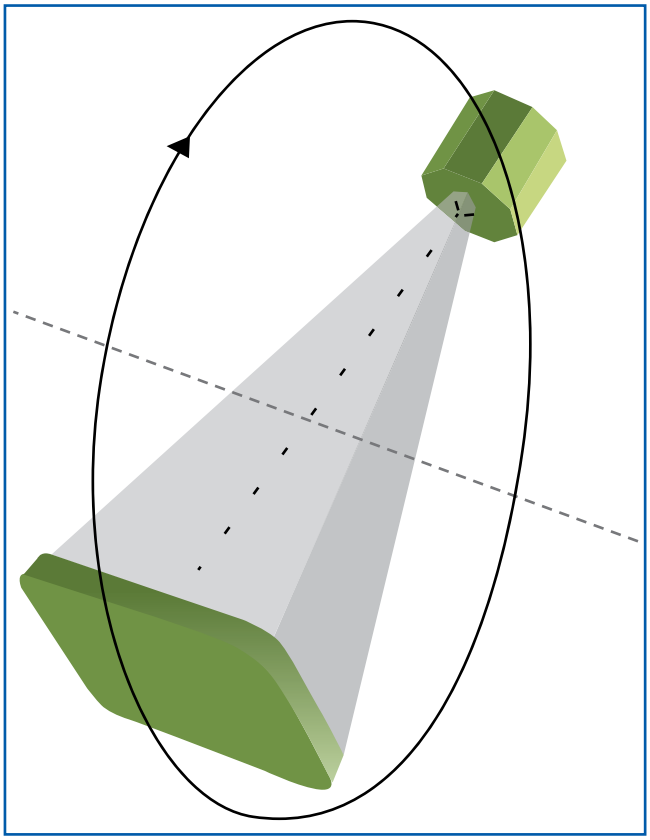

Fig. 2.17 Diagram of a cone beam (CBCT).

we are not working with collimated radiation: the radiation reaching a pixel (therefore, the signal produced) is not only caused by the primary radiation (the useful one, whose direction is that given by the line linking the pixel to the cone beam source), but also by the secondary, random and unpredictable one coming from points outside the primary direction trajectory. CBCT systems exhibit other negative factors (varying pixel gain, electronic noise, etc.). It may be possible to develop new methods so as to reduce these problems, but not to remove them completely. However, according to the use, its advantages may be so important and the quality sufficient enough, that this solution is recommended.

In dentistry, for instance, this is the case. Here, we are focused on the morphology of small, very hard structures whose densities are different from those of the adjacent structures. A high contrast-to-noise ratio is therefore unnecessary. What is really essential is to work with doses which are as low as possible, because high doses, justified when diagnosing diseases affecting the patient's life, are not justified in diagnosing much less dramatic diseases, like common dental disorders.

Depending on the kind of examination required, it could be necessary to have high-resolution capabilities with systems that are able to reproduce volumes with small enough voxels. Based upon physical laws, we know that if we want to maintain the same image quality, the smaller the voxel is, the higher the dose will be.

According to the well-known ALARA principle (as low as reasonably achievable), we are required to use the smallest dose allowing the proper voxel sizes to meet the desired diagnostic goal.

FOV: definition and importance

An essential factor of both CT and CBCT systems is the so-called field of view (FOV). It is strictly linked to the volume sizes. In all cases, the sizes of the receptor, of the beam pro-

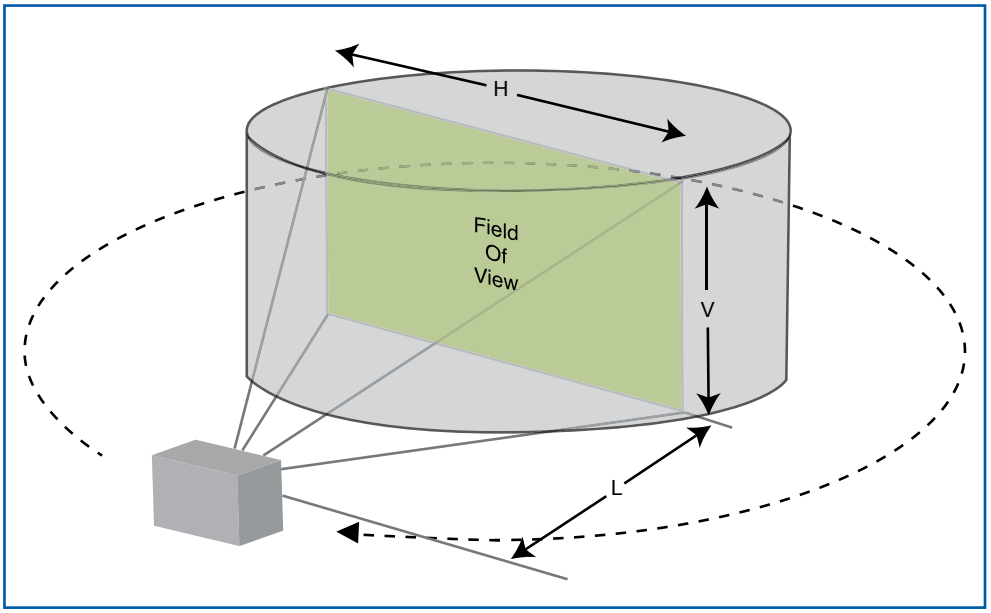

Fig. 2.18 Diagram of an FOV (H = horizontal FOV dimension, V = vertical FOV dimension, L = source distance).

duced, and their positioning with regard to the rotation axis of the volume to be scanned, determine the geometric values. The maximum sizes of the area concerned along the rotation axis depend on these geometric values; this area is known as FOV.

In particular, with CBCT systems the FOV is usually a rectangular area, because this is also the receptor shape. Because of rotation symmetry, it is clear that the volume scanned and then reconstructed will be cylindrical (Fig. 2.18).

With CT systems, the receptor is linear and the FOV is linear as well. The translation along the z-axis together with the rotation will generate in this case, too, a cylindrical volume: the FOV establishes the base diameter of this cylinder and the height will depend on the translation length along z. The FOV size depends on other factors as well. First of all, dose: the larger the volume is, the higher the dose. Since the FOV is essential in establishing the volume (with CBCT the ratio is 1:1 with it), the FOV establishes the dose quantity; as the FOV increases, the dose quantity also increases. The FOV is also connected to the receptor sizes. This is one of the essential parts regarding both costs and performance. It determines the voxel sizes and therefore the detail resolution.

Large sensors relate to larger FOVs (and volumes), but this also implies higher costs and fewer details (larger voxels). If it is possible to work with smaller FOVs and consequently with smaller receptors, we will have lower costs and different technologies that will produce smaller voxels and thus more detailed information.

This is very important in dentistry, where we are required to use lower dose quantities and have a high resolution in order obtain accurate information about very small anatomical areas. The small FOV is therefore essential. According to a common classification, maxillofacial/dental equipment is divided into three groups based on FOV sizes: small FOV systems (portion of an arch), medium FOV (up to two arches), and large FOV (up to the entire skull). In literature, we often find FOV subdivided into medium-small ones (dentoalveolar) and large FOV (craniofacial).

Since 2009, the European Atomic Energy Community's SEDENTEXCT project has been active to study the application of CBCT systems in the maxillofacial and dental sectors, and to develop operative protocols for their use. Twenty guidelines have been established. One of them concerns the FOV, determining the maximum size which can be used by clinicians when operating with CBCT systems (when it is not deemed necessary to call for a radiologist): 80 mm x 80 mm.

Effective dose and volumetric radiological systems

Like any radiological equipment, volumetric systems may be potentially harmful to patients and operators. It is therefore required to know and measure the degree of this risk. As is well known, the size directly linked to risk is the dose quantity, that is, the energy amount that the ionizing radiation releases per mass unit when passing through bodies. According to the kind of radiation and how large and how sensible the organs hit are, the damage caused by the same amount of energy may change (both in absolute and relative terms). This is why we talk about effective dose when speaking about biological damage. The value of effective dose an object takes during a specific exposure is defined as the one that should be released using a uniform beam field along the whole body to cause the same damage or risks.

If a restricted but very sensitive area is irradiated at low energy, the effective dose may be larger than the one resulting from higher and more intense radiation to a less sensitive area. To this end, the international ruling bodies (ICRP) supply tables with radiation weighting factors, through statistical studies, which may be used to establish the values of effective dose based upon the measurements of absolute values, taking into account several factors (sensitivity, kind of radiation, types and ages of patients, etc.).

The unit of measurement of effective dose is the sievert (expressed in joules/kg).

Every day we are exposed to a normal amount of ionizing radiation (cosmic rays, decayed radionuclides, X-rays, etc.), whose average value has been fixed at 6.5 uSv/day. This value varies from area to area and increases as the altitude increases (the thickness of the atmosphere decreases and as a result its screening capacity against cosmic rays decreases as well). This is an excellent reference value to understand the risk any patient runs when performing an X-ray exam. It is clear enough that it is very hard or even impossible to have a precise effective dose value, because it depends on so many factors according to specific operative conditions (patient, his position, geometry, etc.). Therefore, when we talk about effective doses, we often talk about variation intervals and order of magnitude.

It is important to underline that those patients undergoing volumetric radiological exams receive very high doses, usually much higher than those undergoing conventional two-dimensional radiological exams, and it should also be pointed out that the size values may be very different, depending on the systems and protocols employed.

The dose quantities used by CT systems are remarkably higher than those used by CBCT systems, and they all increase as the FOV increases. Small FOV CBCT systems are the best, from this point of view. At present, there are volumetric radiological exams performed in dentistry which use doses with the same size as digital orthopantomography (10 uSv).

This is very impressive if we consider that dental exams performed using CT systems with no optimized protocols may expose the patient to doses above 1000 uSv.

Thus, it is clear that, according to the optimization and justification principles, these systems are not permitted for most dental diagnostic examination systems, while CBCT systems may be used because they meet all requirements—more restricted areas of examination and lower image quality, lower doses. When choosing proper diagnostic instruments (either when we want to buy proper equipment or when we refer our patients to a radiological practice), we should always take into account all these considerations.

Reconstruction

The reconstruction process is of key importance in establising the quality of the resutling 3D data. This process includes all processing operations performed on raw data at the end of the acquisition phase. Its aim is to reconstruct the values to be associated to each voxel forming the digital volumetric radiological imaging of the object.

The algorithms, strategies, and numeric computation procedures used in this phase should be done following not only mathematical rules but also any steps to remove or reduce as much as possible any disturbances resulting from the real conditions (which are not the ideal ones because data are not complete or accurate, numbers are approximate, there is electronic noise, mechanical defects, sensitivity thresholds, etc.).

Mathematical theory and numeric computation

In the previous sections, we described the principle on which volumetric radiological systems are based. In particular, we underlined the crucial role of the raw data processing method. Even though its mathematical concepts are very complicated, and our goal is not to explain these concepts fully, it would be useful to have a rough idea of some concepts in order to understand the limitations and compromises to tolerate when working with this equipment. As we have already said, the basic physics of radiology is related to the interaction processes between matter and radiation. The processes concerning ionizing radiation are a particular case. The interaction between matter and radiation happens when the matter absorbs part of the energy carried by the radiation and it is attenuated. For the sake of simplicity, we can consider just one two-dimensional (xy) section of the entire three-dimensional body. We will take an origin point of this section plane. If we consider a radiation beam along any straight line passing through the xy plane, indicating with $\mu(s)$ the specific attenuation coefficient at a distance s from the origin along the straight line propagation and indicating with I_0 the radiation intensity passing through the origin, the physical law expressing the attenuation process is the following:

$$I = I_0 \cdot e^{-\int \mu(s)ds}$$

According to this law, the radiation intensity and the beam path are strictly connected to the attenuation properties along this path. If we imagine, ideally, a space with no matter but the body irradiated, which occupies a given area, we will have $\mu(s) = 0$ in all points of the plane except for those where the body exposed to radiation is positioned. On the xy plane, our body occupies a given area. If we establish a propagation direction, indicating the angle θ created with the y-axis and consider all passing rays parallel to that direction and measure the attenuation rate of the radiation, thanks to the above equation, we will have the attenuation profile of the body in the established radiation direction, provided that the initial intensity in each ray is always I_0 (Fig. 2.19).
Here, p shows the attenuation rate caused by the body on the AB ray passing through toward θ and at a distance of r from the line passing through the origin and with the same slant. This can be written with the expression:

$$p(r,\theta) = \ln\left(\frac{I}{I_0}\right) = -\int \mu(x,y)ds$$

and taking into account the trigonometric relation:

$$r = x \cdot \cos\theta + y \cdot \sin\theta$$

it can be written as:

$$p(r,\theta) = \int_{-\infty}^{\infty}\int_{-\infty}^{\infty} \mu(x,y) \cdot \delta(x \cdot \cos\theta + y \cdot \sin\theta - r)dxdy$$

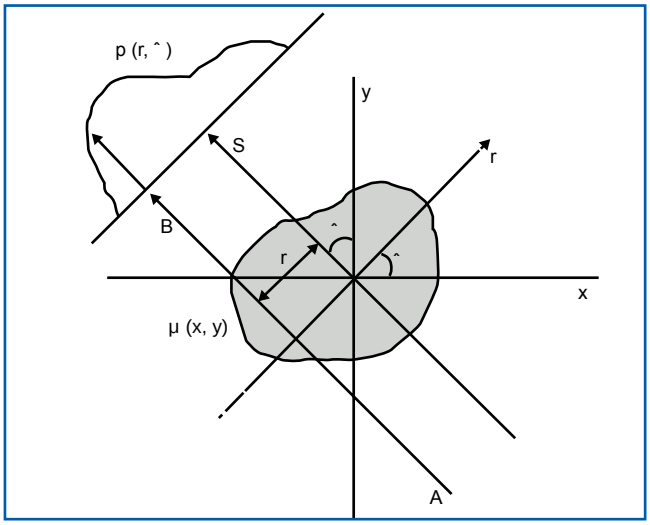

Fig. 2.19 Attenuation profile.

Where δ is always a null function, except for the point where its argument is zero, where its value is one: in our case, since the argument is $x \cdot \cos\theta + y \cdot \sin\theta$, it will always be null except for the points of the direction fixed by θ and r, where it will have the value of one. The operator applied to μ, expressed by the previous formula is called the Radon transform. It is possible to define the inverse mathematical operation, with some work. This operation expresses μ in function of p: when it has been fixed, it will become the key operator to reconstruct the precise volumetric data from the raw ones. Below you will find all the mathematical steps that lead to this fundamental operator.
Similarly to what was seen above with the Radon transform, it is possible to define an operator, which is used a great deal in the signal processing theory: the Fourier transform. In particular, indicating with $P(\omega, \theta)$ the single-dimension Fourier transform of $p(r, \theta)$, in r it is expressed by:

$$P(\omega,\theta) = \int_{-\infty}^{\infty} p(r,\theta) \cdot e^{-j\omega r} \cdot dr$$

replacing the above expression valid for $p(r, \theta)$ we will have:

$$P(\omega,\theta) = \int_{-\infty}^{\infty}\int_{-\infty}^{\infty}\int_{-\infty}^{\infty} \mu(x,y) \cdot e^{-j\omega r} \cdot \delta(x \cdot \cos\theta + y \cdot \sin\theta - r)\, dx\, dy\, dr = \int_{-\infty}^{\infty}\int_{-\infty}^{\infty} \mu(x,y) \cdot e^{-j\omega \cdot (x \cdot \sin\theta + y \cdot \cos\theta)} \cdot dxdy$$

The two-dimensional Fourier transform of $\mu(x, y)$ will be given by:

$$M(u,v) = \int_{-\infty}^{\infty}\int_{-\infty}^{\infty} \mu(x,y) \cdot e^{-j(x \cdot u + y \cdot v)} dxdy$$

It will be demonstrated that the existing anti-transformation Fourier operation expresses a function starting from its transformed operation, in this case μ starting from M; it is given by:

$$\mu(x,y) = \frac{1}{4 \cdot \pi^2} \int_{-\infty}^{\infty}\int_{-\infty}^{\infty} M(u,v) \cdot e^{j(x \cdot u + y \cdot v)} dudv$$

This can be written as follows, remembering the expression previously found with $P(\omega, \theta)$;

$$\mu(x,y) = \frac{1}{4 \cdot \pi^2} \int_{-\infty}^{\infty}\int_{-\infty}^{\infty} P(\omega,\theta) \cdot e^{j\omega \cdot (x \cdot \sin\theta + y \cdot \cos\theta)} \cdot |\omega| d\omega d\theta$$

The last relation is what we were looking for; based on the P and p connection, this relation expresses μ in function of p if p is known in every θ and r. This means that if we know the attenuation profiles from all (infinite) directions, it is possible to calculate the exact μ value in each point of the xy plane. We can therefore have a radiological characterization of the object to examine. Similarly, we can have a three-dimensional characterization of the whole body in all planar sections parallel to the xy one. Since the operator in this last expression for a given direction (fixed by choosing a precise θ value) acts on the projection value $p\ (r, \theta)$, redistributing it along that direction, this action is often called back projection.
These operators, however, are not suitable for the numeric calculation systems; they should be replaced with their discrete equivalent operators, like the discrete Fourier transform.
In this way, the infinite sums of infinitesimal parts determined by these integral operators will be replaced by finite sums of finite parts. The theoretical basis is always the same. In real implementation, a number of measures will be taken to prevent any negative aspects due to the unavoidable, non-ideal, approximate conditions of a real system (noise, lack of precision, sensitivity, etc.) based on numeric calculations (the mathematical concepts just examined are highly affected by noise which is always present in real systems; if we used them with no modifications, we would achieve poor results in quality).
The numerical reconstruction algorithms resulting from the Feldkamp one are those most commonly used by CBCT systems.
We will examine further in the next sections how the aforementioned non-ideal conditions will affect the reconstructed volumetric data and the 2D images derived from that data representing planar sections of the volume.
With the above algorithms, we can follow the three-dimensional radiological characterization; we can therefore calculate the attenuation value—the radiodensity—to be associated to each voxel.
This value is often expressed in Hounsfield units (HU), a pure number that expresses the (radiological) density associated to the voxel, relating it to the (radiological) density of water. In particular, the density in Hounsfield units is defined as follows:

$$HU = K \cdot \frac{\mu_{voxel} - \mu_{H_2O}}{\mu_{H_2O}}$$

Where μ indicates the specific attenuation and K is the coefficient, usually standardized at 1,000. Water density is equal to 0 HU. Materials that are more radio-opaque than water have positive HU; materials less radio-opaque than water have negative HU.
In volumetric radiological systems that must guarantee accurate quantity results, a steady reading of density values is ensured by procedures and protocols of calibration by means of a special phantom containg water. They allow us to determine and accurately adjust the system reading for μ_{H_2O}.

Real system performances: artifacts, noise, and resolution

One of the main issues we face when using volumetric radiology is that of artifacts, which are always present in all reconstructed data. With the term "artifact" we mean any structure present in the data displayed which is, however, not real. All non-ideal conditions of our system, with respect to theoretical considerations, will lead us to produce virtual structures during reconstruction.
It is essential to know the main ones, what they look like, and how they are caused, so as to better understand the information and not to make evaluation errors.

According to their characteristics, they can be divided into: streaking, shading, rings, and distortion (in CT systems with helical scanning).
According to how they are caused, they can be divided into four main groups: physics-based artifacts; patient-caused artifacts; those resulting from the specific reconstruction apparatus of the radiological scanning system; those of section reconstruction.
The most common artifacts of each group are described below.

Physics-based artifacts

They are caused by the physics of the processes involved in the data acquisition sequence.

Noise

This usually means any kind of distortion, with a random or regular distribution, that distorts the real information because it overlaps it.
In the case of volumetric radiology, the most remarkable negative result of noise is the reduced ability to distinguish areas with little contrast. These are areas in which the useful signal value varies only a little (therefore the overlapped noise is more determining).
In volumetric equipment there are two kinds of noise: quantum or that due to scattering.
The former is due to statistical functions which are always present in the flow of photons in the irradiation field. Since these fluctuations are more remarkable the smaller the irradiation field is, and the irradiation field is proportional to mA (and then to dose), this noise will be higher when the systems work at lower doses.
With the same dose, the noise will be higher as the voxel sizes decrease; they are proportional to the pixel sizes of the receptor. The larger the pixel sizes are, the more the variations due to fluctuation will tend to compensate for mutual cancellation. (If the surface is larger, it is more likely to have too little radiation fluctuation in a point and too much fluctuation in another; since the pixel value depends on the average of all values recorded in the whole surface, the opposite values will mutually cancel each other out).
Scattering (Compton scattering) is a way in which X-rays and matter interact. An incident X photon releases part of its energy to the external electron shell of an atom and changes it into an ion (an electron is extracted), modifying its energy and direction according to how the impact occurs. The emerging photon may have a very different direction with respect to that of the primary beam. Any photon changing its primary direction will, of course, increase the noise and interfere with the useful information (the entire reconstruction process occurs when the recorded radiation comes from a given direction—that of the primary beam). The size of this signal greatly depends on the patient's characteristics and on the beam collimation (less collimation means more scattering). Since, compared to CT, CBCT work with lower doses, beams with lower primary collimation, and no secondary collimation (on the beam emerging from the patient), it is unavoidable that they are noisier and have a lower image quality, meant as the contrast-to-noise ratio. Noise usually appears in images as "snow-effect" shading and it is more apparent in the areas with less contrast.

Beam hardening

Any X-ray source emits radiation not with a specific and sole value of frequency, but with different values throughout a given interval of frequencies. Since interactions with any substances change as the radiation frequency changes so that the attenuation rate is higher with lower frequencies (especially due to the photoelectric effect), it usually occurs that the energy distribution beam spectrum varies according to components at different frequencies, when radiation passes through the object (patient) so that the spectrum shows higher frequencies—the so-called "hard beams"—during crossing. This phenomenon is called "beam hardening". It causes different kinds of artifacts.

The so-called "cupping artifact" is visible as a sort of incorrect evaluation of the radiolucency of inner parts. They appear more radiolucent because the beam is more hardened here after passing through thicker structures. The term "cupping" is used because the hardened beam causes the attenuation of a homogeneous (which should be steady) sample as if it went down approaching the center and then went up again, forming a cup profile. In order to avoid this problem, we usually pre-treat the beam with special filters to prevent the beam from being hardened when crossing through the patient.
Another kind of artifact caused by this phenomenon is that of dark streaks. They usually appear when two very dense objects (for instance, two implantations) are present. This occurs because, during scanning, there are angles in which the area between these objects is aligned with both objects, causing the beam to be hardened much more and the resulting attenuation to be lower.

Partial volume
The reconstruction algorithms are based upon the fact that the raw data read the attenuation of the area to be reconstructed. This means that nothing can cause attenuation outside the FOV. This is true with CT systems because they are designed so that the patient is completely within the FOV, but this is almost never the case with CBCT systems. This problem increases when the FOV is smaller than the patient, because there is a larger area that causes attenuation when there is not supposed to be. Huge progress has been made in the algorithms used for CBCT systems in order to avoid this problem, with changes that take into account this residual attenuation. Nevertheless, this is so far the main reason why correct reading in terms of HU is not yet possible with CBCT machines.

Undersampling
If the sampling intervals of raw data acquisition are too large because of the system manufacturing features, with respect to the speed at which the structures scanned vary in the space (corners and profiles rapidly change, very small parts, etc.), the phenomenon known as "aliasing" occurs in the reconstructed data. It appears in the form of very thin streaks in images. Although this artifact is not so determining (the actual anatomical structures usually have no such sudden reactions), it may sometimes be necessary to have systems with proper sampling requirements in order to get useful images for diagnosis.

Photon starvation
Photon starvation appears in the form of deep streaks and is due to the fact that the beam absorption is sometimes so high that the noise in that direction is unbearable. This problem is intensified in reconstruction, causing the effect described above. It may be corrected by increasing the intensity of the beam, but in this way the patient will undergo a useless dose of radiation in the remaining positions. The use of automatic exposure setting mechanisms is therefore recommended. These problems usually occur with CT systems, which scan very different structures (shoulders, where the radiation will cross the entire width of the body, are larger and denser than the chest, which is the structure to be crossed frontally).

Artifacts caused by patients

These depend on each patient being examined.

Movement
The reconstruction algorithm is based upon raw data that are radiographic projections of the same object from different angles. It is clear that if the object moves from one imaging to another, the reconstruction will make even remarkable mistakes. This is one of the most important causes of poor quality in the results of a three-dimensional radiological exam.

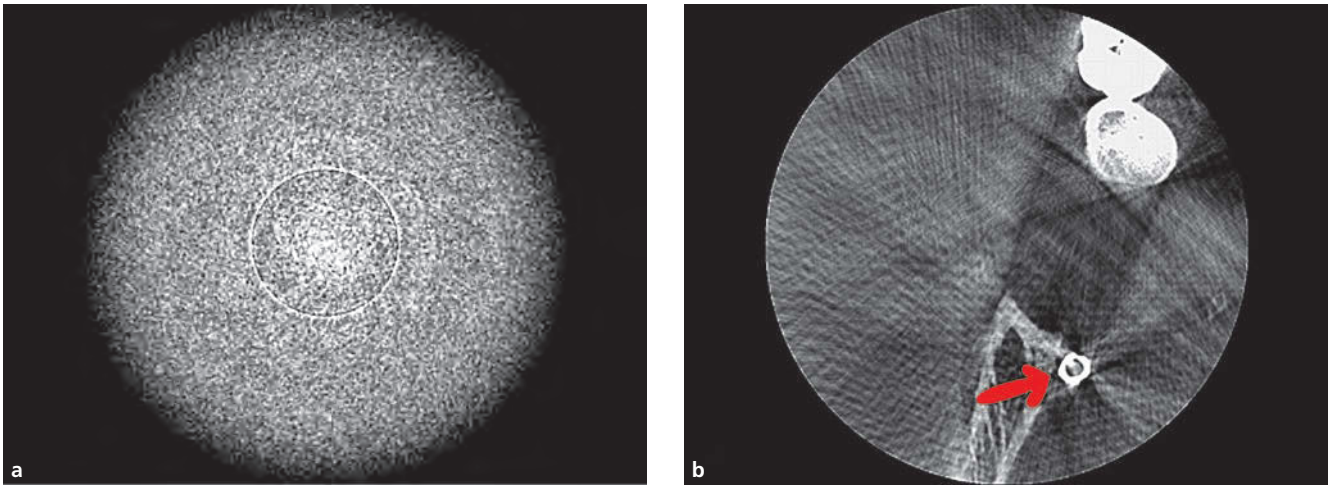

Fig. 2.20 Examples of artifacts: (**a**) ring with steady volume due to a faulty receptor; (**b**) aliasing and streaks due to the metal object indicated by the arrow, a spring.

Small movements will create out-of-focus images obtained by volumetric data, while large movements may cause double images or ghost images. The higher the system resolution is, the more sensitive to movement the quality will be. We must aim at achieving maximum patient stability and the shortest scanning time.

Hyperdensity

Problems and errors in the attenuation value reading made by all systems are caused not only by "beam hardening" but also by the presence of very dense objects which bring the radiation intensity to such low values that the receptor reaches its sensitivity threshold. This will cause light/dark streaks in the reconstructed images, and the quality will be negatively affected.

Since the beam in CBCT systems is conic, this problem will occur in other planes as well, as opposed to CT systems, where this artifact only affects the plane where the object lies.

Artifacts of radiological scanning systems

These are caused by defective volumetric radiological equipment. The most common one is the so-called "ring artifact" caused by faulty or poorly calibrated receptors or incorrect system geometry (Fig. 2.20).

In CBCT systems, for instance, different pixels for different beam positions will detect the attenuation value along the same path; if the pixels are not set in such a way as to have the same response, we will of course have a different reading, causing an error when reconstructing.

Artifacts from section reconstruction

These are caused by the sections calculated from volumetric data and depend on the kind of volumetric data available and on the calculation method used to extract the section images. For further details on the methods and displaying techniques of volumetric radiological data, please refer to the following section in this chapter, "Display".

Because of manufacturing reasons, these artifacts mainly affect CT systems (helical artifacts, "step" artifacts, "zebra" artifacts that are mainly in multiplanar reconstructions of CT and are due to interpolation and non-homogeneous helical scanning).

Simple and complex volumes

According to the optimization and justification principles, our natural aim is to obtain the most possible diagnostic information with the lowest possible dose. This is of course achieved using the smallest possible FOV and the proper operative resolution (the one required to detect the necessary details with high enough quality).
In dental applications, it is therefore generally recommended to use CBCT systems with small FOVs in the dentoalveolar area. In addition, they are cheaper and of medium size.
However, in particular cases these sizes are insufficient.
Most of the advanced CBCT systems now available can perform suitable operative protocols with the aid of special software programs which join together several scans and form groups of volumetric data. This operation is called "stitching" and requires simple scans with suitable overlapping areas.
The system should be equipped with a special operative configuration, performing several subsequent scans with automatic positioning so as to produce two or more simple volumes that are partially overlapped.
After reconstructing data, thanks to proper software programs, a number of points corresponding to the volumes to be joined together will be identified and data will be processed creating a new volume which is a sum of previous ones.
This would be very useful and in some cases absolutely necessary to be able to use other clinically valuable tools like guided surgery or quick prototyping. It should, however, be pointed out that the data usually obtained are not as accurate as those obtained with one single scan of the entire volume. The reasons are clear enough: there is more risk of motion (the scanning times are usually longer), of partial volumes (higher risks with smaller volumes), and of problems with alignment (both in the course of the volume reconstruction or when repositioning the patient after each scan).

Display

The analysis of volumetric radiological data is the most important step in medical diagnosis. It is, however, necessary to know the equipment to use and how this analysis should be performed. As in two-dimensional radiology, the visual test is the most employed in three-dimensional radiology, too.
In this case, it is required to know the proper strategies, principles, and uses, so as to avoid any evaluation mistakes or misunderstandings, or wasting time.

The use of volumetric radiological data

The three-dimensional radiological characterization is generated by a digital system and the information obtained is obviously read by this system and other digital instruments, like suitable software programs. The best-known visual device is the screen, on which the volumetric data will be displayed. How can we reproduce a three-dimensional image on a two-dimensional device like a screen? There are two possible solutions.
The first solution is the easiest, and it consists of a drawing which uses the rules of perspective in order to achieve a realistic three-dimensional image. This is usually known as three-dimensional "rendering".
Rendering software is able to filter data and exclude voxels with given density levels, and it can hide or highlight only the structures to be examined and (virtually) alter the transparency level of overlapped data. We can thus visualize the overlapping soft tissues and bone structures.

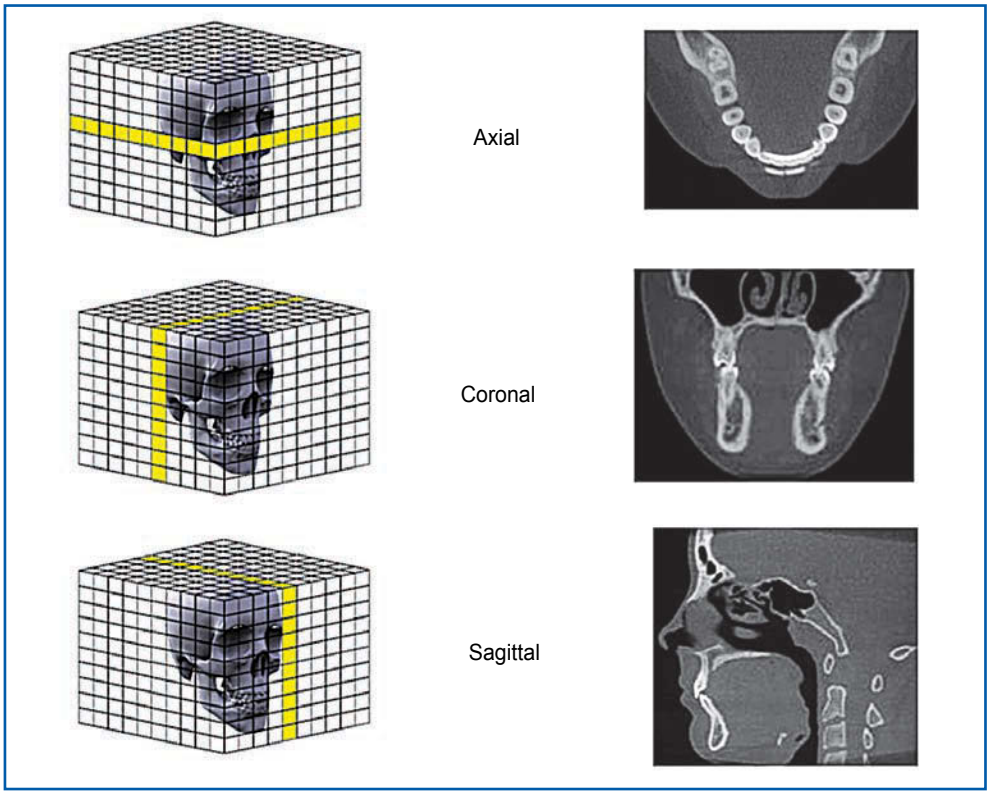

Fig. 2.21 Axial, coronal, and sagittal sections.

The most advanced software is also equipped with devices like implant simulators (they can simulate the implant insertion with photorealistic structures). Moreover, they allow us to carry out rotations in real time and change lighting, and are therefore very useful means of communication and motivation with patients.

As a matter of fact, the "rendering" technique is mainly useful for this, as it is not so effective in diagnosis. Parallel-section imaging should be chosen for diagnosis and all other clinical purposes.

When we talked about the digital volume as a voxel matrix and we compared it with bitmaps, two-dimensional digital images, we underlined that any voxel matrix can be seen as a structure of several flat layers as thick as one voxel, each of which is actually equal to a bitmap. When we examine each layer, the three-dimensional data obtained are the same as if we "cut" our patient "into slices", so as to have a slice as thick as that layer, and we took a two-dimensional radiograph. It is obvious that this could be displayed on our screen.

When any surface crosses a voxel matrix it will cover a given area. Even if it is curved, we can think about stretching it on a plane, translating the voxels concerned, exactly as we do with geographic maps. In this way, a group of voxels aligned according to a flat surface is obtained. They are equal to the bitmap of a two-dimensional image that we can produce on our screen. This operation of extracting the image of a direct section from the volume and according to a given flat surface is known as multiplanar reformatting (MPR).

Following the procedures of the CT systems used in hospitals, the reference orthogonal tern is conventionally fixed in the three-dimensional space, assuming the z-axis is the axis from the patient's feet to head, the x-axis is the one from right to left, and the y-axis is the forward-backward one.

All sections parallel to the xy plane (perpendicular to z) are conventionally considered axial; all sections parallel to the yz plane are considered sagittal, and all sections parallel to the xz plane are considered coronal (Fig. 2.21).

Rendering and planar sections: a new mode of communication and diagnosis

The two main systems of displaying data have been previously described, as well as their differences: rendering is useful for communicating with patients; cross-sectional MPR is preferable for diagnosis.
Actually, MPR can also be useful for communication. Since it is more difficult, it should be used to examine further the aspects and information obtained with rendering. Rendering, too, can be used for diagnosis purposes as an auxiliary method in clinical and surgical planning. We know that the volumetric data can be used in the production protocols of masks for guided surgery or quick prototypes, so as to shape bone fixtures in the pre-surgical phase to improve accuracy and reduce the real surgical times and the infection and failure risks. It is often necessary to have volumetric data without any information about soft tissues (when you need an accurate bone adjustment) or other details (air, etc.). This procedure is known as data segmentation; it allows us to keep only the voxel data corresponding to given values of tissue density (radiological density).
Even though several software instruments permit us to process data in such a way as to execute data segmentation automatically, this is often not effective, especially when there is a lot of noise. In this case (with low-dose CBCT systems) segmentation should be performed in semi-automatic or manual mode; therefore a combined use of rendering and MPR sections would be very helpful to better understand the three-dimensional local anatomical development and whether some voxels are included.
A helpful diagnostic application of rendering is its use as a navigator to position the MPR planes. As a matter of fact, it is not easy to understand the actual positions we are examining. Rendering can display them in perspective and we can easily recognize them. This is why volumetric radiology software is now equipped more and more with the optional display of MPR planes and surfaces inside the rendering.

MPR: general considerations and dental applications

When we first analyze volumetric radiological data by means of MPR sections, we are puzzled because we see images which are different from those of conventional two-dimensional radiology.
First of all, we must understand where the section surface is oriented and what it looks like. We will then be sure that we are examining exactly what we want to and in a proper way. One of the most interesting advantages of MPR analysis of volumetric data with isotropic voxels (cubic voxels, with the same size in all directions of the Cartesian system) is to perform accurate linear and angle measurements of the anatomical structures in the sections extracted. All modern CBCT systems work with isotropic voxels and enable dentists to measure an implant location, the bone thickness, as well as the distance from the mandibular nerve, with no distortions and in full scale.
We will get accurate results provided that we use the correct evaluation section. In the case reported in Figure 2.22, the correct section is that where the bone thickness is the smallest, the one obtained in the plane perpendicular to the arch directrix and tilted according to the direction of the main axis of the implant to be positioned, usually that along the directrix on which the roots and crown of the original tooth develop.
All MPR software is usually able to simultaneously display the axial, coronal, and sagittal sections passing through a point set by the user. This position may often be easily and interactively modified in real time, for a quick and orderly scrolling of volumes of adjacent sections

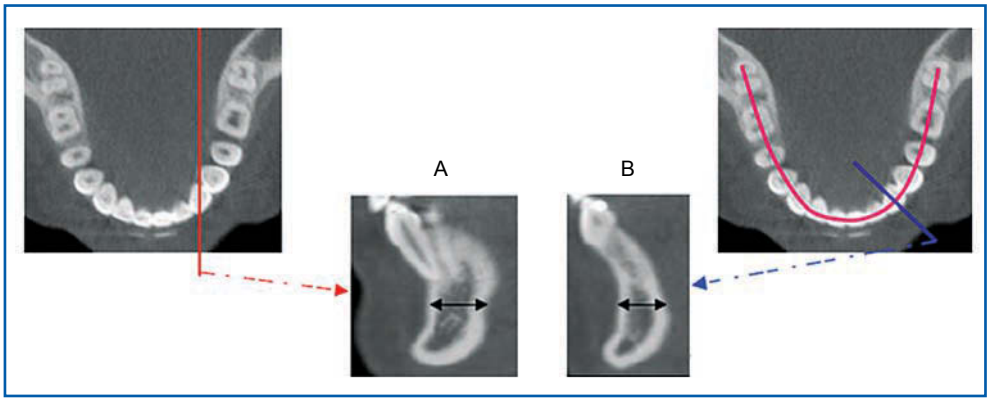

Fig. 2.22 Incorrect (A) and correct (B) selection of the transversal section to evaluate the bone thickness in an implant location.

in the directions perpendicular to the three sections. This scrolling can help to understand the anatomical structures better than with fixed images, especially when there is noise.

In dentistry, one of the most used MPR reconstructions is the panoramic one. The user chooses the most suitable axial section for his purpose. Then he identifies a curve on that plane, through points automatically joined together by the software. This curve usually covers the median area of the patient's arch or portion. The software will build a virtual surface perpendicular to the axial planes and as bent as the curve that identifies the group of intersecting voxels. If we develop this section on a plane, the transversal section too will be displayed perpendicular to the axial plane and the perpendicular projection. If we tilt this section with respect to the axial plane and keep it perpendicular to the arch, we will get the correct section to measure the smallest thickness of the bone and the distance as seen in the above example of the implant (Fig. 2.22).

The generation of multiple MPR sections perpendicular to a direction and at the same distance is very useful. In the case of implant location, we can examine how the bone structures evolve both in the whole area concerned and in the surrounding areas.

MPR sections are also used with software tools that are able to draw graphic elements on them in order to highlight the important structures (i.e. the alveolar nerve) or to simulate prosthetic elements (i.e. implants) that can be displayed by rendering. In the case of implant simulations, we usually work with a panoramic MPR to produce the correct transversal section of the area concerned, where the simulation graphic system is positioned in 1:1 scale.

The ATM is also useful in dentistry, because these sections are aimed at studying diseases of the temporomandibular joint. This is usually made of a group of sections of each condyle area. Every group is made up of a group of parallel sections in the forward-backward direction and of a group of parallel sections perpendicular to those of the previous one.

It could be better to bin voxels, provided that accuracy is respected and the function is available. Binning will reduce noise and improve the image quality. Binning is a sort of aggregating of the starting voxels into larger voxels with an average value of the original ones. When carrying out this operation, noise, which is a random process, will be reduced. In some cases, this procedure can only be done in the direction perpendicular to a section. This will result in an image with the same resolution, but its points will correspond to a value obtained by the average values of the same points of the adjacent parallel sections.

How to choose a suitable system for the practitioner's needs

Clinical requirements, radiation risk, image definition

Emanuele Ambu

Criteria for choosing an "ideal system" and FOV for any clinical practice

Manufacturers and dealers are continuously offering clinicians new CBCT systems, emphasizing the qualities of their products and criticizing those of their competitors.
This can be very confusing for the clinician, who often has only a faint idea about the kind of system he really needs. This technology is likely to soon become the gold standard for diagnosis in our field. We have, however, to understand first which CBCT systems are useful in our daily practice, and then we must choose the most suitable system from a large number of machines available on the market.
In my opinion, the following questions should be considered:

1. What clinical job do I do?
2. How many volumes do I have to perform for any treatment?
   What is the maximum radiation exposure to patients?
3. What level of image definition do I need for diagnosis?

These criteria will be discussed further in the following sections.

Choosing a system based on our daily practice

What job do you do? Are you a general practitioner or a specialist? What are you specialized in? If you are a specialist in endodontics, you will probably need a system that is suitable for examining a small area, reducing both the irradiation area and the patient's exposure.
The smaller the FOV, the smaller the voxel; the smaller the voxel, the higher the image resolution. If we use a medium FOV system, the smallest size of voxel will be 200 µm, which is the minimum size necessary to detect disruption in the periodontal ligament space (Scarfe et al. 2009).
However, we often need voxels which are smaller than 200 µm to detect smaller areas or ancillary or calcified root canals and vertical root fractures.
The only contraindication of small FOV systems in endodontics could be a radiolucency larger than the examined area. To this end, the stitching technique has recently been introduced; stitching together three "small FOV" areas, we can have almost a full arch view.
According to the Joint Position Statement of the American Association of Endodontics and the American Academy of Oral and Maxillofacial Radiology (Use of Cone Beam Tomography in Endodontics), limited-volume CBCT should be used rather than large-volume CBCT in most endodontic applications, for the following reasons:

1. Higher spatial resolution to achieve more accurate endodontic results.
2. Higher spatial resolution to achieve a satisfactory signal-to-noise ratio for our purpose.
3. Lower radiation exposure to the patient.
4. Time savings due to interpreting smaller volumes.

Fig. 3.1 CS 9000 3D device.

If you are an oral surgeon, you will probably require a medium FOV or a large FOV system. As already mentioned, the introduction of stitching has made it possible to have almost the same images as those obtained with a medium FOV system, using a small FOV system. In this case, the minimum voxel size will be 200 µm and the irradiation rate will be particularly high, although lower than that of medium FOV systems. Nevertheless, the volume of data collected, though very accurate, is often too small to be properly read by the guided technology, especially when examining the full arch.

As a result, the characteristics of our daily practice will be binding when choosing a suitable system: if we need a high-definition system, we will choose a focused FOV system, like the CS 9000 3D (Fig. 3.1) that provides very thin "slices" with an irradiation rate that is sometimes the same as that of intra-oral X-rays. This feature allows us to use the system not only for diagnosis but also for subsequent checkups (as required by endodontic treatments). A medium FOV system with a minimum voxel size of 200 µm may lose too much information and give patients too much radiation exposure. On the contrary, this would become acceptable when planning a guided implant or oral surgery. In this case, we have to examine a larger area only one time. The exposure rate to patients would be much lower than that supplied by a CT exam.

The ALARA principle and choosing a system based on the patient's radiation dose

When choosing the most suitable system for our purposes, we must take other factors into account, like the patient's radiation exposure.

The larger the FOV, the higher the irradiation rate that the patient will be exposed to, whereas the definition level will decrease as the minimum voxel size increases.

Those who choose a medium FOV system should take into account the radiation exposure and choose the one with as low irradiation rate as possible and image definition which is high enough to offer a correct visualization (Fig. 3.2).

This falls within the legal duties of optimization, summarized with the acronym ALARA (as low as reasonably achievable). This means that the radiation exposures resulting from the

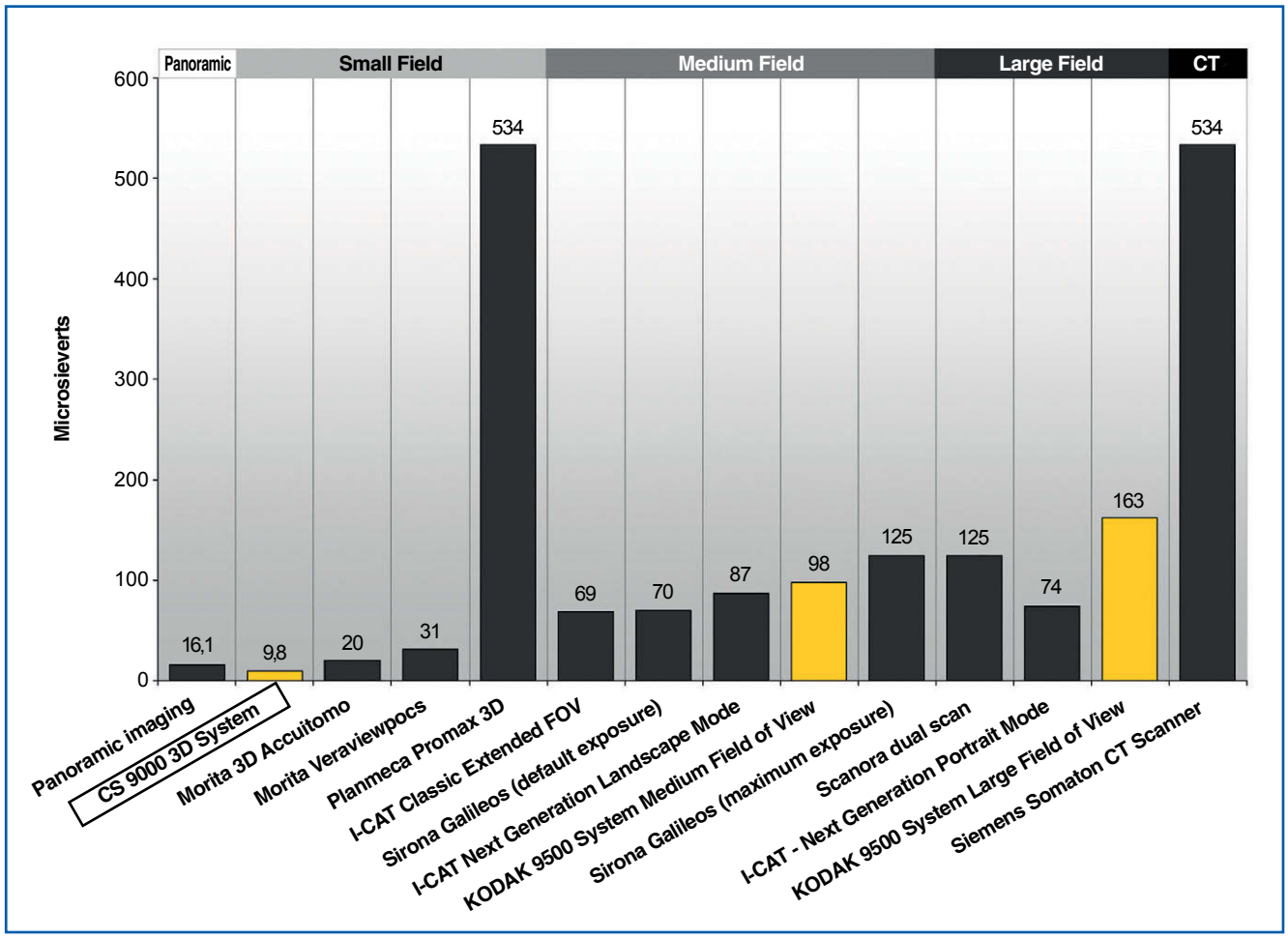

Fig. 3.2 Comparison of effective dose of some small, medium, and large FOV devices (source: ICRP 2007).

exam must be reduced to the lowest level possible, considering the cost of such a reduction in dose. It is possible to look at specific websites, like conebeam.com, to find a good comparison system and download a comparison chart of various models with the features declared by manufacturers.

With large FOV systems, it should be taken into account that the area scanned by these systems is not only that concerned in dental diagnosis; therefore information which is potentially important to patients may not be detected in an exam performed by a dentist who has had no specific training about extra-oral areas in his education. This failure to inform the patient could lead to medical legal disputes.

We will examine further the laws governing the use of 3D radiology in dentistry.

Legislative aspects

In Italy, the use of radiological systems is regulated by Act 187/2000, which states that the use of these systems by dentists is allowed in performing their own ancillary radiodiagnostic activities or, as stated by Act 2.1.b, in "activities of direct aid to the specialist medical surgeon or dentist to perform specific interventions of their discipline, provided that they are performed in concomitance with, in completion of the specialized procedure and that they cannot be postponed".

The dentist, after receiving his Ph.D., should take periodical refresher courses.

The specific use of CBCT systems has been further explained by the Department of Health with a notice, published in the Gazzetta Ufficiale no. 124 of 29 May 2010, stating once again that dentists are allowed to use CBCT systems as indicated by Act 187/2000, making it compulsory for dentists to give their patients a (digital) copy of their volumetric exams and to have their written consent prior to the exam.
In my opinion, this law is defective, and I am eagerly awaiting a clear outline of the law to be enacted by the European Union.
The EU, through its agency Euratom, had charged the SEDENTEXCT Consortium, through its Guideline Development Plan, to come up with evidence-based guidelines dealing with justification, optimization, and referral criteria as applied to CBCT. At the end of the Plan in 2011, guidelines were introduced, developed together with the European Academy of Dental and Maxillofacial Radiology, which became its own guidelines in 2009 (Horner et al. 2009).
When examining these guidelines, it is possible to find the proposed instructions.
Guideline no. 18 states that dentists using such equipment are required to attend "a period of additional theoretical and practical training that has been validated by an academic institution (University or equivalent)".
Guideline no. 19 quotes verbatim: "For dento-alveolar CBCT images of the teeth, their supporting structures, the mandible and the maxilla up to the floor of the nose (e.g. 8 cm x 8 cm or smaller fields of view) clinical evaluation (*'radiological report'*) should be made by a specially trained DMF Radiologist or, where this is impracticable, by an adequately trained general dental practitioner".
Under these guidelines, the use of radiological systems exclusively in the dental sector is limited to dental practitioners with a specialization in DMF radiology or to otherwise suitably trained dental practitioners, as stated by guideline no. 18.
According to guideline no. 20, "For non-dento-alveolar small fields of view (e.g. temporal bone) and all craniofacial CBCT images (fields of view extending beyond the teeth, their supporting structures, the mandible, including the TMJ, and the maxilla up to the floor of the nose), clinical evaluation (*'radiological report'*) should be made by a specially trained DMF Radiologist or by a Clinical Radiologist (Medical Radiologist)", and it is excluded that dental practitioners can use larger fields of view than the area of dental concern. Larger areas should be examined by either dental or medical radiologists.

Conclusion

We do not know either when an EU law will be enacted or to what extent it will take into account the guidelines as stated by SEDENTEXCT. However, it is clear that there is a sharp disparity between dental practitioners and medical ones. Dental practitioners are not allowed to create diagnostic centers for dental radiology, in spite of a twenty-year separation of education and career paths.
A lot of EU member countries have not yet started specialization courses in dental and maxillofacial radiology; however, dental practitioners who have graduated in those countries are not prevented from receiving their Ph.D. abroad.
At the end of this chapter, we can only hope that this problem will be solved, not by preventing "medical" practitioners from performing these exams, but by allowing practitioners who are specialized in the diagnosis and treatment of oral pathologies (who are suitably trained with post-graduate courses) to use these powerful new diagnostic instruments, even if it means restricting their practice to diagnostics.

Radiological anatomy of the oral cavity and adjacent areas

Roberto Ghiretti

The use of 3D devices allows us to examine anatomical structures without any of the limitations of 2D radiology. These limitations are often due to the superimpression of anatomical structures or the presence of areas with a higher density. Today, we have the fantastic new possibility of examining an anatomical structure from all directions, using CBCT devices that guarantee images with high definition and low radiation doses to the patient. Still, the passage from 2D to 3D can be very difficult for clinicians, as they are often used to reading only 2D plane images, like conventional X-rays, OPT, and teleradiography. Therefore, we have to learn to identify anatomical structures and related pathologies in three new, different planes belonging to 3D, or "orthogonal", radiology: coronal, sagittal, and axial, respectively (Fig. 4.1). The following images can help clinicians become familiar with these planes. We will compare 2D images (in gray scale) with the 3D rendering processed ones. We have avoided labelling all the anatomical structures, limiting ourselves to those which can help the observer to locate anatomical areas. All of the following images have been captured using a large FOV device (Kodak 9500) and processed using CS 3D imaging software (Carestream) with a PC, or OsiriX 64-bit with an Apple Mac Pro.

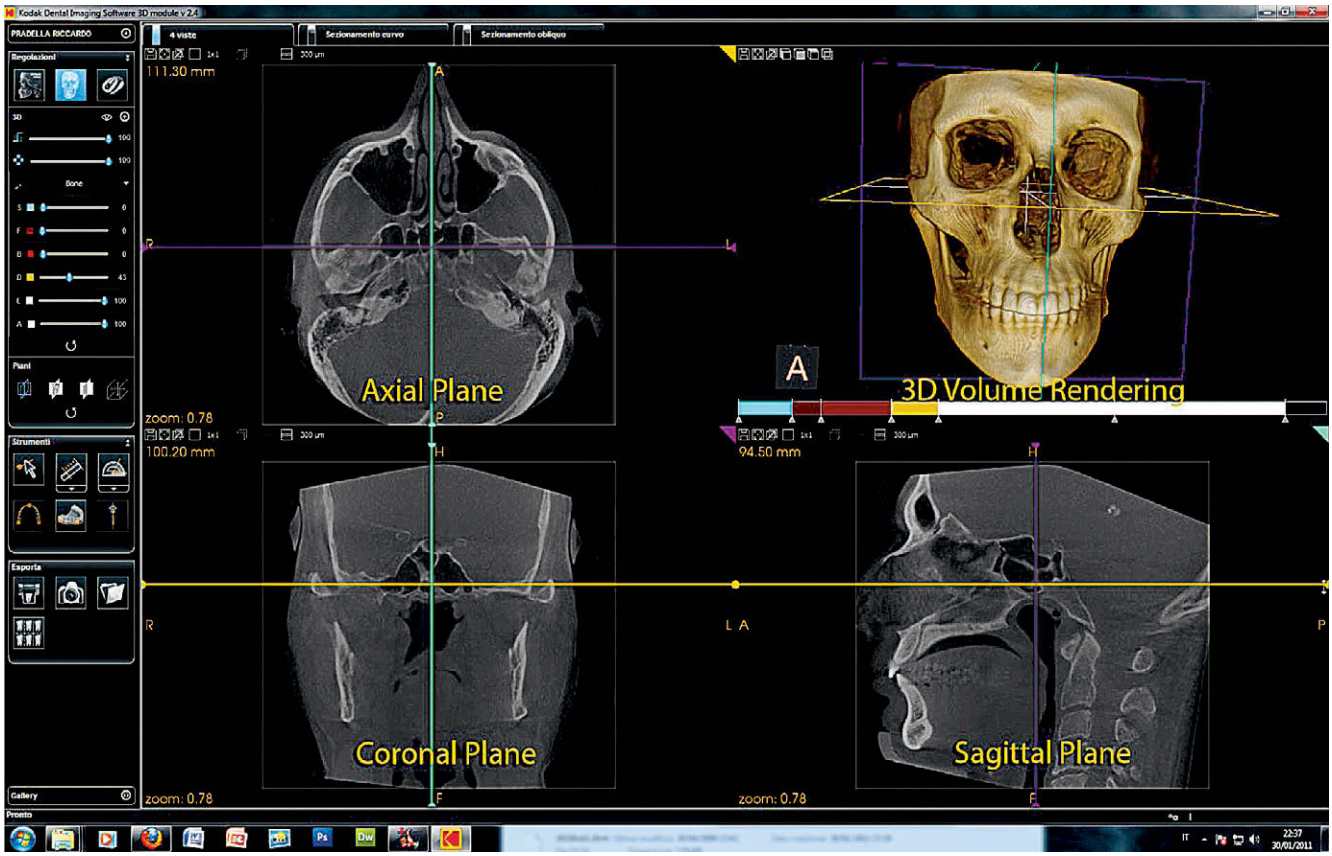

Fig. 4.1 The main screen developed by CS 3D imaging, which shows the three orthogonal planes and the 3D rendering. The 3D reconstruction and the 3D rendering, as well as the colored "cutting" lines (yellow for axial, green for sagittal, and purple for coronal, respectively) help observers locate the exact space-position of the examined area. We can scroll any plane and put our "colored line" on the structures that we want to examine.

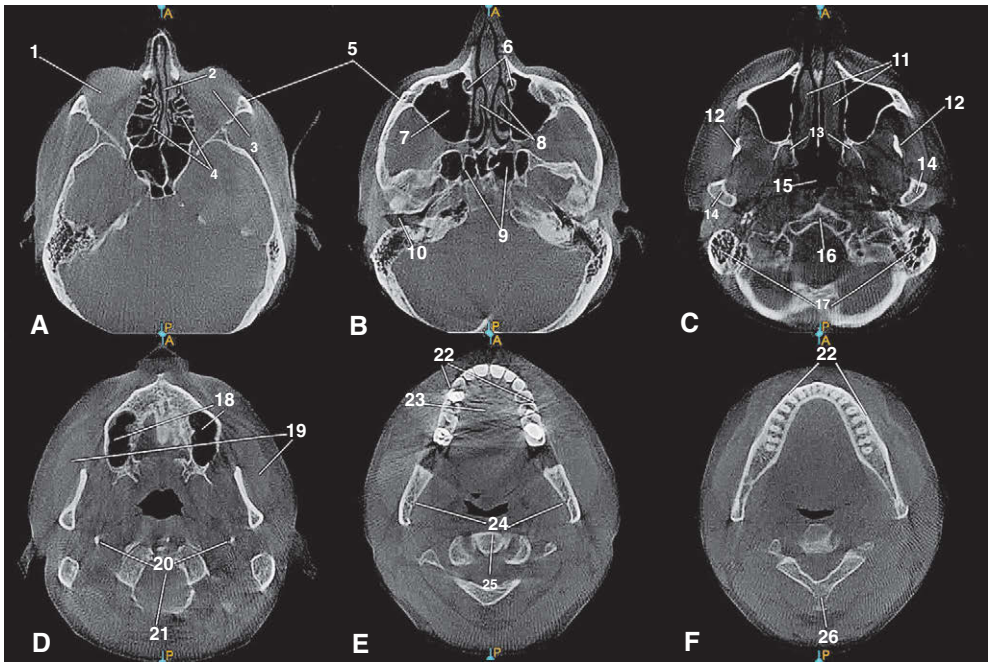

Fig. 4.2 1. Eyeball; 2. Nasal septum; 3. Eyeball; 4. Ethmoid cells; 5. Zygoma; 6. Nasolacrimal duct; 7. Maxillary sinus; 8. Middle nasal concha; 9. External acoustic meatus; 11. Inferior nasal concha; 12. Coronoid process; 13. Pterygoid process; 14. Mandibular condyle; 15. Fossa of Rosenmuller; 16. Anterior arch of atlas; 17. Mastoid cells; 18. Inferior portion of maxillary sinus; 19. Masseter muscle; 20. Styloid process; 21. Foramen magnum; 22. Maxillary arch; 23. Hard palate; 24. Mandibular foramina; 25. Dens Axis; 26. Spinous process of C2.

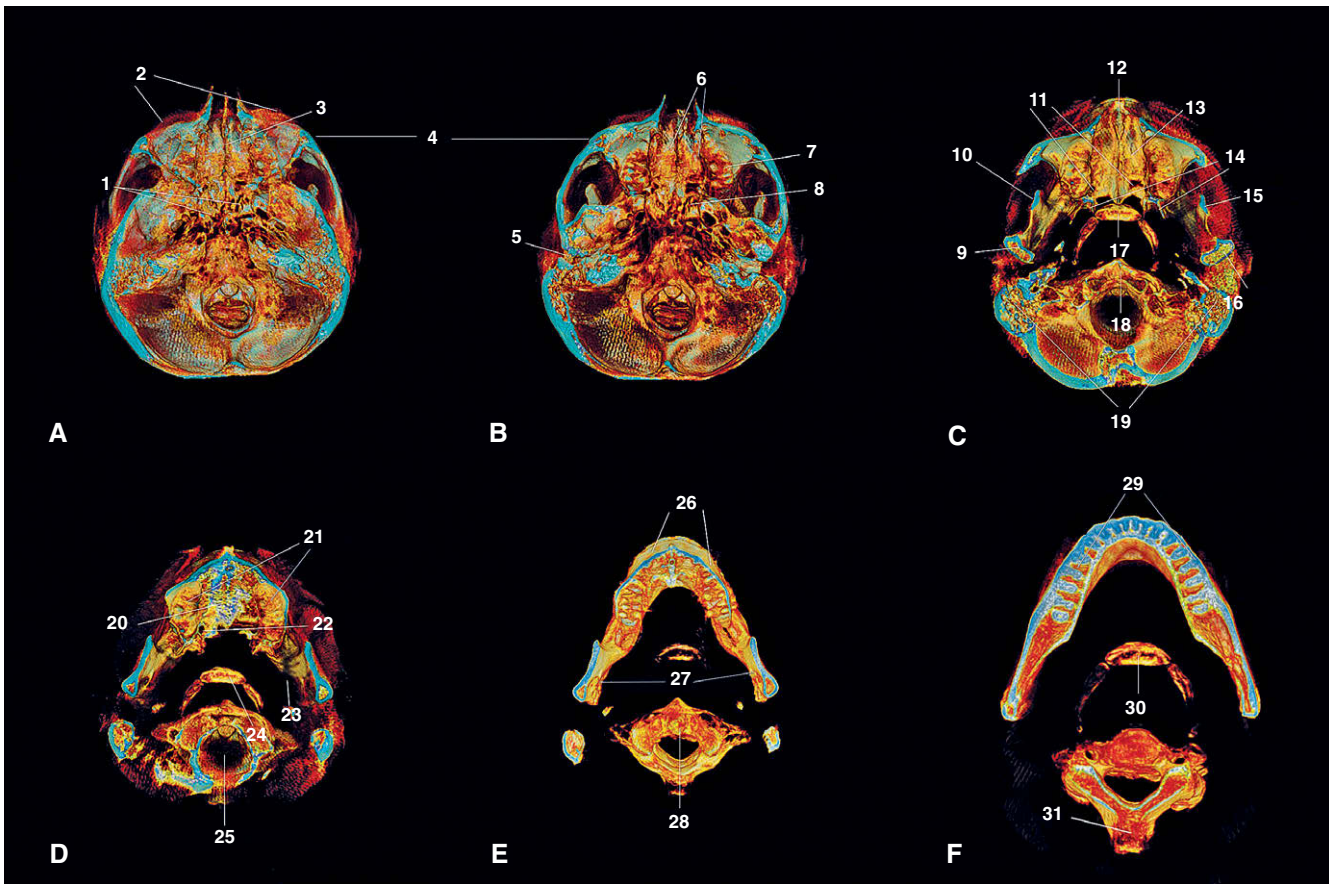

Fig. 4.3 1. Ethmoid cells; 2. Eyeball; 3. Nasal septum; 4. Zygoma; 5. External acoustic meatus; 6. Middle nasal concha; 7. Maxillary sinus; 8. Sphenoid cells; 9. Mandibular condyle; 10. Coronoid process; 11. Foramen palatinum magnum; 12. Incisive foramen; 13. Hard palate; 14. Pterygoid process; 15. Coronoid process; 16. Mandibular condyle; 17. Hyoid bone; 18. Anterior arch of atlas; 19. Mastoid cells; 20. Hard palate; 21. Inferior portion of maxillary sinus; 22. Foramen palatinum magnum; 23. Styloid process; 24. Hyoid bone; 25. Foramen magnum; 26. Maxillary arch; 27. Mandibular foramina; 28. Dens Axis; 29. Mandibular arch; 30. Hyoid bone; 31. Spinous process of C2.

Axial plane

In figure 4.2 we can observe some anatomical structures that we can identify in several axial planes from the orbital cavity to the body of the mandible. Looking at the same axial sections from figure 4.2 processed using 3D rendering software (Fig. 4.3), we can obtain useful information for a correct analysis of the anatomical structures examined with the CBCT.

Sagittal plane

In figure 4.4 we can observe the different structures, starting from the median section (A), passing to a paramedian one (B), and, lastly, a section passing through the TMJ (C).
In figure 4.5 the 3D rendering of two different sections, the median and a more superficial one, allows us to locate anatomical structures that are very important in our analysis.

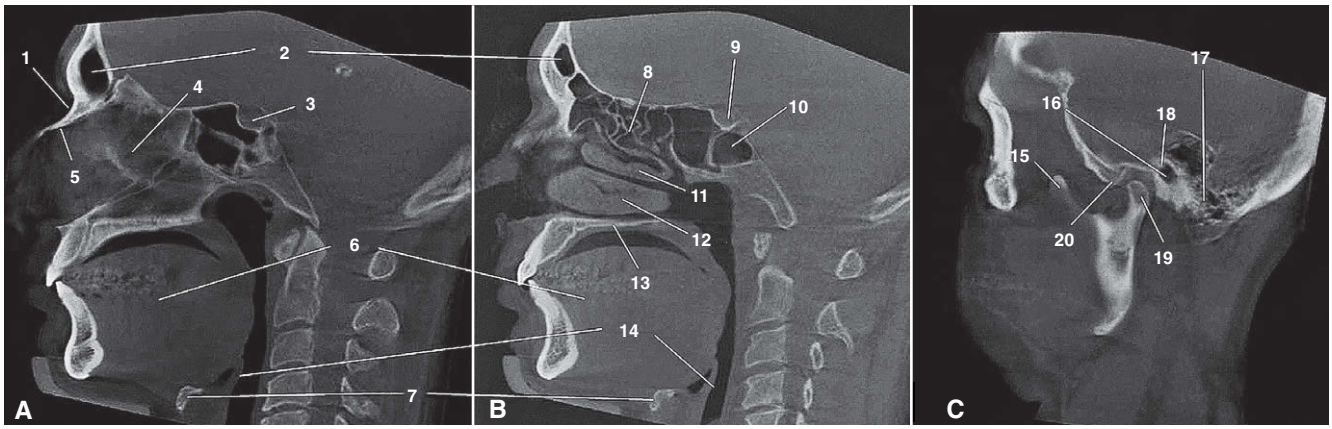

Fig. 4.4 1. Nasion; 2. Frontal sinus; 3. Sella turcica; 4. Nasal septum; 5. Nasal bone; 6. Tongue; 7. Hyoid bone; 8. Ethmoid cells; 9. Sella turcica; 10. Sphenoidal cells; 11. Middle nasal concha; 12. Inferior nasal concha; 13. Hard palate; 14. Epiglottis; 15. Coronoid process; 16. Internal acoustic meatus; 17. Mastoid cells; 18. Stapes; 19. Mandibular condyle; 20. Eminence of temporal bone.

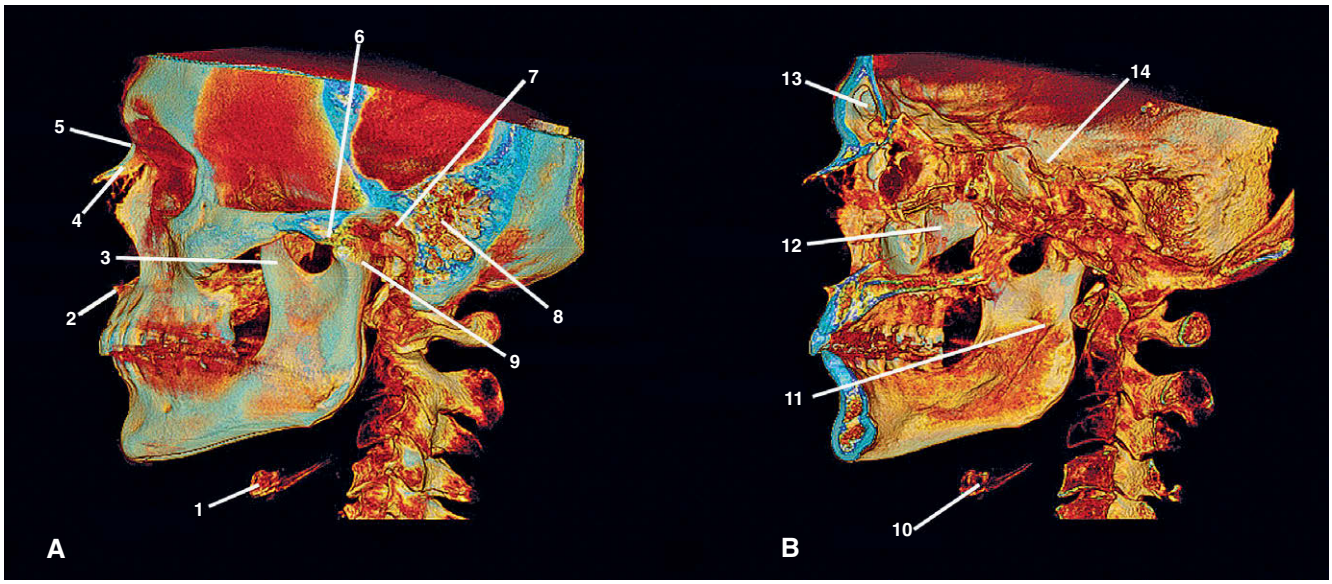

Fig. 4.5 1. Hyoid bone; 2. Anterior nasal spine; 3. Coronoid process; 4. Nasal bone; 5. Nasion; 6. Eminence of temporal bone; 7. External acoustic meatus; 8. Mastoid cells; 9. Mandibular condyle; 10. Hyoid bone; 11. Mandibular foramen; 12. Nasal septum; 13. Frontal sinus; 14. Sella turcica.

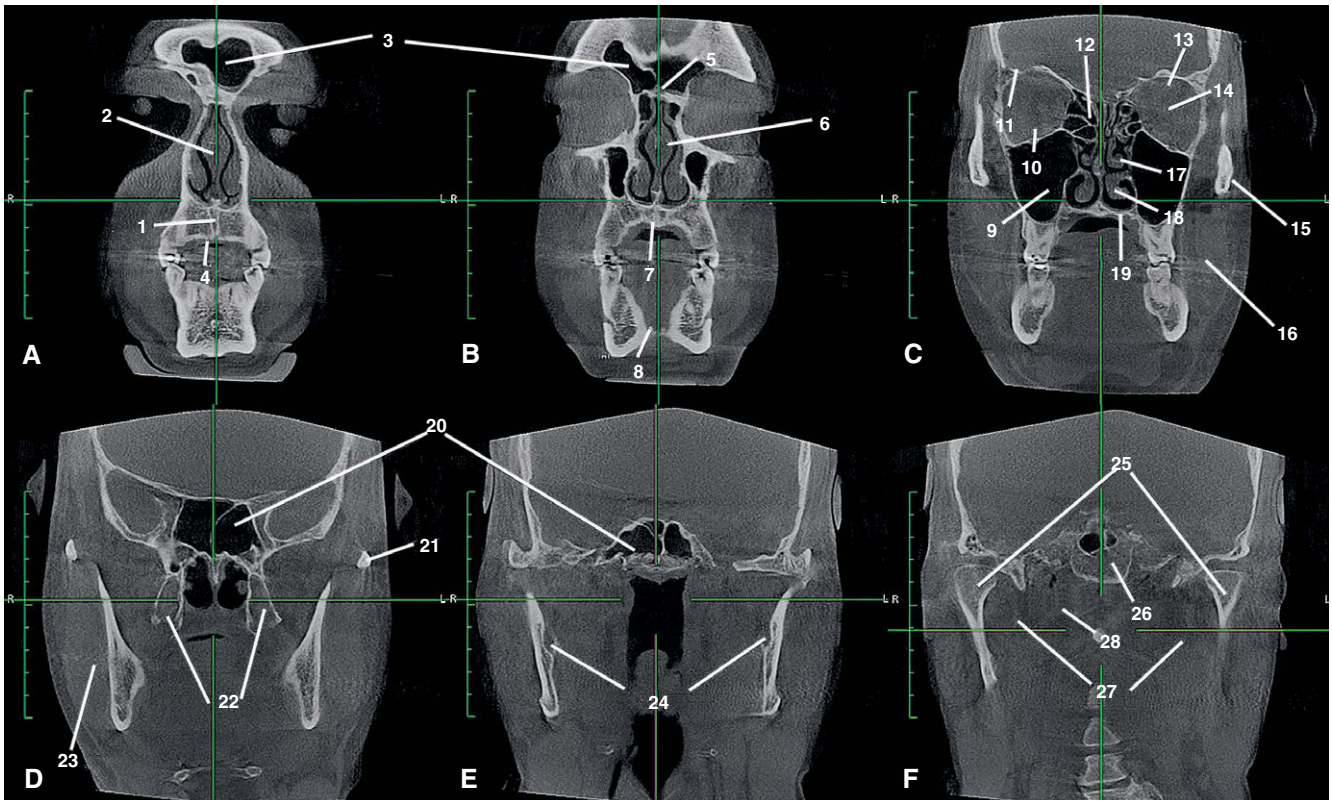

Fig. 4.6 1. Incisive foramen; 2. Nasal septum; 3. Frontal sinus; 4. Hard palate; 5. Crista galli; 6. Nasal septum; 7. Hard palate; 8. Genial tubercles; 9. Maxillary sinus; 10. Inferior rectus muscle; 11. Lateral rectus muscle; 12. Ethmoid cells; 13. Superior rectus muscle; 14. Optic nerve; 15. Zygoma; 16. Masseter muscle; 17. Middle nasal concha; 18. Inferior nasal concha; 19. Hard palate; 20. Sphenoidal cells; 21. Zygoma; 22. Pterygoid process; 23. Masseter muscle; 24. Mandibular foramina; 25. Mandibular condyle; 26. Base of sphenoid bone; 27. Styloid process; 28. Anterior arch of C1.

Coronal plane

The coronal sections, going in an anteroposterior direction, gradually show a lot of the structure of the odontostomatological area (Fig. 4.6).
These 3D images (Fig. 4.7) show the high quality and definition levels that this kind of exam can achieve. The anatomical structures are immediately identifiable, allowing a complete, thorough, and reliable diagnosis.

Upper respiratory tract exam

Another important use of volumetric radiology is the examination of the upper respiratory tract, which is very useful in orthodontics and in the diagnosis of sleep apnea syndrome. Recently, this syndrome has attracted the attention of dentists because of some intra-oral devices which work on the tongue position (TRD, tongue retaining device) or on the mandibular position (MAD, mandibular advancement device) to reduce the more aggravating symptoms of this disorder.
This 3D image (Fig. 4.8) of the midsagittal, or median, plane shows the air spaces (in light blue) from the frontal sinuses to the epiglottis.

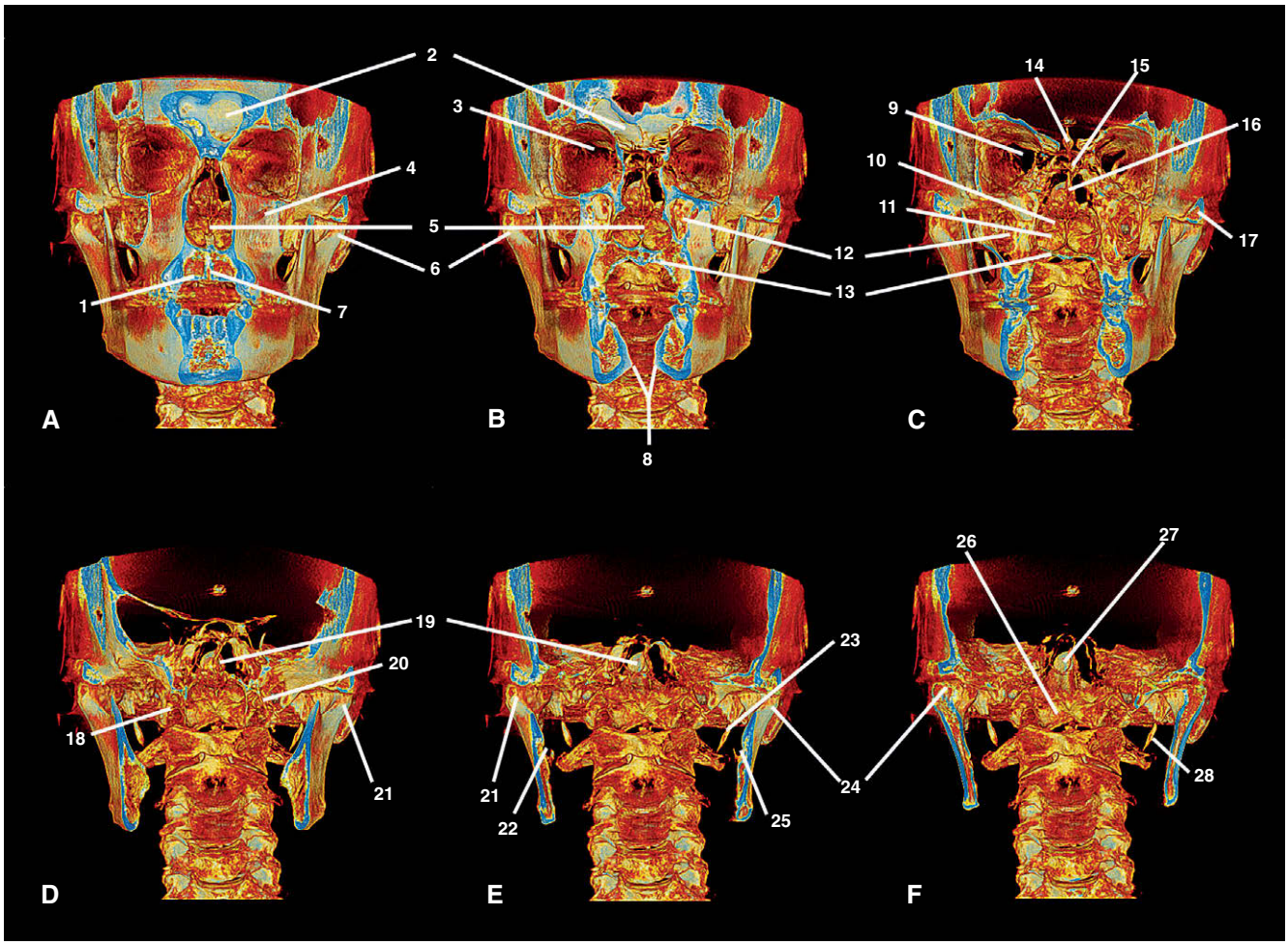

Fig. 4.7 1. Hard palate; 2. Frontal sinus; 3. Superior orbital fissure; 4. Infraorbitarium foramen; 5. Nasal septum; 6. Mandibular condyle; 7. Incisive foramen; 8. Genial tubercles; 9. Superior orbital fissure; 10. Middle nasal concha; 11. Inferior nasal concha; 12. Maxillary sinus; 13. Hard palate; 14. Crista galli; 15. Ethmoid cells; 16. Nasal septum; 17. Zygoma; 18. Pterygoid process; 19. Dens axis; 20. Pterygoid process; 21. Mandibular condyle; 22. Mandibular foramina; 23. Styloid process; 24. Mandibular condyle; 25. Mandibular foramina; 26. Base of sphenoid bone; 27. Dens axis; 28. Styloid process.

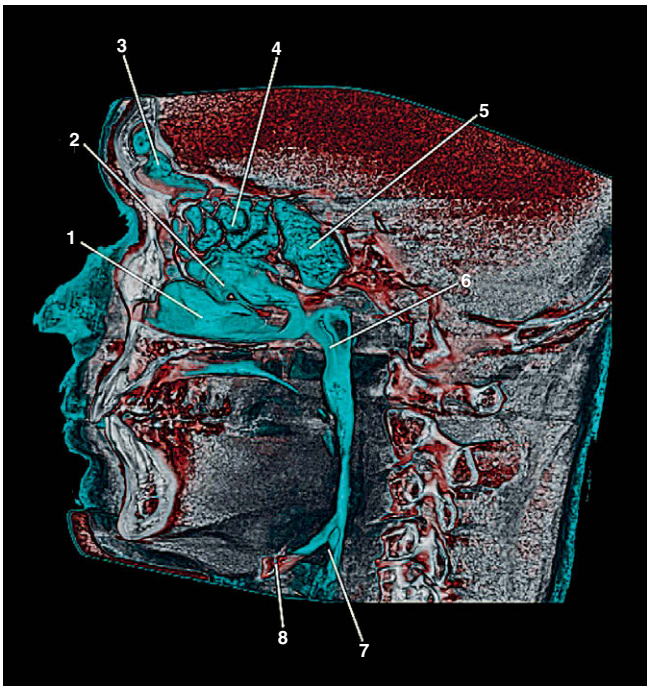

Fig. 4.8 1. Inferior nasal concha; 2. Middle nasal concha; 3. Frontal sinus; 4. Ethmoid cells; 5. Sphenoidal cells; 6. Pharyngeal airways; 7. Epiglottis; 8. Hyoid bone.

When examing children, the area of the pharyngeal recess must be carefully examined for the presence of adenoids that, causing difficulty in breathing, can lead to dentoalveolar malpositions.

The analysis of coronal planes (Fig. 4.9) can help clinicians in morphological exams of choanae and paranasal sinuses. Some diseases of these areas can have an important influence on dental pathologies.

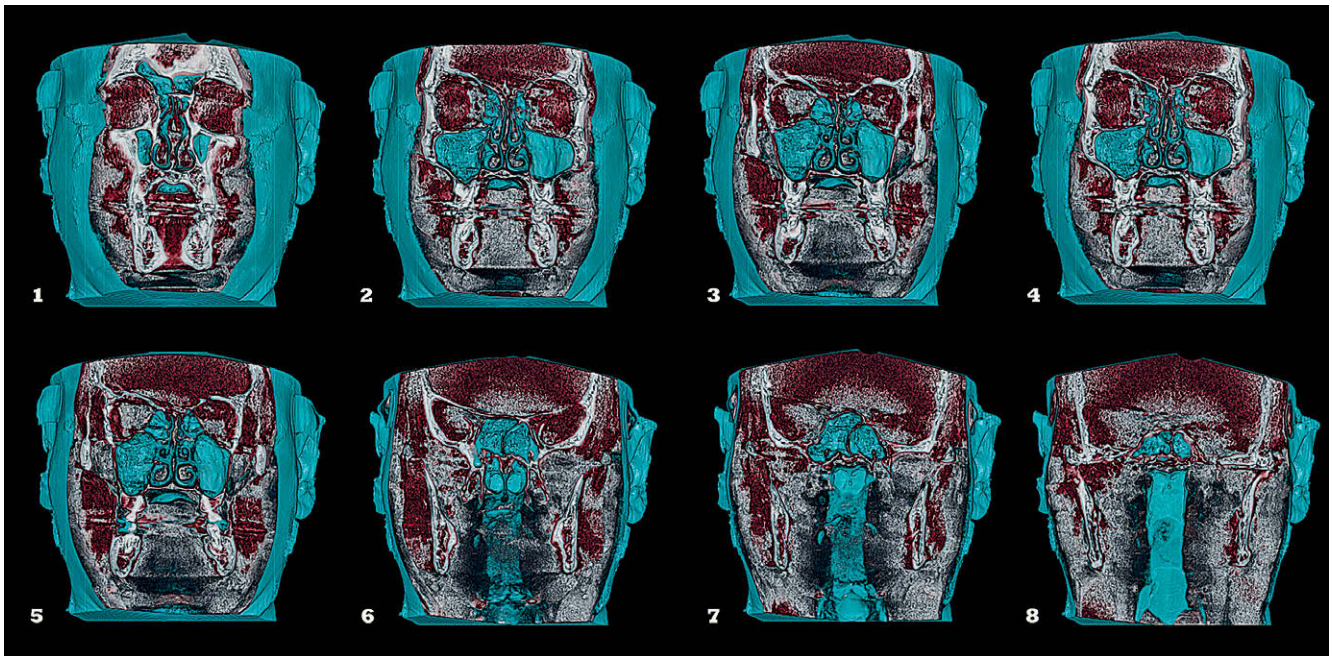

Fig. 4.9 Analysis of coronal planes.

Three-dimensional rendering of models using data from CBCT

Roberto Ghiretti

From virtual to actual models

Three-dimensional rendering is the 3D visualization of computer-generated objects using special software. It was introduced in the 1970s, and since then it has commonly been employed in video editing, video games, simulators, and special effects in film and television, as well as in architecture to get a realistic model of projects (Fig. 5.1). With the introduction of computed tomography (CT), it soon began to be used in the medical sector to obtain a three-dimensional visualization of tissues, thanks to computed tomography, magnetic resonance imaging (MRI), and positron emission tomography (PET).

The image obtained is called "pseudo-realistic", because it shows tissues, like skin, muscles, and bones, with colors chosen by the operator so as to highlight and contrast them.

These various radiographic systems (CT, MRI, PET) can examine a given sector of the human body, creating sections with different thicknesses. Subsequently, these sections are

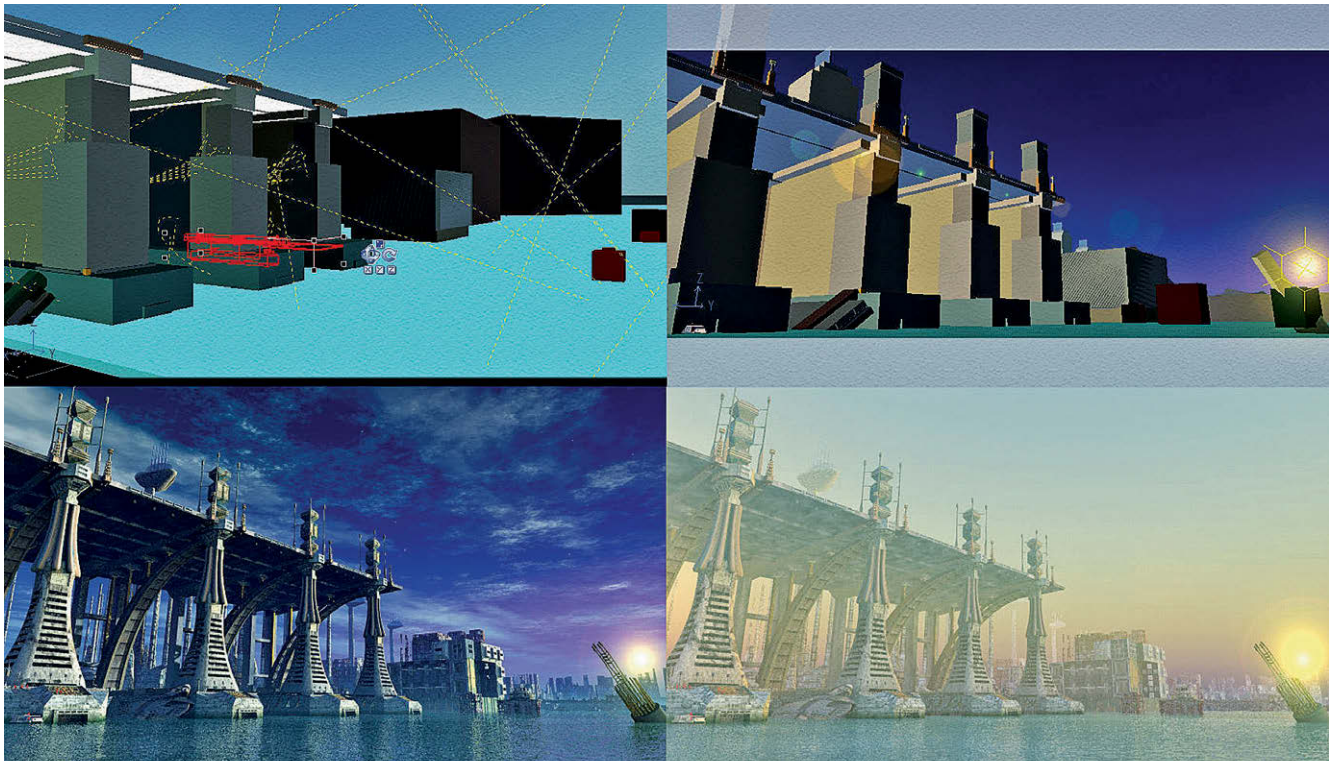

Fig. 5.1 This picture clearly demonstrates how modern three-dimensional rendering technologies can process very sophisticated images, starting from a computer-generated three-dimensional model, even creating very different environments, simulating various weather conditions based on specific requirements (e-on software Vue Infinite 5).

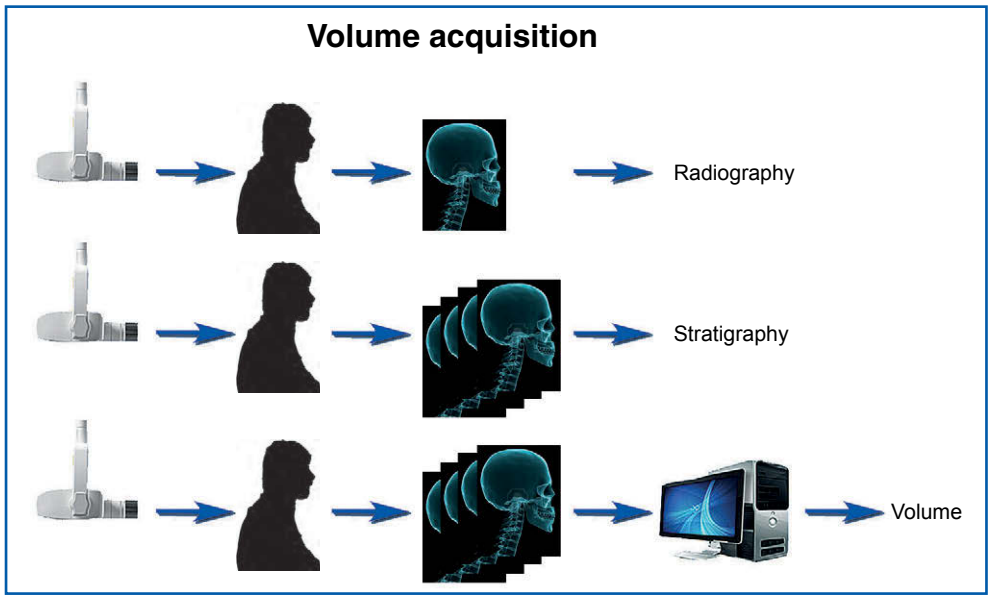

Fig. 5.2 In standard X-rays, the ray beam hits different tissues. According to their specific density, these tissues will either be passed through by the X-rays or they will not, until they strike a radiographic plate on which the final image is reproduced. With stratigraphy, with particular artifacts, we are able to investigate various planes of the organ using a number of plates. In computed tomography, similarly to stratigraphy, we can examine various layers of a volume of our body, obtaining a number of data that will be stored and then processed to reproduce either two-dimensional images on the three Cartesian axes or three-dimensional images with 3D rendering.

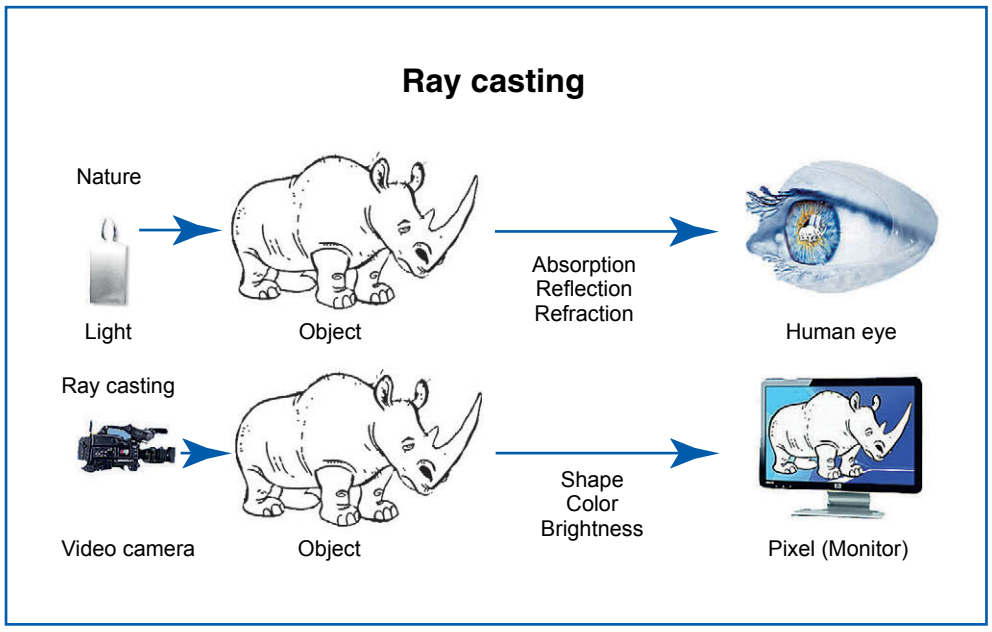

Fig. 5.3 This diagram shows the difference between ray casting and what happens in nature, where the light hits an object which "filters" the information to our eyes according to its own characteristics. In ray casting a video camera records a scene where the objects, created virtually, with preset shape, color, and brightness, are reproduced by the pixels of our monitor.

assembled by a computer to create a volume. Once reconstructed, this volume will become a three-dimensional image through so-called 3D rendering (Fig. 5.2).

The three-dimensional images of volumes are usually processed by so-called "ray casting". In nature, light usually hits objects. According to their features, these objects can either absorb, reflect, or refract the light until our eye's retina is stimulated and sends the information to our brain, which will record an image of the objects.

During ray casting, a video camera records the shape, color, and brightness of an object that will be reproduced on a monitor in the form of pixels (Fig. 5.3). Ray casting starts from the camera (the point from which the object to be examined is seen) and then colors every single point (voxel), forming the object according to its opacity. This process makes every element opaque and composes and colors it so as to create interplay between light and shadow, resulting in a three-dimensional effect. We can thus observe the volume to be examined from the outside or even "cut it into slices" to explore its inside. We can also observe some tissues only, because they will behave differently when hit by rays and supply different data to our

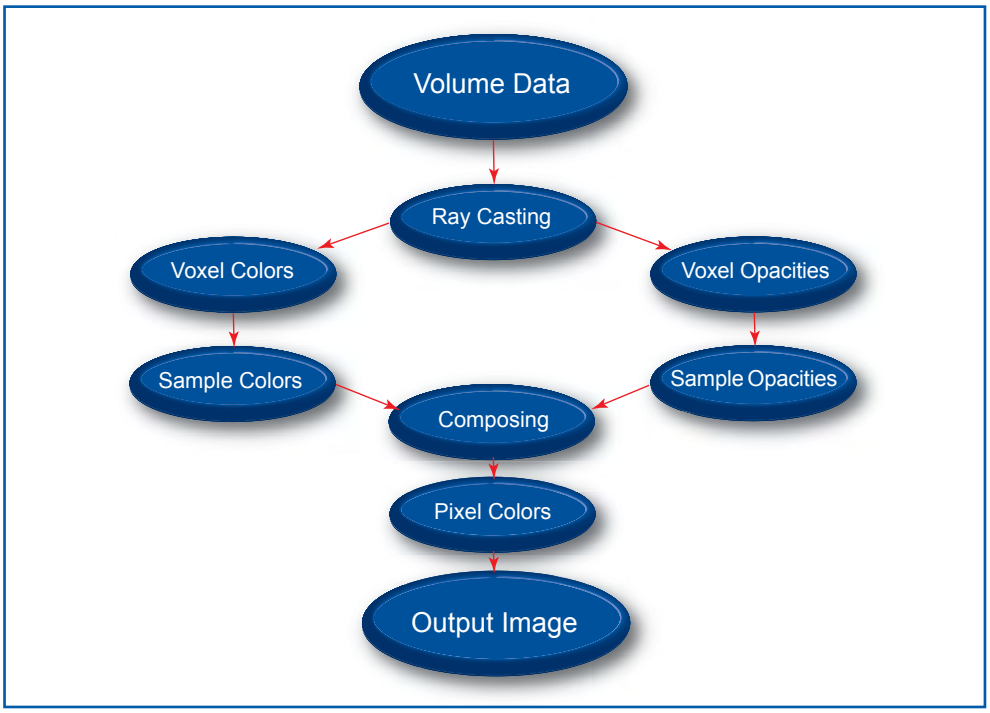

Fig. 5.4 This diagram has been taken from the User's Manual for OsiriX and shows how an image is reproduced on our monitor from the data supplied by CBCT.

computer (Fig. 5.4). As in architectural models, in medicine, too, several kinds of rendering have been studied, and we can now take advantage of mathematical algorithms, like volume ray casting, splatting, shear warp, or texture mapping. However, like in architecture, in 3D rendering it is of the upmost importance to use the GPUs (graphic processing units) that are suitable for performing this complicated mathematical calculation.

The final result obtained with these procedures will be displayed on our monitor in different ways according to our requirements.

The most frequently used system is 3D surface rendering, because it allows us to quickly visualize the bone surface only, and to send our data to advanced three-dimensional printers and get 1:1 models for sophisticated surgery planning.

However, for graphics, 3D volume rendering is excellent because it can create very realistic three-dimensional color models which can help us accurately diagnose the diseases we encounter. This is possible thanks to a gray scale histogram made out of the specific analysis curves of the sectors examined.

Clinical use of models processed using 3D rendering

In many cases, a 3D rendering system can facilitate diagnosis.

We have tested various software models specifically designed for rendering. After discarding those with obvious performance limits usually used by the suppliers of three-dimensional systems, we have chosen the software OsiriX, which is free in the 32-bit version, and cheap in the 64-bit version but with better performance. The 3D volume rendering in OsiriX is sophisticated, but it can only be used with Apple products since it is an Apple application and requires advanced and expensive systems. The rendering results shown in this chapter have been obtained using an Apple Mac Pro with an 8-Core Intel processor and 20 GB RAM. In our opinion, however, these results are wholly satisfactory and help us achieve better diagnosis and communication with our patients than those achievable up to now (Fig. 5.5).

Fig. 5.5 This image clearly demonstrates what we can obtain from computed tomography. Its data help analyse any tissue layers, from skin to bones. (Analysis taken from the OsiriX file, available on the program's website and performed with a contrast medium. Processed by OsiriX 64-bit with Apple Mac Pro.)

Three-dimensional volume rendering can have various dental applications: from extraction surgery to implant planning; from diagnosis in several sectors, like traumatology, to ATM diseases (Figs. 5.6-12). For example, an oroantral fistula can barely be detected with either conventional radiology or a two-dimensional image from CBCT, but the 3D rendering can show us a clear image of the damage (Fig. 5.6).

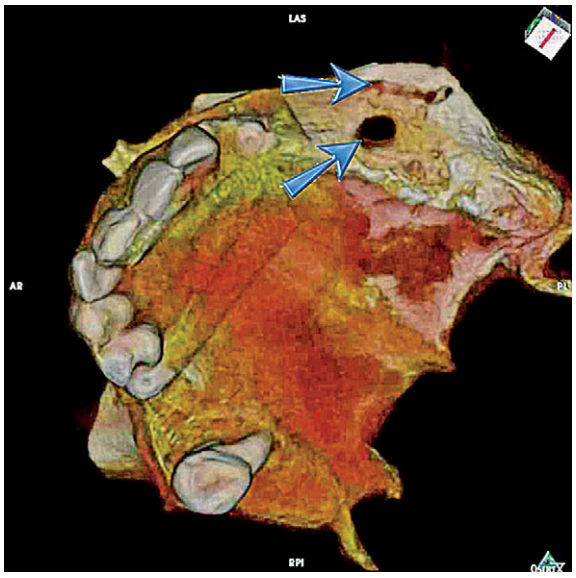

Fig. 5.6 This 3D rendering from CBCT performed with a CS 9000 3D (OsiriX 64-bit with Apple Mac Pro) shows in detail this double oroantral iatrogen fistula and would help in planning a suitable surgical treatment to solve the problem.

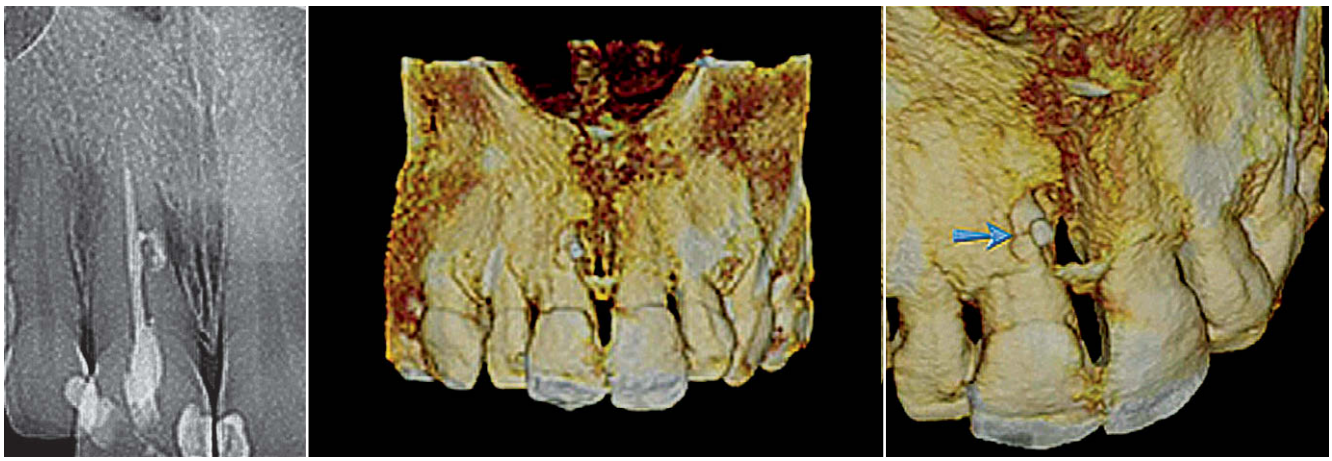

Fig. 5.7 This root fracture had only been suspected with an intra-oral X-ray. It is made clear in this 3D volume. We can make out the large bone lesion between the upper central incisors. (Exam performed with a CS 9000 3D. Rendering processed by OsiriX 64-bit with Apple Mac Pro.)

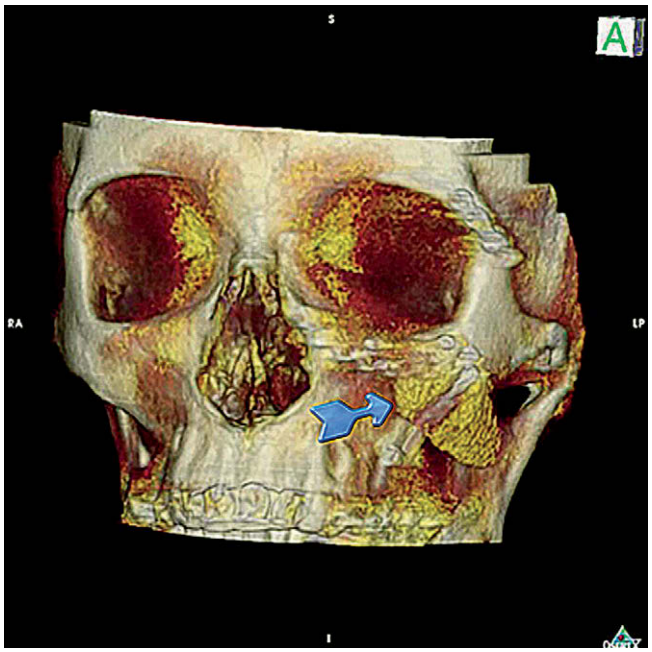

Fig. 5.8 This image shows a case of malpositioning of a Proplast implant, located to correct a previous unsuccessful treatment of restraint reduction of the left orbito-malar complex. This image clearly facilitates our surgical approach to correct the dislocation. (NewTom 3G. Rendering with OsiriX 64-bit with Apple Mac Pro.)

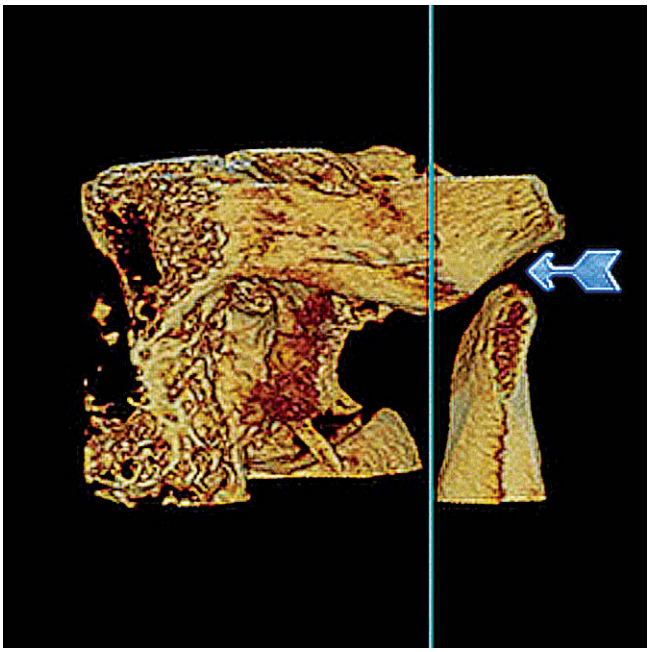

Fig. 5.9 The ATM exams reprocessed in a 3D volume rendering may give us useful direct and indirect details of any morphological and structural alterations of the joint. In this case, no morphological alterations of articular bones were detected but a habitual dislocation of the right mandibular condyle appeared far beyond the tuber eminence (marked with a vertical blue line). The correct joint space, indicated with an arrow, is an indirect sign of the maintained coordination between the condyle and the meniscus even during the condylar translation movement. (CS 9000 3D. Rendering with OsiriX 64-bit with Apple Mac Pro.)

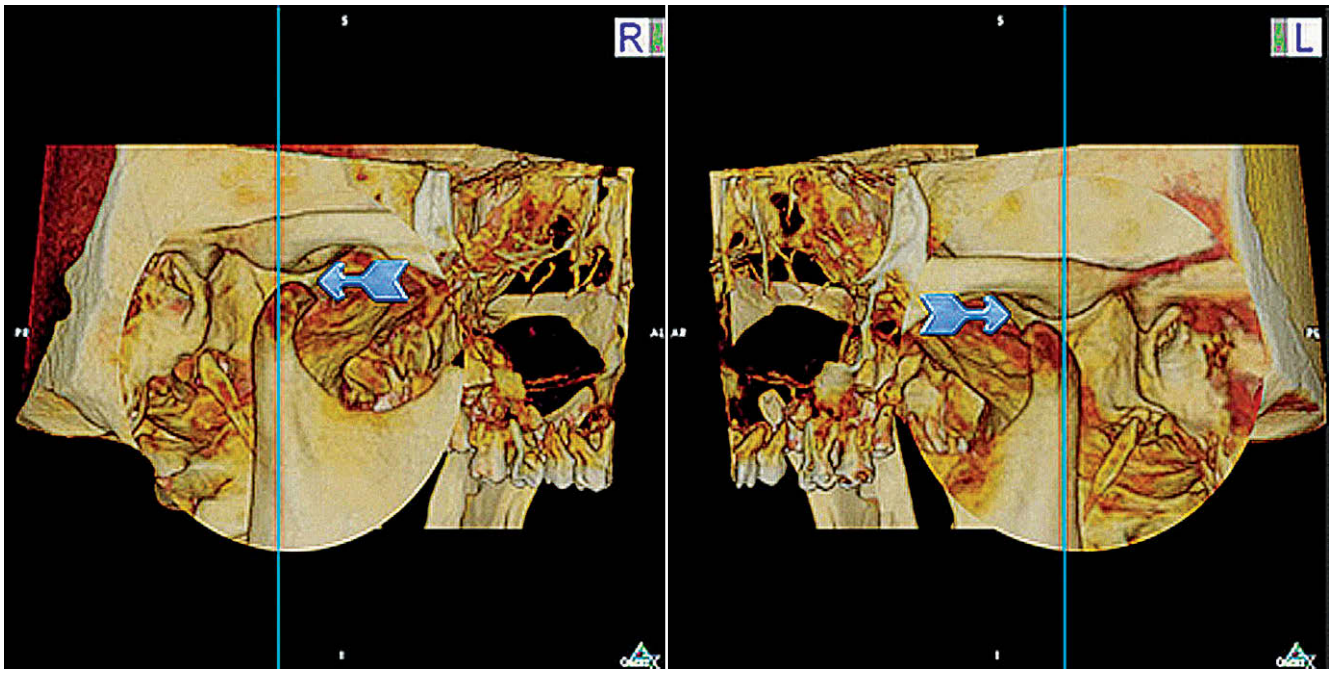

Fig. 5.10 This case clearly demonstrates that, while the right joint movement is correct, there is a slight habitual dislocation of the ATM in the left side with a small joint space—an indirect sign of the lack of coordination between the condyle and the meniscus in that space. (NewTom VGi. Rendering with OsiriX 64-bit with Apple Mac Pro.)

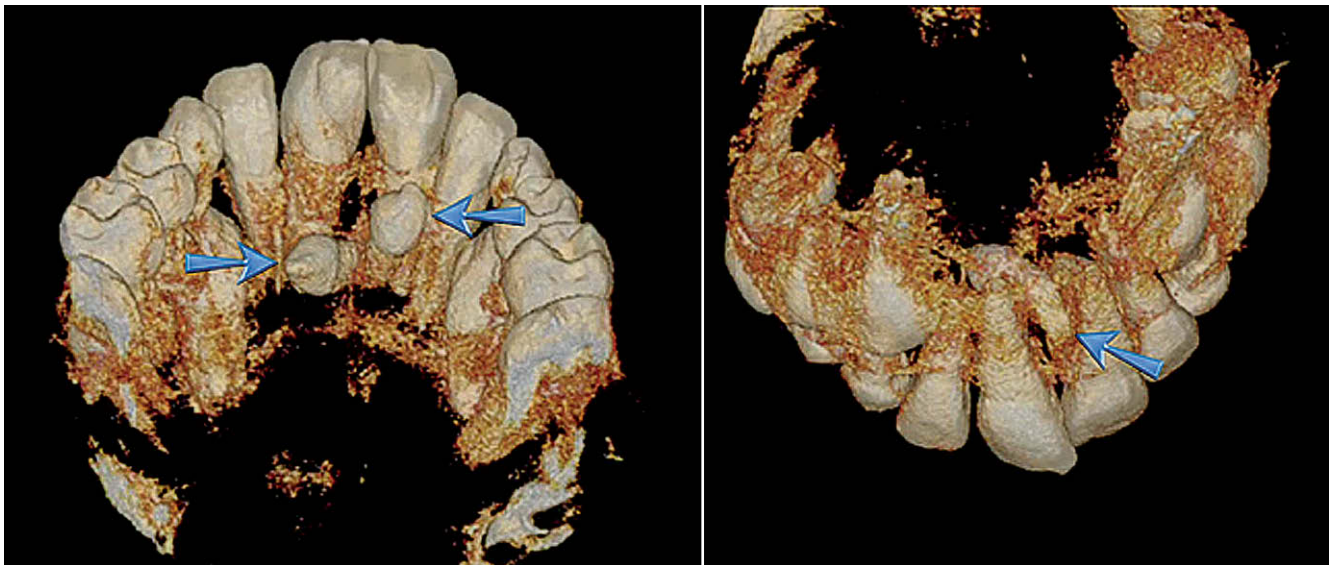

Fig. 5.11 This case shows clearly that it is sometimes very useful in diagnosis and surgical planning. Two supernumerary teeth appear in the palate; thanks to the suitably processed 3D volume rendering, we can see a high hook-like curvature of the right tooth. (CS 9000 3D. Rendering with OsiriX with Apple Mac Pro.)

Fig. 5.12 This example shows how useful 3D rendering may be in evaluating a cyst neoformation of the lower maxilla reaching the mouth floor. On the left, we can see a good rendering of bone tissues showing a large lesion of hard tissues destroying a wide area of the inner cortical up to the soft tissues of the mouth floor. On the right, a sophisticated background elimination of the neoformation gives an accurate pre-surgical view to evaluate the approach. This analysis, however, requires a radiological device with a power of over 100 kV. Moreover, it is necessary to isolate the neoformation from the soft tissues of the mouth floor, using a virtual cleavage plane that could only be detected by someone very experienced. (NewTom VGi. Rendering with OsiriX 64-bit with Apple Mac Pro.)

Using 3D rendering to communicate with patients

In our daily practice, it is essential to communicate with our patients as clearly as possible. As a matter of fact, it is often very difficult for us to describe a clinical pattern that appears objectively slight to the patient, but actually seems severe to us clinicians. It should be emphasized that 3D rendering is often not very helpful, but it can be in some cases (Figs. 5.13-15).

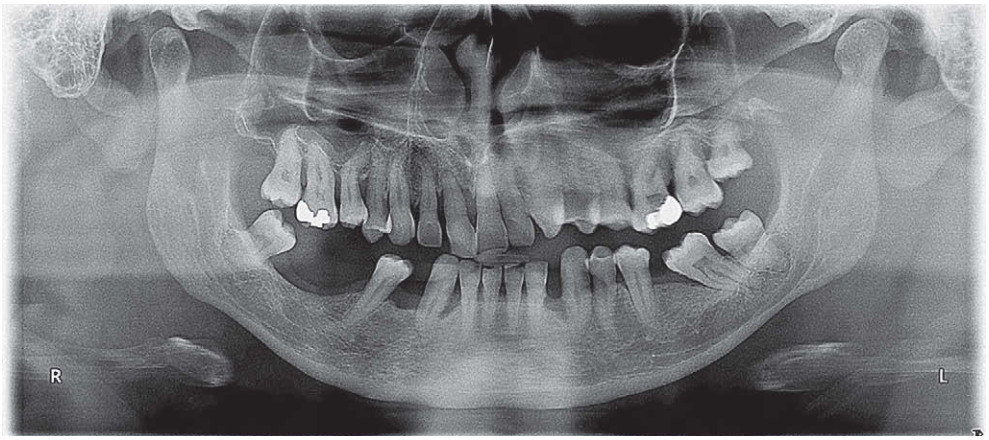

Fig. 5.13 Ordinary orthopantomography can supply useful data. Along with a proper objective exam and radiological status of dental arches, we can make a reliable diagnosis of our patient's disease. We encounter difficulties, however, when we have to explain to our patient that a large portion of his masticatory apparatus is compromised and that he should undergo several extractions of teeth that do not appear unstable, because they are closely overlapped. Our patient may be affected psychologically, and we have to give a detailed and accurate description of the clinical pattern with the aid of very clear images. Orthopanthomography may be unsatisfactory in this case.

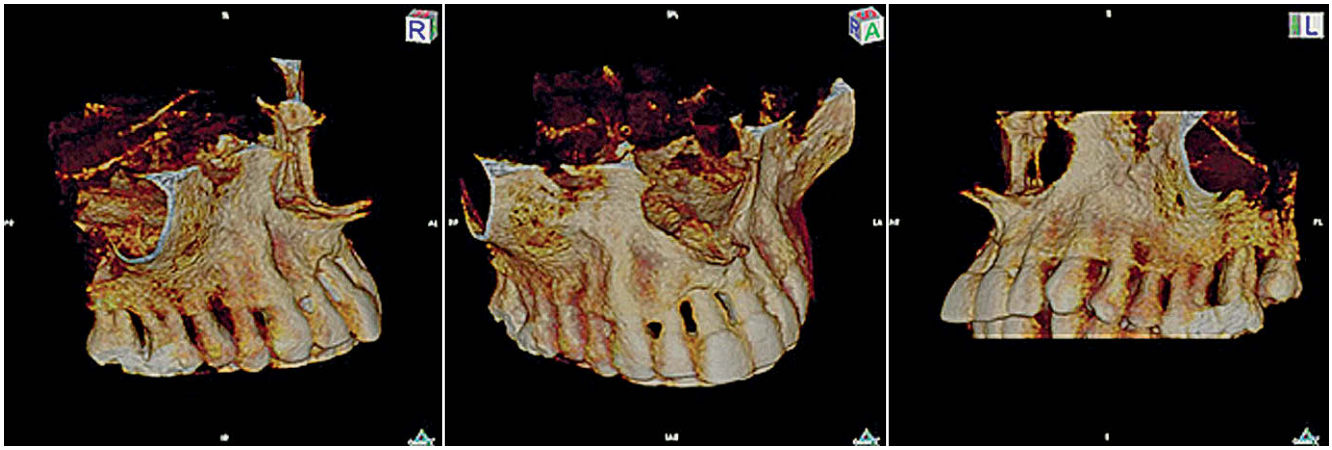

Fig. 5.14 These are three images taken from a QuickTime VR format exported with OsiriX. This is a particular format which is useful in observing this rendered "object" because we can rotate it so as to see it from multiple angles. Since the images are extremely lifelike and realistic, the patient can easily understand his actual clinical pattern and could be willing to accept a treatment that he may have otherwise refused. (NewTom 3G. Rendering with OsiriX 64-bit with Apple Mac Pro.)

Fig. 5.15 This is a very explicative case, which shows an edentulous lower jaw with a "blade-shaped" alveolar crest. This patient had been insisting on having several implants put in to stabilize a fixed prosthesis, after reading a number of articles published on the Web. The QuickTime VR format exported with OsiriX convinced him that the peculiar anatomy of his residual alveolar crest would not allow this approach unless several bone grafts were made to recover a proper volumetric morphology of the crest. (NewTom 3G. Rendering with OsiriX 64-bit with Apple Mac Pro.)

We will now summarize what 3D volume rendering can offer, as a new frontier in modern medicine and a valid support in our daily practice, with the analysis of data obtained from CBCT. Is it useful?

Yes, it is. Is it easy to perform? It requires experience and training. Can it be applied to any device? Of course it can, although the results will differ, and, in our opinion, more powerful devices will offer faster analysis without any "cleaning" of soft tissues.

Is it expensive? Of course it is. Every 3D data processing system is equipped with software that is able to display a 3D model, but this is usually an unsophisticated rendering. If we use a software like OsiriX to obtain a simple analysis, it takes us at least thirty to forty minutes, plus thirty more minutes of rendering, and we are forced to use an Apple Mac. Certainly, it is possible to start with a "basic" MacBook Pro, but it will soon require more RAM, ranging from 6 to 32 GB, and NVIDIA Quadro 4000 (with 2 GB RAM DDR5) for video, which is quite expensive. As its use increases, it will be necessary to add an SLI video card (two cards working together will get more accurate and faster results). This is how things will go, and with time the technology is going to become more sophisticated and cheaper, so that almost everyone will take advantage of it.

The use of CBCT in dentistry

Introduction

In this section, the various uses of CBCT systems in each specialty will be described in everyday clinical practice. Clinical cases will often be described in detail and step by step so as to underline the three phases when these systems may be really useful to clinicians: diagnosis, treatment planning and follow-up.

It is therefore a kind of a handbook aimed at leading the reader to the various clinical uses of these systems.

This section is subdivided into seven subsections:

1) Implants
2) Endodontics
3) Dental traumatology
4) Oral surgery
5) Periodontics
6) Orthodontics
7) Maxillary sinus diseases

Each of them is set up with an introduction and a brief discussion of various indications following the scientific literature and describing some clinical cases.

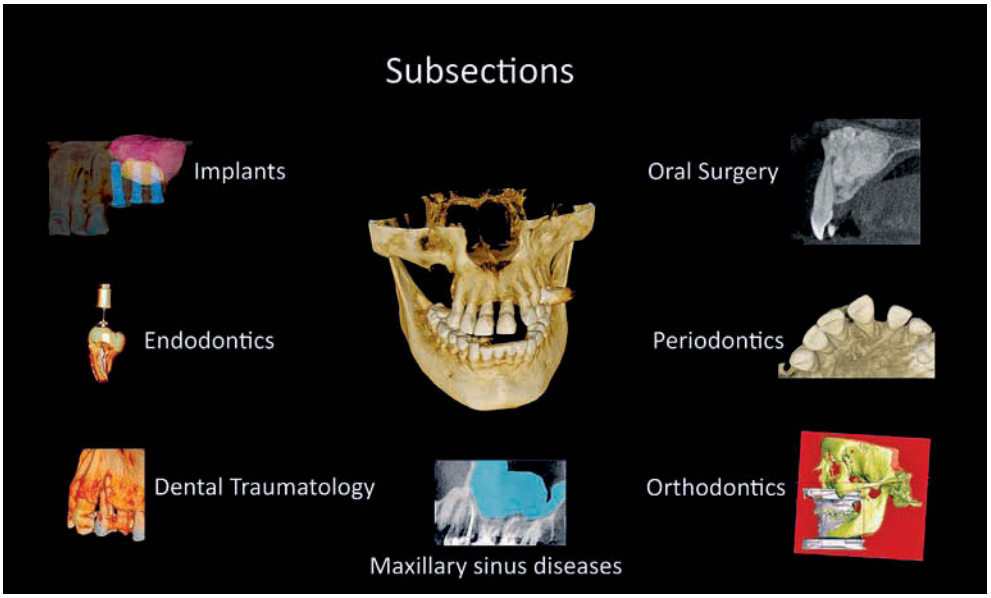

Implants

Emanuele Ambu - Roberto Ghiretti

The use of CBCT in implant surgery

According to many clinicians, volumetric radiology is strictly and almost exclusively recommended for dental implant and oral surgery. As a matter of fact, until some years ago patients used to be exposed to a large amount of radiation because volumetric exams were performed in hospitals with CT systems. These exams were justified only in cases of potentially dangerous surgery. Possible injuries to anatomical structures, like the maxillary sinus or nerve, or large lesions resulting from oral and maxillofacial surgery justified the use of CT.

In 2002, a team from the European Association of Osseointegration established guidelines for diagnostic imaging in implant dentistry (Harris et al. 2002), describing the use of "cross-sectional imaging."

They determined that "[c]linicians should decide if a patient requires cross-sectional imaging on the basis of the clinical examination, the treatment requirements and information obtained from conventional radiographs." Moreover, "[s]tandard imaging modalities are combinations of conventional radiographs" and "[c]ross-sectional imaging is applied to those cases where more information is required after appropriate clinical examination and standard radiographic techniques have been performed." It was, however, emphasized that "[t]he technique chosen should provide the required diagnostic information with the least radiation exposure to the patient."

Their article did not mention the CBCT that had been introduced only some years before. The introduction of this system has provided such advantages as to largely modify the conclusions of these guidelines.

With some of these systems patients are exposed to very low radiation rates. Two-dimensional radiology can never supply exhaustive information about the patient's anatomy, even with several multiple projections. This means that they risk being exposed to a higher radiation dose (with less information) than that of one volumetric scan. This is especially true when the areas to be looked at are within a volume that can be examined with a small FOV system.

In these guidelines, it is recommended to establish a good rapport with radiologists, giving them as much information as possible about the aims of the exam. Moreover, it is recommended that clinicians use the absolute best technique rather than the best one they have in their practice. CBCT systems are suitable for clinicians' direct use in their own practice, which avoids any misunderstandings in communication with radiologists, and clinicians are able to read immediately and directly all data required.

CT images were not so useful: they were processed by systems designed to examine other parts of the body (with lower resolution, of course). Clinicians could examine images showing planes that had been chosen by radiologists. They were only seldom useful for implant dentistry.

In 2003, Hatcher et al. were the first to point out that CT, used up to then for diagnosis and pre-surgical assessment in implant dentistry, could not be very helpful to clinicians for diagnosis or to patients because of its high costs and biological risks (Hatcher et al. 2003). The authors stressed that CBCT would soon be developed (we are talking about nine years ago!) and would spread beyond their exclusive use in maxillofacial surgery.

According to the authors, this new radiological system is extremely important in implant dentistry. Thanks to suitable software, clinicians can find the best planes for their clinical requirements (Clinical Case 1).

CLINICAL CASE 1

Massimo Frosecchi

This 58-year-old female patient came to my practice to have her bridge on missing teeth replaced from the upper left incisor to the upper left first molar. As shown by the clinical examination, the patient was suffering by a serious periodontitis, also confirmed by the panoramic X-ray that she had brought to me (Fig. 1.1). According to the volumetric exam, there was a large bone loss both in the area of her first and second molars and in the area of her canine. In order to ensure the patient to keep an adequate aesthetic level over the entire treatment period, we planned to insert a temporary denture on implants immediately after extracting her teeth. Because of the small quantity of bone available, we planned to insert a tilted implant in the area of her upper left second premolar (Figs. 1.2 and 1.3). During surgery, after extracting her teeth, an implant was inserted in the area of her upper left lateral incisor and one in the area of her upper left second premolar. This latter has been tilted so as to make the abutment in the area of the first molar be raised. This would reduce the cantilever effect (Fig. 1.4). Thanks to the primary stability of the nasal and sinusal cortical bones, we were able to execute a temporary denture of acrylic material on metal caps, screwed and placed on site, removing any contacts with the antagonist arch (Fig. 1.5). This procedure will give the patient a good aesthetic level and a good social life until she has her temporary denture replaced with a ceramic one on golden alloy (Fig. 1.6).

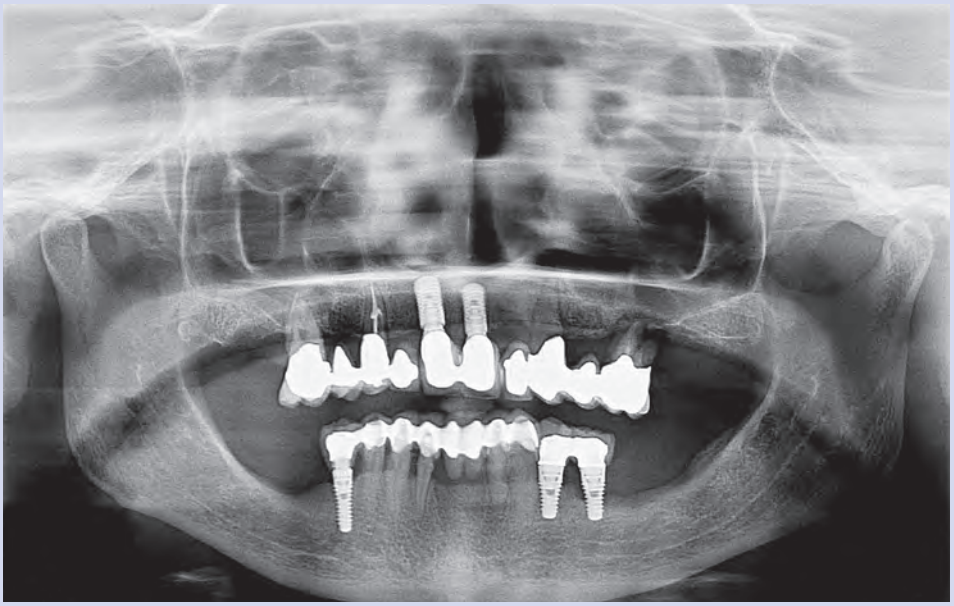

Fig. 1.1

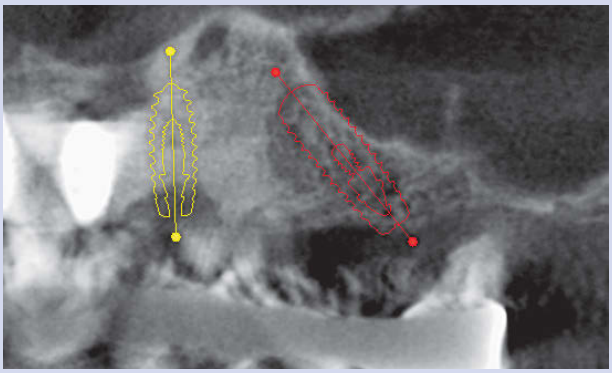

Fig. 1.2

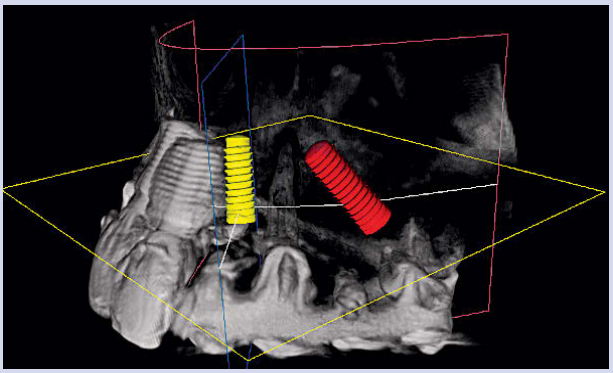

Fig. 1.3

CLINICAL CASE 1 ***(cont'd)*** **Massimo Frosecchi**

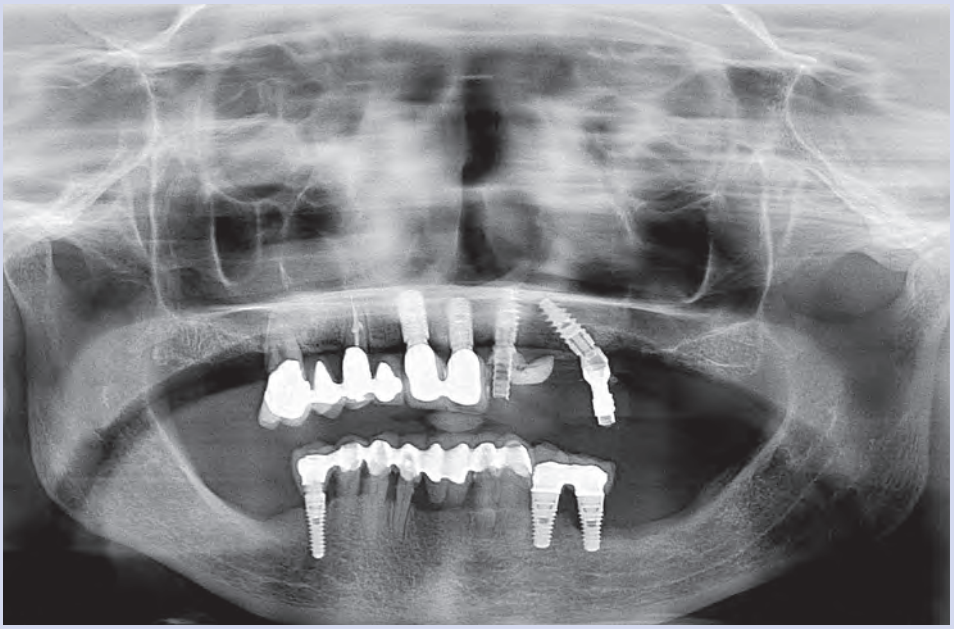

Fig. 1.4

Fig. 1.5

Fig. 1.6

The use of CBCT is highly recommended in dentistry, because it is easy and the radiation dose to patients is relatively low. Nevertheless, there are still some problems connected to this kind of radiological device. As highlighted by Draenert et al., a multidetector computed tomography (MDCT) device supplies better images in post-operative checkups because there is a smaller amount of beam hardening artifacts than with CBCT (Draenert et al. 2007).
As we have already seen, the E.A.O. guidelines of 2002, though not dealing with CBCT, focus their attention on the problem of "cross-sectional imaging", which is the "first-choice" criterium in pre-implant evaluation and treatment planning. The use of a three-dimensional exam is recommended in these guidelines only if "there is a need for assessments in situations where some kind of complications have occurred, such as nerve damage, post-operative infection in relation to nasal and/or sinus cavities close to implants." These assumptions, as already mentioned, had been made about the radiation quantity produced by multislice spiral computed tomography (MSCT) systems, and not by CBCT ones. While awaiting the new guidelines urgently required from the E.A.O. (SEDENTEXCT 2011), clinicians should take into account, in any single case, the ratio between the amount of radiation to which patients are exposed (varying according to the type of CBCT used, the examined area, and

the patient's characteristics) and the quantity of data supplied for diagnosis and planning, and then compare these values with those supplied by conventional radiological systems or by exams which are much more dangerous to patients, like those performed by MSCT. It is recommended to read the conclusions reached by the SEDENTEXCT group in their 2011 guidelines, stating: "for cross-sectional imaging prior to implant placement, the advantage of CBCT with adjustable fields of view, compared with MSCT, becomes greater where the region of interest is a localized part of the jaws, as a similar sized field of view can be used." To evaluate the "cross-sectional imaging," essential for a proper image arrangement, one of the main factors is the geometric accuracy in linear measurements supplied by the CBCT software. Over fifty scientific articles have been published about this matter because of its importance in implant dentistry and orthodontics. Though there has been no systematic review, they have been reviewed by the Panel of SEDENTEXCT, and they came to the conclusion that there was little difference between the values measured by CBCT and the standard references, and that the linear measurements obtained by CBCT are extremely accurate (SEDENTEXCT 2011).
Several other papers have focused their attention on the possibility of evaluating bone quality with the images obtained by CBCT. This evaluation had been done up to then using MSCT (de Oliveira et al. 2008). Barone et al. have been suggesting since 2003 to use Hounsfield units (HU) to evaluate the bone density quality in implant sites (Barone et al. 2003). Since then, a lot of studies have proved that a correlation exists between the HU values obtained by CBCT and the bone density measured by other devices (Aranyarachkul et al. 2005; Nomura et al. 2010).
There are also some studies, however, which have disputed this assessment: Lee et al. (2007) have found a low correlation between the resistance of bone to drilling and HU values, while more recently Nackaerts et al. (2011) have stated that this correlation is valid with MSCT but unreliable with CBCT because the values depend on the system type, imaging parameters, and positioning of the field of view.
The use of cross-sectional imaging is advantageous in some situations (E.A.O. guidelines 2002):

- Lower risk of damage to adjacent anatomical structures.
- Assessment of critical clinical cases, such as horizontal and vertical sizes of the bone where the implant is going to be inserted.
- Assessment and planning of implant positioning and axial direction so as to improve the biomechanical, functional, and aesthetic results.

The Consensus Report of the International Congress of Oral Implantologists has recently been published, based upon the systematic review of literature published between 1 January 2000 and 31 July 2011 (Benavides et al. 2012). According to this report, "the literature supports the use of CBCT in dental implant treatment planning particularly in regards to linear measurements, three-dimensional evaluation of alveolar ridge topography, proximity to vital anatomical structures, and fabrication of surgical guides. Areas such as CBCT-derived bone density measurements, CBCT-aided surgical navigation, and post implant CBCT artifacts need further research."

Lower risk of damage to adjacent anatomical structures

There are several articles in international literature dealing with the importance of the use of CBCT to localize some anatomical structures which should be safeguarded during surgery, including the lower alveolar nerve (LAN) (Angelopoulos et al. 2008; Oliveira-Santos et al. 2011), the incisive canal in the mandibular interforaminal region (Madrigal et al. 2008; Sokhn et al. 2011; Uchida et al. 2009), the maxillary sinus (Pelinsari Lana et al. 2011), and the nasal cavity.

CLINICAL CASE 2

Marco Vigna

A sixty-year-old female patient came to the practice to receive implant-prosthetic rehabilitation of her right lower rear sector. The panoramic radiograph the patient gave to us (Fig. 2.1) did not allow us to assess the actual bone thickness in the area concerned. Therefore, we decided to perform a volumetric exam to make a diagnosis. The exam was performed with a small FOV CBCT and showed an alveolar nerve split in two paths. Just before the foramen, the nerve moved in a cranial direction (Fig. 2.2).

Virtually placed implants helped dental technicians build the radiological guide on the diagnostic wax-up. A second exam allowed us to assess the accuracy of the areas chosen to receive fixtures (Fig. 2.3). A follow-up CBCT showed that the implants had been placed to safeguard the nervous structures (Fig. 2.4).

We would like to point out that the dentist preferred to place shorter implants than planned, though he placed them as suggested.

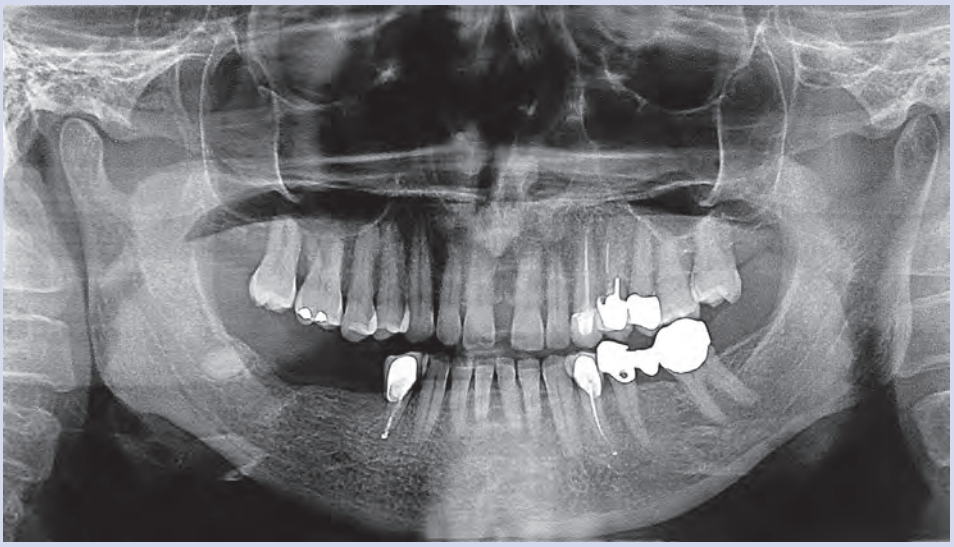

Fig. 2.1

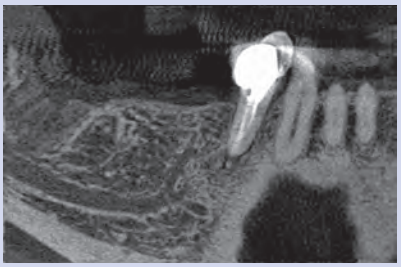

Fig. 2.2

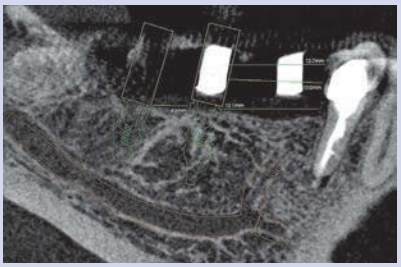

Fig. 2.3

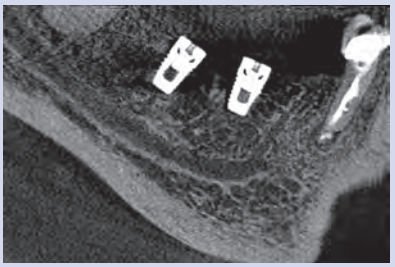

Fig. 2.4

This exam is extremely useful to assess the alveolar nerve path in implant planning (Clinical Case 2).

The CBCT exam can be used to investigate cases of paresthesia after surgery, allowing the dentist to plan the most suitable treatment to resolve this complication (Clinical Case 3).

CLINICAL CASE 3

Antonino Cacioppo

A sixty-four-year-old female patient came to the office thirty days after the insertion of four dental implants. In the days following surgery, she had suffered from paresthesia in the area of her left lip and chin, as was shown by mapping the area. She also reported both spontaneous and stimulated acute pain in her left lower jaw. The panoramic radiograph given to us by the patient did not permit an accurate assessment of the fixture's relationship to the lower alveolar nerve (Fig. 3.1). A volumetric exam was performed. The tomographic (axial, paraxial, and panorex) sections (Figs. 3.2 and 3.3) and the 3D volume (Fig. 3.4) showed that the implant inserted in the area of the lower first molar was in contact with the walls of the nerve canal.

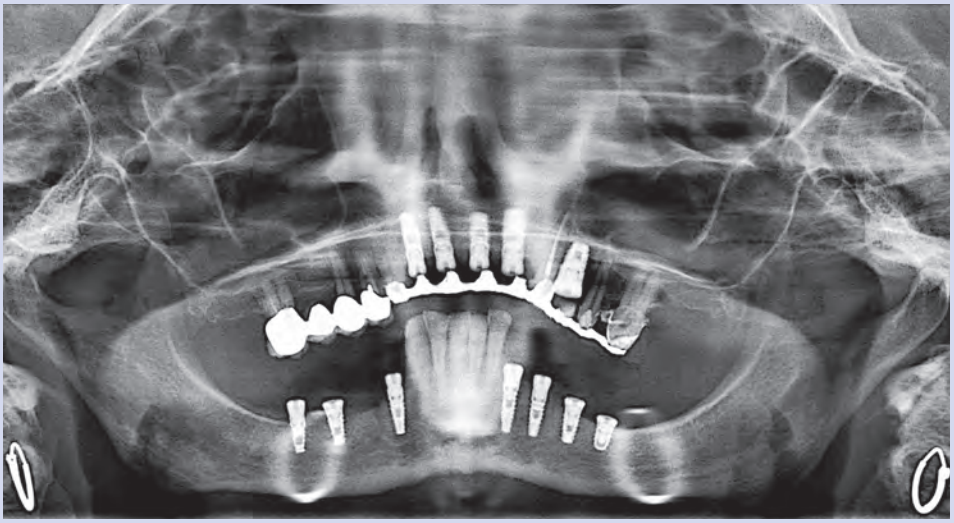

Fig. 3.1

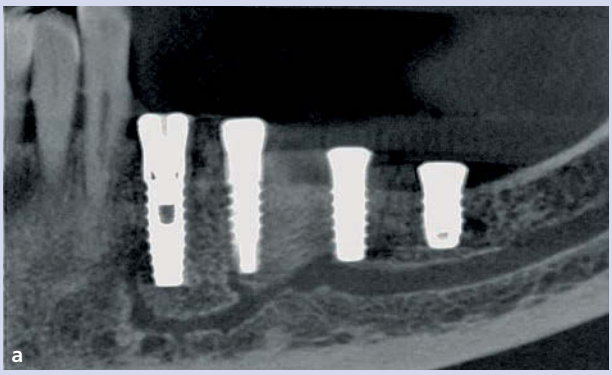

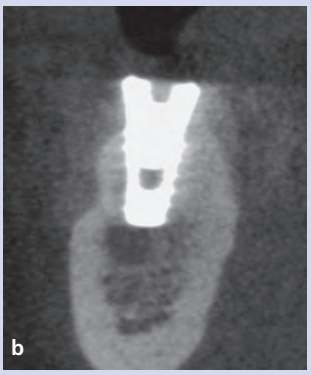

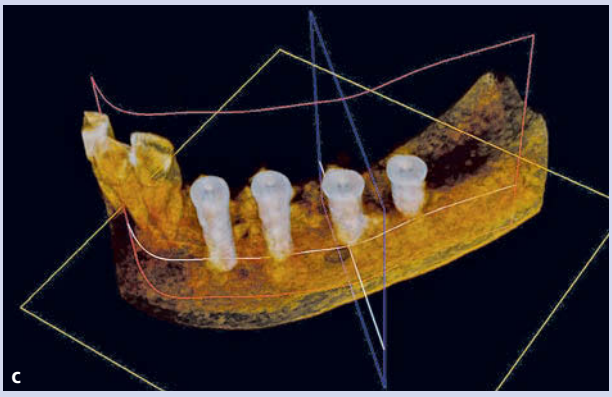

Fig. 3.2 a-c

CLINICAL CASE 3 *(cont'd)*

Antonino Cacioppo

The upper cortex of the left mandibular canal was blocked, but there was no sign of damage to the middle third and lower third section of the canal, in paraxial slices. The implants placed in the area of the lower first and second molars were in contact with two branches of the incisal nerve.

This diagnostic evidence justified the patient's symptoms, which were caused by a compression of the inferior alveolar nerve. Since the canal had only been slightly damaged, we decided to wait for the symptoms to disappear on their own. As a matter of fact, the symptoms gradually decreased and disappeared completely after ninety days.

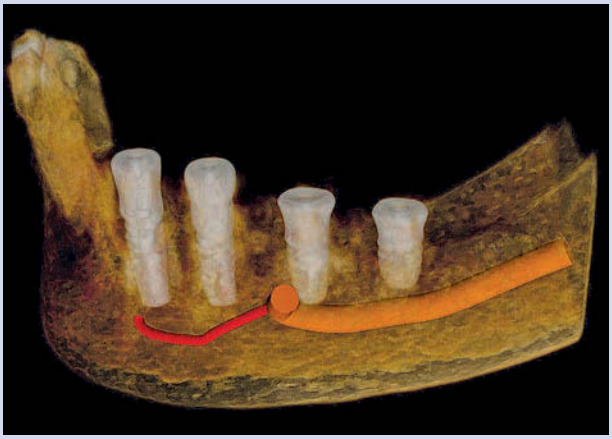

Fig. 3.3

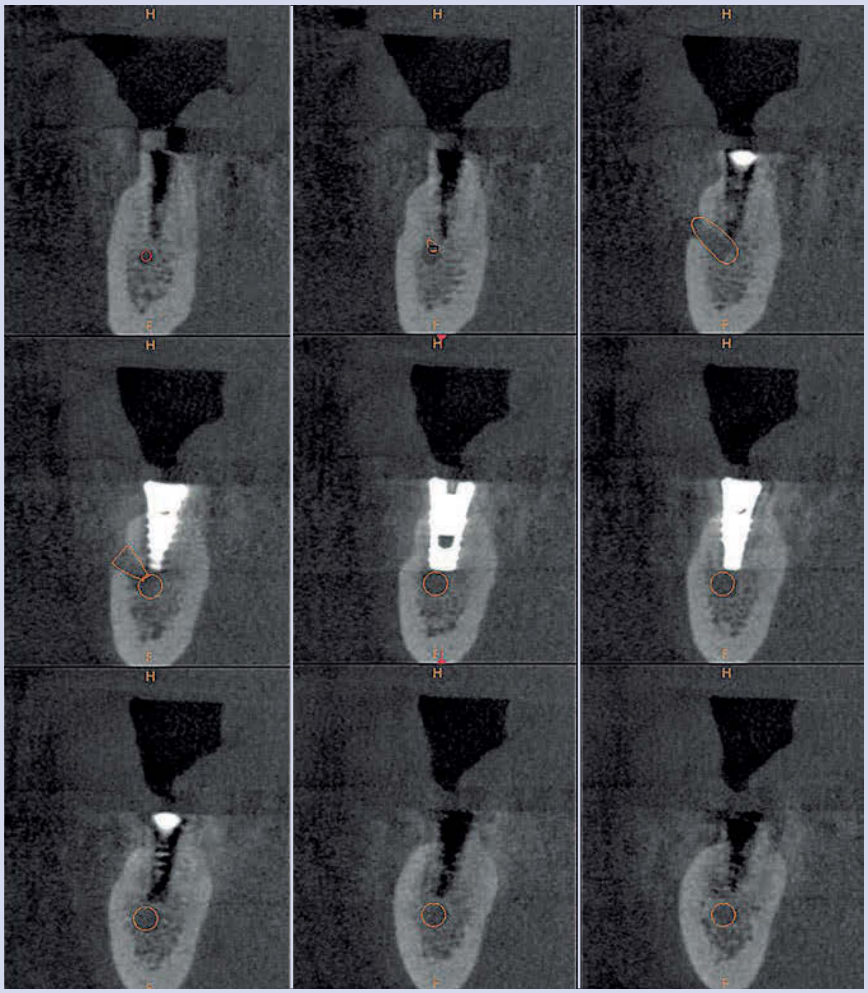

Fig. 3.4

The CBCT exam also permits us to assess the maxillary sinus area during preimplant planning (Clinical Case 4).

CLINICAL CASE 4

Roberto Ghiretti

The 40-year old female patient came to my practice to have prosthetic rehabilitation of the area of her upper left first molar, extracted one year before by a colleague. The patient had brought a panoramic X-ray and we decided to perform a CBCT exam to evaluate the best prosthetic procedure to follow. The presence of the maxillary sinus often hinders the insertion of implants suitable to the upper arch without bone grafts. In this case, the vertical size of the bone useful to insert an implant was less than 9 mm (Fig. 4.1). With an accurate study of the area made with the CS 3D software Imaging, we were able to measure the vertical space obtained by tilting our fixture (Fig. 4.2). We followed this way after simulating a distal-mesial tilting of 11° (Fig. 4.3). During surgery we performed an intra-oral X-ray (Fig. 4.4), after creating the guide with a 1.8-mm pilot bur. We were able to realize that our approach to the implant site was correct and the post-operative CBCT exam (Fig. 4.5) showed the good result of the insertion of a 5 x 9.5 implant with a 9° tilting obtained with no surgical guide and keeping to the maxillary sinus line.

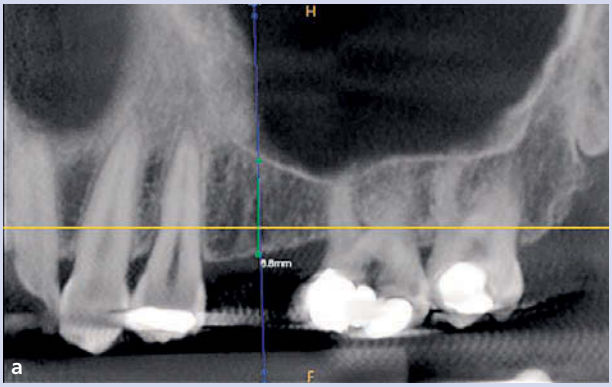

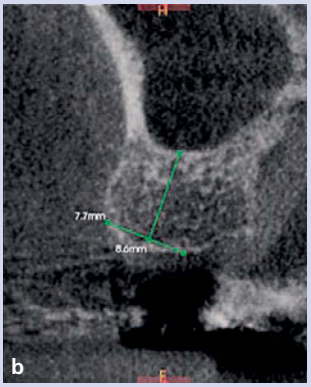

Fig. 4.1 a-b

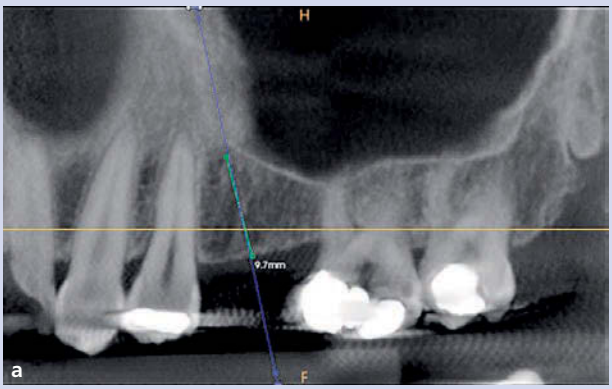

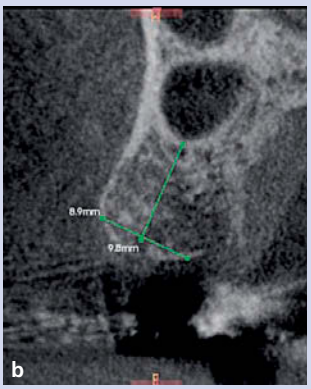

Fig. 4.2 a-b

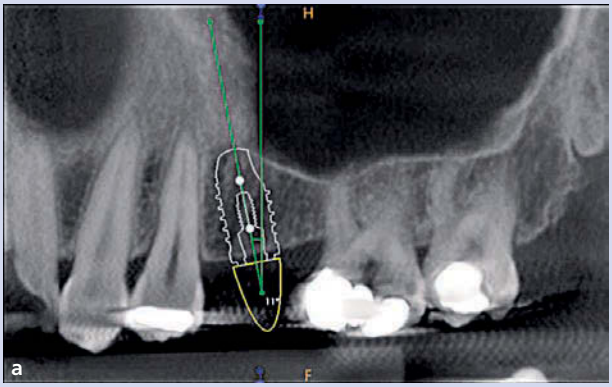

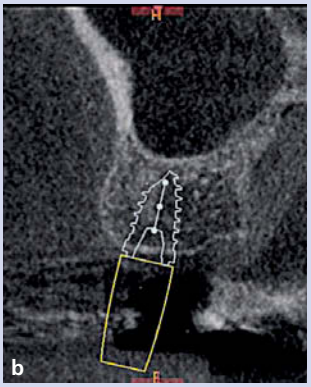

Fig. 4.3 a-b

CLINICAL CASE 4 *(cont'd)* | **Roberto Ghiretti**

Fig. 4.4

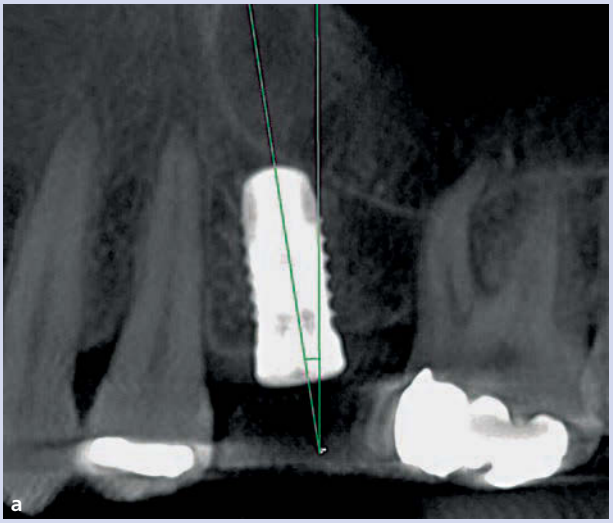

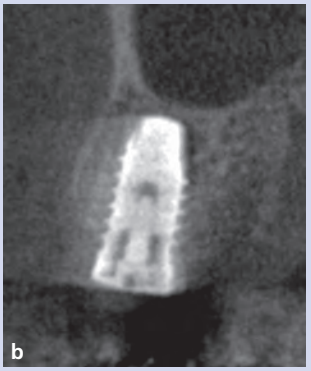

Fig. 4.5 a-b

Assessment of critical clinical cases (bone horizontal and vertical sizes)

Several works have been published about the use of CBCT in implant dentistry (Hatcher et al. 2003; Guerrero et al. 2006; Peck and Conte 2008). In a 2010 article, Worthington et al. emphasized that various parameters should be examined with CBCT in the pre-surgical planning phase (Worthington et al. 2010). For example, in the lower maxillary bone the presence and path of the mental nerve should be evaluated along with all possible abnormalities, as well as any bone grafts prior to the implanting phase. In the upper maxillary bone, the buccal concavity should be checked in the lateral incisor region, as well as the paranasal bone area in the canine region, and any bone to be used in the pterygoid area. Special attention should be paid to detect abnormal maxillary septa of the maxillary sinus that could obstruct the membrane lifting and to evaluate the status of grafts previously placed in the site.

We will examine further some cases in which we had to expand the implant site after assessment of the anatomical area sizes.

One of the main uses of this exam is to assess the maxillary sinus area in implant planning (Clinical Case 5).

CLINICAL CASE 5

Roberto Ghiretti

A sixty-four-year-old male patient came to the office to receive rehabilitation for his upper left rear area, toothless from the first premolar to the third molar.
The 3D exam allowed us to plan the implant insertion, simulating the position using images chosen from the software library.
We were also able to note that the bone thickness was enough to insert an implant in the area of the first premolar and that we needed to perform a sinus lift to insert implants in the area of the second premolar and first molar (Fig. 5.1).
We also noticed a mucous secretion probably of ENT origin in the most declivous area of the maxillary sinus.

Analyzing further, we were able to follow the anastomosis between the rear upper alveolar artery and the infraorbital artery. This path would not interfere with the necessary maneuvers to have a lateral access to the maxillary sinus (Fig. 5.2), because it went in a cranial direction with respect to the area concerned.
Planned in this way, the surgery did not seem difficult and the radiological examination after the surgery showed we had accurately inserted the bone and implants in the correct position (Fig. 5.3).
The 3D rendering and graphic processing (Fig. 5.4) highlighted the implant relations with the graft material (in yellow) and the maxillary sinus (in pink).

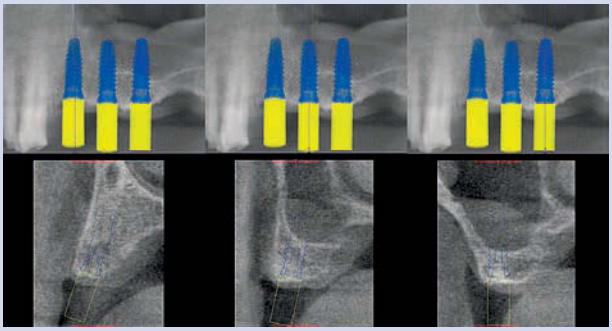

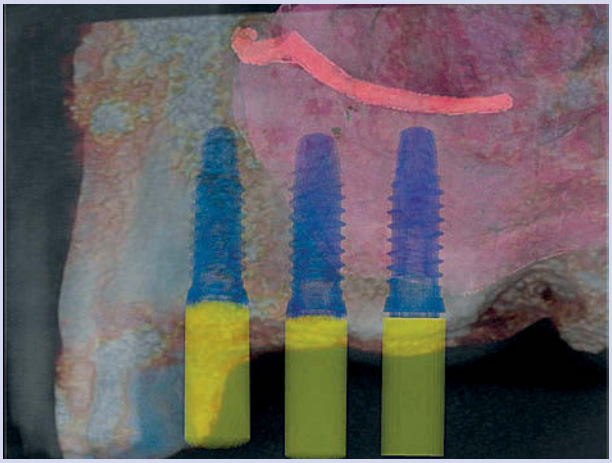

Fig. 5.1 and 5.2

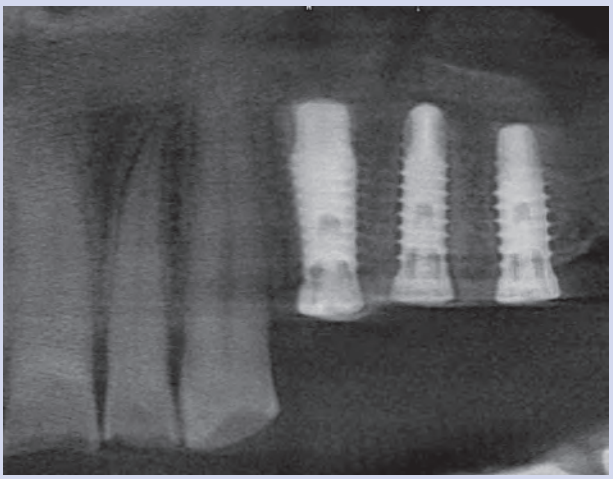

Fig. 5.3 and 5.4

The CBCT exam can also be very useful for block grafts with stereolithographic planning (Clinical Case 6).

CLINICAL CASE 6

Roberto Ghiretti

A forty-nine-year-old male patient came to the oral surgeon's office with serious atrophy of his lower right alveolar process, as shown in the panoramic radiograph (Fig. 6.1). The first volumetric exam showed a serious vertical bone defect and that the useful bone of the molar region was only eight millimeters thick (Fig. 6.2).
It was decided to rebuild the insufficient alveolar process with a block graft of heterologous material (Bioteck) with stereolithographic planning (Fig. 6.3). A full-scale model was made based upon the DICOM data of the first volumetric exam. A further exam of the model and graft (Fig. 6.4 a, b) proved that the volumetric increase was adequate. These preliminary procedures facilitated the bone graft and the titanium grid insertion (Fig. 6.5). This grid was useful for avoiding any material fragmentation due to the osteosynthesis screws. The volumetric exam performed at the end of surgery confirmed that the graft was positioned correctly (Fig. 6.6 a, b).

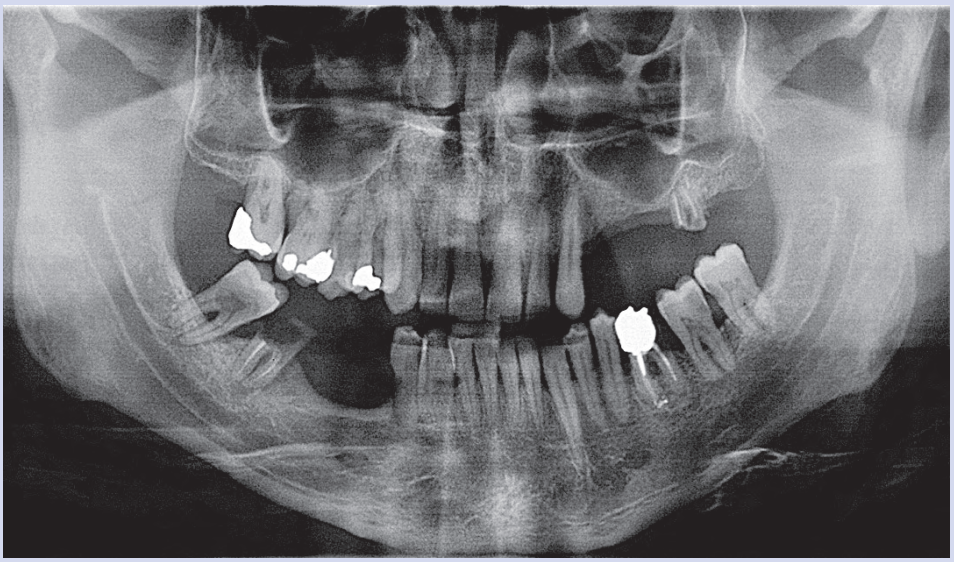

Fig. 6.1

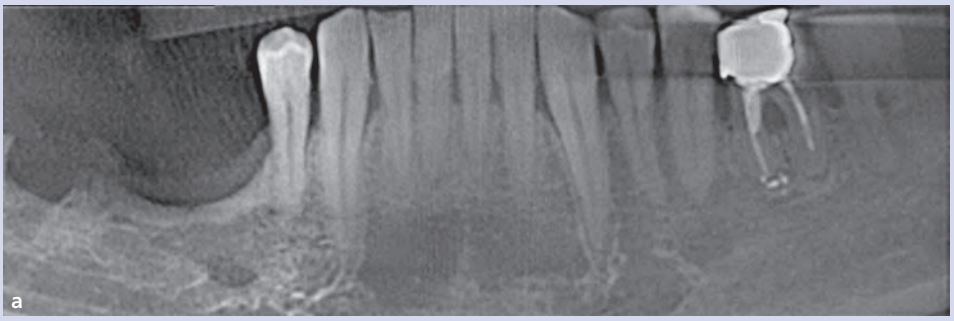

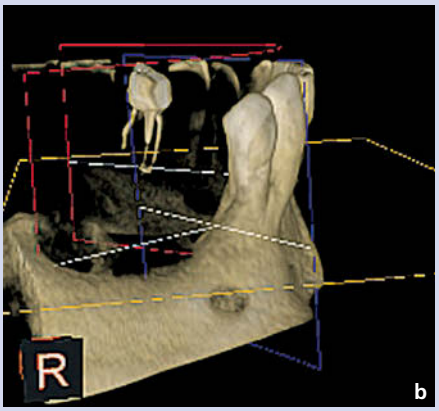

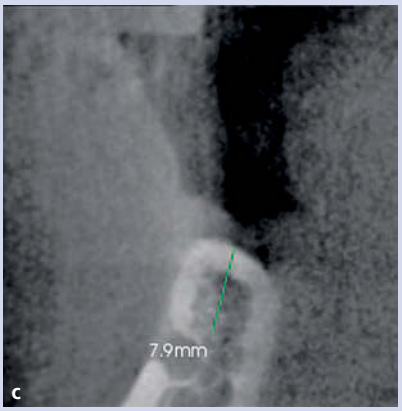

Fig. 6.2 a-c

CLINICAL CASE 6 *(cont'd)*

Roberto Ghiretti

Fig. 6.3

Fig. 6.4 a

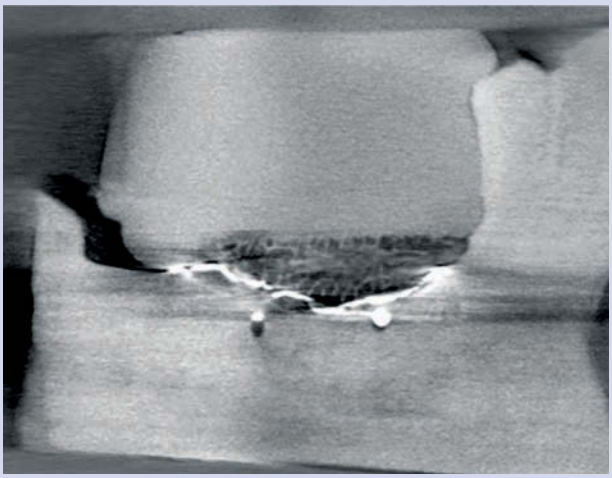

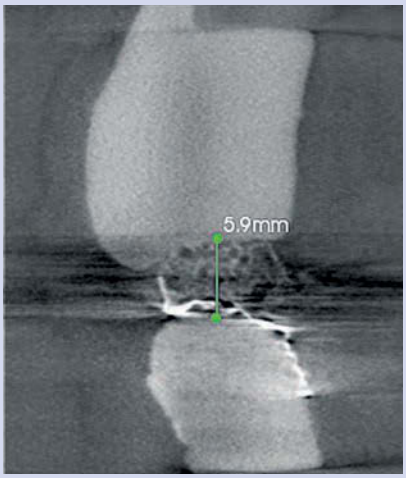

Fig. 6.4 b

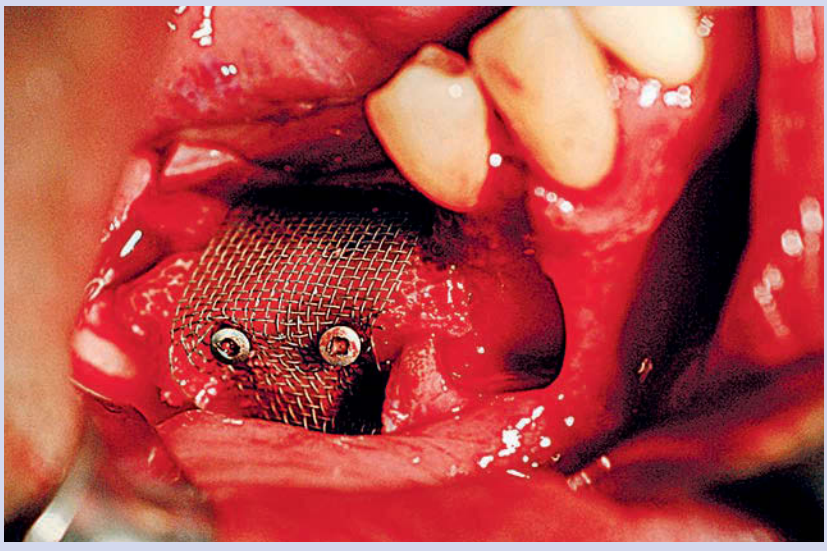

Fig. 6.5

CLINICAL CASE 6 *(cont'd)*

Roberto Ghiretti

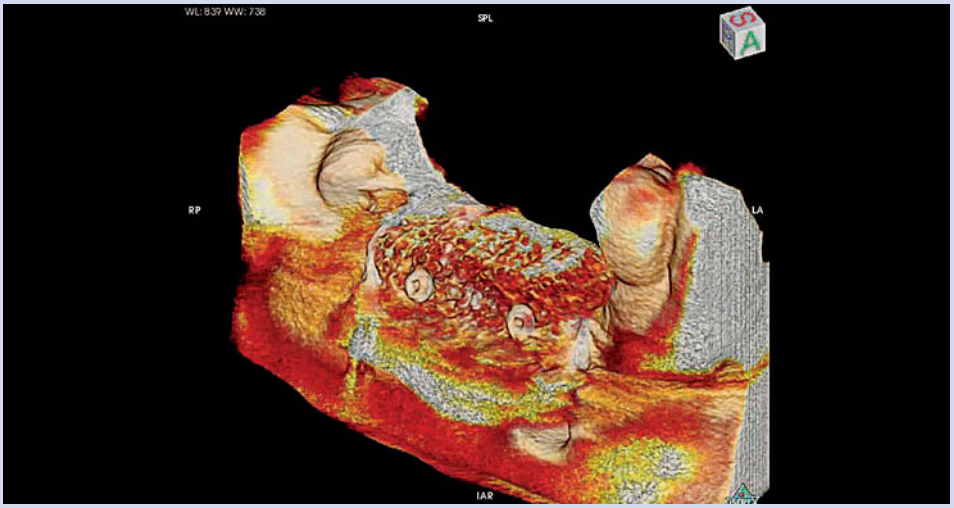

Fig. 6.6 a

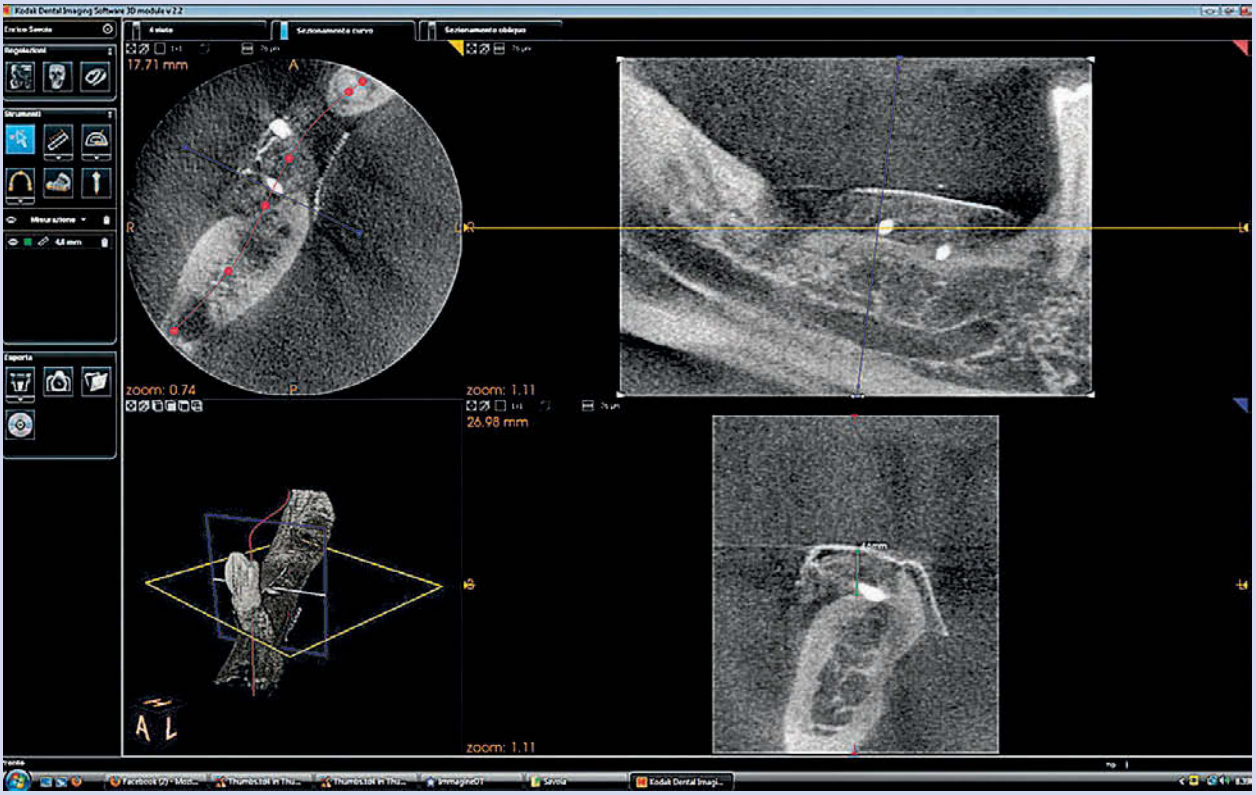

Fig. 6.6 b

As shown in the following case, the CBCT exam permits us to plan the premaxillary area increase, using mixed autologous and heterologous bone (Clinical Case 7).

CLINICAL CASE 7

Roberto Ghiretti

A fifty-three-year-old female patient came to the office reporting persistent abscesses in her upper arch, especially in the central incisor region where fixtures had been placed. A 3D exam performed with a small FOV system in stitching mode with 200 µm images showed diffuse periodontal diseases and periapical lesions in all elements with unsuccessful endodontic treatments (Fig. 7.1 a, b). Both fixtures appeared exposed on their vestibular side, causing repeated abscesses in this region.
Two months after removal of both fixtures in the incisor area, the extraction of all upper elements was agreed upon with the patient and the alveolar process was rebuilt. This had been seriously damaged on its transversal side because of chronic inflammation in the teeth which had been poorly treated endodontically. Two miniplates were applied to create a suitable gap that was filled with heterologous material according to the PRF procedure (Fig. 7.2). Six months later regeneration was assessed (Fig. 7.3) and four fixtures were inserted to stabilize an overdenture on a milled bar (Fig. 7.4 a, b).

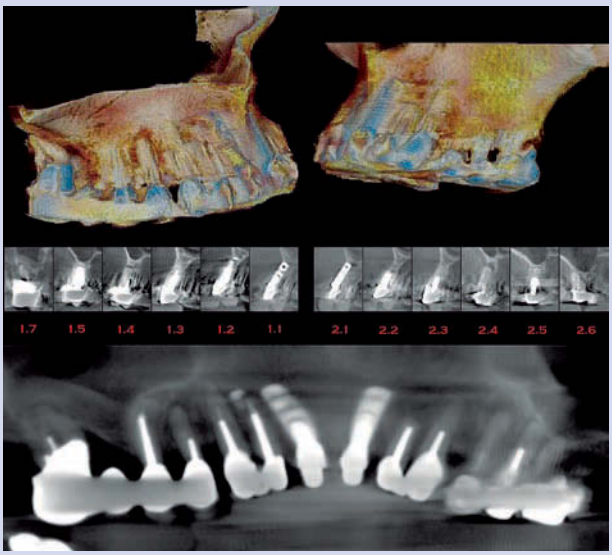

Fig. 7.1 a

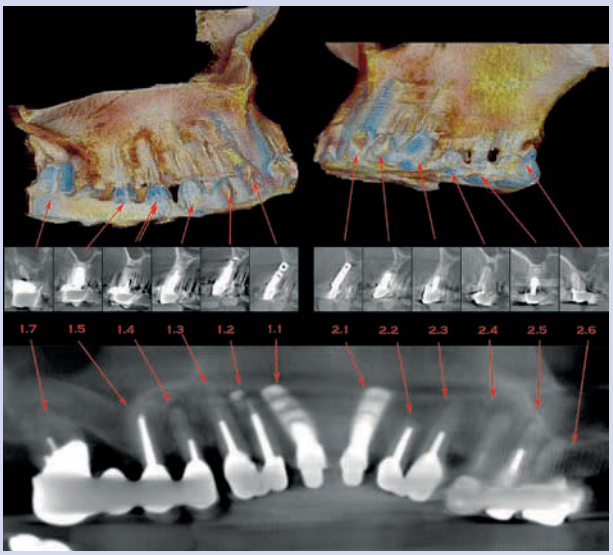

Fig. 7.1 b

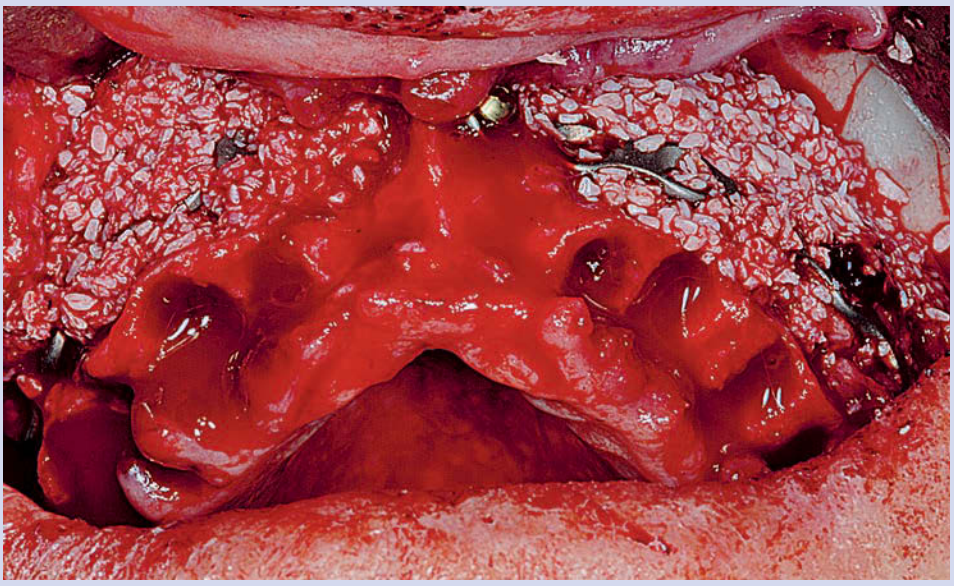

Fig. 7.2

CLINICAL CASE 7 *(cont'd)*

Roberto Ghiretti

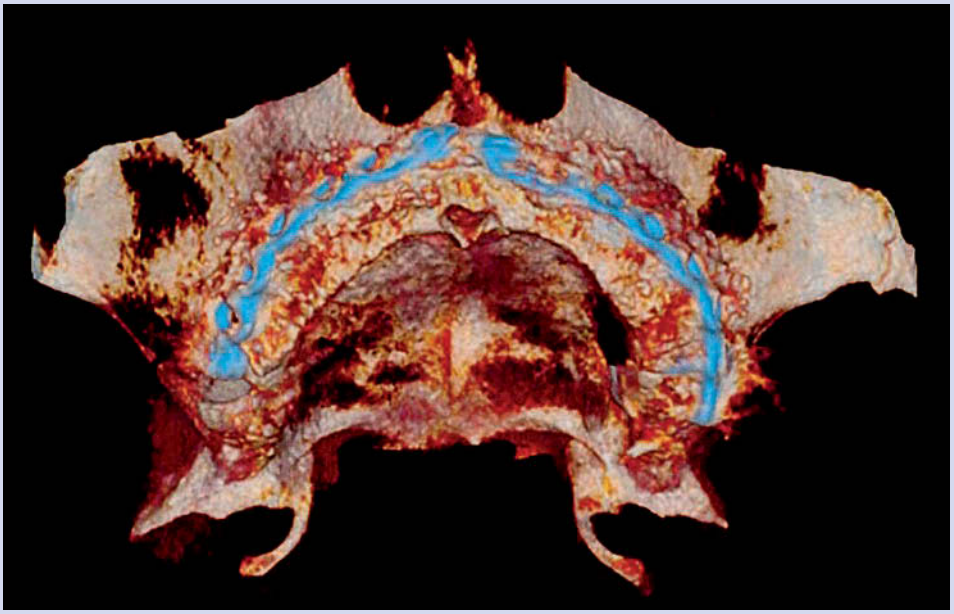

Fig. 7.3

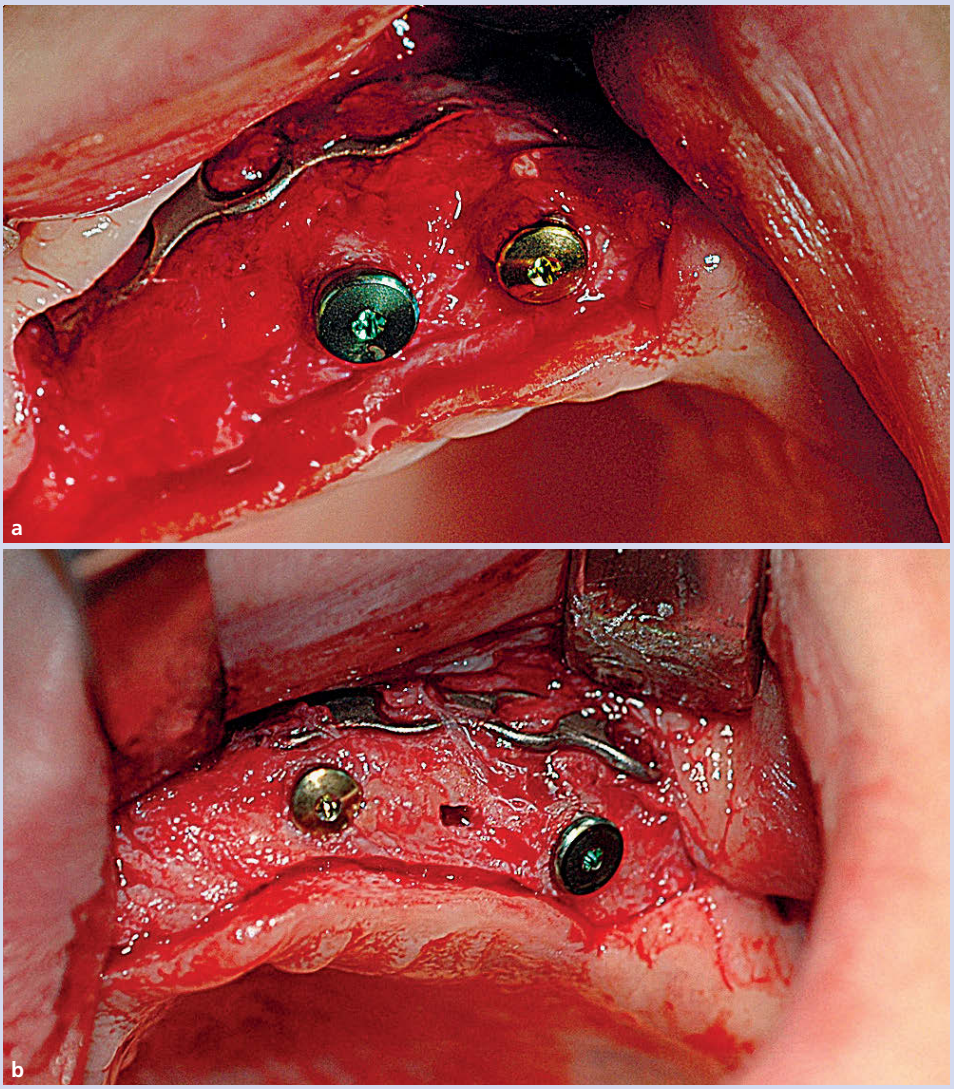

Fig. 7.4 a-b

Finally, the CBCT exam allows us to detect radiolucent lesions reaching the implant insertion area (Clinical Case 8).

CLINICAL CASE 8

Marco Vigna

A fifty-four-year-old male patient came to the office for aesthetic and functional recovery of the area from his upper right first premolar to his first molar (Fig. 8.1). The two-dimensional exam performed with a periapical radiograph (Fig. 8.2) showed such a large periapical lesion of his second premolar that extraction was decided upon. The CBCT performed two months later to plan the insertion of a fixture showed a large radiolucent area from the mesial-buccal root of the first molar to the alveolar area of the element extracted (Fig. 8.3).
The endodontic retreatment of the molar was planned. This treatment was performed by Dr. Ambu. Seven months later, the hard tissues seemed to be in the advanced stages of healing (Fig. 8.4).
The virtually planned implant insertion appeared successful (Fig. 8.5).

Fig. 8.1

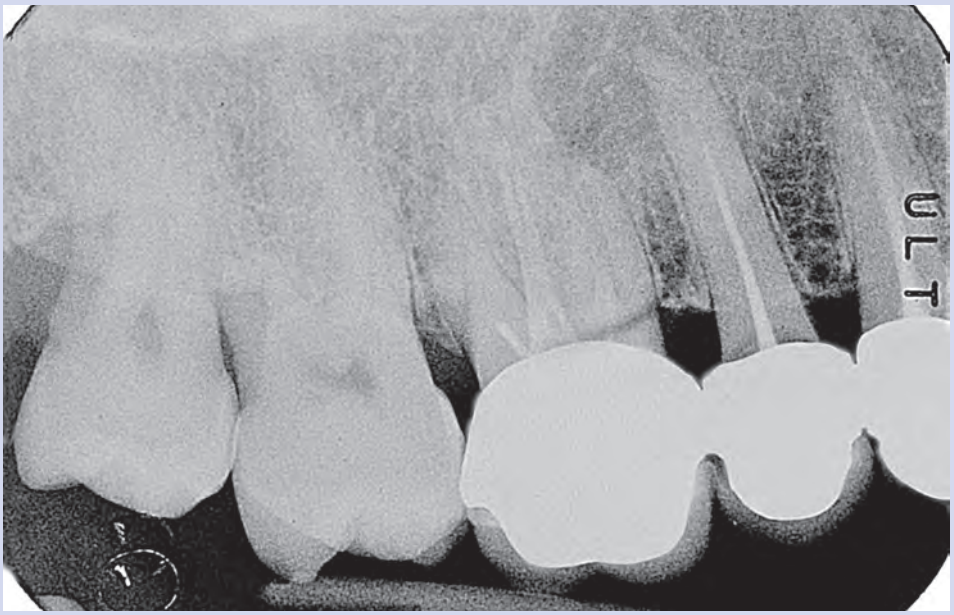

Fig. 8.2

CLINICAL CASE 8 *(cont'd)* | **Marco Vigna**

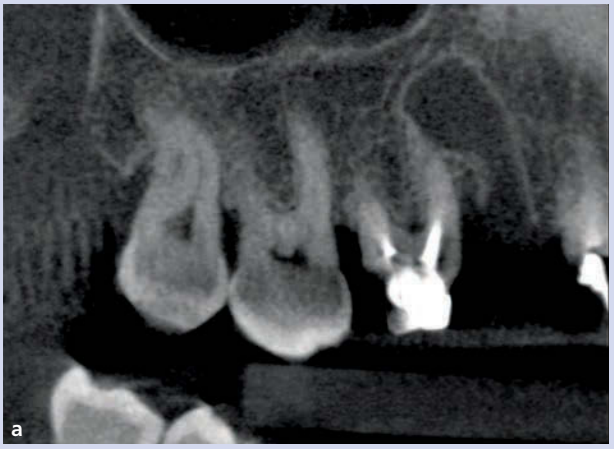

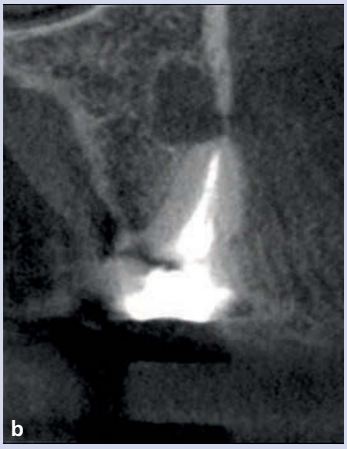

Fig. 8.3 a-b

Fig. 8.4 a-b

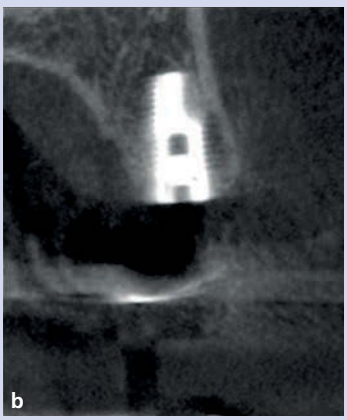

Fig. 8.5 a-b

Assessment and planning for implant insertion and axial direction to improve the biomechanical, functional, and aesthetic results

As suggested by the E.A.O. guidelines, this application will often require "the use of radiopaque reference points and restorative templates, even though data will be safely and accurately transferred through suitable programs for computer-aided surgery".
In this case, too, there are several articles confirming that the introduction of CBCT was successful in specialized practices that, for quite some time, had been taking advantage of CT in planning and clinical practice (Fortin et al. 2003; Nickenig and Eitner 2010).

The use of a template with radiopaque reference points helps the clinician to insert the implant correctly. Simpler systems have been devised to locate the position of implant placement, using surgical templates with radiopaque reference points, as suggested by Peck and Conte (2008) (Clinical Case 9).

CLINICAL CASE 9

Emanuele Ambu

A sixty-seven-year-old male patient came to the office to receive implant-prosthetic rehabilitation of the area of his lower left second premolar and first molar. After a diagnostic wax-up, we performed a radiological stent (Fig. 9.1). A hole was drilled in the stent, in the center of the occlusal face of the elements. This hole was filled with radiopaque material (gutta-percha). With the aid of the volumetric exam, we planned the accurate insertion of fixtures, taking into account the bone structure available and the prosthetic position (Fig. 9.2). Once the insertion axis was amended, the radiological stent was used as a surgical guide for fixture insertion. A second CBCT exam showed the accurate insertion of the implants (Fig. 9.3).

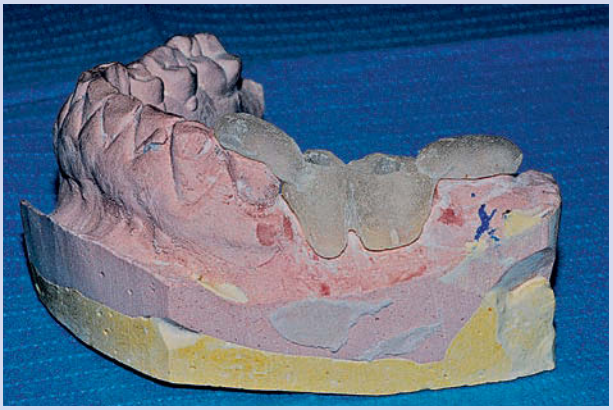

Fig. 9.1

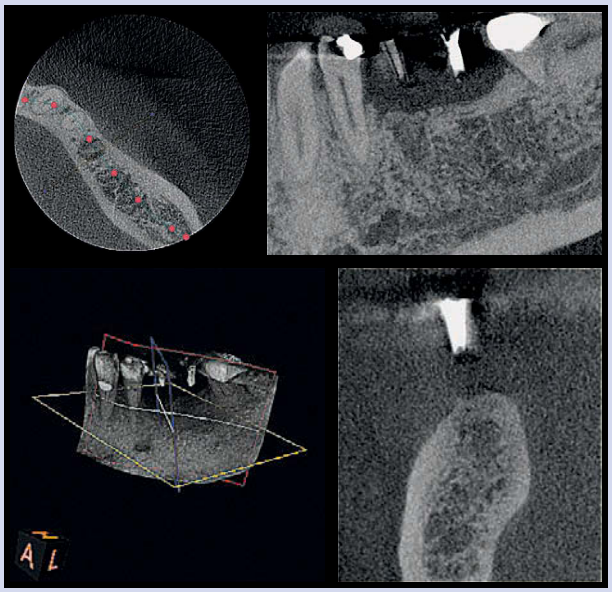

Fig. 9.2

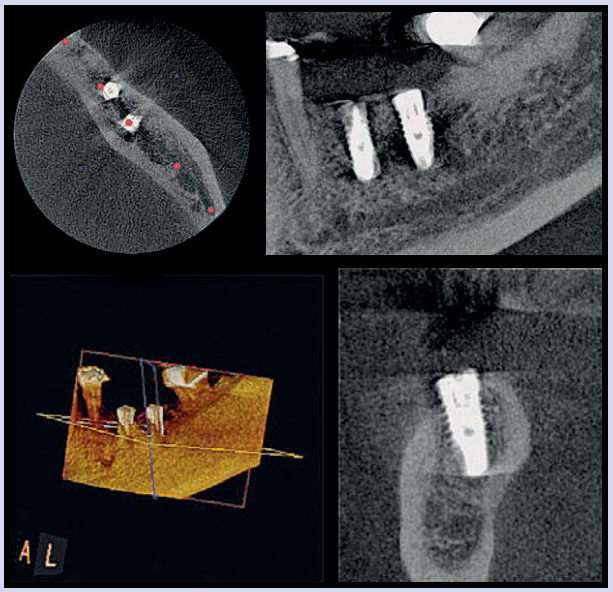

Fig. 9.3

The use of CBCT has widely increased thanks to computer-aided implantology systems. Ganz has shown the use of software in planning procedures to lift the maxillary sinus and to aid implant placement in the upper maxillary bone and implant rehabilitation in the lower maxillary bone, highlighting the path of various vascular and nervous systems (Ganz 2005). There are now several systems available that permit computer-aided implant placement starting from 3D volumetric images (Clinical Case 10).

CLINICAL CASE 10

Antonino Cacioppo

A fifty-seven-year-old female patient came to the office to receive functional rehabilitation of her upper right arch (from the first premolar to the second molar). We performed a panoramic radiograph (Fig. 10.1) and a volumetric exam (Fig. 10.2), and decided to perform implant prosthetic rehabilitation with a computer-guided system. This was aimed at exploiting the residual bone (anatomical function) and at inserting fixtures according to prosthesis requirements. The volumetric exam with a template supplied files in DICOM format so as to plan the implant insertion using implant 3D software (Media Lab) (Fig. 10.3). By means of a Ray Set system, we transformed the radiological template into a surgical one. At the end of the computer-guided insertion using a flapless technique, we positioned a temporary pre-built restoration. The post-op checkup with a panoramic radiograph showed the implant in the first premolar area was in contact with the canine area and the implant in the first molar area appeared to go into the maxillary sinus (Fig. 10.4). The CBCT performed to assess the actual implant insertion, proved that the procedure had been carried out properly (Fig. 10.5) and in compliance with the guided implant prosthesis planning (Fig. 10.6). There is a clear discrepancy between the 2D exam and the 3D one. The latter appears better and more reliable for a proper post-op control of implant insertions; it also exposes patients to less radiation (9.8 µSv vs. 7 µSv with OPG).

Fig. 10.1

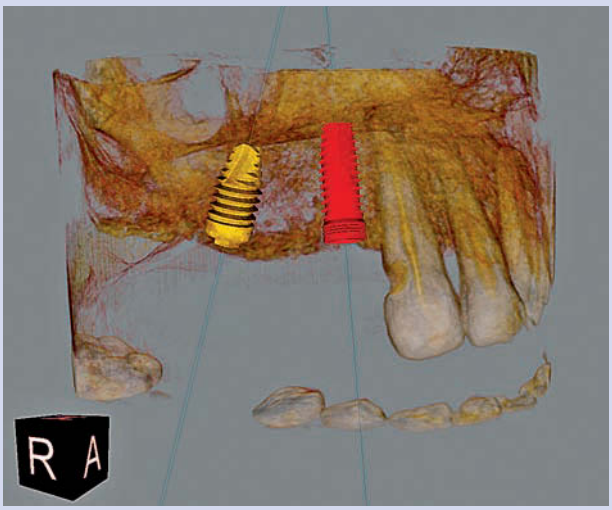

Fig. 10.2

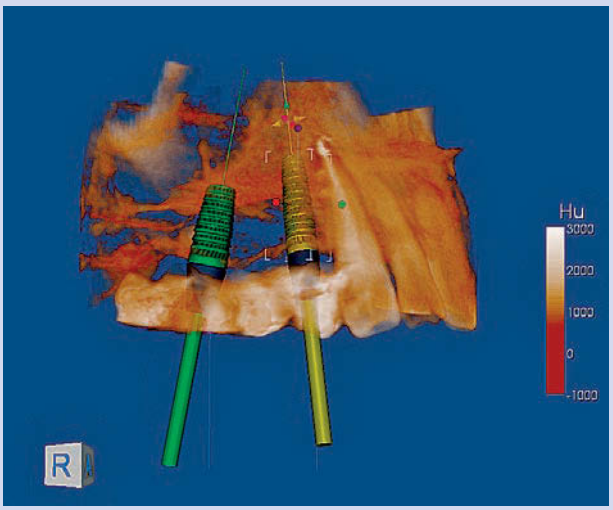

Fig. 10.3

CLINICAL CASE 10 *(cont'd)* | **Antonino Cacioppo**

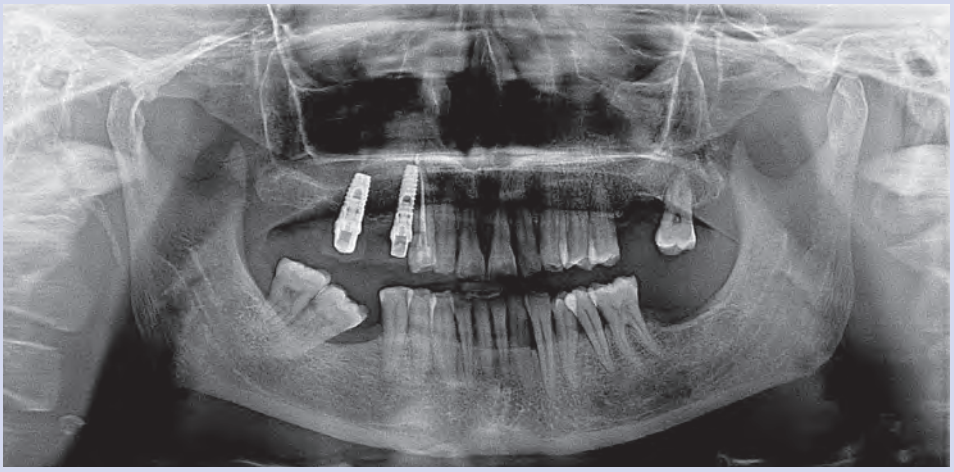

Fig. 10.4

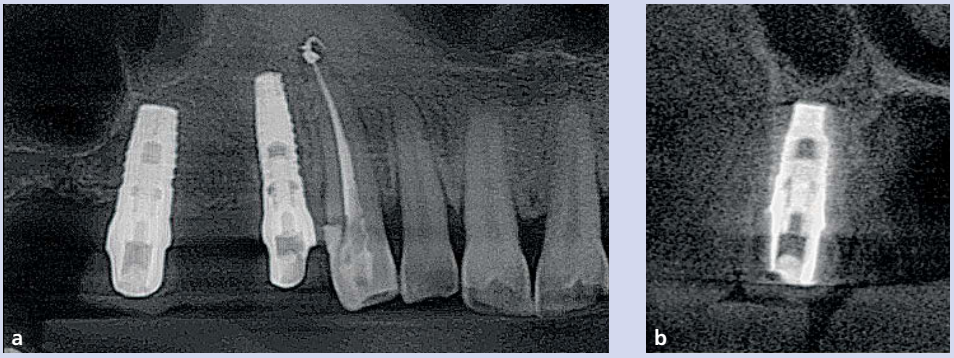

Fig. 10.5 a-b

Fig. 10.6

Finally, the use of CBCT with or without surgical templates was described in the placement of implants in front areas from an aesthetic perspective (Ganz 2008) (Clinical Case 11).

CLINICAL CASE 11

Vittorio Ferri

This patient had been complaining about recurrent abscesses in his upper right central incisor. The CBCT exam (Fig. 11.1) and the probing performed lead us to diagnose a vertical root fracture, which was confirmed after the extraction of the element (Fig. 11.2).

Fig. 11.1

Fig. 11.2

After the insertion of a conic implant (4 mm in diameter and 13 mm in length), we filled with biomaterials (Endobon BIOMET 3i and Hyaloss META) the 2 mm gap which we had voluntarily obtained between the implant margin and the gingival one (Fig. 11.3) so as to guarantee an attractive aesthetic result (Fig. 11.4).
The alveolus conditions did not permit us to place a temporary restoration, therefore we protected the material with a grafting of connective tissue taken from the palate (Fig. 11.5). Five months later, we checked the regeneration with a volumetric exam (Fig. 11.6) and then positioned the final restoration (Fig. 11.7).
In this case the use of a CBCT system made it possible to have excellent planning and performance of all surgical and aesthetic aspects.

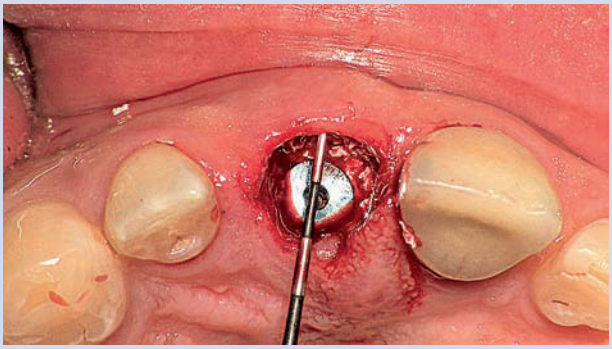

Fig. 11.3

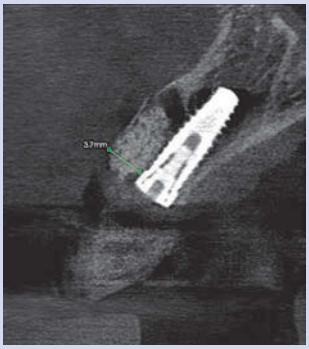

Fig. 11.4

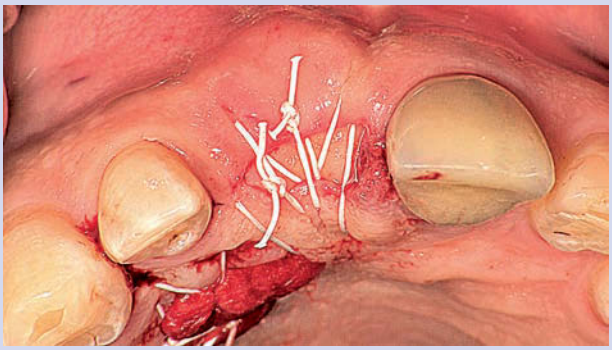

Fig. 11.5

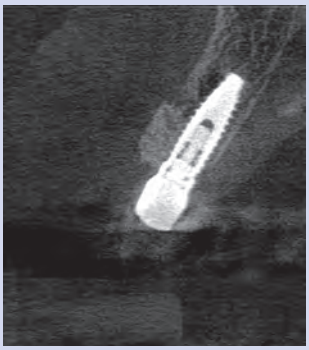

Fig. 11.6

Fig. 11.7

Endodontics

Emanuele Ambu

CBCT in endodontics

Scarfe et al. (2006) were the first to suggest the use of CBCT in endodontics. Medium FOV CBCT devices seem poorly effective in this particular sector, and the use of limited volume FOV is strongly suggested by some authors (Cotton et al. 2007; Patel et al. 2007; Patel et al. 2009). As we previously pointed out in chapter 2, limited volume FOV CBCT devices have been designed to supply high spatial resolution images thanks to the dimension of the voxel: the smaller the voxel, the greater the possibility of detecting very small structures. For example, if we have to detect a calcified root canal with a diameter of under 100 µm, we have to use a device that allows reconstructing slices with a smaller voxel. In his master's thesis, Bauman pointed out that accuracy in checking the MB2 canal in the upper first molar was over ninety-three percent with a 120-µm resolution, while it was reduced to lower than forty percent with a 400-µm voxel resolution (Bauman 2009).

According to the Joint Position Statement of the American Association of Endodontists and the American Academy of Oral and Maxillofacial Radiology, it is recommended to use CBCTs with a limited volume FOV in most endodontic applications, for the following reasons:

- Increased spatial resolution to improve such tasks as the visualization of small features, including accessory canals, root fractures, apical deltas, calcification, etc., which are essential in endodontics.
- Highest-possible spatial resolution with a diagnostically acceptable signal-to-noise ratio.
- Time savings due to smaller volume to be interpreted.
- Finally, limited volume FOV devices decrease radiation exposure to patients, while allowing us to examine an area with twice the size of that of conventional X-rays.

According to the summary of the aforementioned Joint Position: "Limited field of view CBCT systems can provide images of several teeth from approximately the same radiation dose as two periapical radiographs, and they may provide a dose savings over multiple traditional images in complex cases."
Limited volume FOV devices are very useful in the following applications in endodontics:

- Localization of root canal systems
- Presence, position, and size of periradicular/periapical radiolucency
- Identification and position of broken instruments
- Extension of root canal calcification
- Presence and position of root perforation
- Vertical root fractures (VRF) (see section on dental traumatology)
- Root resorptions (external, internal, invasive/cervical)
- Endodontic surgery planning
- Follow-up and failure analysis
- Differential diagnosis with non-endodontic diseases

We will now examine all of these applications further.

Presence and position of root canal systems

Today, CBCT imaging is the "gold standard" of *in vivo* epidemiological studies where differences in root canal anatomy in human populations are examined (Neelakantan et al. 2010; Tian et al. 2012).

Thanks to their high spatial resolution, limited volume FOV devices (CS 9000 3D, in this paper) seem to be very useful in *in vitro* root canal findings (Michetti 2010). Blattner et al. have underlined how essential CBCT systems are in finding the MB2 root canal in first upper molars (Blattner 2010), while La et al. highlighted CBCT imaging for accurate diagnosis and management of a third root canal system in the mesial root of a lower first molar (La et al. 2010).

Baratto Filho et al. demonstrated that the combined use of an operative microscope and CBCT was important for locating and identifying root canals in upper first molars, while CBCT devices could be chosen as a good diagnostic method for the first identification of the internal morphology of these teeth (Baratto Filho et al. 2009). Lastly, CBCT volumetric data provide largely accurate and reliable measurements of tooth and root length (Sherrard et al. 2010) (Clinical Case 12).

Presence, position, and size of periradicular/periapical radiolucency

In one third of cases it is impossible to diagnose the presence of a periapical lesion using conventional X-rays, because of anatomical and technical problems (Barthel et al. 2004). Lofthag-Hansen et al. have noted that limited volume FOV CBCT exams allow us to find all lesions that are not detected by conventional 2D radiology (Lofthag-Hansen et al. 2007). In this paper, lesions were detected in eighty-six roots using a small FOV CBCT device, while conventional 2D radiographs detected fifty-three lesions. The data supplied by Barthel et al. were confirmed by Low, who found that thirty-four percent of lesions were not detected by conventional X-rays (Low et al. 2008).

Lesions are often not detected when apices are very close to the maxillary sinus, or when the bone between the lesion and sinus floor is thinner than one millimeter.

Estrela et al. have compared the performance rates of OPG, X-rays and CBCT in detecting periapical lesions. The results were 17.6%, 35.3%, and 63.3%, respectively, examining 1,425 endodontically treated teeth, and 21.7%, 36.1%, and 74.7%, respectively, examining eighty-three untreated teeth (Estrela et al. 2008). The same group has proposed a new PAI (periapical index) to detect periapical lesions using CBCT devices (PAICBCT) (Estrela et al. 2008). The PAICBCT has been modified by Esposito et al., who suggested an image acquisition and processing method to have reproducable and standardized data (Esposito et al. 2011).

CLINICAL CASE 12

Emanuele Ambu

A sixty-nine-year-old female patient was referred to me because of persistent pain after endodontic treatment of her lower left third molar. The control X-ray showed a successful endodontic treatment, but a periapical radiolucency was detected in the apical area of the mesial root (Fig. 12.1).

The volumetric exam highlighted a radiolucency starting from the apical area of the mesial root and extending to the lingual periradicular bone, thus suggesting a vertical fracture. But, since the root appeared "L-shaped," as seen from the axial sections (Fig. 12.2), it was then possible to hypothesize the presence of a third canal. This was subsequently detected clinically and treated endodontically. The volumetric exam performed at the end of the treatment detected a lateral canal in the lingual side of the mesial root besides the three canals. This could explain the origin of the lesion in the corresponding bone area (Fig. 12.3).

The 3D reconstruction before (Fig. 12.4) and after this treatment (Fig. 12.5) displayed the peculiar endodontic anatomy of this element.

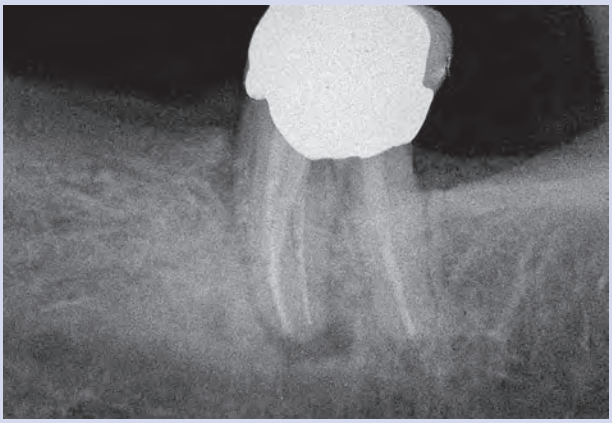

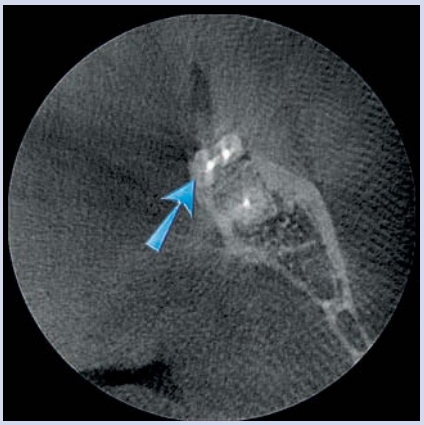

Fig. 12.1

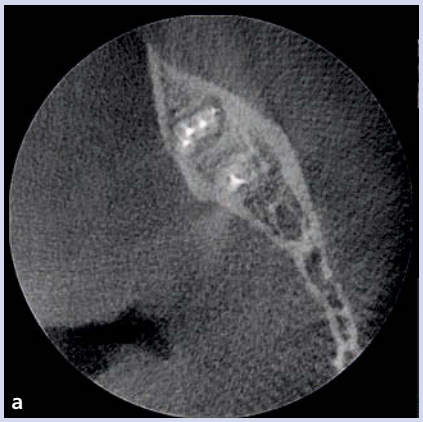

Fig. 12.3 a-b

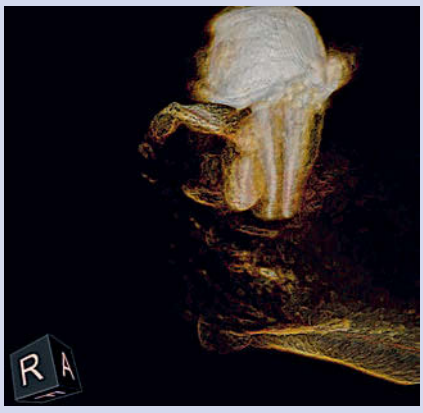

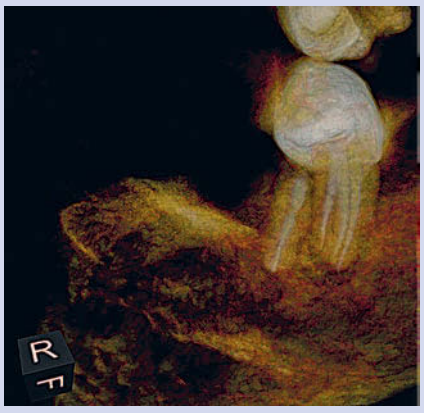

Fig. 12.4

Fig. 12.5

Some studies have focused their attention on the accuracy of CBCT devices in the differential diagnosis of cysts and granulomas.
Simon et al. pointed out that CBCT systems cannot perform a differential diagnosis of cysts and granulomas, but they are able to check whether the content of the area is liquid or solid (Simon et al. 2006).
On the contrary, Rosenberg et al. have found no accuracy of CBCT devices in this kind of differential diagnosis; according to them, an accurate diagnosis is only possible after surgery and a subsequent histological exam of the lesion (Rosenberg et al. 2010).
Kaya et al. have recently stated that it is possible to assess the changing bone density levels of periapical lesions before and after treatments, using Hounsfield units (Kaya et al. 2012) (Clinical Cases 13 and 14).

CLINICAL CASE 13

Emanuele Ambu

This male patient, a forty-eight-year-old dentist, came to my practice to have his two upper left incisors treated. The presence of a wide lesion already detected by the intra-oral X-ray performed in his practice (Fig. 13.1), was confirmed by the volumetric exam showing its real dimensions (Fig. 13.2). The follow-up digital X-ray he performed after fifteen months showed a sharp reduction in the size of the lesion (Fig. 13.3), which was also confirmed by the volumetric exam (Fig. 13.4). Afterwards, the follow-up digital intra-oral X-ray showed that the lesion had disappeared completely (Fig. 13.5), while the volumetric exam showed a good healing process but that the lesion was still there, although restricted to the medullary bone (Fig. 13.6). The volumetric exam also showed that the cortical area had reformed, and this is why the clinical pattern appeared to be completely resolved when using two-dimensional radiology.

Fig. 13.1

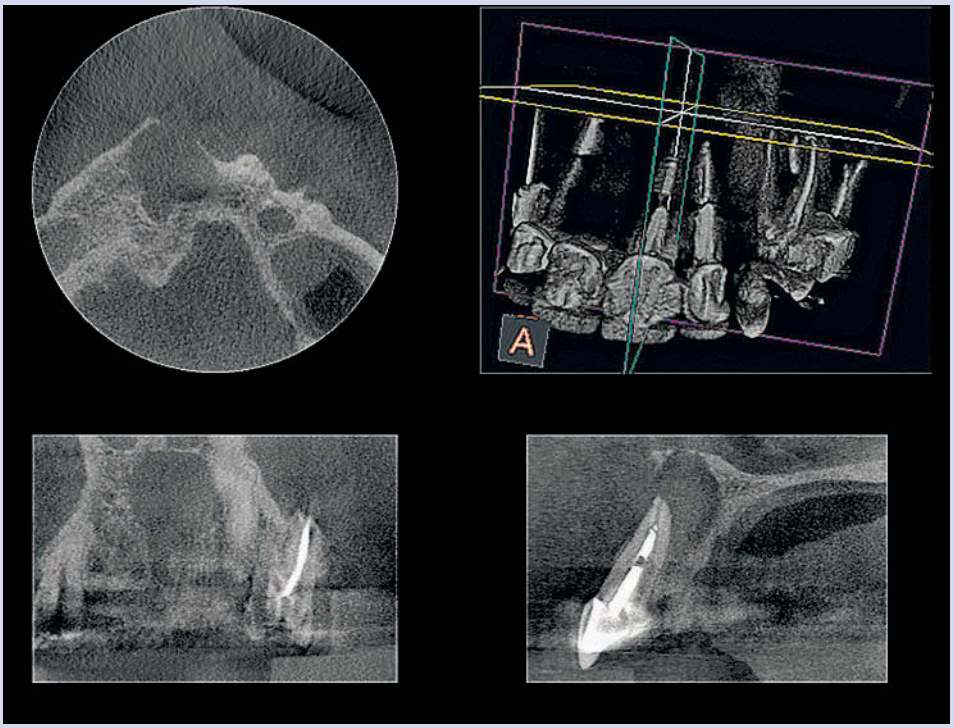

Fig. 13.2

CLINICAL CASE 13 *(cont'd)*

Emanuele Ambu

Fig. 13.3

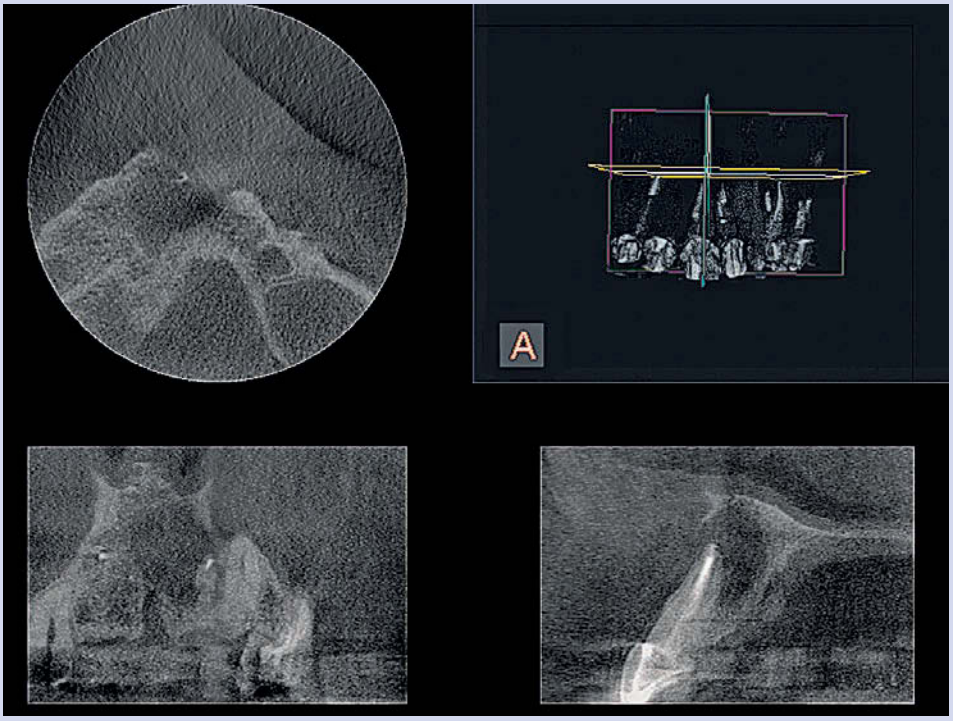

Fig. 13.4

Fig. 13.5

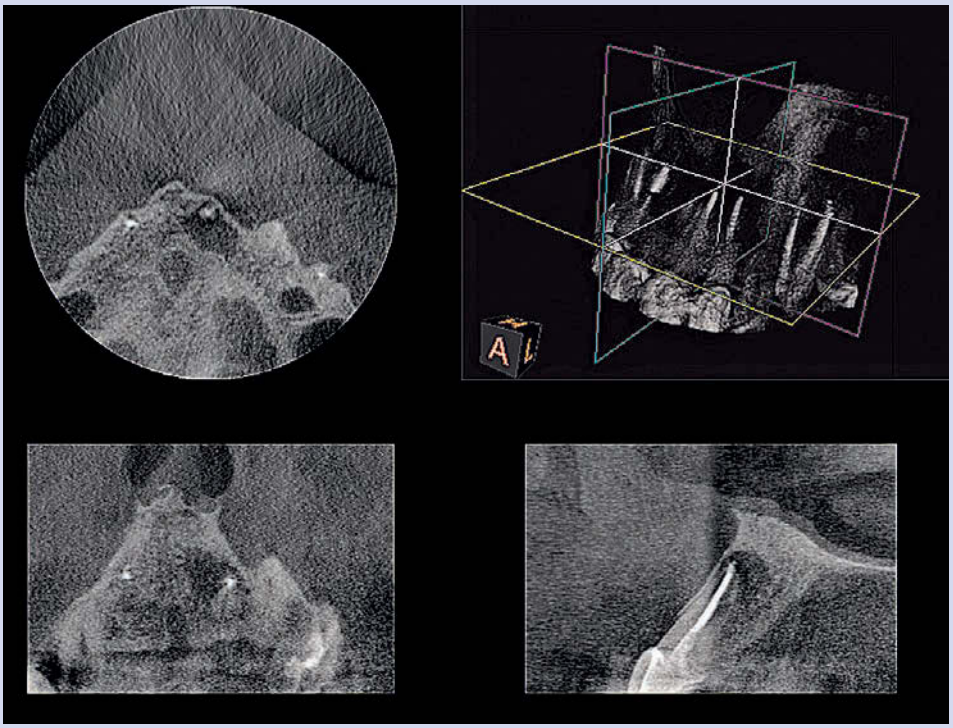

Fig. 13.6

CLINICAL CASE 14

Emanuele Ambu

This young female patient was referred to me because of pain in her upper left central incisor when biting. The conventional X-ray showed a large periapical lesion of the central incisor, which had been endodontically treated (Fig. 14.1). Furthermore, the patient reported frequent swelling in the palatal side of the same area, but closer to the lateral incisor apex.

Fig. 14.1

Fig. 14.2

The conventional X-ray showed no periapical radiolucency of this tooth, but an overfilling of cement was detected (Fig. 14.2). The CBCT exam showed the presence of a "liquid" radiolucency around the apex of the central incisor. A fragment of broken instrument inside the lesion was discerned (Fig. 14.3). A large "solid" radiolucency and the presence of extruded endodontic cement were detected around the apex of the lateral incisor (Fig. 14.4). Both teeth underwent endodontic surgical treatment and the diagnosis of a cyst in the central incisor was confirmed (fluid contents, presence of a connective wall). Histological exams allowed the diagnosis of foreign body granulomas, a lesion of 1.5 cm in the lateral incisor. The follow-up CBCT performed one year later showed good clinical success of both treatments (Figs. 14.5 and 14.6).

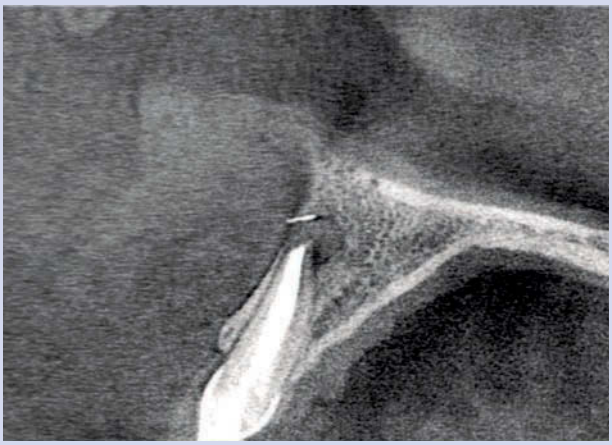

Fig. 14.3

Fig. 14.4

Fig. 14.5

Fig. 14.6

Localization and position of broken instruments

Although scientific literature is lacking, 3D imaging can help remarkably in detecting any problems clinicians may encounter during endodontic retreatments.
One of the main problems in endodontic retreatments is the presence of fragments of broken instruments inside the root canal system. As is well known, the position of the fragment and its relationship with the anatomical configuration of root canal systems may affect the feasibility of the treatment and, consequently, its outcome. If we bypass the fragment, we will be able to shape, clean, and seal the whole root canal system, allowing the periapical disease to heal. In the case of confluent root canals, we can reach the shared apical third through the "free canal," solving the problem clinically without removing the broken instrument. At any rate, it is often very difficult to detect the root canal confluence using 2D radiology, even if we take multiple pre-op and intra-op X-rays with different beam angles. The use of a 3D device allows us to explore the endodontic anatomy, checking the position of the fragment and the presence of confluent root canal systems (Clinical Case 15).

CLINICAL CASE 15

Emanuele Ambu

This twenty-two-year-old female patient was referred to me because of a fragment of an endodontic instrument in the mesial root of her lower right second molar. The root canals of this root showed a severe double curvature, and in the opinion of other clinicians, endodontic retreatment was almost impossible because this complex curvature made it very hard to remove the fragment with ultrasonic devices (Fig. 15.1).

The 3D exam allowed us to detect that the mesial-lingual canal, where the fragment had been broken, was confluent to the "free" mesial-buccal one (Fig. 15.2). This canal was first shaped, and the action of instruments pulled out the fragment, allowing the glide path of the mesial-buccal canal too. This canal was shaped up to the confluence, so both endodontic systems were cleaned and sealed with warm gutta-percha (Fig. 15.3).

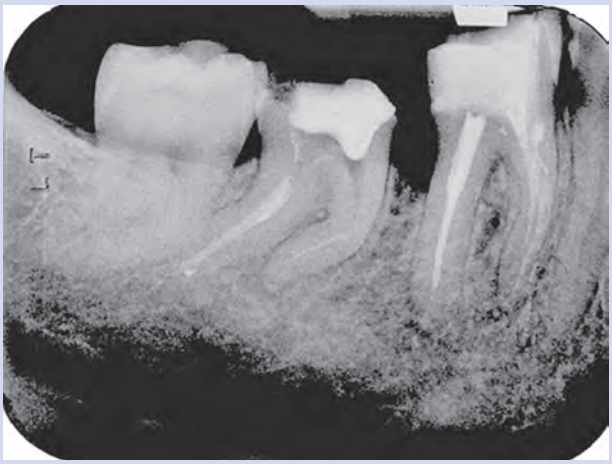

Fig. 15.1

Fig. 15.3

CLINICAL CASE 15 ***(cont'd)*** **Emanuele Ambu**

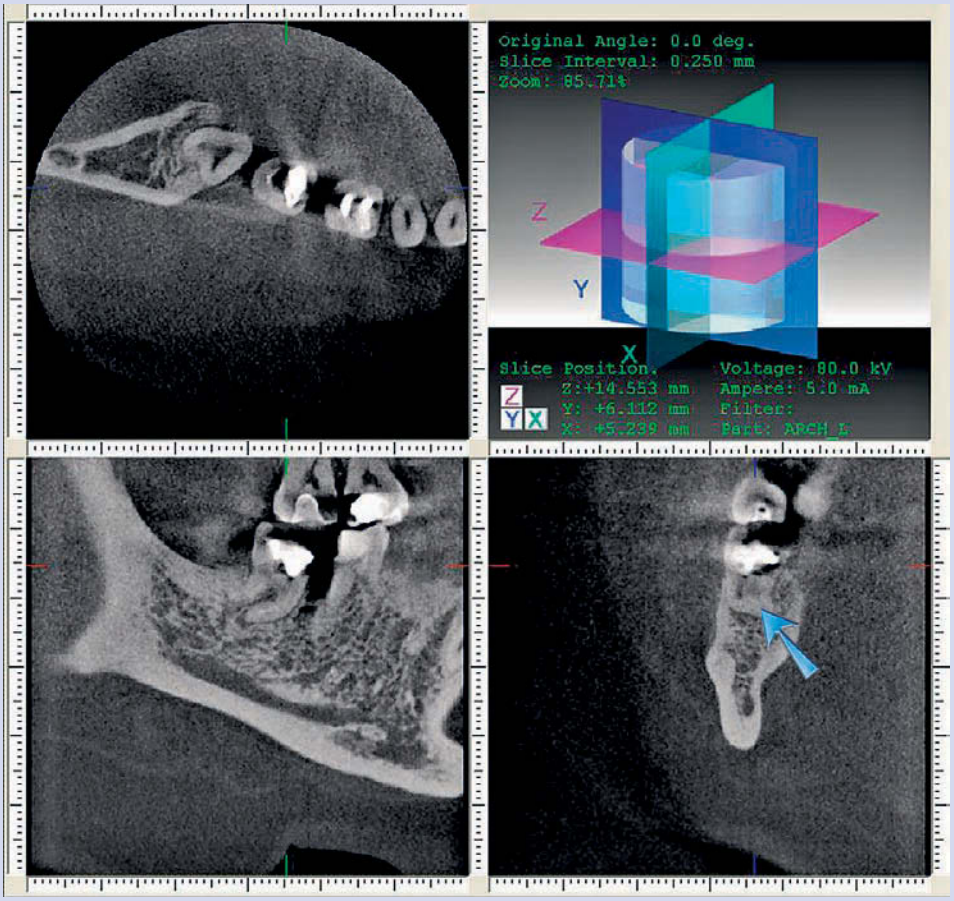

Fig. 15.2

Extension of root canal calcification

Calcifications often occur in endodontic treatments. We can often find them in upper incisors because of accidental traumas and in lower ones because of chronic traumas. Calcifications can appear in teeth with incorrect endodontic treatments and are due to the reaction caused by the cement. If the pulp is completely drawn back, the canal space is filled with the calcification tissue and there is no periapical radiolucency, the root canal treatment will be avoided; on the other hand, if the pulp is necrotic and we can see empty parts of the canal and periapical radiolucencies, endodontic therapy will absolutely be recommended. This treatment may be very difficult in the case of deep calcification, and the use of an operative microscope will be very helpful. The CBCT exam allows us to detect the presence of periapical radiolucency and to evaluate how deep the calcification is, enabling the correct diagnosis. If there is no root canal image and the periapical bone is healed, endodontic treatment will not be required. If there is a periapical radiolucency, we will have to check the extent of the root canal calcification and any contamination in the root canal system (Clinical Case 16).

CLINICAL CASE 16

Emanuele Ambu

This forty-four-year-old female patient was referred to my practice because of a wide calcification of her upper central left incisor. The referring colleague had made a perforation in the vestibular side of the coronal third of the root to find the root canal system. The volumetric exam showed the canal perforation and position. The canal looked calcified (Fig. 16.1). It was detected by an operating microscope (Fig. 16.2) and then treated. Both the canal and perforation were then sealed with warm gutta-percha and MTA, respectively (Fig. 16.3). The follow-up volumetric exam showed that the treatment had been performed successfully (Fig. 16.4). It should be noted that, by performing these two volumetric exams with a CS 9000 3D system, the patient was exposed to almost the same radiation dose as she would have been exposed to with an ordinary intra-oral X-ray (5.3 μSv vs. 5 μSv).

Fig. 16.1

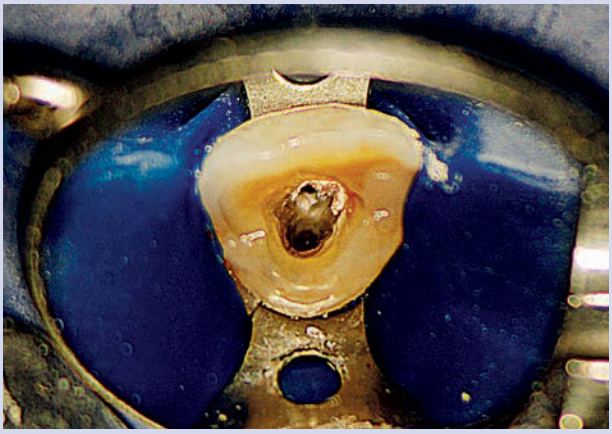

Fig. 16.2

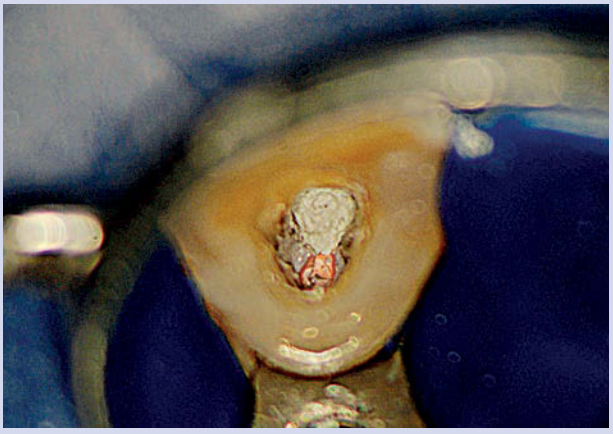

Fig. 16.3

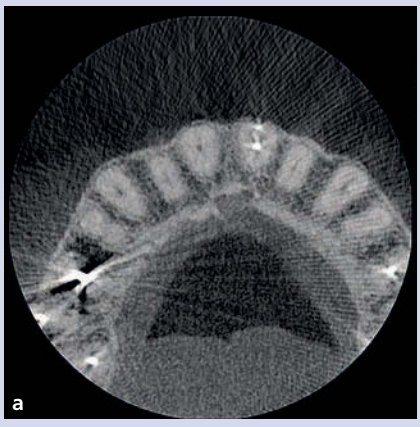

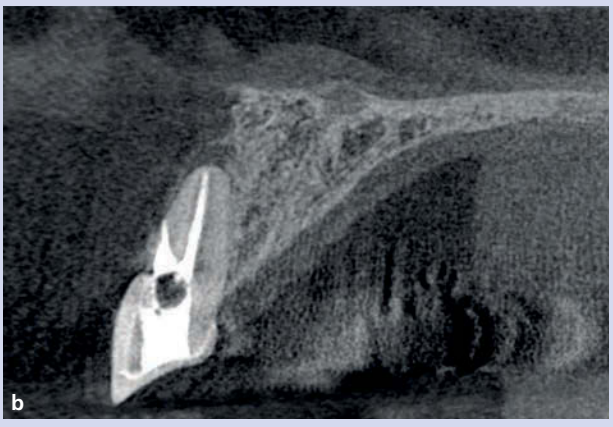

Fig. 16.4 a-b

Presence and position of root perforation

Perforations in endodontic systems can occur in several cases: in the floor and walls of the pulp chamber, "strip perforations" and perforations due to deviation in performing the dowel space. In most cases, the CBCT exam gives us clear and accurate information, but when used to diagnose root perforations, some clinical conditions may make the interpretation of data more difficult.

We do not have many studies in the literature about this matter. Young was the first to suggest the use of CBCT in a clinical case where 2D conventional radiology had been unsatisfactory in locating the perforation (Young 2007). In a laboratory study performed by D'Addazio et al. (2011), they reported that CBCT could identify root perforations in one hundred percent of samples, while periapical radiographs could not detect eighty percent of them (eighty percent inaccurate and twenty percent accurate samples). Furthermore, CBCT exams could accurately identify sixty percent of post deviations (forty percent of identifications turned out to be inaccurate); while twenty percent of post deviations were not detected by periapical radiographs, sixty percent of those detected turned out to be inaccurate and only twenty percent were accurately detected (D'Addazio et al. 2011). The results of this study are very interesting, despite the small number of samples, the presence of a single observer, and the use of a 0.2-mm slice.

In another laboratory study, Shemesh et al. showed that the risk of misdiagnosing strip perforations was high using both CBCT and periapical radiographs (Shemesh et al. 2011). Both *in vitro* studies had used human teeth in human bones and this could have highly affected this study because there is no periradicular radiolucency in the perforation area.

Metal post and core and gutta-percha inside the root canal and in strips or perforations reduce CBCT accuracy in detecting strips and perforations because of the well-known "beam hardening" problem. As a matter of fact, artifacts like scatter and beam hardening caused by very dense adjacent structures, such as gutta-percha, metal posts, pins, and crowns, may reduce the quality of CBCT exams (Mischkowski et al. 2007). Reis Bueno et al. suggested the use of a strategy to minimize artifacts due to the presence of cast metal post in root perforations. A dynamic examination of axial slices of each root from coronal to apical (or vice-versa) allows a "map-reading" (Rais et al. 2011). By scrolling the images, we can see where the shaped canal and the periodontal space with radiolucent areas meet. In this way, we can suggest the presence of root perforations. In the four cases shown, the presence of periodontal radiolucency connected to the perforation was highly emphasized. Another advantage of this "map-reading" approach is that, as the slices are located near the post tip, the "beam hardening" effect is reduced because the amount of metal is lower. These authors anticipate the development of new software filters to reduce the metal artifacts in CBCT images (Clinical Case 17).

Root fractures

(see Dental traumatology, page 104)

Root resorption

Root resorptions are a heterogeneous group of diseases with different pathogenesis, including external, internal, and cervical resorptions. Resorptions can be easily detected using CBCT, so a large amount of research has been published about these kinds of diseases.

CLINICAL CASE 17

Emanuele Ambu

This thirty-four-year-old female patient was referred to me because of persistent pain after an endodontic treatment. Her dentist reported the treatment of four root canals, the MB1 and the MB2 in the mesial-buccal root. The conventional X-ray pre-op exam did not help to diagnose the problem (Fig. 17.1). The CBCT exam allowed us to detect the perforation of the mesial-buccal root due to an incorrect shaping of the MB2 root canal. In addition, the confluent MB2 canal had not been shaped (Fig. 17.2). The MB1 canal was retreated, and the MB2 was shaped, showing the presence of an isthmus. The root perforation was sealed using MTA, while the root canal systems were sealed using warm gutta-percha (Fig. 17.3). The six-month follow-up CBCT exam showed the healing of periapical tissues (Fig. 17.4).

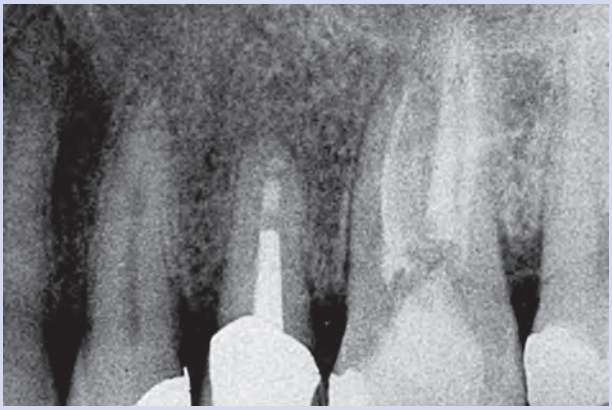

Fig. 17.1

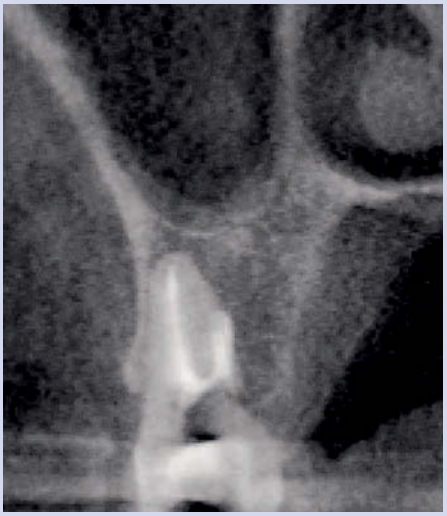

Fig. 17.2

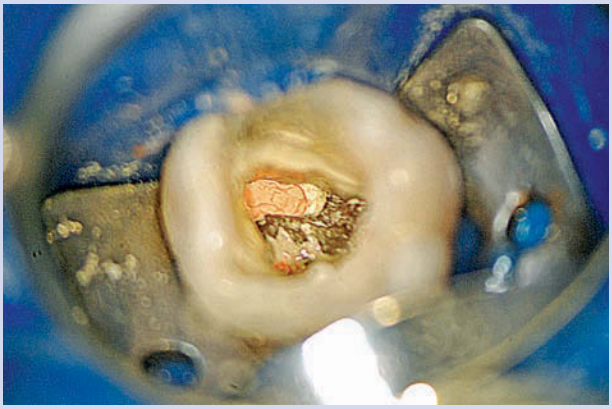

Fig. 17.3

Fig. 17.4

External root resorption (ERR)

Several papers have thoroughly described the use of serial cross-sectional CT to diagnose external resorptions (Kim et al. 2003; da Silveira et al. 2007). Cotton et al. suggested the use of CBCT devices to detect external resorptions (Cotton et al. 2007). The dimensions of the voxel are very important in the detection of ERR. Liedke et al. recommended a minimum voxel resolution of 300 µm to detect external lesions (Liedke et al. 2009). However, according to Ludlow, CBCT become more accurate as the voxel resolution of the volumetric data set increases (Ludlow 2008). Several laboratory and *in vivo* studies have been performed to examine the accuracy of CBCT in detecting ERR. One *in vivo* study showed that CBCT is more accurate in detecting resorption lesions than digital intra-oral radiography (Patel et al. 2009); according to D'Addazio et al., CBCT exams are remarkably accurate in detecting ERR (D'Addazio et al. 2011), and the same conclusion has been reached by two more *in vitro* studies (Liedke et al. 2009; Durack et al. 2011), although this experimental model has not been compared with the clinical situation. In fact, clinical conditions can be better detected because the radiolucency adjacent to the ERR and the resorption cavity may be different from the drilled defects prepared for research studies (Clinical Case 18).

CLINICAL CASE 18

Emanuele Ambu

A thirteen-year-old female patient was sent to my practice about sixty days after a sports trauma that had affected her two upper incisors.
The intra-oral X-ray (Fig 18.1) lead us to suspect an external resorption of the distal wall of her 2.1. Although the patient assumed that both elements were sensitive to cold, the volumetric exam showed that there was a periapical reaction of both teeth and that there was an external hemispherical resorption of the 2.1 (Fig. 18.2). Both elements were treated endodontically. The apex of the central incisor were sealed with MTA because it was very large (Fig. 18.3). The two-year follow-up volumetric exam showed that the clinical case had been resolved with a gap that was then restored with cement (Fig. 18.4).

Fig. 18.1

Fig. 18.3

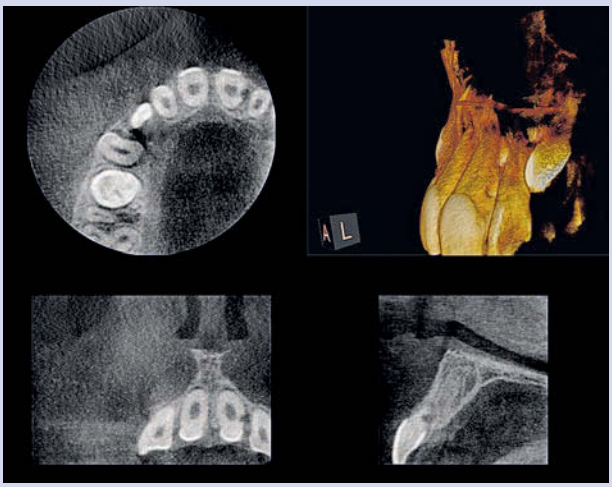

Fig. 18.2

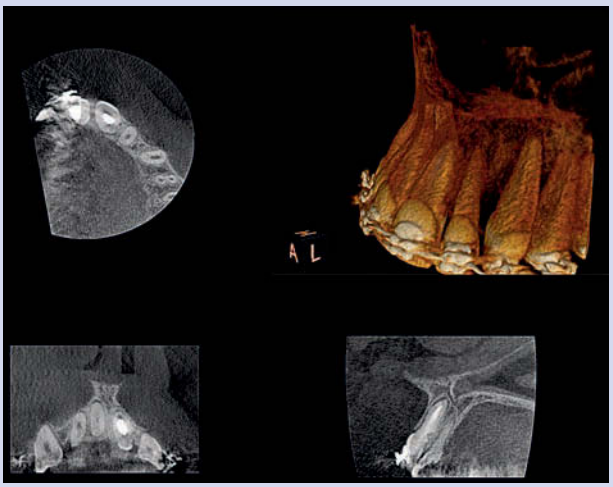

Fig. 18.4

Internal root resorption (IRR)

Except for pulpectomized deciduous teeth, internal root resorption is a rare pathologic finding, where multinucleated cells have destroyed predentin and odontoblasts as a result of chronic pulp infection or trauma.

Often asymptomatic, IRR could be detected as a well demarcated, round radiolucency widening out of the root canal. We can find it more frequently in the coronal part of the root, especially in the cervical area, but we might see it in all the areas of the root canal system. Patel et al. have compared conventional 2D radiology and CBCT (Patel et al. 2009). They discovered that the sensitivity level of X-rays is high (ROC Az 0.78) when diagnosing IRR, but the sensibility level of CBCT is all the more excellent (Az 1.00). According to the authors, CBCT is much more accurate than conventional radiographic techniques in assessing root resorption lesions.

Conventional and digital intra-oral radiographic techniques are most commonly used to detect IRR, but a differential diagnosis with ERR is often required. In the case of external resorptions, the area of radiolucency will show movements when multiple radiographs are taken from the mesial and distal angles, whereas in the case of internal resorptions, the defect will still appear close to the canal (Frank and Torabinejad 1998).

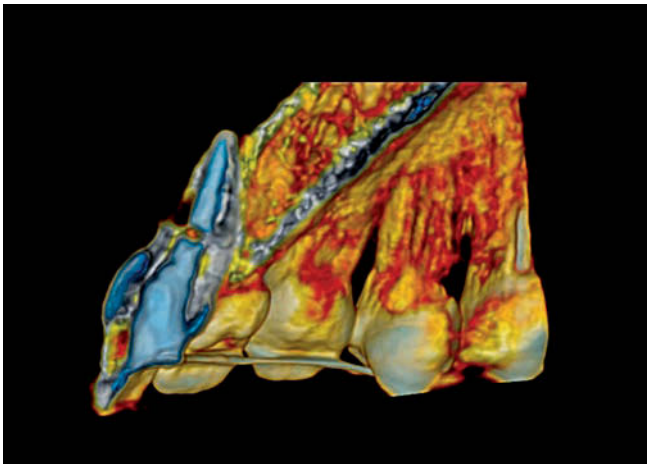

Kleoniki et al. have suggested taking three radiographs—an orthoradial one and two with a 20° horizontal variation in the mesial and distal angles, respectively—to diagnose the IRR (Kleoniki et al. 2002). To accomplish this, the patient would be exposed to a large amount of radiation. Moreover, detecting internal resorption using conventional intra-oral techniques also depends on the size and location of the lesion, with small apical defects that are hard to diagnose.

In conclusion, several factors may reduce the performance of conventional or digital radiographs in IRR diagnosis: beam angle, overlapping anatomical structures, patient-related factors, and the limitations of 2D radiology in detecting 3D structures.

Bhuva et al., describing the treatment of a perforated internal root resorption, have stressed the features of small fields of view in its diagnosis and the management of this disease (Bhuva et al. 2011). The CBCT scan facilitated the pre-operative actual localization of the perforation which could not be determined with conventional radiology.

Furthermore, CBCT helped clinicians in surgical procedures where a palatal perforation five millimeters away from the apex could not have been detected by conventional radiographs or direct visualization, and the position of the root-end resection was easily determined directly below the perforation. According to the authors, the low radiation dose to the patient and the large amount of information obtained using a small FOV CBCT justified its use in IRR treatment (Clinical Case 19).

CLINICAL CASE 19

Elisa Cuppini

This twenty-thee-year-old female patient came to my dental practice because of swelling in the palatal area of her upper left central incisor. The tooth had been retreated one year before. The conventional X-ray did not show any sign of endodontic failure (Fig. 19.1), so a CBCT was performed. An examination of the data showed the presence of a palatal radiolucency, close to the medial third of the root, where a round enlargement of the canal was noticed (Fig. 19.2 a, b). IRR was diagnosed. A surgical treatment was planned.

After flap lift, the position of the internal resorption was marked on the vestibular bone according to the CBCT image. Then, the vestibular bone and the root wall were removed and the resorption area was found (Fig. 19.3), cleaned using ultrasonic tips, and sealed with MTA. Root-end surgery and retrograde filling were also performed, and the flap stitched. The six-month follow-up CBCT exam showed that the periradicular tissues had been restored and the resorption area was properly sealed (Fig. 19.4 a, b).

Fig. 19.1

Fig. 19.2 a

Fig. 19.2 b

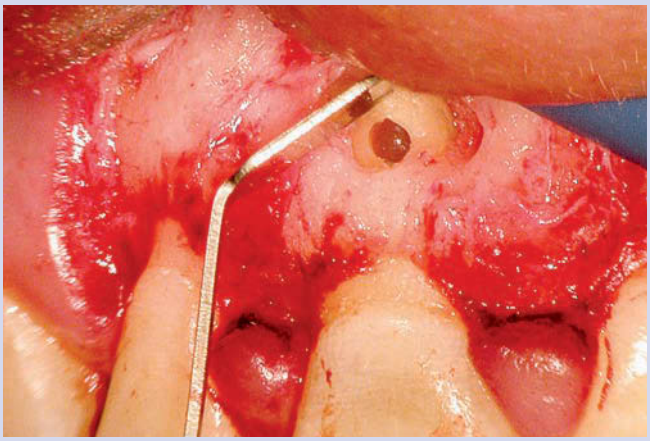

Fig. 19.3

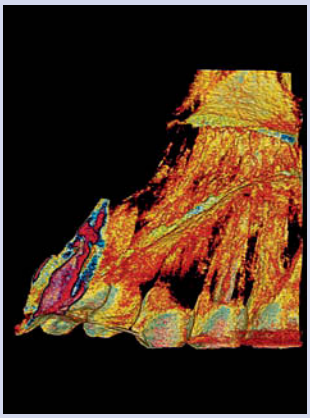

Fig. 19.4 a

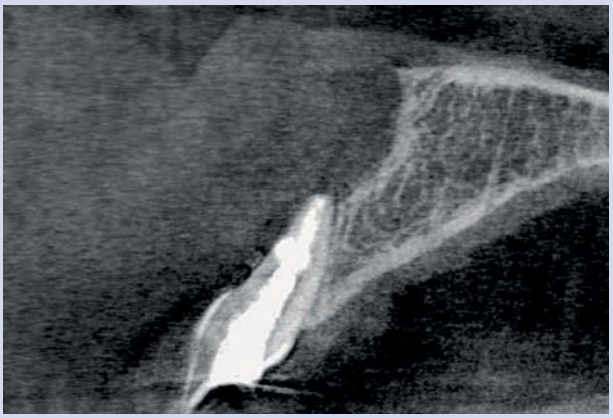

Fig. 19.4 b

Invasive cervical resorption (ICR)

Invasive cervical resorption is a type of external resorption which affects mineral dental tissues (cement and dentin), while pulp tissues are preserved longer because the layer of predentin is unmineralized.

ICR starts taking effect below the epithelial attachment and may reabsorb the root almost entirely. Heithersay established a clinical classification of ICR based on four classes according to the degree of damage of mineralized tissues (Heithersay 1999). Using conventional 2D radiology, ICR appears at the beginning as a cloudy radiolucency in the cervical area of the tooth; its borders are usually poorly defined (Patel et al. 2009). The root canal walls should be visible and running vertically through the radiolucent defect, indicating that the lesion does not lie within the root canal (Heithersay 1999). A second exposure, performed according to the "parallax technique," may confirm the presence and the location of the defect (Haapasalo and Endal 2006).

In any case, intra-oral radiographs cannot detect the true size of the lesion (Kim et al. 2003). Furthermore, the defect may spread in all directions inside the root, and this could not affect the size and position of the radiolucency detected on the radiograph (Patel and Dawood 2007). Cohenca et al. have underlined the limits of conventional radiology in the diagnosis and management of ICR (Cohenca et al. 2007b).

Kim et al. suggested the use of CT in detecting ICR (Kim et al. 2003); one of the advantages of CBCT over CT scanners is the lower radiation exposure (Cotton et al. 2007; Patel et al. 2007; Scarfe and Farman 2008). The use of CBCT in the diagnosis and management of an isolated case of ICR has been reported (Cotton et al. 2007: Patel et al. 2007; Patel and Dawood 2007; Scarfe and Farman 2008). Cohenca et al. described the use of CBCT in the treatment of ICR lesions due to dentoalveolar traumas (Cohenca et al. 2007).

Patel et al. compared the accuracy of intra-oral periapical radiography and CBCT, and concluded that CBCT was much more accurate than conventional radiography. They also underlined that "CBCTs superior diagnostic accuracy also resulted in an increased likelihood of correct management of resorption lesions" (Patel et al. 2009).

Recently, two case reports describing the use of CBCT in diagnosis and management of ICR have been published. Estevez et al. have reported the conventional and surgical endodontic treatment of a central incisor affected by a large ICR: the use of CBCT in diagnosis, management, and follow-up was stressed (Estevez et al. 2010). Yu et al., reporting a case of multiple idiopathic cervical resorptions, underlined that CBCT has shown that the lesions were larger and more widely distributed than what was seen using conventional radiography (Yu et al. 2011).

The use of CBCT in the diagnosis of multiple idiopathic cervical resorptions was strongly suggested (Clinical Case 20).

CLINICAL CASE 20

Emanuele Ambu

This twenty-eight-year-old female patient was referred to me because of a large periapical lesion of her 1.6. The element's response to cold tests was positive. A twelve-millimeter-deep pocket was probed in the mesial-buccal area (Fig. 20.1). The CBCT exam confirmed the presence of this periapical lesion and also detected a resorption area due to ICR (Fig. 20.2).

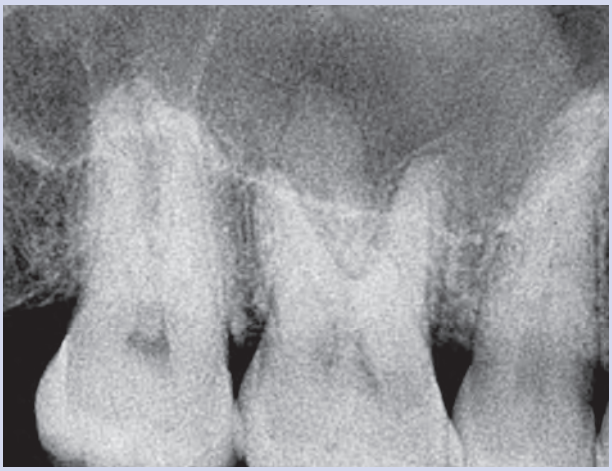

Fig. 20.1

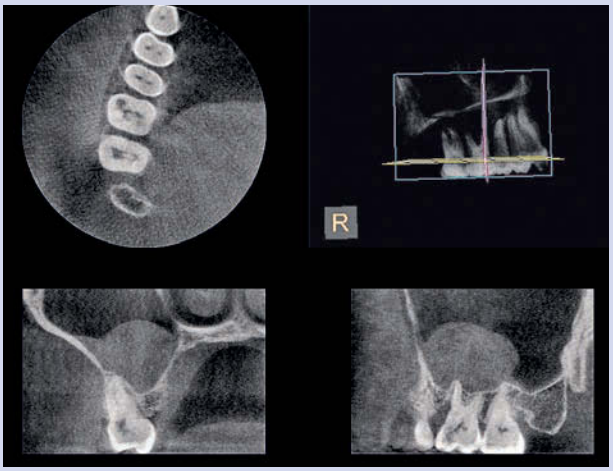

Fig. 20.2

By removing the resorption tissue, it could be seen that the lesion had extended to the pulp chamber, necrotizing the vascular nervous system of only the MB1 canal (Fig. 20.3). The element was treated endodontically (Fig. 20.4) and the resorbed tissue was restored with MTA (Fig. 20.5) in the subgingival areas and with composite to reconstruct the crown, respectively.

Fig. 20.3

Fig. 20.4

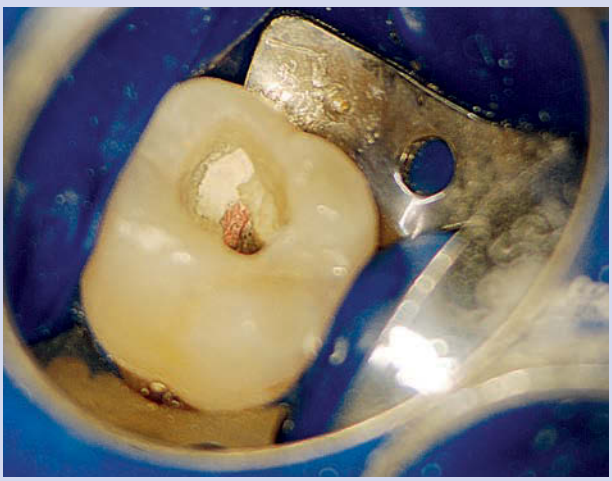

Fig. 20.5

Endodontic surgical planning

Rigolone et al. were the first to suggest the features of CBCT in endodontic surgery (Rigolone et al. 2003). They studied the mean distance between the palatal root of forty-three upper first molars and the vestibular cortical bone, and the presence of lateral sinus recesses lying between the buccal and palatal roots. These data may help clinicians choose from which side, either buccal or palatal, to approach the palatal root. They concluded that CBCT could play an important role in planning the vestibular access to the palatal root during endodontic surgery. Nakata et al. presented a case report where a periradicular lesion was located in a specific root and underlined the importance of CBCT when planning apical surgery of teeth adjacent to the maxillary sinus (Nakata et al. 2006). Tsurumachi and Honda described the use of CBCT in localizing a fractured endodontic instrument protruding into the maxillary sinus prior to endodontic surgery (Tsurumachi and Honda 2007). Pinsky et al. introduced the use of a computer to create surgical guides in endodontics (Pinsky et al. 2007). The aim of this study was to compare apical access accuracy using a guide versus the conventional "freehand method." It followed that that the apex was more precisely and consistently located using a guide based on computer-aided technology. Buchanan, during the AAE Annual Session in San Diego in April of 2010, showed a CT-guided endodontic surgery. He used the treatment planning software SimPlant, which is commonly used in implantology, to create a guide to access the apical area (Mortman 2011) (Clinical Case 21).

CLINICAL CASE 21

Emanuele Ambu

This thirty-five-year-old female patient was referred to me because of persistent pain when chewing, after endodontic retreatment of her lower left first molar. The X-ray showed an excellent treatment but also the presence of radiolucent lesions in both apices. We then decided to perform the surgical endodontic treatment of both roots. Before treatment, we performed a volumetric exam to plan the surgery (Fig. 21.1).

At the end of the surgery, we performed one more volumetric exam to check whether the retrograde sealings had been properly positioned (Fig. 21.2). The one-year follow-up exam showed that the periapical hard tissues had completely recovered (Fig. 21.3). Comparing both three-dimensional renderings, one performed at the end of surgery (Fig. 21.4) and the other performed one year later (Fig. 21.5), we could estimate the healing.

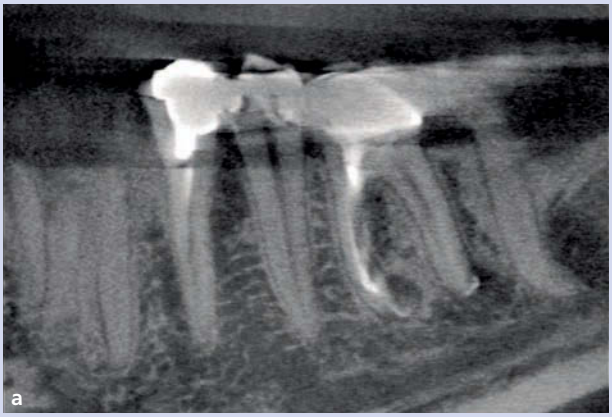

Fig. 21.1 a-b

CLINICAL CASE 21 *(cont'd)*

Emanuele Ambu

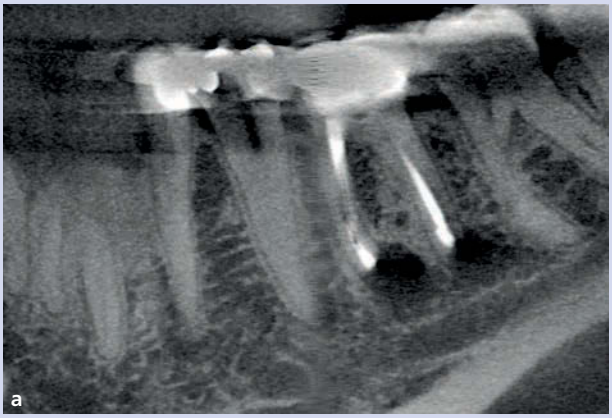

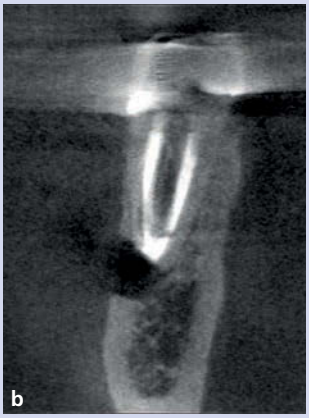

Fig. 21.2 a-b

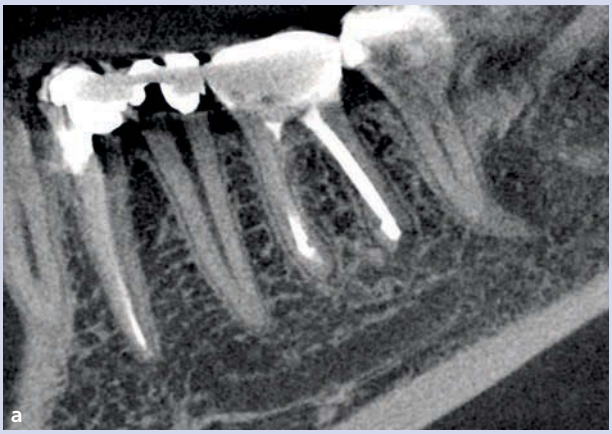

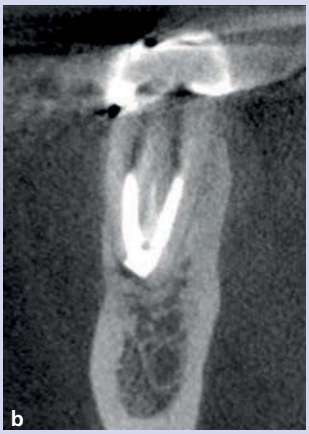

Fig. 21.3 a-b

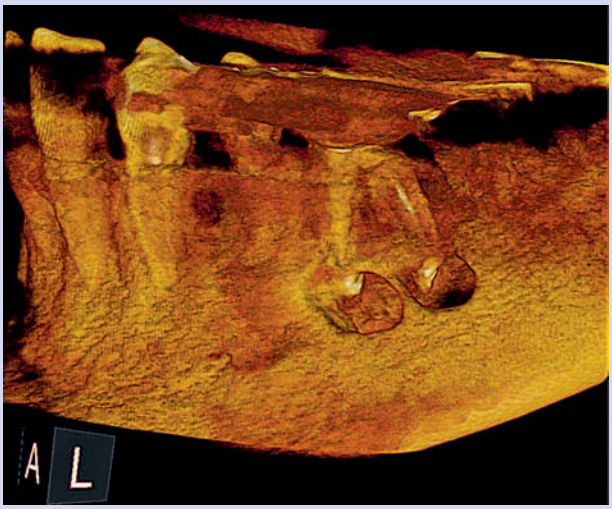

Fig. 21.4

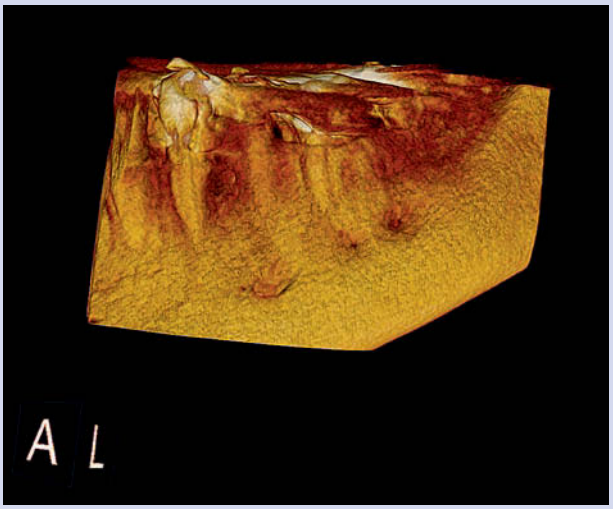

Fig. 21.5

The following case shows the advantages of using volumetric exams to plan endodontic surgery when there is a large lesion (Clinical Case 22).

CLINICAL CASE 22

Emanuele Ambu

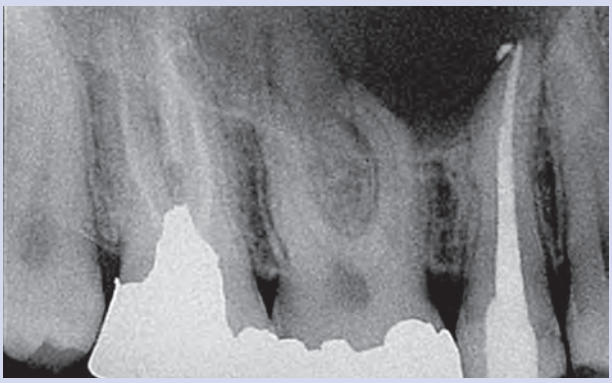

Fig. 22.1

Although the upper right second premolar of the female patient had been properly treated, her periradicular disease had not been healed (Fig. 22.1).
The eighteen-month follow-up exam showed that there was still a large liquid lesion (Fig. 22.2). Once the flap had been lifted, the lesion was removed (Fig. 22.3), an apicoectomy was performed and the retro-cavity was sealed (Fig. 22.4).
The post-op X-ray showed that the retrograde sealing had been properly positioned (Fig. 22.5). The six-month follow-up volumetric exam showed that all periradicular tissues had completely recovered (Fig. 22.6).

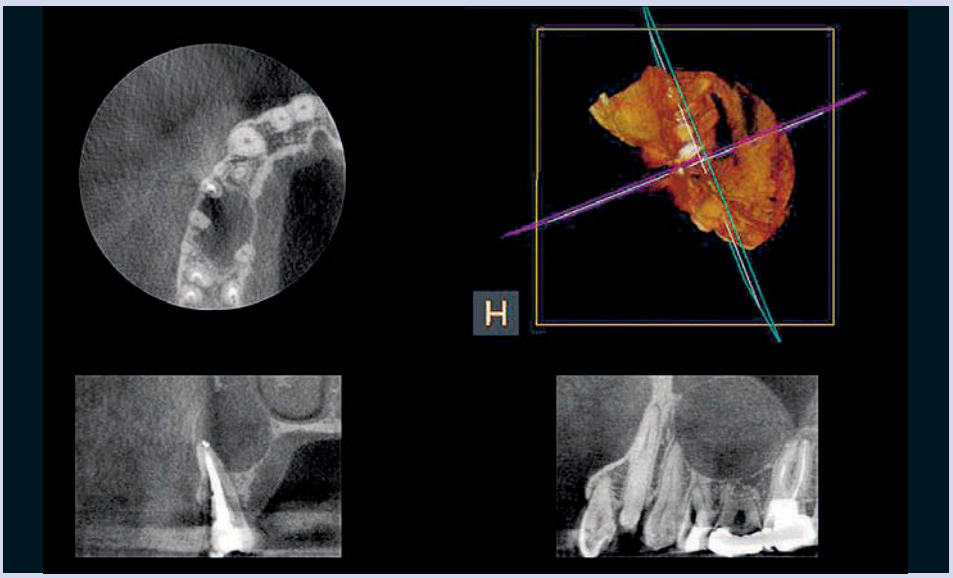

Fig. 22.2

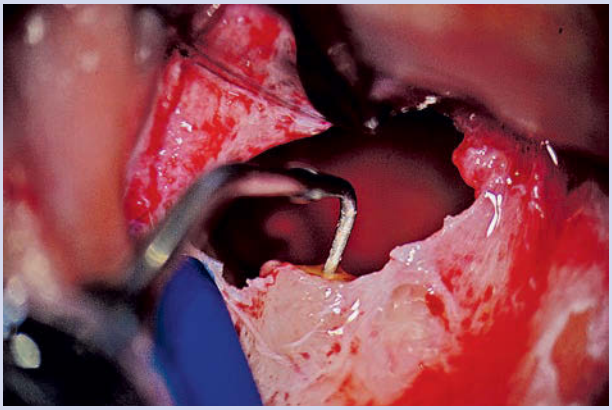

Fig. 22.3

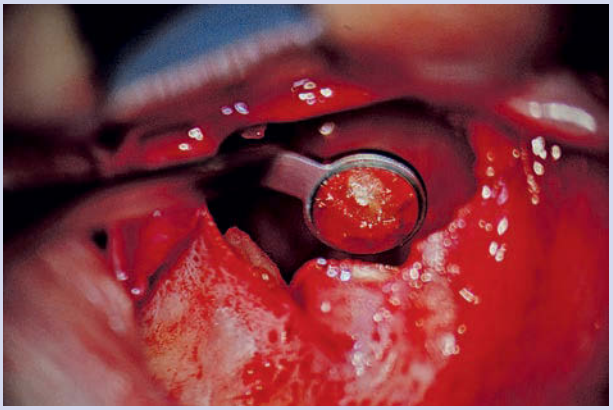

Fig. 22.4

CLINICAL CASE 22 ***(cont'd)*** **Emanuele Ambu**

Fig. 22.5

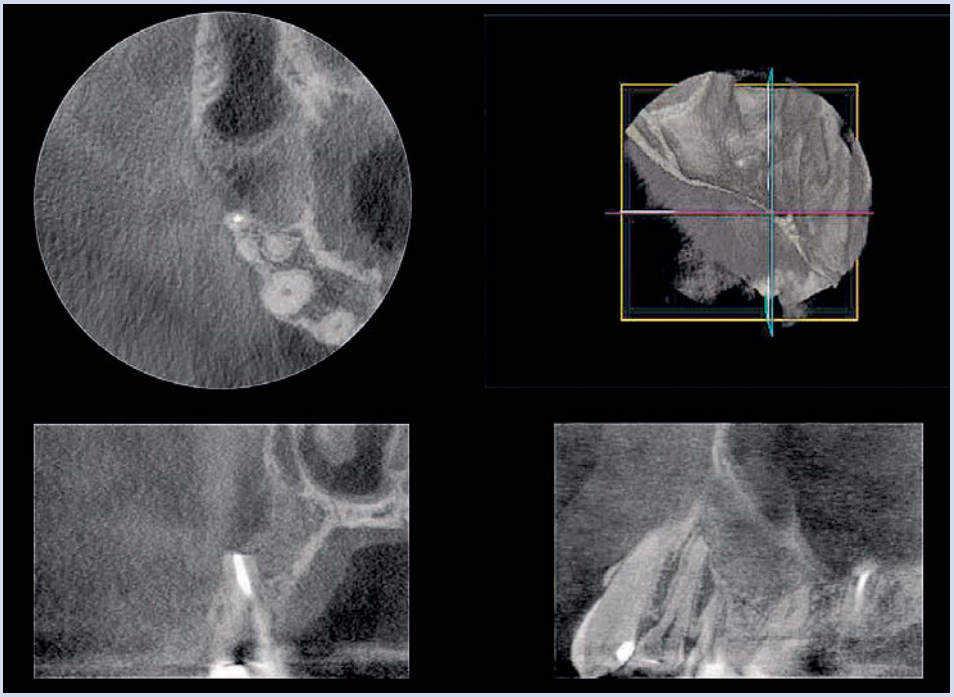

Fig. 22.6

Follow-up and failure analysis

It is well known that two-dimensional radiographs do not provide reliable information in endodontic epidemiologic investigations and clinical outcome studies, due to their limitations in the detection of periapical radiolucencies (Clinical Case 23).

CLINICAL CASE 23

Emanuele Ambu

This forty-six-year-old female patient was referred to me because of persistent pain in her upper right first molar, which had been previously accurately treated. She had been treated in a practice with no three-dimensional radiological systems. The intra-oral X-ray had shown a radiolucent lesion in the mesial-buccal root (Fig. 23.1), suggesting that it was possible to surgically treat only the two canals of this root (Fig. 23.2).

Fig. 23.1

Fig. 23.2

At the six-month follow-up, the patient still complained of persistent pain, even though the intra-oral X-ray showed that the problem had been resolved. A volumetric exam was then performed showing that the lesion in the mesial root had disappeared (Fig. 23.3), but that there was a periradicular lesion at the apex of the distal-buccal root (Fig. 23.4). One more treatment was performed and the clinical case was finally resolved (Fig. 23.5).

Fig. 23.3

CLINICAL CASE 23 *(cont'd)*

Emanuele Ambu

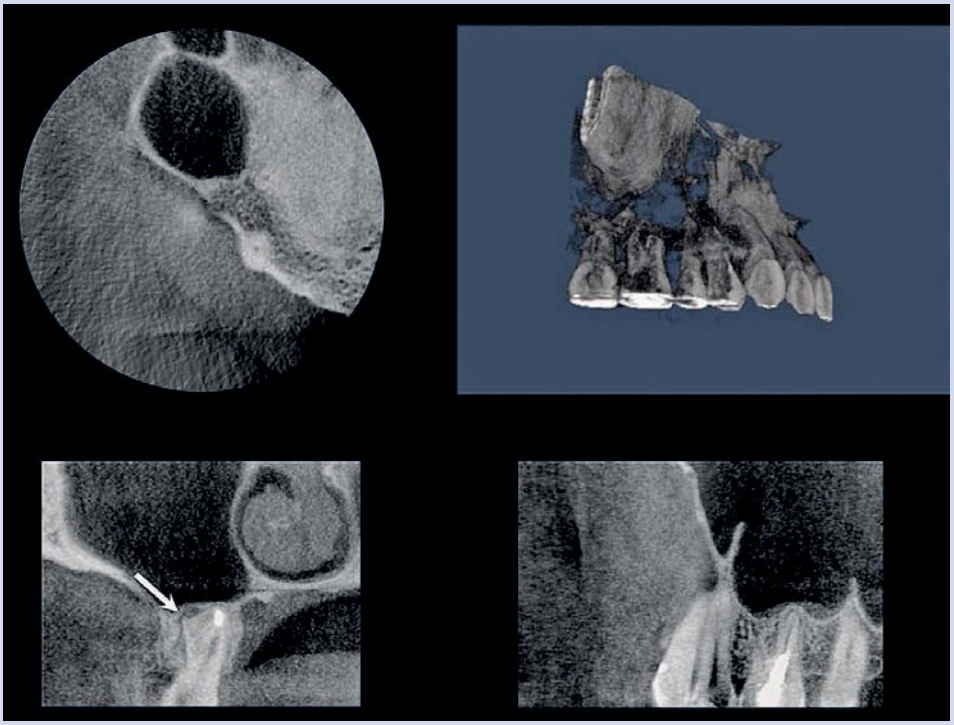

Fig. 23.4

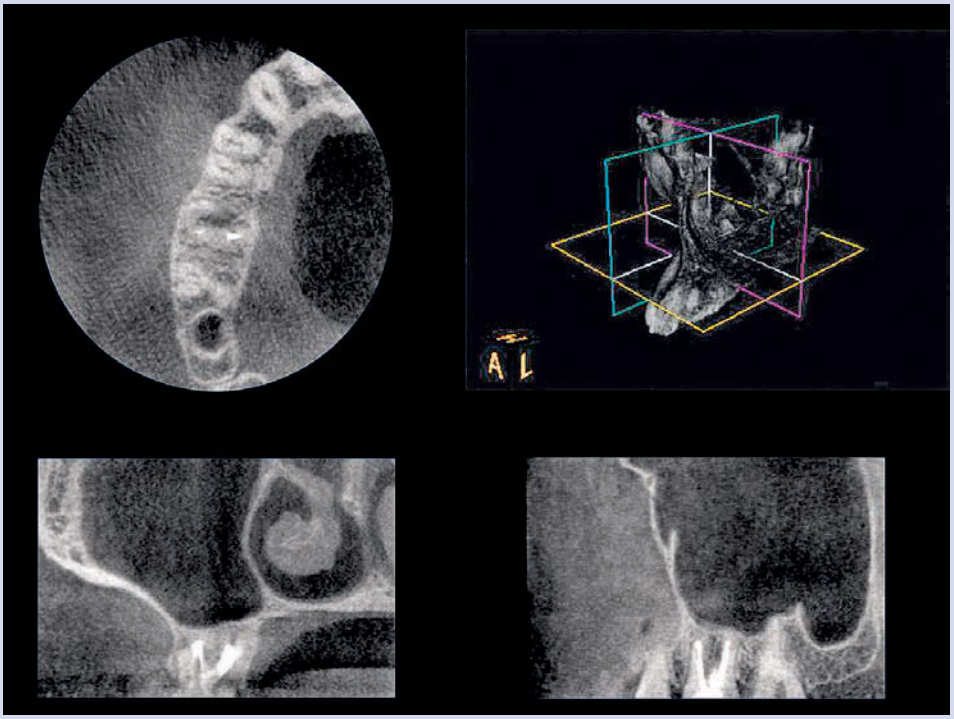

Fig. 23.5

The presence of almost one third of endodontic periapical lesions could be underestimated during diagnostic procedures; the same problem occurs after treatment in the follow-up of these cases. Unless radiolucency around an apex is detected using conventional X-rays, and if a CBCT exam is required, the same exam will be required in the follow-up to check the healing of the lesion. As previously mentioned, Wu et al., underlining the limits of outcome studies based on traditional radiological exams, suggested a re-evaluation in long-term longitudinal studies using CBCT exams (Wu et al. 2009).

According to the authors, most cases which were diagnosed healthy by periapical X-ray actually showed periapical periodontitis as confirmed by the CBCT exam and histhological test.

In teeth, where the reduction of radiolucency was diagnosed by the periapical X-ray and then supposed to lead to periapical healing, actually the enlargement of the lesion is often confirmed by CBCT.

Furthermore, the recall rate of longitudinal clinical studies is below 50% because of the too long follow-up period of time (4 years).

In their letter to the editor of the International Endodontic Journal, published in 2011 (Wu et al. 2011), these authors suggested to reduce the follow-up period (from 4 to 1 year) using CBCT and the effective/ineffective concept. "Effective" treatment is defined as the absence of symptoms and complete or partial resolution of the preoperatively existing periapical radiolucency 1 year after treatment. "Ineffective" treatment is defined as the development or enlargement of radiolucency and/or the persistence emergence of symptoms and signs 1 year after treatment.

Adopting this system would mean to increase the recall rate reducing the number of appointments and radiographs and to reduce the number of unnecessary retreatments.

And finally the use of the "effective" and "ineffective" concept would permit checking whether the treatment is necessary or not.

Any radiological exam should be performed after a correct analysis of the costs and benefits to the patient. When a CBCT exam is prescribed, you must adhere to the ALARA principle (as low as reasonably achievable). In any case, as suggested in the Joint Position Statement of AAE and AAOMR, the smallest FOV should always be chosen for endodontic purposes. Small FOV devices provide very low radiation doses to patients, in some cases almost the same as those of a conventional X-ray, but 2D radiographs do non provide reliable information in the evaluation of clinical outcomes. According to Durack et al., adjusting the exposure parameters reduces the effective dose without affecting the diagnostic yield of the CBCT scan (Durack et al. 2011). We have to inform patients that 2D radiological exams could be useless; in these cases, considering its diagnostic value and the limited radiation exposure, a CBCT exam should be suggested to confirm the presence of apical periodontitis.

The use of small FOV CBCT exams in these new follow-up procedures could be strongly recommended: comparing the pre-op CBCT scan with the one-year follow-up CBCT scan, we can check whether the radiolucency has decreased and whether the cancellous bone has been regenerated. This evaluation will let us classify the results.

This protocol is made in compliance with ALARA principle: e.g. using a CS 9000 3D, one of the most common small FOV CBCT devices, in the diagnosis and follow-up of a periapical lesion of an upper central incisor, the patient will be exposed to 10.6 µSv divided over two scans, one pre-op and a one-year follow-up—almost the same dose as with two conventional periapical X-rays. However, contrary to 2D imaging, the 3D imaging allows us to evaluate the changes in the lesion. Further studies will be necessary to determine the correct use of small FOV CBCT scans in the follow-up of endodontic treatments. For this reason, we will look again at clinical case 13, which was that of the colleague that came to my office because of a large radiolucency in the periapical area of his upper left central and lateral incisors. Endodontic retreatments of both elements were performed. The one-year

follow-up X-ray, performed by the colleague in his office, showed a small reduction in the area of radiolucency, while the two-year follow-up periapical X-ray showed a complete healing of the periapical lesion. According to Friedman, the lesion after one year was still "healing," while after two years it had "healed." Performing a CBCT follow-up after one year, we saw a small reduction of radiolucency, while the two-year CBCT showed a wide reduction of the periapical lesion. The radiolucency was limited to a small area of the cancellous bone, and the bone of the buccal cortical plate was completely restored. According to Friedman, after two years this lesion was still "healing" and further checkups were required. Using the new "effective/ineffective" concept, the treatment of this disease is "effective" after one year, and no more checkups should be necessary. In fact, the reduced volume of the lesion as it appears comparing the pre-op and the one-year follow-up CBCT proves that the treatment was very effective in treating the endodontic disease.

Finally, as underlined by Wu and Colleagues in a Letter to the Editor pubblished in 2011 in the *Journal of Endodontics*, most false negative diagnoses of periapical lesions based on periapical X-rays make it dfficult to relate AP to systemic diseases. These authors suggest performing new epidemiologic investigations with the CBCT so as to modify the official AAE position statement disproving any potential connection between endodontic lesions and subsequent systemic health events. The Authors have also underlined the fact that in endodontics the best diagnostic devices should be the CBCT ones with the smallest FOV. Similarly to X-rays, the potential benefits obtained by CBCT scan would outcome the potential risks. Since two-dimensional X-rays are not able to supply reliable information in endodontic epidemiological investigations or in clinical outcome studies, the CBCT system should be used with the lowest irradiation to patients.

To this purpose the Editorial Board of the *Journal of Endodontics* has been invited to start an open discussion on the issues of CBCT imaging in endodontology.

Differential diagnosis with non-endodontic diseases

The features of differential diagnosis (DD) of endodontic and non-endodontic large radiolucencies will be further discussed in the section on oral surgery. Now, we would like to underline how useful CBCT can be to clinicians in differential diagnosis. The use of CBCT to make a differential diagnosis of endodontic periapical periodontitis and the nasopalatine duct cyst has been described by Faltaroni et al. (2011). In this clinical case the nasopalatine cyst seems to overlap the apex of an endodontically treated tooth, in the endoral X-ray. This would suggest an endodontic disease. The CBCT exam has shown the actual nature of the lesion, permitting the planning of the correct surgical treatment. In any case, according to the authors, histopathological tests are mandatory for a definite diagnosis. The use of CBCT in differential diagnosis of focal osseous dysplasia may be suggested. The sensitivity test is usually enough to allow an accurate diagnosis; besides, if this disease is strictly related to the apex of an endodontically treated tooth, DD could be very hard. As we can see in the clinical case below, the CBCT exam can help us make the correct diagnosis (Clinical Case 24).

CLINICAL CASE 24

Emanuele Ambu

This fifty-four-year-old male patient was referred to me because of a fistula in the buccal area of his lower right central incisor. The conventional X-ray, performed by a colleague, showed the presence of a poor endodontic treatment (Fig. 24.1); the X-ray showed multiple radiolucencies in the periapical area of other teeth. The CBCT showed radiolucencies in all teeth, from the right canine to the left first premolar; except for the right central incisor, where the cortical plate was lost due to endodontic problems, all radiolucencies appeared peculiar, with the cortical plate intact and an "island" of compact bone within the lesion (Fig 24.2). A multifocal cemento-osseous dysplasia was diagnosed; only the right central incisor was successfully retreated by the colleague.

Fig. 24.1

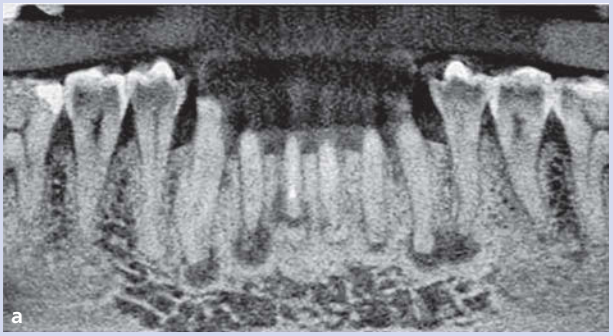

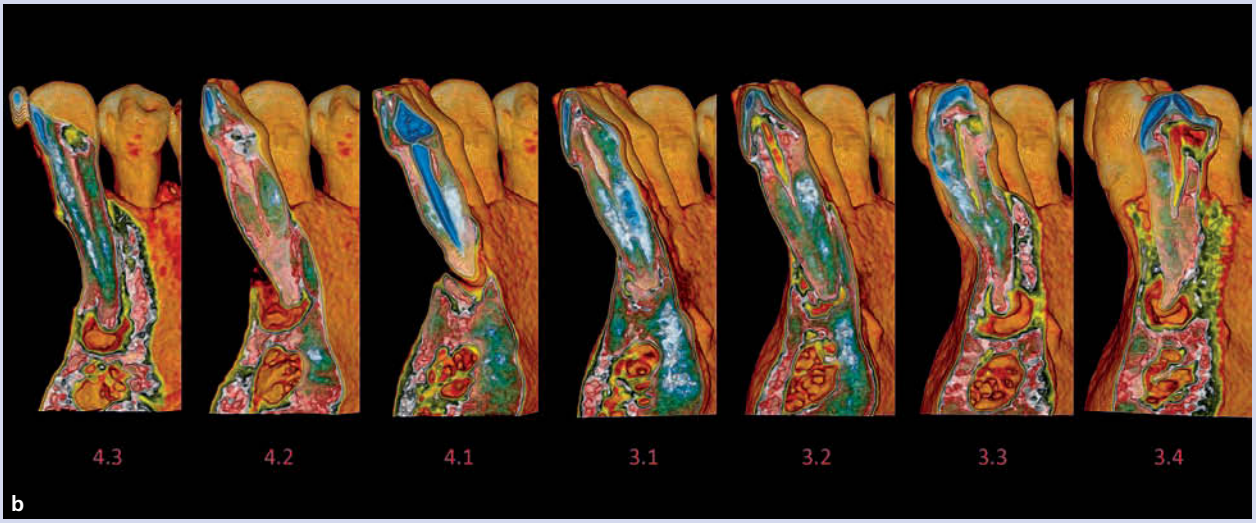

Fig. 24.2 a-b

Dental traumatology

Emanuele Ambu - Roberto Ghiretti

Dental traumatology includes a number of injuries to teeth, to periodontal soft and hard tissues, to gingiva, oral mucosa, lips, and oral muscles, as a result of trauma. According to the World Health Organization's Application of International Classification of Diseases to Dentistry and Stomatology, Andreasen et al. subdivided these injuries into the following elements (Andreasen et al. 2011):

- Soft and hard dental tissues
- Dental hard tissues, pulp, periodontal ligament, and alveolar process
- Dislocated teeth
- Lips and oral cavity

For didactic reasons, we would also like to include vertical root fractures (VRFs). Direct, acute traumas often cause a horizontal fracture while VRFs are the result of a persistent chronic occlusal trauma in endodontically treated or compromised teeth.
We will focus our attention on those diseases that clinicians can diagnose with the aid of CBCT: crown fractures, horizontal root fractures, vertical root fractures, alveolar process fractures, and tooth dislocations.

The use of CBCT in dental traumatology

Most injuries due to trauma to the maxillofacial area usually affect either dentition (50%) or dental elements along with the adjacent soft tissues (36%). Maxillofacial fractures amount to only 13.6% of injuries (Cohenca et al. 2007a). The diagnosis, treatment plan, and prognosis of an injured element are a real challenge because conventional radiology based on endoral X-rays is not sensitive enough to detect small dislocations or fractures in the dentoalveolar area, since there may be anatomical overlapping, geometrical projections, or procedure mistakes. The use of volumetric radiology is widely recommended in dental traumatology. The external position of its detector facilitates its use with injured patients (Kanagasingam et al. 2011), especially children. Children and teenagers are those most exposed to traumas, especially to upper incisors, due to falls or accidents during sports training or games (Andreasen and Andreasen 1994).
Shintaku et al. have underlined in one of their review articles that the investigation method should be evaluated according to the ALARA principle, depending on the entity of the trauma (Shintaku et al. 2009). Conventional radiological systems provide patients with the lowest radiation dose but, since they supply two-dimensional images, a lot of important information may be lost. CT is able to supply information both about soft and hard tissues, but with a high radiation dose to patients. Furthermore, this system is very expensive and used almost exclusively in hospitals. Magnetic resonance imaging (MRI) is very useful to identify injuries to soft tissues, but a large amount of information about hard tissues may be lost in the course of the exam. It is especially recommended in cases of suspected fractures affecting the paranasal sinus or large areas of soft tissues. Similarly to CT, it is very expensive and its use is almost exclusively limited to hospitals. CBCT is suggested by these authors as an excellent alternative, although they are aware of the loss of data concerning the damage to soft tissues. Stuebmer et al. also prefer CBCT to CT in airgun injuries, because the images obtained by CBCT produce fewer artifacts from the metal of bullets and give much more defined images (Stuebmer et al. 2008). The use of CBCT in the diagnosis and treatment of dentoalveolar traumas has also been suggested by Cotton et al. (2007), by Patel et al. (2007b), and by Cohenca et al. (2007).

Crown fractures

Crown fractures are usually diagnosed without any radiological examination. In some cases, however, a radiological investigation with an X-ray or a CBCT with small FOV systems may be necessary to detect foreign bodies (fragments of the crown, small rocks, fragments of asbestos) (Cohenca et al. 2007).
Small FOV CBCT systems produce a very low radiation dose (sometimes even as low as that of conventional X-rays, in upper anterior sectors). This kind of examination is also particularly recommended in the case of large traumas combined with coronal fractures, in order to check for any other fractures of roots or the alveolar area.

Horizontal root fractures

Horizontal root fractures are usually due to sports or car accidents and especially affect the upper anterior elements. Wang et al. presented three cases of horizontal fractures of the palatal root of the maxillary first molars in patients, usually risulting from chewing food very hard (Wang et al. 2011).
The diagnosis was made evaluating the mobility, which is highly dependant on the fracture portion (third coronal, medium, or apical of the root).
The prognosis varies considerably and depends on the fracture position. In twenty-five percent of cases the dental pulp will encounter necrosis, therefore early diagnosis is necessary (Kamburoglu et al. 2009). The radiological diagnosis will require a number of radiograms in different projections, because the fracture will only be visible when the ray direction is perpendicular to the root fracture direction (Flores et al. 2007).
According to these guidelines, it is recommended to have first a projection at 90° with respect to the element investigated, then an occlusal projection, and finally one going from mesial to distal.
Fractures often become apparent only when the edema or the granulation tissue has separated both fragments. According to Kamburoglu et al., the small FOV CBCT permits a much better diagnosis of this pathological pattern than any other endoral system, either digital or analog (Kamburoglu et al. 2009). According to another work, CBCT has permitted the diagnosis of fractures in all the investigated cases (Bornstein et al. 2009).
Moreover, the three-dimensional exam has made it possible to detect the correct direction of the fracture. In a high percentage of cases the fracture had an oblique slope, starting from the third medium or apical in the vestibular portion and going to the third coronal in 68.2% of cases. This figure is particularly important because it is related to a poor prognosis depending on the coronal enlargement of the fracture line. These authors have proved that the prognosis shown in literature and based on two-dimensional radiological exams is incorrect, and they have suggested performing other examinations and evaluating the case again.
In conclusion, when using two-dimensional radiological systems, at least three projections are necessary to perform a not always correct diagnosis; on the other hand, the small FOV CBCT is able to diagnose this kind of fracture accurately, with a dose as low as that of an intra-oral X-ray (especially in front elements) to patients (Clinical Case 25).

CLINICAL CASE 25

Emanuele Ambu

The sixty-three-year-old male patient was introduced to me by a colleague who was unable to conclude the endodontic treatment because he could not determine the working length of the palatal canal of the upper right first molar. The patient had reported an abscess of this element some months before (Fig. 25.1).

During the endodontic treatment, the canal negotiation caused bleeding and pain at the length where the electronic locator signaled the end of the canal. Comparing the length of other canals and the control X-ray of the working length of the canal investigated, we found that the length reached by the instrument was too short for the root length. The volumetric exam allowed us to detect in all projections a horizontal/oblique fracture of the palatal root (Fig. 25.2).

This fracture was not easily detectable using the intra-oral X-ray because of anatomical overlapping, such as the floor profile of the maxillary sinus. When asked whether he had suffered any traumas, the patient answered that he had had a chewing trauma twelve years before. An endodontic retreatment of vestibular roots was performed and the palatal root extracted (Fig. 25.3).

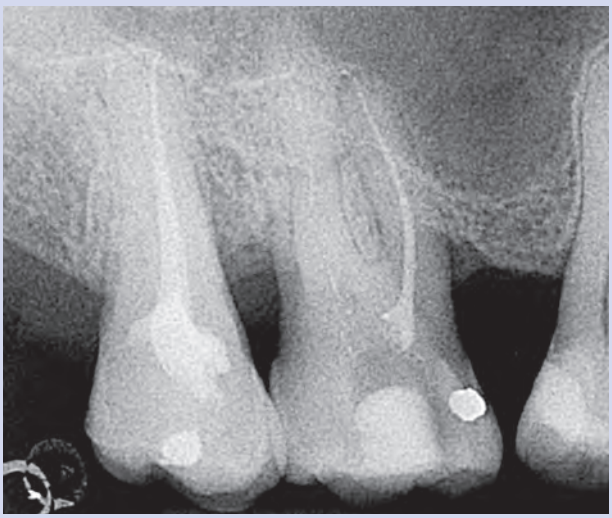

Fig. 25.1

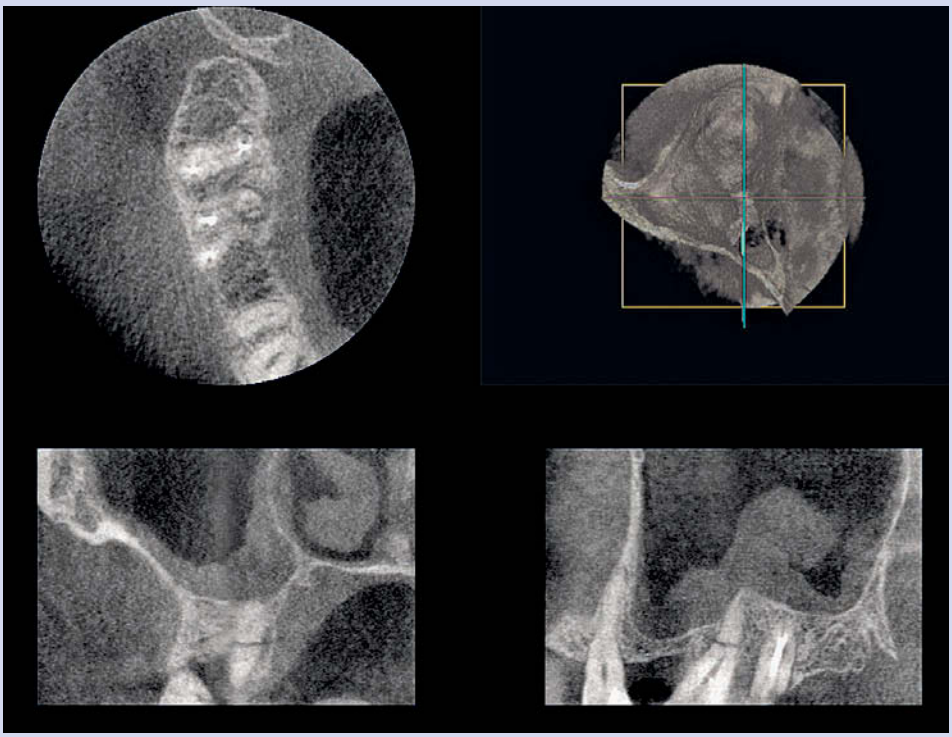

Fig. 25.2

Fig. 25.3

Vertical root fractures

Vertical root fractures are unusual in non-endodontically treated teeth. They are often due to chewing problems or incorrect occlusion (Yang et al. 1995). VRFs are more often detected in endodontically treated teeth, in the elements (especially premolars) used as the last abutment teeth of a bridge reconstructed with metal posts, as well as in pontics with cantilever bridges (Testori et al. 1993).

Since VRFs are not usually accompanied by symptoms, they are often ignored. VRFs are often signaled by little pain and are associated with abscesses in only fifty-two percent of cases.

Intra-oral X-rays usually show periapical and lateral radiolucency (the so-called "halo type"). During probing, a spot-like periodontal pocket (often twice as large at the opposite sides of the root) may be detected.

Since it is hard to reach a satisfactory diagnosis of this problem, useless invasive interventions are often performed.

All the X-rays shown in the paper by Andreasen (2011), as already mentioned, are excellent two-dimensional intra-oral projections.

We must, however, take into account that any lesions due to bloody traumas caused by road or sports accidents or even violent acts leading to horizontal lesions are seldom detected in dental practice. These can be easily diagnosed with conventional 2D X-rays.

On the other hand, clinicians often deal with vertical lesions in endodontically treated teeth, which are often difficult to diagnose.

As early as 1970, Rud and Omnell had already come to the conclusion that if fractures were not so apparent, conventional radiology could not help to find them (Rud and Omnell 1970). In 1980 Meister et al. stressed the importance of signs like "halo type" that would appear over time (Meister et al. 1980), as also mentioned by Tamse (1988) and by Testori et al. in 1993 (Testori et al. 1993). These are radiographic signs appearing one or two years later, as reported by Moule and Kahler (1999). They noticed that only 35.7% of cases were diagnosed and only after this amount of time had lapsed.

Thanks to the introduction of volumetric radiology and its (however slow) diffusion in dental practice, the way in which we deal with this kind of lesion has changed, and we are now able to see diseases that would have otherwise remained undetectable.

The use of CT to detect VRFs was suggested by Youssefzadeh et al. (1999); they proved that this kind of exam was much more reliable and precise than intra-oral X-rays. These authors also found that the presence of artifacts, like metal posts or endodontic sealing material could hide the fracture line.

Bernardes et al. pointed out the limits of CT: patients are exposed to a larger dose of radiation as the number of artifacts increases (due to so-called "beam hardening" and "streak artifacts"), low space resolution, and reduced capacity for early diagnosis (Bernardes et al. 2009). In their paper, the authors stated that CBCT can improve the diagnosis of VRFs, as compared to that using intra-oral X-rays. In their study, a radiologist and an endodontist (both very skilled) were asked to perform a "blind" study of two-dimensional and volumetric exams of twenty cases of vertical root fractures.

The fractures detected by each operator through endoral X-rays were eight and six, respectively; whereas those detected by each of them using 3D radiology were eighteen. The two cases which were not detected were due to metal artifacts from prosthetic elements close to the lesion.

The authors stressed that that the fracture may not be apparent in the two-dimensional exam when the rays are not exactly parallel to the rim. Moreover, the presence of several overlapping anatomical structures may confuse the clinician further.

Comparing the results of CT and CBCT, the authors noticed a reduction in artifacts due to endodontic materials, even though they make the exam less sensitive. As highlighted by Zhang et al., root canal gutta-percha causes streak "star-like" artifacts similar to fracture lines, thus reducing the observer's confidence in the diagnosis of VRFs (Zhang et al. 2007).
Hassan et al. performed an *in vitro* exam with eighty artificially fractured teeth to evaluate any interference with root canal filling materials (Hassan et al. 2009). The aim of this study was to evaluate the sensitivity level of both exams (high sensitivity equals low probability of false positive results) and their specificity (high specificity equals low probability of false negative results). The ability to detect fractures (sensitivity) was much higher with CBCT (79.4% of cases), regardless of the presence of root filling material; whereas the average number of cases detected by intra-oral X-rays was 37.1%, with a percentage of 26.6% in teeth that had been endodontically treated and of 47.5% in non-endodontically treated teeth. These results prove the sharp and unfavorable interference of root canal treatments in two-dimensional analysis.
The presence of radiopaque material inside root canals increases the number of false negative results even in analysis with CBCT, probably because of star-like artifacts that reduce the observer's confidence in the diagnosis of VRFs. Furthermore, if on the one hand it is very hard to diagnose palatal/lingual fractures using intra-oral X-rays, it is absolutely impossible to diagnose the mesio-distal ones with this kind of exam. With regard to the specificity level, the percentages found were almost the same (90%). This means that when the signs of a fracture are detected, the fracture is real, regardless of the kind of analysis performed.
It is essential to note the fact that a vertical tooth fracture can be detected in twice as many cases by 3D radiology as compared to conventional radiology. According to the authors, this is due to several factors: 3D analysis is multi-angular and multiplanar, and its images show very thin layers with higher contrast.
As proved by Hassan et al., the ability of a system to detect VRFs depends on the FOV and voxel sizes (Hassan et al. 2010). According to the authors, the axial projection is the one which enables us to identify the fracture more accurately. The smaller FOV provides a higher image resolution.
Özer has proved that when the voxel is smaller, it permits greater sensitivity and better specificity in diagnosing VRFs (Özer 2011). According to the results shown in this paper, with 125-micron voxels the most accurate values (equal to 97%) can be achieved, even though the author inexplicably concludes that the 200-micron voxel is the best from the clinical point of view.
In conclusion, whereas two-dimensional radiology has proved to be useless for diagnosing VRFs, volumetric exams seem to give reliable results. However, as is always the case when performing a diagnosis, the use of radiology should be an aid to any approach that takes into account all the symptoms that are typical of this clinical pattern.
We will now highlight some different radiological patterns using clinical cases which show various degrees of vertical root fracture (Clinical Cases 26-29).

CLINICAL CASE 26

Roberto Ghiretti

The element was endodontically retreated according to an intra-oral X-ray showing no VRFs (Fig. 26.1). Since the symptoms persisted, a volumetric radiological exam was performed (Fig. 26.2). This showed considerable bone loss (Fig. 26.3), which had been hidden in the 2D image by the overlapped root and a fracture line (Fig. 26.4).

Fig. 26.1

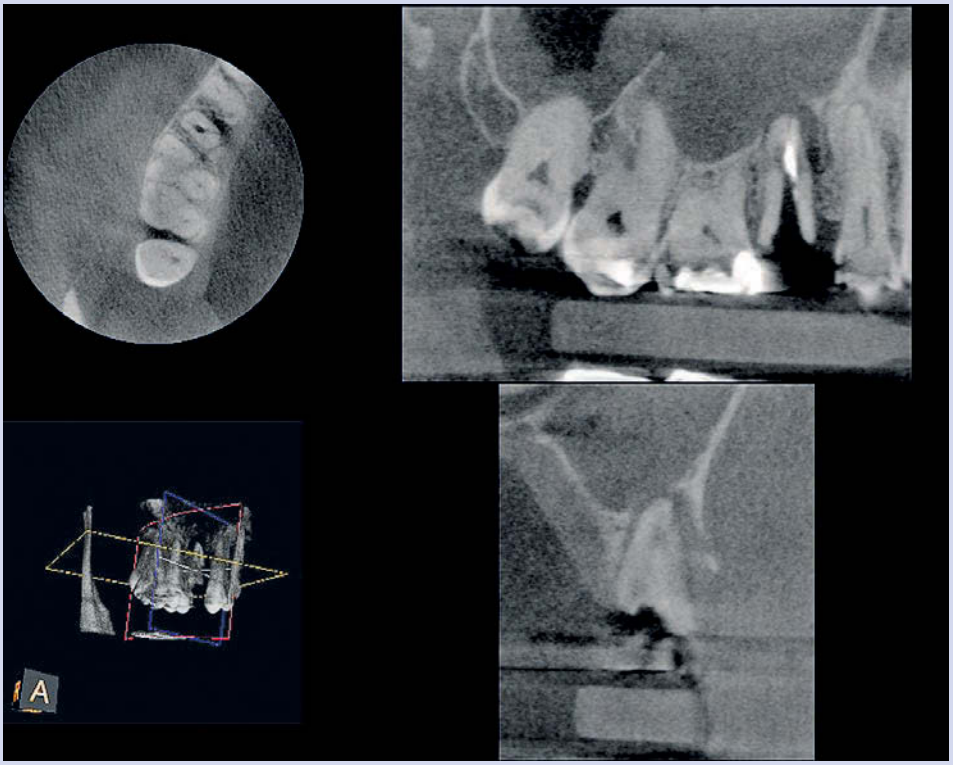

Fig. 26.2

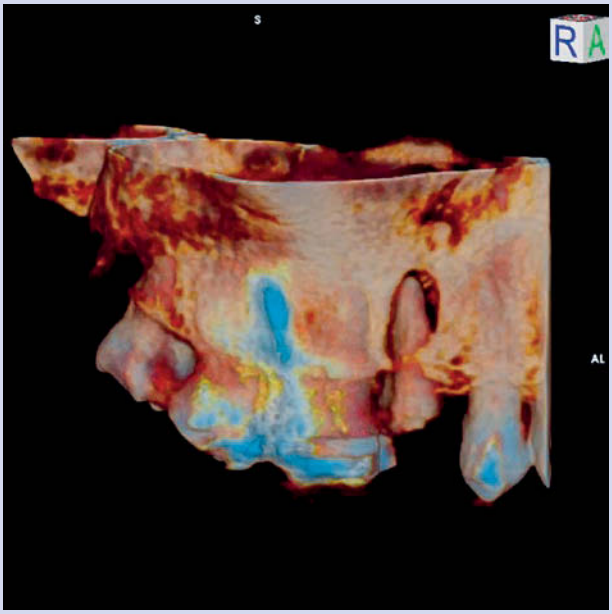

Fig. 26.3

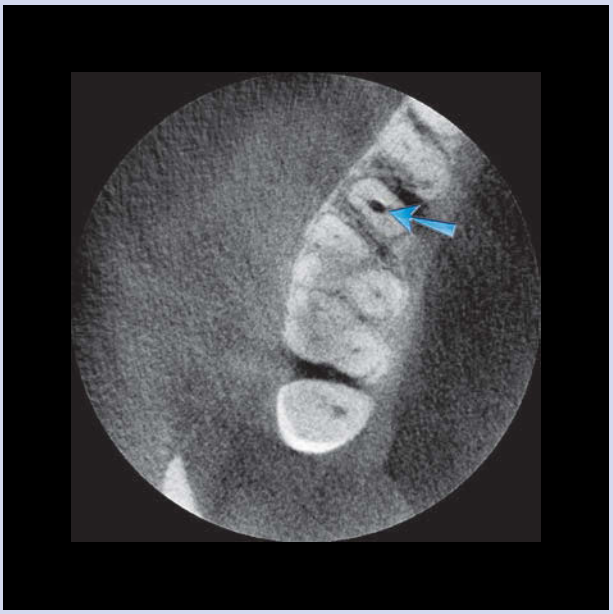

Fig. 26.4

CLINICAL CASE 27

Emanuele Ambu

This patient suffered from a fistula in her vestibular mucosa. No periradicular radiolucency appeared in the intra-oral X-ray (Fig. 27.1). On the contrary, the volumetric exam showed a small lesion with vestibular cortical bone expansion (Fig. 27.2).

The 3D rendering showed an oval lesion in the vestibular cortical bone, suggesting the presence of a lateral canal (Fig. 27.3). Only performing a surgical flap was it possible to detect the unexpected presence of a vertical root fracture (Fig. 27.4).

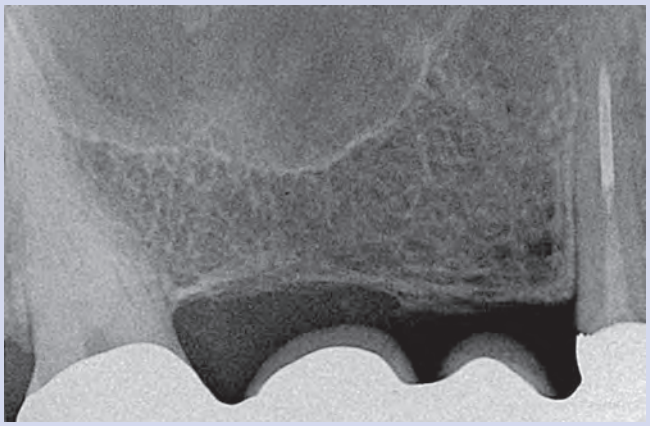

Fig. 27.1

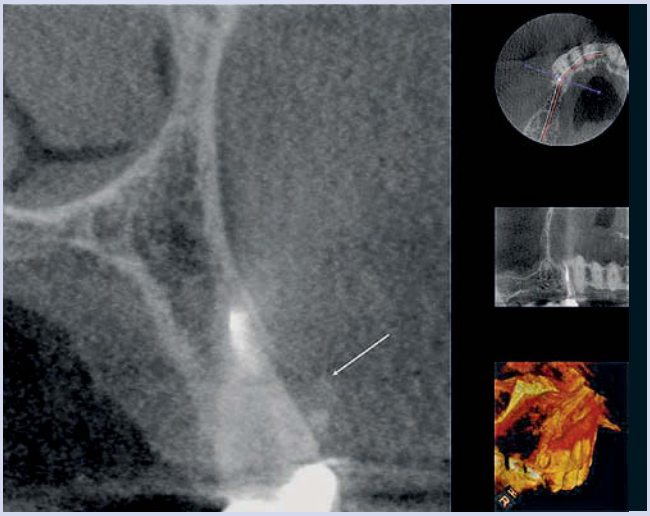

Fig. 27.2

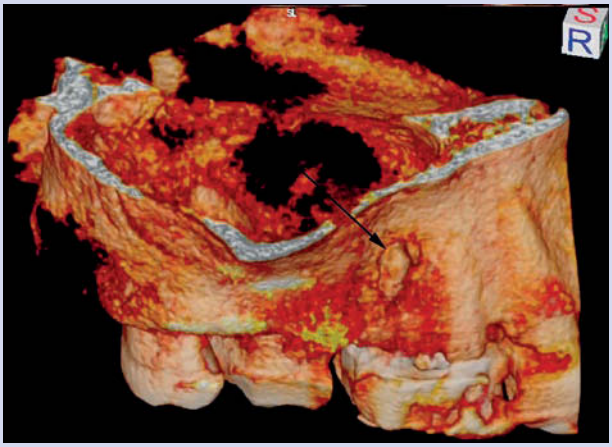

Fig. 27.3

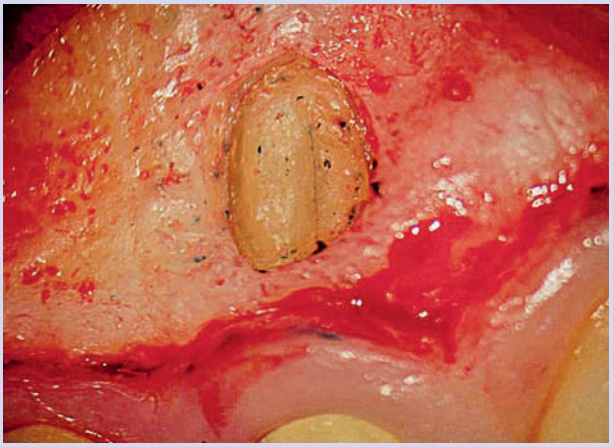

Fig. 27.4

CLINICAL CASE 28

Emanuele Ambu

Probing a vestibular path had caused us to suspect a fracture. The CBCT exam confirmed our suspicion (Fig. 28.1). A surgical flap clearly showed this fracture (Fig. 28.2) and confirmed the fistulous path (Fig. 28.3).

Comparing the clinical image with the sagittal view we can see that the digital image is perfectly in compliance with that the clinician will find during surgery.

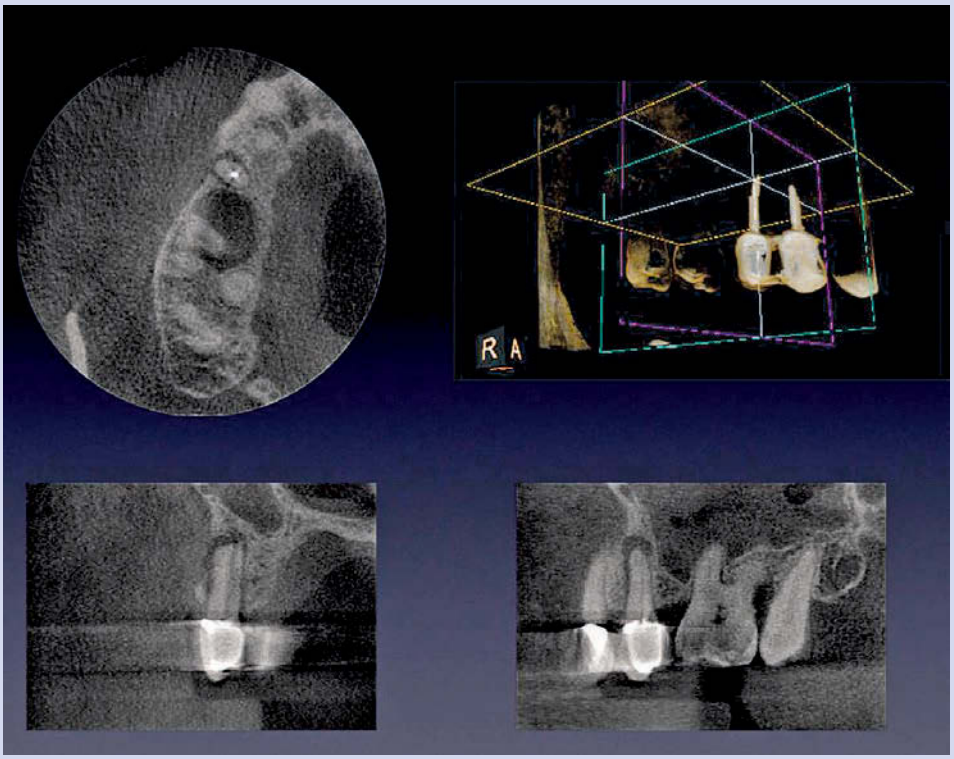

Fig. 28.1

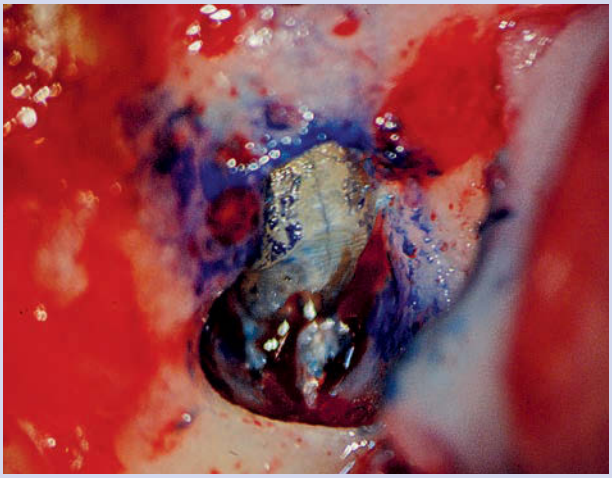

Fig. 28.2

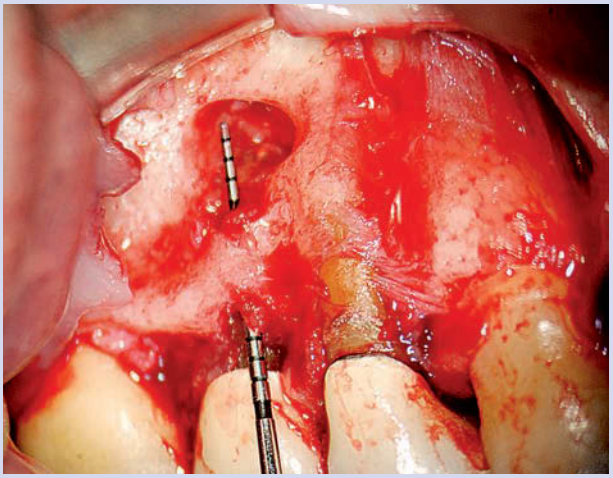

Fig. 28.3

CLINICAL CASE 29 | **Roberto Ghiretti**

The diagnosis of an obvious fracture cannot be clearly defined in a two-dimensional image (Fig. 29.1). It becomes clear in the 3D imaging (Fig. 29.2) and rendering (Fig. 29.3). This case, too shows the huge advantages resulting from the use of CBCT systems in daily clinical practice. The cost/benefit ratio suggests patients to undergo radiographic exams with CBCT systems with the lowest FOV and the lowest radiation dose.

Fig. 29.1

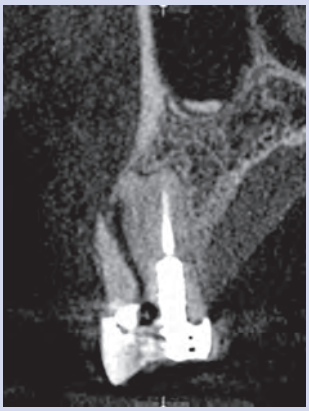

Fig. 29.2

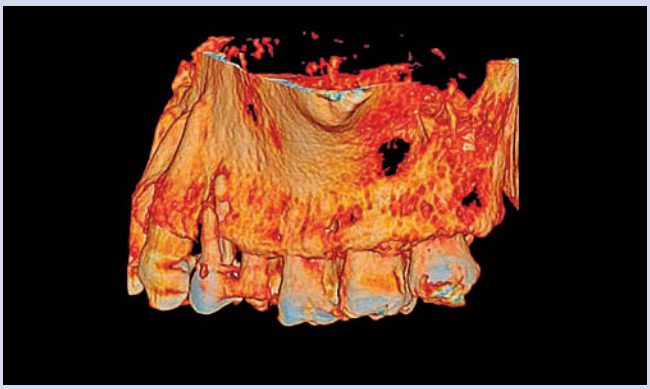

Fig. 29.3

Dentoalveolar fractures

As highlighted by Cohenca et al. (2007) and by Patel et al. (2007b), CBCT is very useful for detecting the cortical bone by means of its multiplanar images. Cohenca et al. have published a clinical case in which the exam helped clinicians to reposition the elements and to remove a crown fragment embedded in the soft tissues, besides being useful for determining the dislocation extension.

The use of volumetric exams to detect multiple fractures of the jaw, alveolar bone and root has been described by Dölekoglu et al. (2010). Palomo and Palomo (2009) have devoted an entire article to the use of CBCT in traumas, concluding that CBCT is better than OPG at detecting the fractures of the alveolar bone, because it can not only determine the presence but also the exact positions of fractures. Moreover, jaw fractures may not be detected by CT, while CBCT, which is more accurate and sensitive, supplies more detailed information than conventional radiology and CT (Ilgüy et al. 2009) (Clinical Case 30).

CLINICAL CASE 30

Emanuele Ambu

A twenty-one-year-old male patient was sent to our practice with a total dislocation of his 11 and 12, after a sports trauma (Fig. 30.1).
After repositioning and splinting the elements, we could not see the root status with an intra-oral X-ray (Fig. 30.2). A horizontal root fracture was suspected, but the volumetric exam showed that the fracture had affected the whole alveolar bone of both elements (Fig. 30.3). After sixty days, the endodontic treatment of both teeth was performed.
The follow-up CBCT showed a complete healing of hard tissues (Fig. 30.4) and the clinical exam detected a complete healing of soft tissues as well (Fig. 30.5).

Fig. 30.1

Fig. 30.2

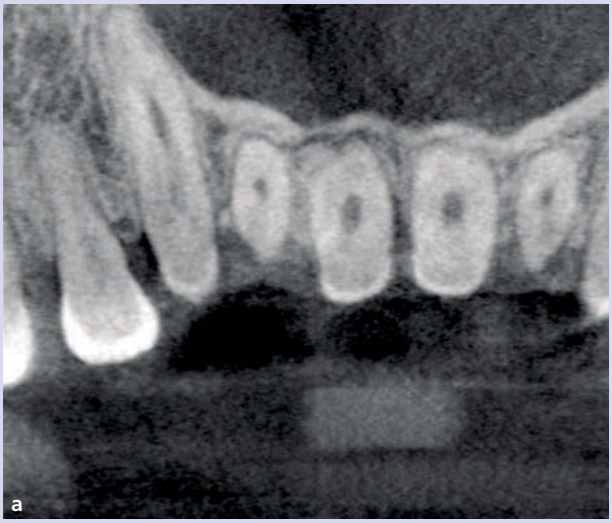

Fig. 30.3 a-b

CLINICAL CASE 30 *(cont'd)*

Emanuele Ambu

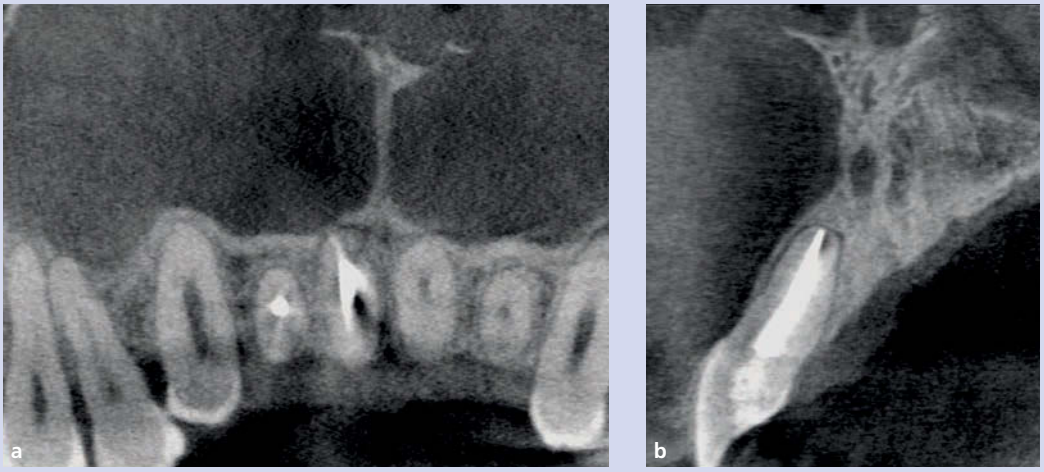

Fig. 30.4

Fig. 30.5

Oral surgery

Emanuele Ambu - Roberto Ghiretti

The use of CBCT in oral surgery

The introduction of CBCT in oral surgery and maxillofacial surgery will be further discussed in the section on maxillofacial surgery. The aim here is to give a brief and sufficiently clear idea about this complex topic. Three-dimensional diagnostic exams have always been used in oral surgery, both because this kind of surgery is particularly complex and because it is necessary to know exactly the lesion's size and its relation to the surrounding structures in order to minimize the risk of permanent lesions in nervous or other delicate tissues. In the past, this risk justified the use of CT systems, in spite of the high radiation exposure to patients. As underlined by Ahmad et al., CBCT systems have been widely used thanks to their small size, easy use, and fairly economical prices (Ahmad et al. 2012). Nevertheless, the use of multidetector computed tomography (MDCT) and MRI is still relevant—as we already pointed out in the section on traumatology—because MRI and soft-tissues window CT can offer excellent analysis of soft tissues, and MRI alone can supply the results required when the main aim is to analyze these tissues. According to the authors, the use of CBCT is especially suitable for such clinical situations as surgical extractions of third molars, impacted teeth, tracing of the inferior alveolar canal, implant planning, evaluation of cysts and tumors, fracture diagnosis, orthognathic surgical planning and follow-up, inflammatory conditions of the jaws and the sinuses, evaluation of temporomandibular joints, and as an aid in diagnosing unexplained symptoms and pain. We will deal with some of these indications below, while others will be explained further in specific sections.

Radiolucent lesions (relating to or not relating to cysts)

A large number of classifications of maxillary cysts have been published. For the sake of simplicity, we will refer to the WHO classification published in *Histological typing of odontogenic tumours* (Kramer et al. 1992), as described by Roberto Barone et al. (1999). In addition, it is necessary to include radiolucent lesions not relating to cysts. At the radiographic exam they resemble cysts, and it is therefore necessary to know their various aspects in order to make a differential diagnosis (Tab. 6.1). The diagnosis of lesions relating to cysts cannot be accurate enough with intra-oral X-rays and OPGs, because these are two-dimensional exams. Better results will be possible with further projections at a 90° tilt, as compared to previous exams. Only if the margins of the lesions can be clearly detected, will this procedure supply information on their size. The analysis of the internal structure and of the spatial relations of lesions will, however, be difficult due to the overlapping of other anatomical structures.
CBCT systems, on the other hand, can supply multiplanar images with one exam. With some CBCT systems this means a radiation exposure equal to or even lower than that of 2D systems requiring multiple exams. Three-dimensional images also supply important information, such as the presence and extent of bone resorption, sclerosis of surrounding bone, cortical expansion, internal and external calcifications, and proximity to other vital anatomy (Kaneda et al. 2003). The use of multiplanar images is more effective, the deeper the lesion is (Hashimoto et al. 2000). Furthermore, CBCT systems can supply 0.1-mm-thick "slices," offering better visualization of the lesion margins, especially if they are not well defined. To this end, Ahmad et al. suggested the use of CBCT in the follow-up of the margins of lesions that may have a high recurrence rate (Ahmad et al. 2012). There are many types of expansive or substitutive

Tab. 6.1 - **Classification**

Cysts	Radiolucent non-cystic lesions
Developmental dysembriogenetic origin cysts A) Odontogenic • Gingival cyst of infants (Epstein pearls) • Gingival cyst of adults • Dentigerous (follicular) cyst • Eruption cyst • Lateral periodontal cyst • Odontogenic keratocyst • Glandular odontogenic (sialo-odontogenic/ mucoepidermoid-odontogenic) cyst B) Non-odontogenic • Nasopalatine duct (incisive canal) cyst • Nasolabial (nasoalveolar) cyst	**Non-neoplastic bone lesions** • Solitary (traumatic/simple/hemorrhagic) bone cyst • Aneurysmal bone cyst **Stafne's bone cavity** **Odontogenic benign tumors** • Ameloblastoma • Pindborg tumor • Odontogenic calcifian cyst • Ameloblastic fibroma • Odontogenic mixoma
Inflammatory cysts • Radicular cyst (apical/lateral) • Residual cyst • Paradental lateral cyst (inflammatory collateral)	**Malignant neoplasms**

lesions affecting the maxillary bones: benign or malignant tumors, acute or chronic inflammatory lesions, dysplasia or developmental cysts, or lesions resembling a cyst. All of them could originate from odontogenic or non-odontogenic tissues. It can be a pathologist's dream or a nightmare, because these kinds of lesions can offer a mixture of different histological, morphological, and clinical aspects. This book, however, is not aimed at becoming a reference text for the classification of different lesions found in the oral and maxillofacial area. Its purpose is to analyze the most common diseases detected in our dental offices, spurring the reader to a more sophisticated study through CBCT exams. We will describe the 3D radiological aspects of some of these cysts below. One should always remember that a definite diagnosis is always possible only after the histological exam following surgery.

Developmental odontogenic cysts

Odontogenic keratocyst

An odontogenic keratocyst (OKC) is a lesion which originates from remnants of dental lamina. It can be located in any area of the maxillary bones that is occupied by teeth. It is, however, ideally located in the rear portion and in the ascending branch of the mandible. It accounts for three to ten percent of all odontogenic lesions. In the case of multiple lesions, especially in children, Gorlin syndrome should be suspected.

It appears radiologically as a unilocular or multilocular lesion with defined, slightly sclerotic margins. Diagnosis can be certain only after a histological test. Since it can recur after a period of time (in about thirty percent of cases), follow-up is absolutely recommended for years. The use of CBCT for OKC diagnosis has been emphasized by Koçak-Berberoglu et al. (2012). They have underlined the limitations of OPGs in detecting the lesion margins,

especially in the upper maxillary bone; whereas CBCT is essential for defining the borders of the lesions overlooking the maxillary sinus. CBCT also supplies important details about the relations of the lesion borders to the surrounding anatomical structures, which are essential to surgical planning (Clinical Case 31).

CLINICAL CASE 31

Emanuele Ambu and Alberto Bianchi

A sixty-year-old female patient came to my office with a wide lesion in the area of a devitalized tooth. The volumetric exam showed a wide lesion and thin bone walls, expanded by the lesion (Fig. 31.1). The patient was sent to a maxillofacial ward to have the lesion removed. The histological exam confirmed the diagnosis of a keratocyst.

She then came back to my office to undergo endodontic treatment of her lower left first molar and of her teeth with a negative vitality test after surgical interruption of their neurovascular bundles. The volumetric exam performed eight months after the treatment showed good healing of all hard tissues (Fig. 31.2).

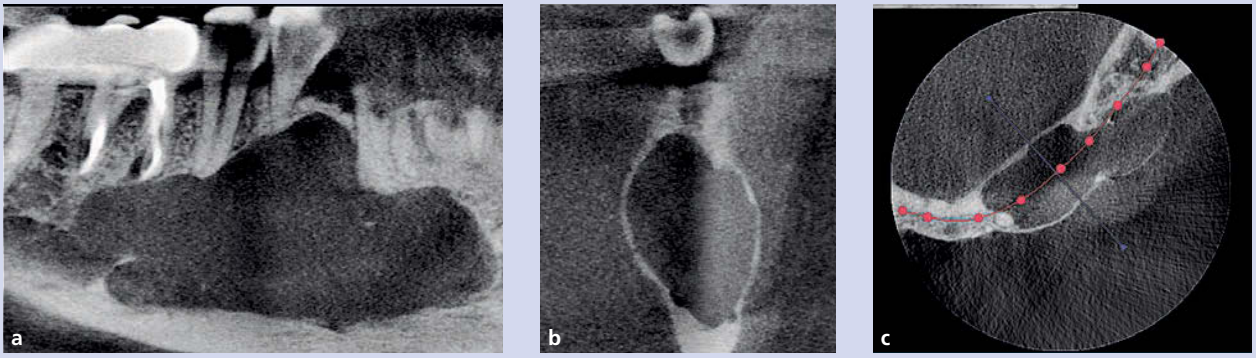

Fig. 31.1 a-c

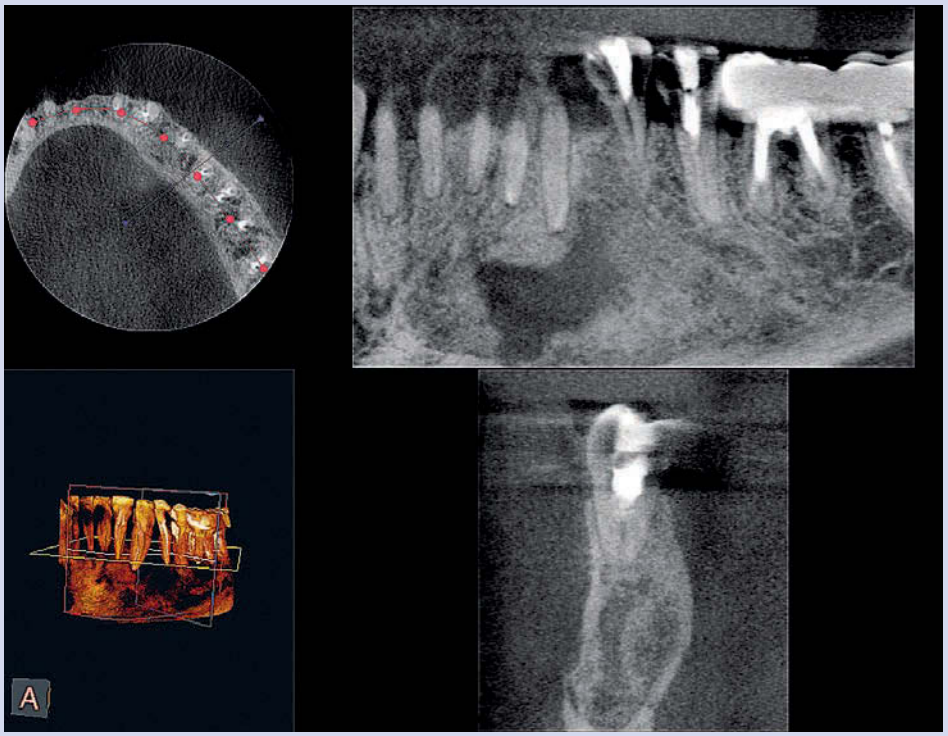

Fig. 31.2

Gorlin syndrome

Gorlin syndrome, or nevoid basal cell carcinoma syndrome, is an inherited medical condition. The gene is passed down through families as an autosomal dominant trait. This syndrome appears in the form of multiple keratocysts, cysts on the skin, calcifications of falx cerebri, coast nerve and spine, prominent frontal bossing and hypertelorism. The first symptoms, appearing before the age of twenty, are scattered basals and multiple keratocysts in eighty percent of patients. The diagnostic and therapeutic approach to this syndrome will depend on its clinical manifestations, but, since keratocysts tend to recur and the risk of developing tumors increases, long and careful follow-up is absolutely recommended (Ficarra 2010) (Clinical Case 32).

CLINICAL CASE 32

Emanuele Ambu

An eleven-year-old girl came to my office because of radiolucent areas detected by an OPG performed to investigate the delayed eruption of her permanent teeth (Fig. 32.1). A volumetric exam detected large lesions that had enlarged the corticals and caused the retention of several dental elements (Fig. 32.2).

After a quick exam of the girl's skin, the presence of nevi was detected and the girl's mother confirmed that the young patient had already had some of them removed surgically. She was sent to a maxillofacial ward with a preliminary diagnosis of a Gorlin syndrome, which was later confirmed by subsequent analysis.

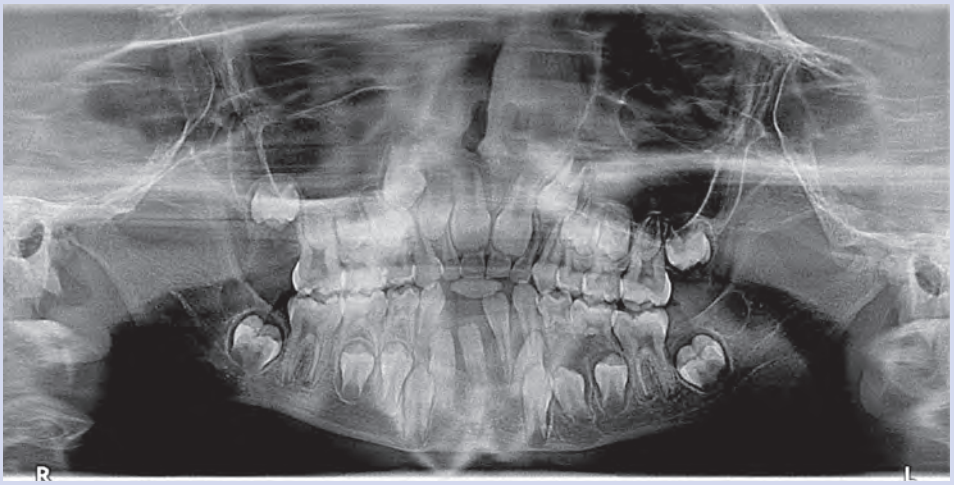

Fig. 32.1

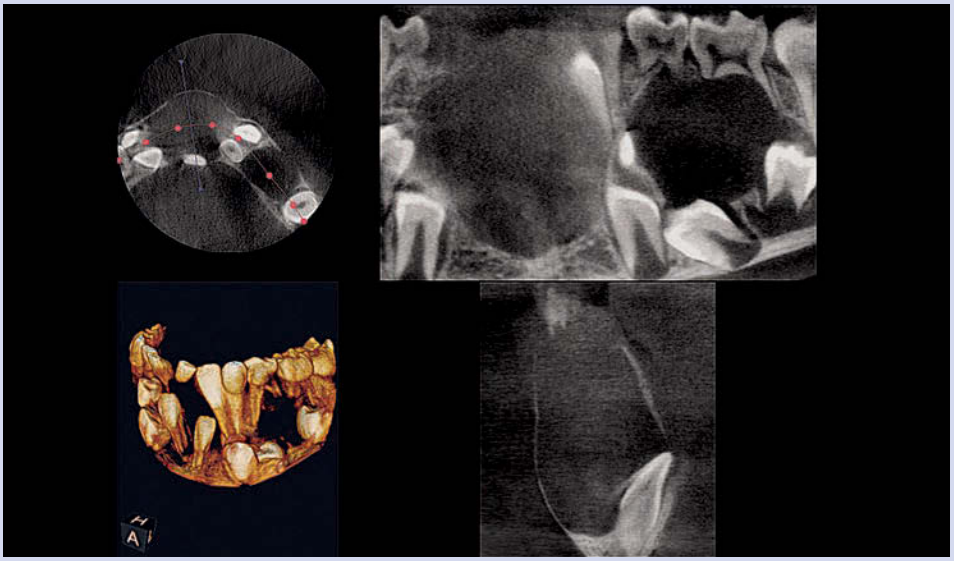

Fig. 32.2

Dentigerous, or follicular, cysts

This kind of cyst develops around the crown of impacted teeth, and it is caused by the accumulation of fluid between the enamel epithelium and the coronal surface of the tooth. It often appears in patients between the ages of ten and thirty, and usually affects the third molars, canines, and second molars. Pain is associated with infection, which usually occurs when the cyst affects a tooth which is only partially erupted. The X-ray shows unilocular radiolucency with clear margins at the crown of an impacted tooth. Since OKC is often associated with an impacted tooth (25-40%), it is recommended to pay special attention, confirming the diagnosis of odontogenic cysts with a histological test of a sample removed surgically (Clinical Cases 33 and 34).

CLINICAL CASE 33

Roberto Ghiretti

A thirty-year-old female patient came to my office, with a history of recurrent abscesses and a skin fistula in her left cheek. This had first appeared twelve months earlier. Her lip sensitivity was preserved. The CBCT exam highlighted the borders of the lesion (Fig. 33.1); the image rendering (Fig. 33.2) showed the lesion of the vestibular coronal giving rise to the skin fistula (arrow 1), and it also showed the neurovascular bundle dislocated by the lesion more toward the cauda (arrow 2). A further three-dimensional reconstruction (Figs. 33.3 and 33.4) showed the tongue extension. The surgeon should pay attention to the area indicated by the arrow where the lingual nerve passes through.

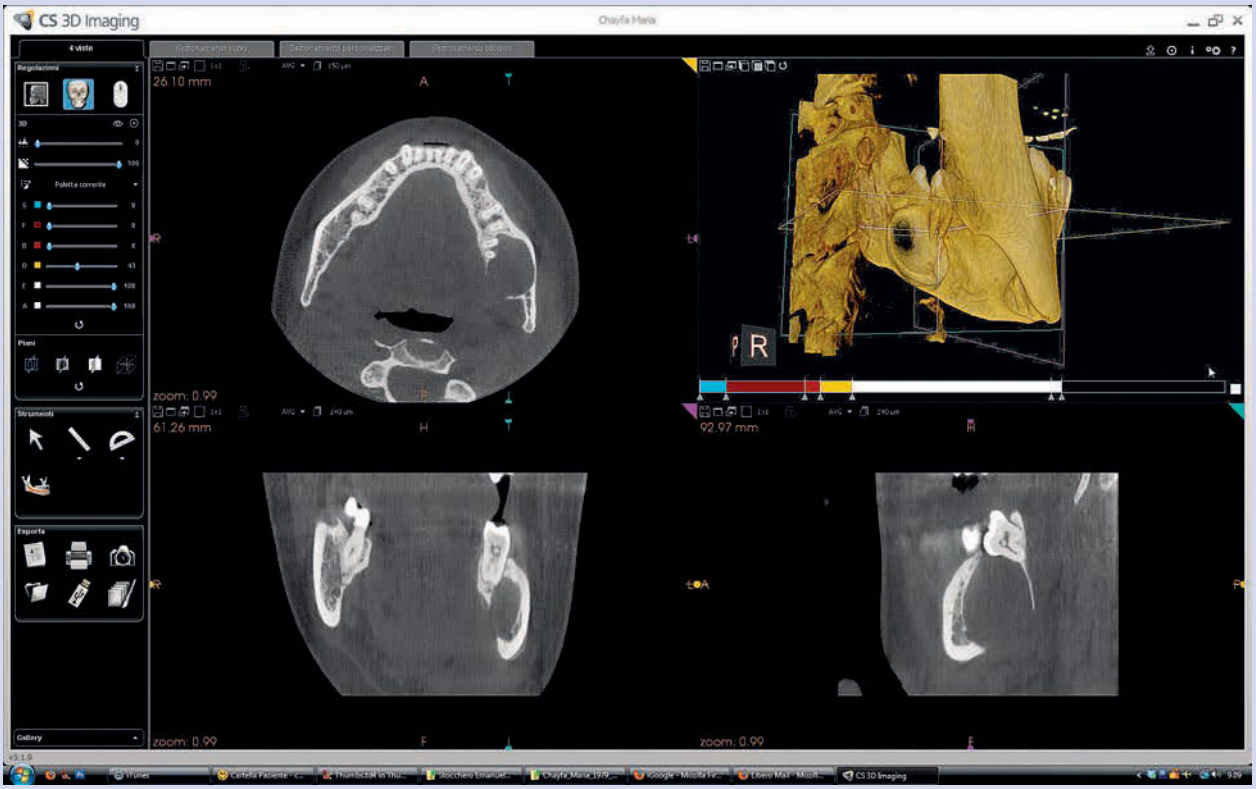

Fig. 33.1

CLINICAL CASE 33 *(cont'd)*

Roberto Ghiretti

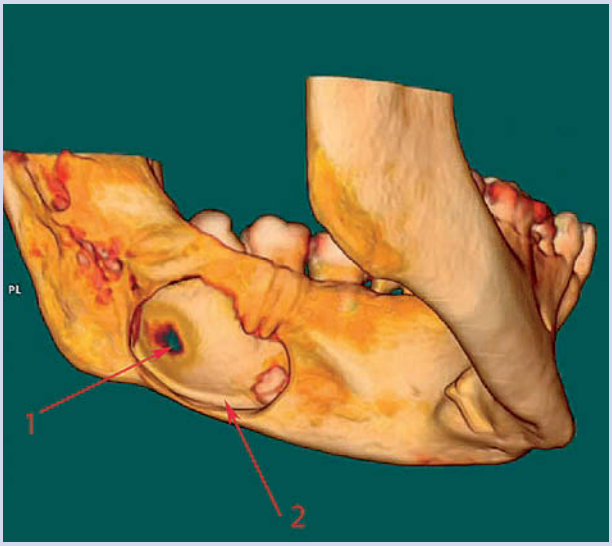

Fig. 33.2

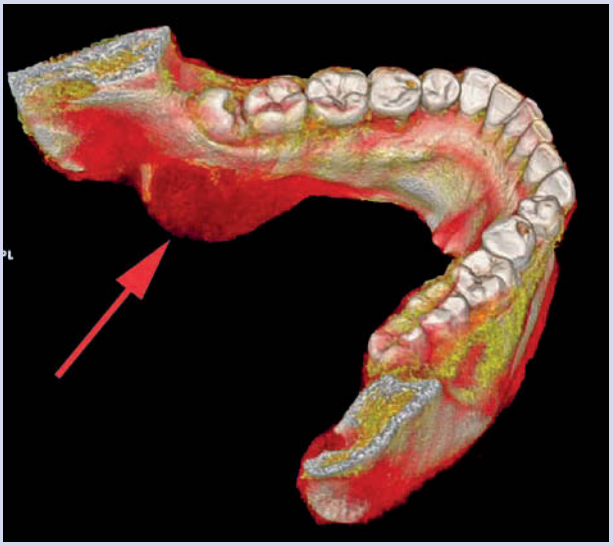

Fig. 33.3

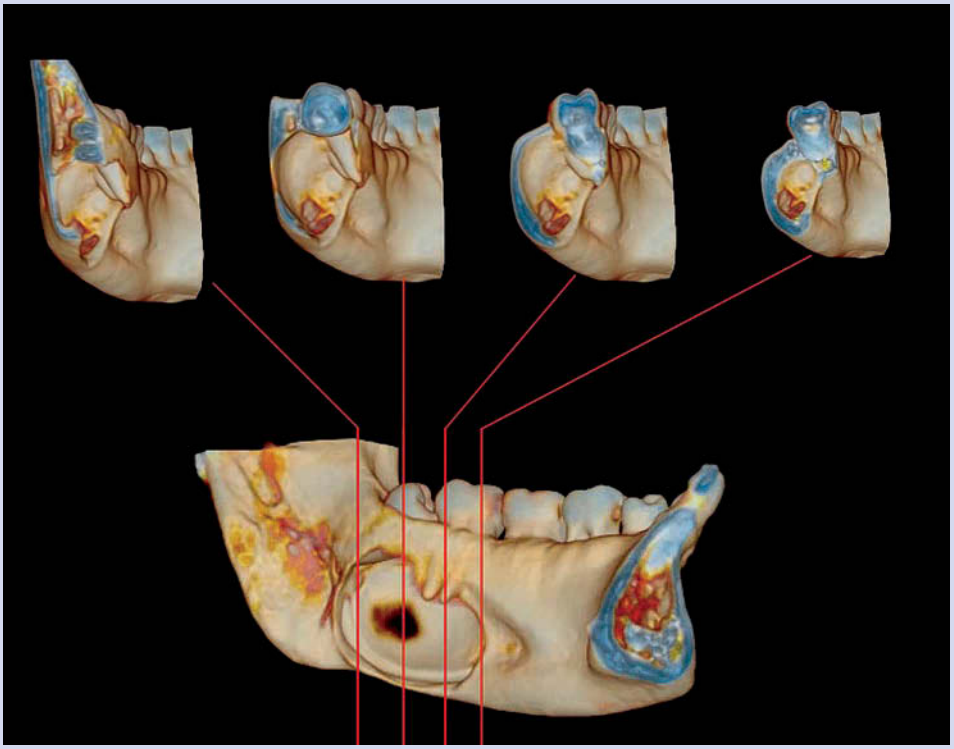

Fig. 33.4

CLINICAL CASE 34

Roberto Ghiretti

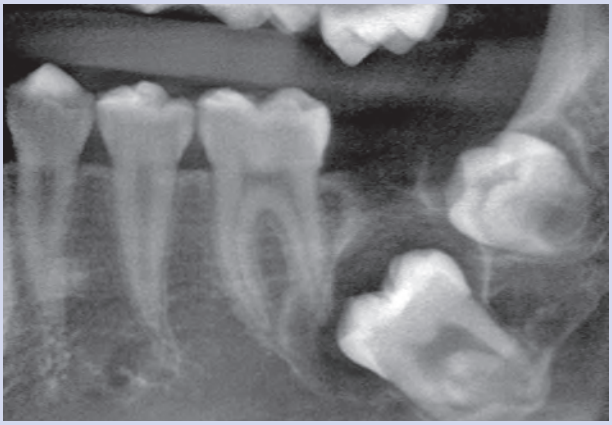

Fig. 34.1

This sixteen-year-old female patient came to my office lacking her lower left second molar.
The OPG showed the impacted tooth and a pericoronal cyst (Fig. 34.1).
The CBCT exam highlighted the exact size of the lesion and its anatomical relations to 3.6 and 3.8 (Fig. 34.2), while the analysis of the alveolar nerve showed its close relation to the roots of the impacted tooth (Fig. 34.3).

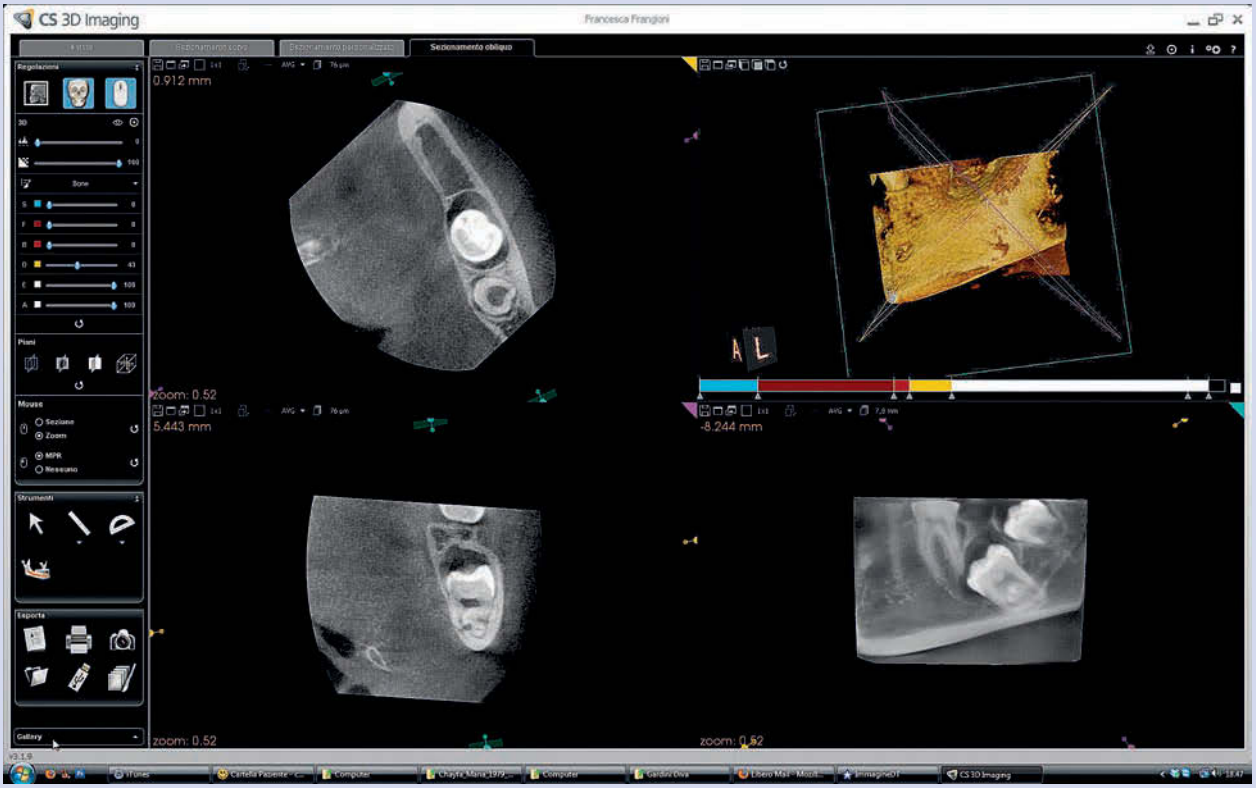

Fig. 34.2

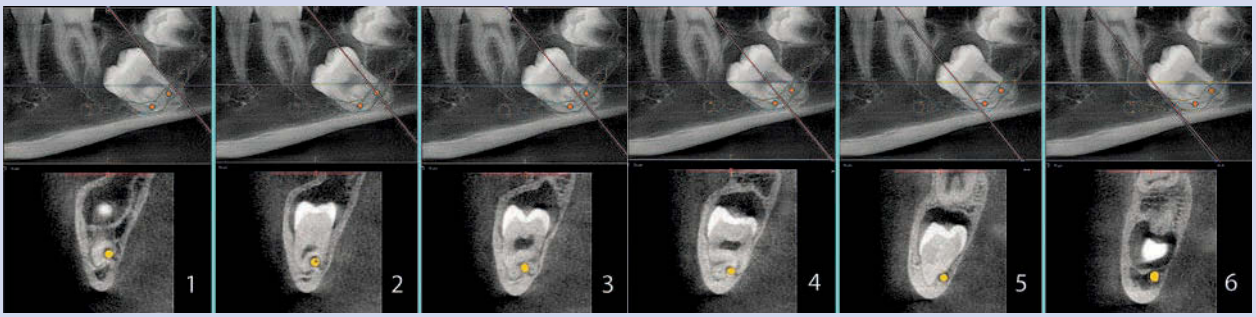

Fig. 34.3

Developmental non-odontogenic cysts

Nasopalatine, or incisive canal, cysts

They originate in the nasopalatine duct on the median close to the incisor foramen. This is one of the most common non-odontogenic oral cysts, especially in male patients from forty to seventy years old. It usually appears with palatal tumefaction between the two central incisors and often without any symptoms. The OPG shows a well-defined oval or round radiolucent area between the roots of the two upper central incisors. As highlighted by Faitaroni et al. (2011), the CBCT exam turns out to be very useful in the initial diagnosis and surgical planning for these lesions. The final diagnosis, however, should absolutely be performed after the histological exam (Clinical Case 35).

CLINICAL CASE 35 — **Emanuele Ambu**

This forty-two-year-old female patient came to my office because of a palatal tumefaction. The two-dimensional exams—OPG and an intra-oral X-ray (Fig. 35.1)—the patient gave us had caused us to suspect an endodontic lesion of the upper right incisor.

The vitality test, however, did not confirm this hypothesis: all front dental elements were vital. The volumetric exam allowed us to perform an initial diagnosis of a lesion of the nasopalatine duct (Fig. 35.2). The 3D reconstruction showed the lesion size (Fig. 35.3).

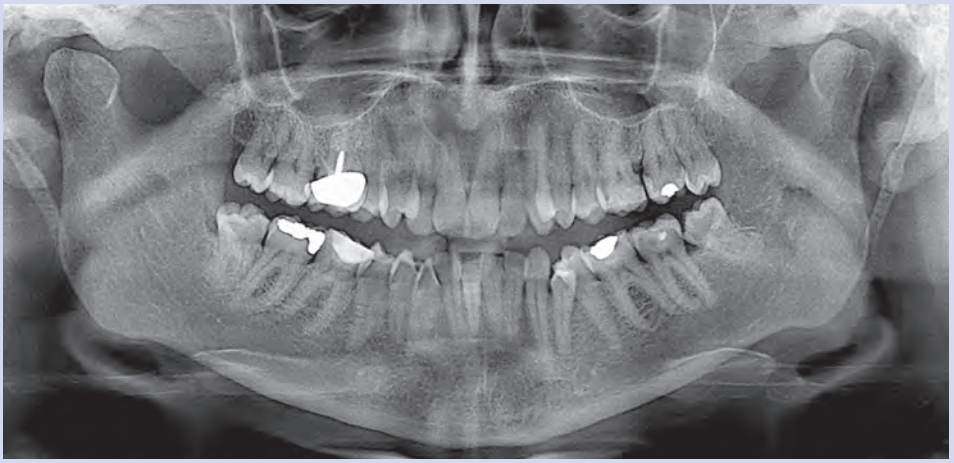

Fig. 35.1

Fig. 35.2

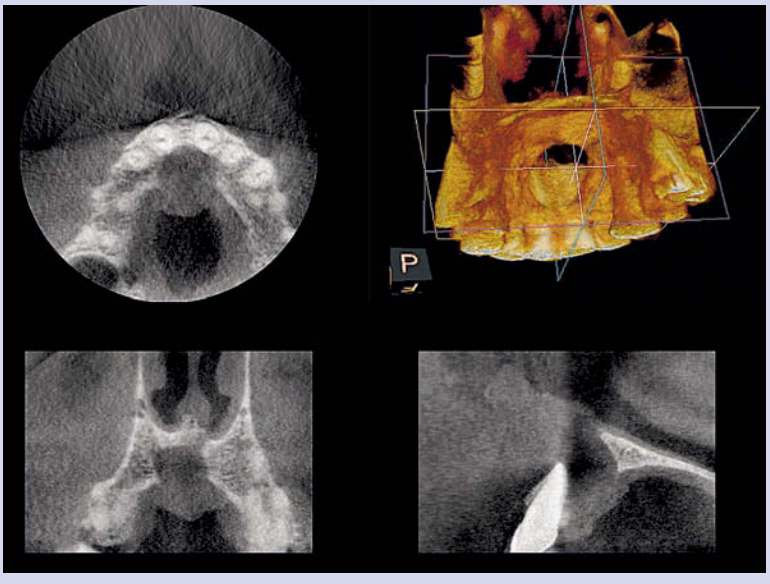

Fig. 35.3

Inflammatory cysts

Radicular cysts

Radicular cysts are definitely the most common cysts of maxillary bones; they account for fifty percent of cases. The radiographic representation is a radiolucent area with well-defined margins at the apex or around the root of the non-vital tooth. We have already dealt with these lesions in the section on root resporption. Here we would like to show a clinical case that exhaustively explains the advantages of CBCT in the diagnosis and resolution of this disease (Clinical Case 36).

CLINICAL CASE 36 — **Emanele Ambu and Roberto Ghiretti**

Despite accurate retreatment, the wide radiolucent lesion of this upper left second molar had not disappeared.
The CBCT exam highlighted its size and relations to the sinus and pterygoid fossa (Fig. 36.1).
The lesion was removed surgically (Fig. 36.2) and an apicoectomy was performed.

We then retro-prepared (Fig. 36.3) and sealed the four canals and the isthmus among them (Fig. 36.4a). The three-dimensional reconstruction of the data obtained by the follow-up exams after surgery showed good apical sealing (Fig. 36.4b). The CBCT exam performed after one year showed that the case had been resolved (Fig. 36.5).

Fig. 36.1

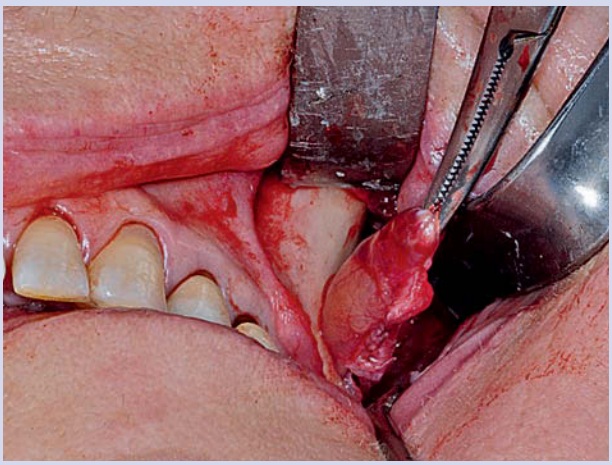

Fig. 36.2

Fig. 36.3

CLINICAL CASE 36 *(cont'd)*

Emanele Ambu and Roberto Ghiretti

Fig. 36.4a

Fig. 36.4b

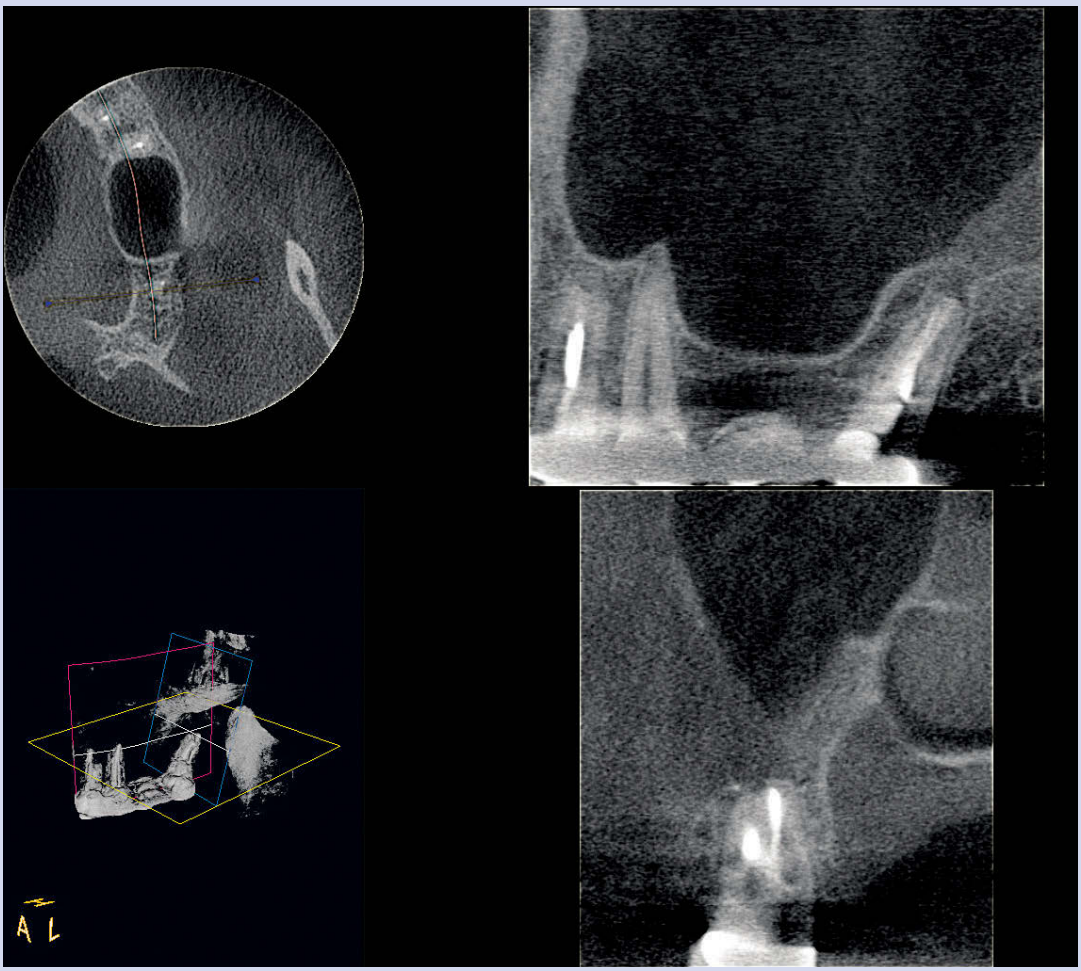

Fig. 36.5

Residual cysts

The origin and development of so-called "residual cysts" has been well explained by Nair (2006). These account for ten percent of cases in which lesions do not disappear after the extraction of the dental elements supporting them (Oehlers 1970) (Clinical Case 37).

CLINICAL CASE 37

Roberto Ghiretti

A seventy-two-year-old female patient came to our office complaining about a persistent abscess in the area of the bridge positioned among the elements 34-36. We found a slightly painful tumefaction after palpation, with no signs of paresthesia in the area of the mental nerve. The volumetric exam (Fig. 37.1) showed a radiolucent roundish lesion in the area of the lower left second premolar that had been extracted.
A diagnosis of residual cysts was performed. As we can see, the image taken during surgery (Fig. 37.2b) corresponds exactly to the three-dimensional reconstruction that allowed us to plan the surgery (Fig. 37.2a).

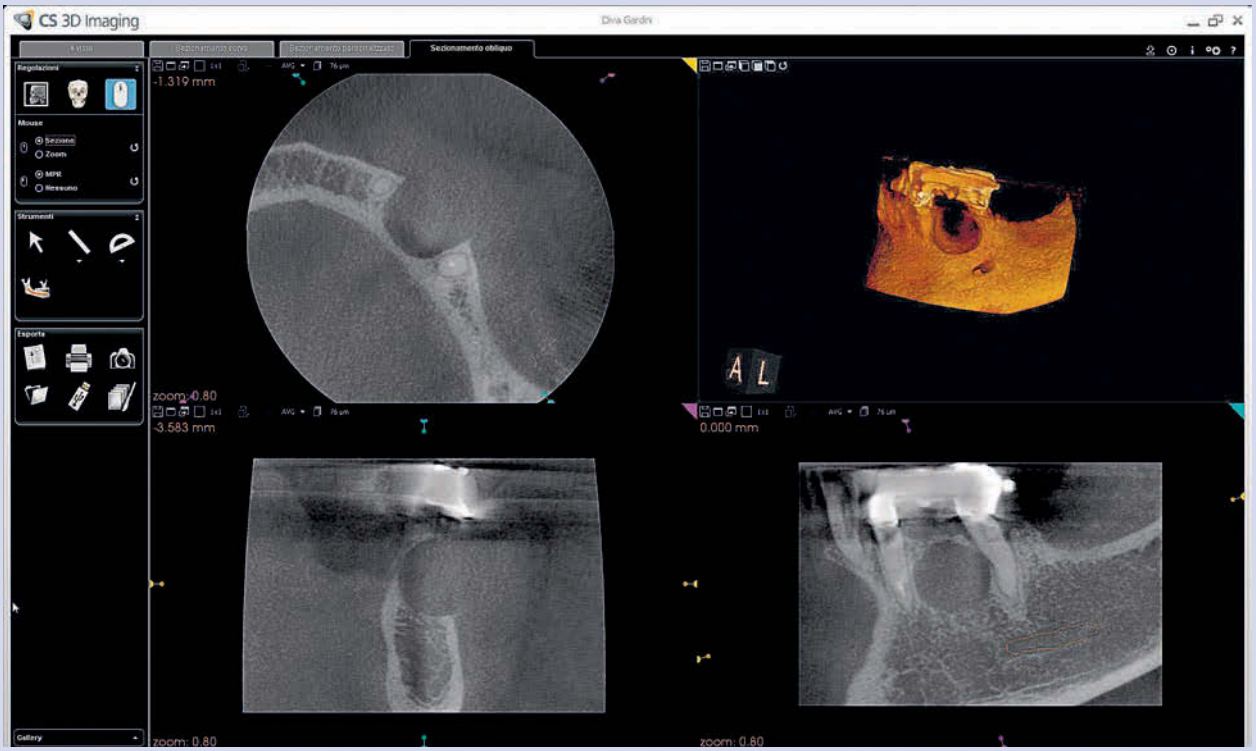

Fig. 37.1

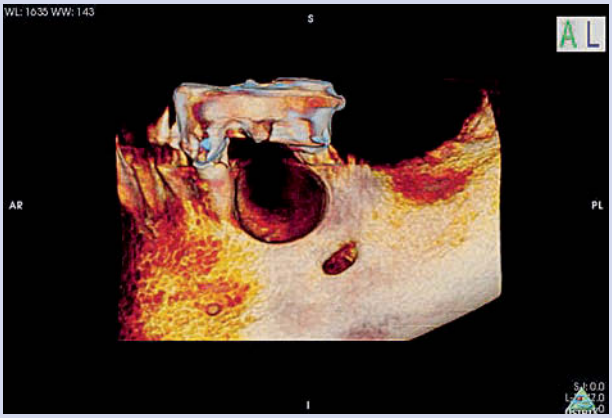

Fig. 37.2 a

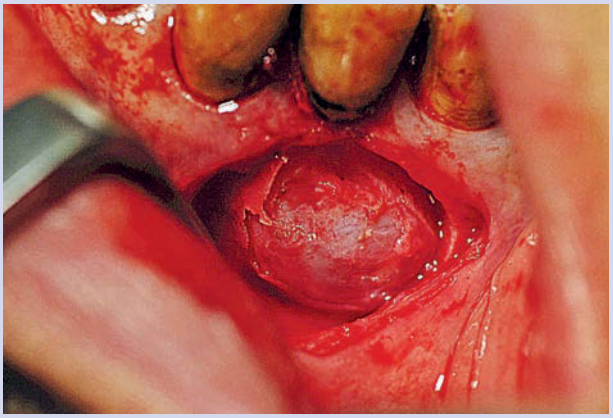

Fig. 37.2 b

Radiolucent non-cystic lesions

Hemorrhagic cysts

These lesions, whose origins are not yet clear, are known as traumatic, empty, or solitary cysts. They appear as empty cavities with no epithelium. The diagnosis of these lesions can be performed during surgery (Kumar et al. 2011). The use of CBCT in the diagnosis of these lesions has been described by Mathew et al. (2011) (Clinical Case 38).

CLINICAL CASE 38 — **Roberto Ghiretti**

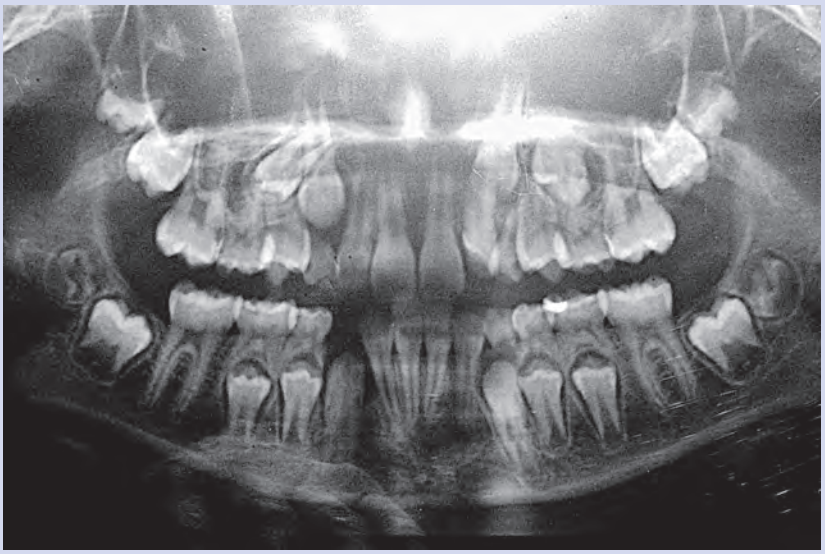

Fig. 38.1

During a routine checkup, the OPG showed an area of periapical bone rarefaction in the elements from the lower left lateral incisor to the lower right central incisor (Fig. 38.1).
After tests, these elements turned out to be vital.
The CBCT confirmed the osteolytic area and showed its size (Fig. 38.2).
The hemorrhagic cyst diagnosis was confirmed by surgery.
An osteolytic area appeared empty and with no epithelial membrane (Fig. 38.3).
The volumetric exam performed one year later showed the complete re-formation of bone tissues (Fig. 38.4).

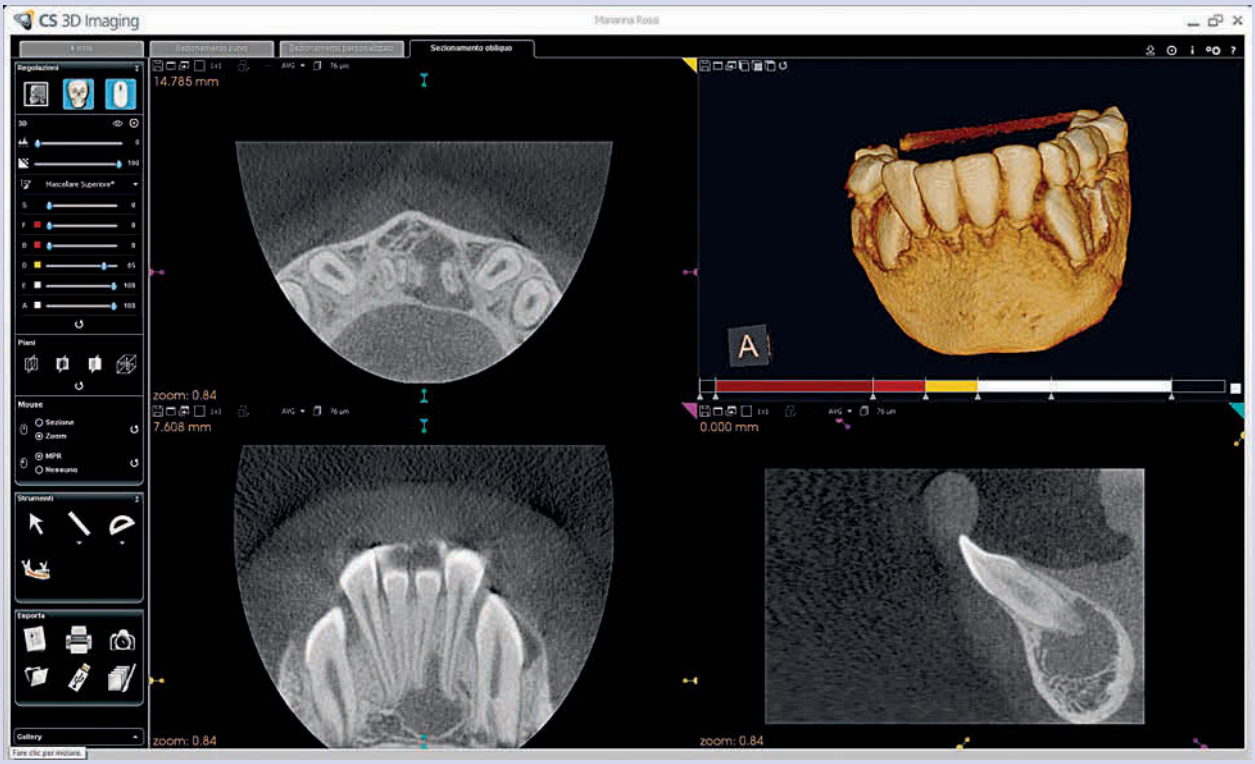

Fig. 38.2

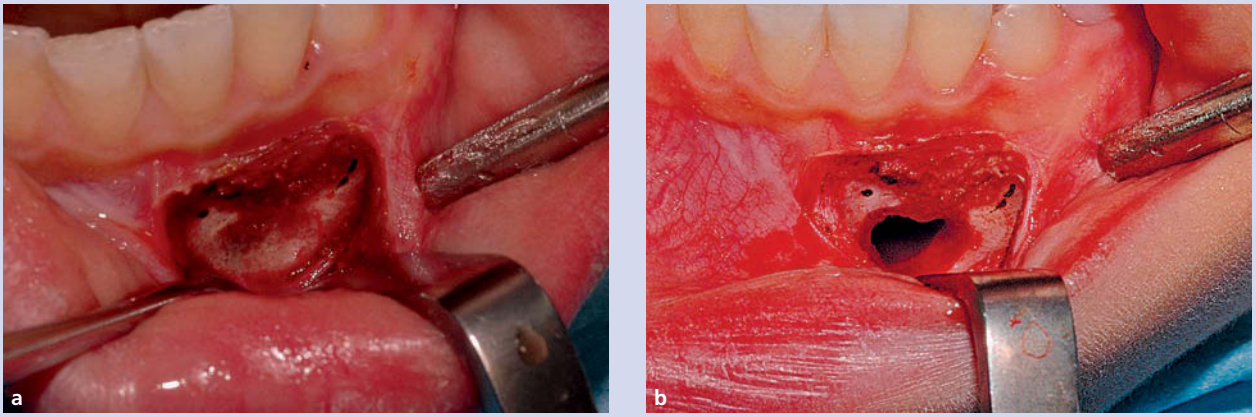

Fig. 38.3

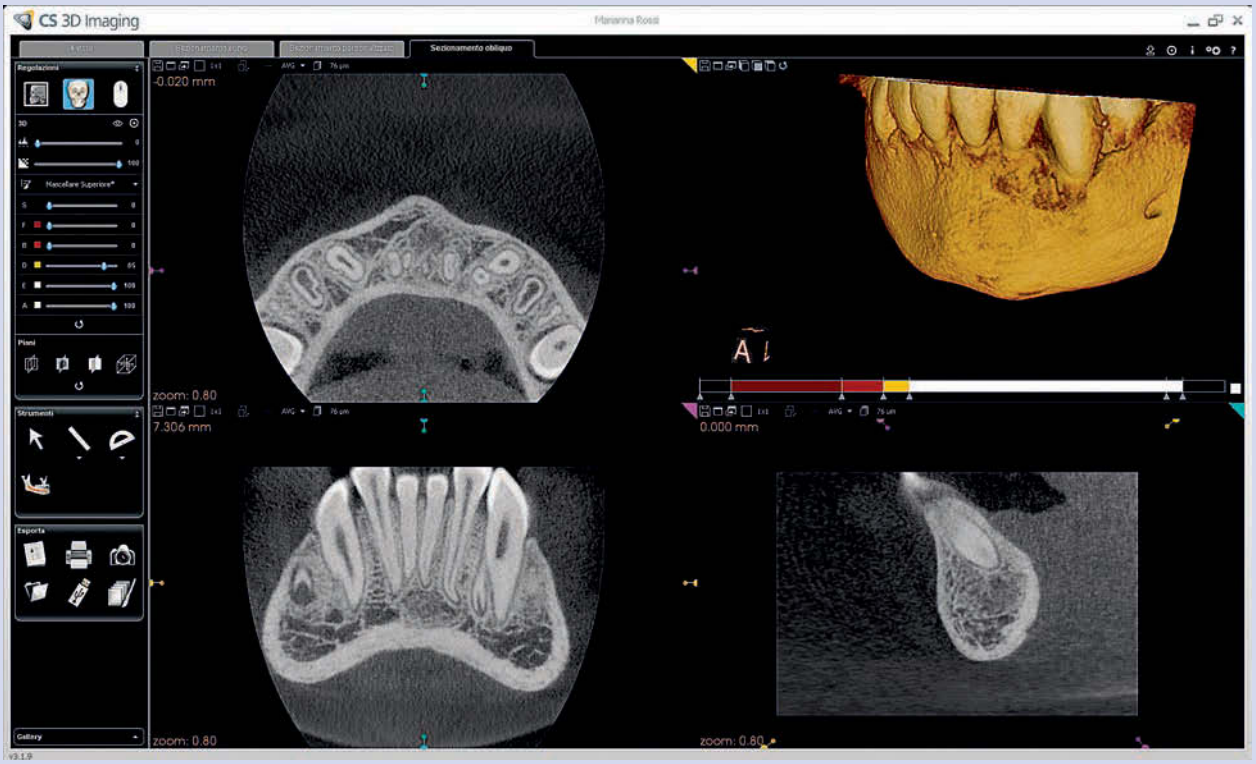

Fig. 38.4

Malignant and benign tumors

Malignant tumors

As will be further explained in the section on maxillofacial surgery, the CBCT exam is not the most recommended exam for diagnosing malignant tumors. We would like to underline here the features of a clinical pattern that should warn clinicians, so they can send patients to suitable health facilities (Clinical Case 39).

CLINICAL CASE 39

Marco Vigna

This sixty-eight-year-old male patient came to me one year after the extraction of his left second molar (Fig. 39.1), with a lesion in that area. The clinical exam (Fig. 39.2) alarmed the clinician, who performed a radiological volumetric exam. The image showed the complete lack of bone structures in the area (Fig. 39.3). The patient was immediately sent to the maxillofacial ward and underwent a surgical intervention within a few days. The histological exam confirmed an adenocarcinoma of the salivary glands.

Fig. 39.1

Fig. 39.2

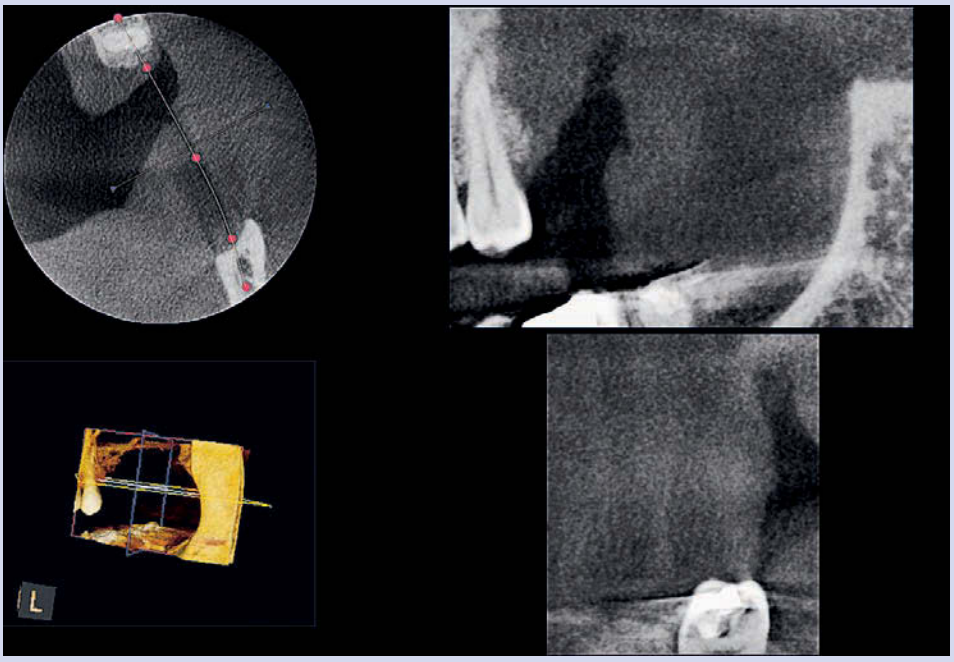

Fig. 39.3

Benign tumors

Osteomata

An osteoma is a benign bone tumor which most commonly develops on the skull and jaw bones. It can be subdivided into cancellous, compact, or both, tumors. It is characterized by a bony protuberance of mature lamellar or woven bone that usually arises in membranous bones. It is not fully clear yet whether an osteoma is a neoplasm or hamartoma. An osteoma may be either solitary or multiple, occurring on a single bone or numerous bones. The lesion slowly enlarges, and is painless until its size or position interferes with function. Multiple osteomata of the jaws as well as of long bones and the skull are a characteristic manifestation of Gardner syndrome and familial adenomatous polyposis (FAP).

The diagnosis of an osteoma is made after a radiographic examination. It is usually detected in the mandible rather than in the maxilla. The most common locations are: the posterior aspect of the mandible on the lateral aspect of the ramus, below the lower molars, coronoid process, or mandibular condyle. An osteoma is usually round or oval and appears as a homogenous radiopaque projection on a broad base, but rarely will it be pedunculated. Its margins are smooth, well defined, and well corticated. The cancellous type has a normal trabecular bone pattern. Large osteomata can displace soft tissues such as muscles and can cause dysfunction. The use of CBCT in the diagnosis of osteomata is suggested by Kamel et al. (2009) as a useful instrument for early detection and evaluation of osteomata and dental anomalies with accurate assessment of their relationship to adjacent anatomical structures (Clinical Case 40).

CLINICAL CASE 40 — **Roberto Ghiretti**

This forty-four-year-old female patient was referred to me with a large bone thickening in her upper frontal area, as detected by the panoramic radiograph performed during a routine checkup (Fig. 40.1). The patient showed no symptoms at all; her dental elements in the area examined had normal responses to vitality tests. A hard but painless area was detected by palpation. The volumetric exam showed a thickened area, diagnosed as an osteoma, and we could assess its size. The anatomical borders were further clarified by the 3D reconstruction (Figs. 40.2 and 40.3).

Fig. 40.1

CLINICAL CASE 40 *(cont'd)* **Roberto Ghiretti**

Fig. 40.2

Fig. 40.3

Odontomas

Odontomas are composed of enamel, dentin, cementum, and pulp tissue. Since they grow slowly and are well differentiated, they are generally considered hamartomas rather than neoplasms. They can be either compound or complex.

A compound odontoma is a collection of small radiopaque masses, some of them or all may be tooth-like structures, "denticles" of sorts. It usually occurs in the anterior maxilla (sixty-two percent of cases) and is generally associated with the crown of an impacted canine. It is caused by an exuberant growth of the dental lamina or due to proliferation of the enamel organ. A complex odontoma is composed of haphazardly arranged hard and soft dental tissues. It does not look like a normal tooth. It usually occurs in the posterior maxilla or in the mandible (seventy percent of cases).

Odontomas are the most common odontogenic tumors and they interfere with the eruption of permanent teeth. They begin to develop as normal dentition does and cease when tooth

development ends. There is no sex predilection. They ideally occur in teenagers. They are usually asymptomatic and are discovered during routine radiographic exams when there are permanent tooth eruption delays. They occur in both the maxilla and the mandible. Radiologically, their borders appear well defined, often with a cortex surrounding a soft tissue capsule. The internal structure is largely radiopaque. They often interfere with the normal eruption of teeth. They can be associated with impacted teeth, malposition, malformation, and displacement of adjacent teeth (Clinical Case 41).

CLINICAL CASE 41

Andrea Nakhleh, Santiago Isaza Penco

A thirty-one-year-old female patient with a severe malocclusion came to the practice for orthodontic treatment. After a routine OPG pre-treatment (Fig. 41.1), a strange image which resembled a "soap bubble" was identified mesial to the lower right canine. Thus, a CBCT was performed in this area to evaluate the radiopacity more accurately (Fig. 41.2). The CBCT allowed us to visualize a lesion like multiple odontoma. In order to perform the orthodontic treatment, this lesion was removed surgically. The response of histological analysis confirmed the multiple odontoma lesion. The patient was then ready to start orthodontic treatment.

Fig. 41.1

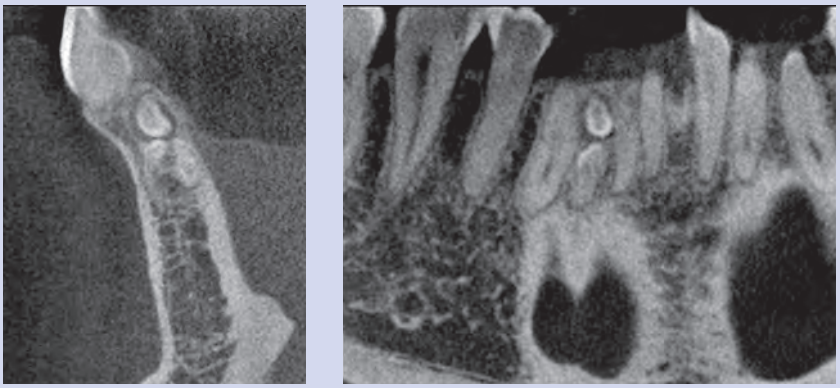

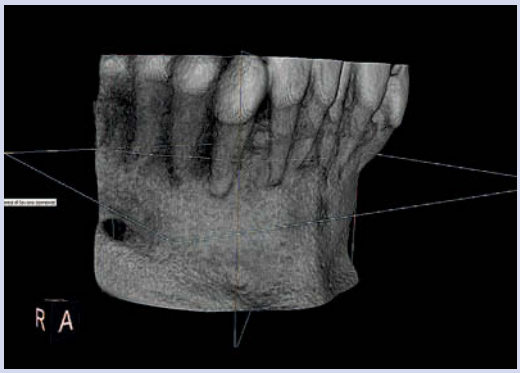

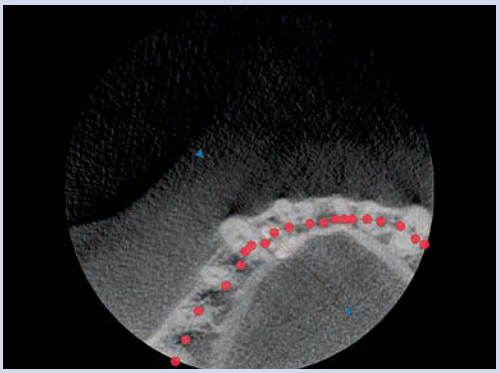

Fig. 41.2

Exodontic surgery

Three-dimensional radiology is particularly useful for exodontic surgery. It allows us to observe the exact anatomical relations of dental elements and adjacent structures, avoiding all problems related to two-dimensional radiology, like the overlapping of different structures.

Extraction of lower third molars

One of the necessary procedures to reduce the risk of complications is to locate the canal of the inferior alveolar nerve, if this is closely adjacent to the roots of the element to be removed. The identification procedures with two-dimensional radiology are well known (Rood and Shehab 1990); the nerve path, however, may be tortuous and have two or even three canals which cannot be easily detected by two-dimensional radiology (Mizbah et al. 2012). The use of CBCT has recently been discussed for detecting the retromolar canal before surgery, usually detectable in twenty-five percent of cases (von Arx et al. 2011).
Besides allowing surgical planning, CBCT permits better risk assessment, as compared to panoramic radiography (Ghaeminia et al. 2011). After reviewing the CBCT images, this study has made it possible to classify a higher number of subjects as being at a lower risk for inferior alveolar nerve (IAN) injury as compared to the panoramic radiograph assessments. This change in risk assessment also resulted in a significantly different surgical approach. Consequently, CBCT has encouraged more adequate surgical planning (Clinical Case 42).

CLINICAL CASE 42 — **Roberto Ghiretti**

This twenty-two-year-old male patient came to my office because of dysodontiasis of his lower right third molar. The panoramic radiograph (Fig. 42.1) suggested performing a CBCT to assess the relations of the neurovascular bundle nerve and the tooth roots (Fig. 42.2).

As pointed out by the arrows (Fig. 42.3), the nerve goes between the tooth roots with partial bone inclusion and the dentist will be forced to act with great care when extracting the element.

Fig. 42.1

CLINICAL CASE 42 *(cont'd)*

Roberto Ghiretti

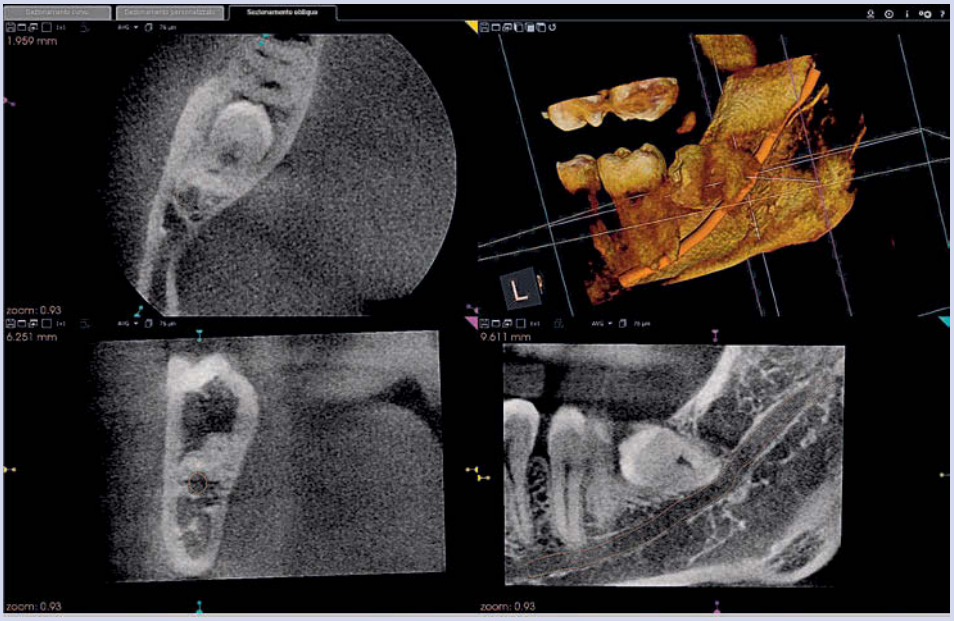

Fig. 42.2

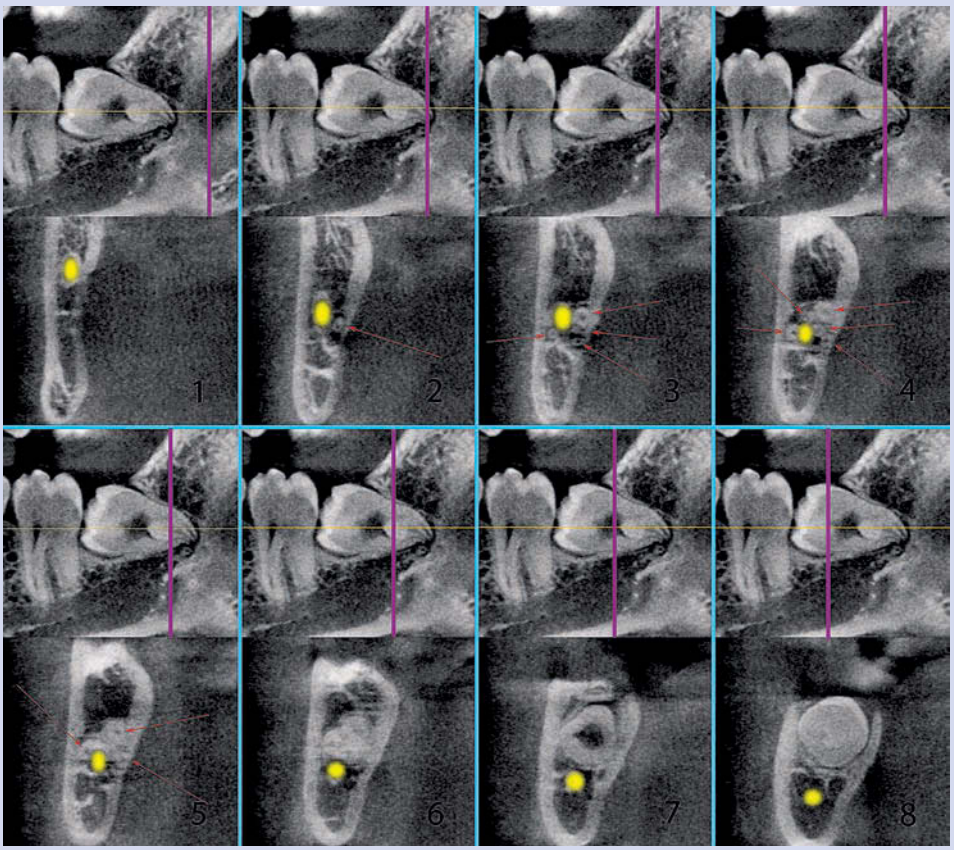

Fig. 42.3

Extraction of upper third molars

In this case, the three-dimensional exam is essential for assessing the position of the element, the maxillary sinus, and the roots of the adjacent teeth (Clinical Case 43).

CLINICAL CASE 43

Emanuele Ambu and Alberto Bianchi

This fifty-four-year-old male patient came to the practice complaining about persistent abscesses in his upper right second molar, which had already been properly treated endodontically. The CBCT made it possible to plan the removal of a cystic lesion, the extraction of his upper right third molar, and the endodontic surgery of his adjacent second molar, contemporaneously. All canals were subject to apicoectomy and retrograde filling (Fig. 43.1). The follow-up exam performed one year later showed perfect healing of all tissues (Fig. 43.2).

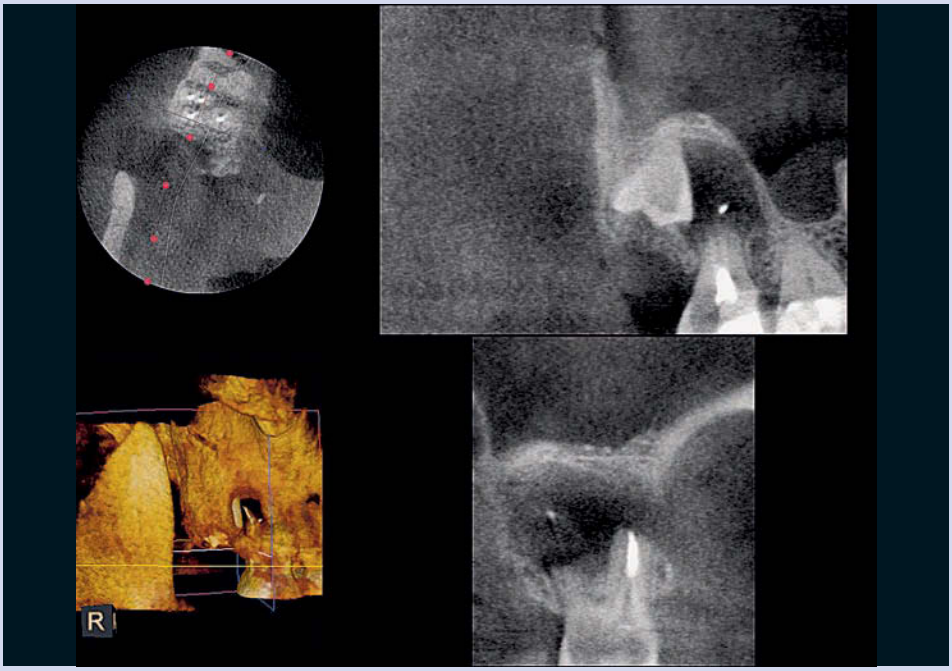

Fig. 43.1

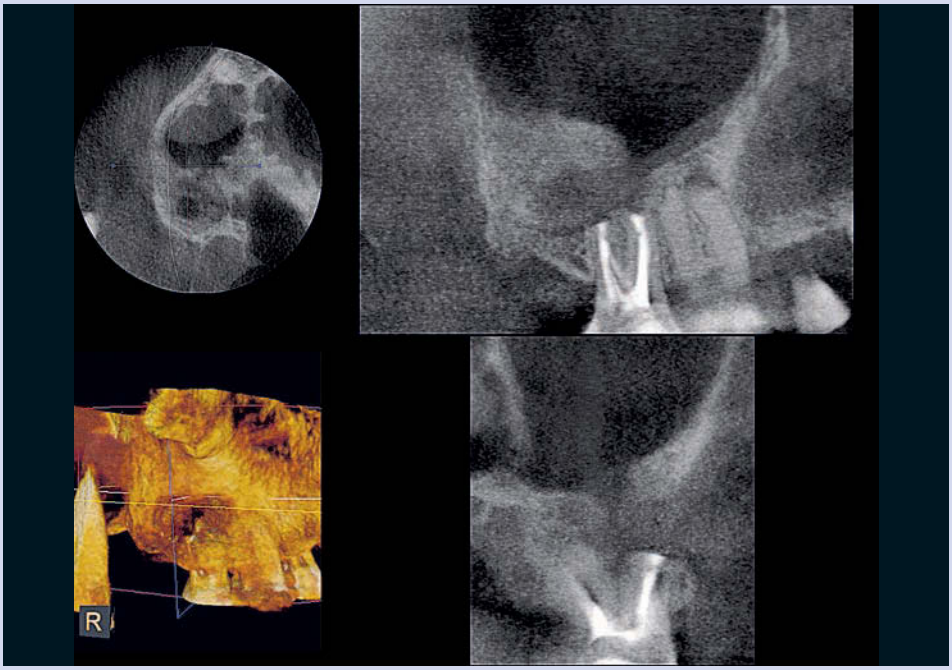

Fig. 43.2

Dental anomalies in shape, number, and location

In this case, too, CBCT has been useful in providing better planning of the treatment to perform, because there is no risk of overlapping of the anatomical structures, unlike with two-dimensional radiology. Furthermore, rendering has made it easier to understand the anatomical relationships and to communicate with patients or their parents.
Below, some cases are shown with anomalies in shape, number, and location.

Abnormal shapes

The use of CBCT has been suggested in studying abnormal shapes, both to overcome the problems of a single element (Patel 2010), and to assess the genetic disorders in a family (dos Santos Neto et al. 2011) (Clinical Case 44).

CLINICAL CASE 44 — **Emanuele Ambu**

Fig. 44.1

This seven-year-old girl was referred by her orthodontist to confirm the abnormal shape of her upper premolar, as suggested by an intra-oral X-ray (Fig. 44.1).
The CBCT, however, showed the presence of two erupting premolars, the second being displaced (Fig. 44.2).

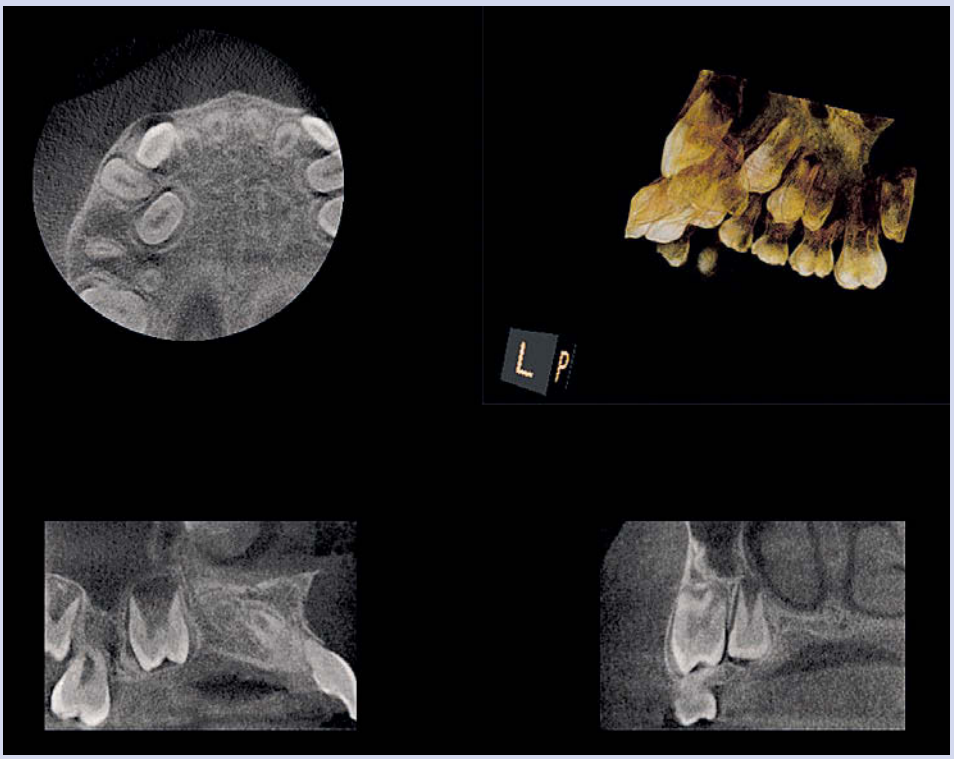

Fig. 44.2

Supernumerary teeth

Santiago Isaza

Supernumerary teeth are not rare anomalies of the maxillofacial complex (Ruprecht et al. 1984). Some associated complications have been reported, including interference with the eruption of adjacent teeth, crowding, and displacement of these teeth, root resorption, dentigerous cyst formation, and loss of vitality of the adjacent teeth associated with severe root resorption (Stafne and Gibilisco 1975; Becker et al. 1982; Most and Roy 1982; Shafer et al. 1983). The periapical radiograph taken with the paralleling technique is considered

CLINICAL CASE 45

Andrea Nakhleh, Santiago Isaza Penco

A seven-year-old boy came to the practice due to the presence of two lateral incisors (Fig. 45.1). The panoramic radiograph (Fig. 45.2) showed both teeth. A 3D exam was necessary to decide which tooth was eligible for extraction, according to its anatomy and position (Fig. 45.3 a, b). We then performed the extraction of the right tooth (Fig. 45.4), because it was shorter than the left one and because the crown of the permanent canine was very close to its root apex.

Fig. 45.1

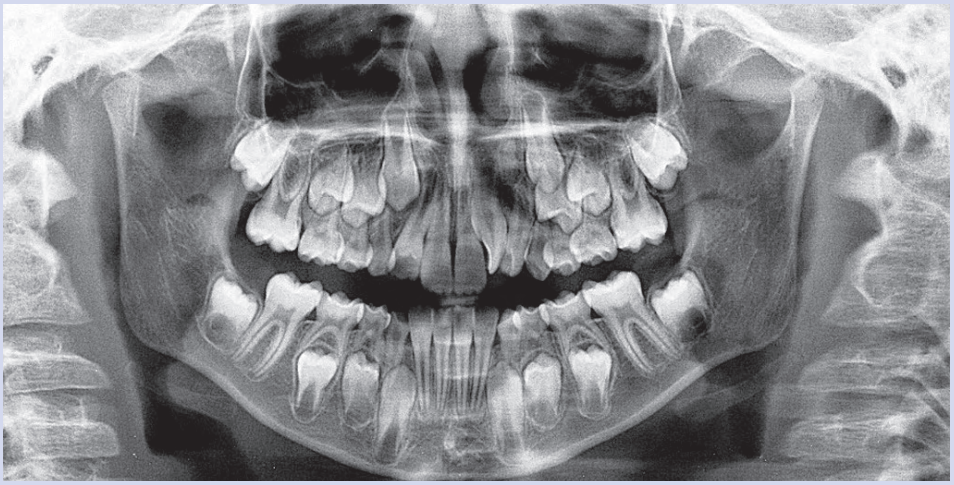

Fig. 45.2

the gold standard of clinical procedure to measure tooth length and estimate root resorption (Sameshima and Sinclair 2001; Årtun et al. 2005). However, periapical radiographs are subject to errors in procedure, orientation, or projection. The orientation errors and overlapping problems of periapical radiographs can be overcome with cone beam computed tomography. For clinical purposes, CBCT voxel sizes of 0.2, 0.3, and 0.4 mm should be considered at least as accurate and reliable as periapical radiographs for tooth length and root length assessments (Sherrard et al. 2010). Furthermore, CBCT imaging yields accurate three-dimensional pictures of local dental and bone structures, and it is helpful for pre-treatment evaluation of supernumerary teeth (Liu et al. 2007) (Clinical Case 45).

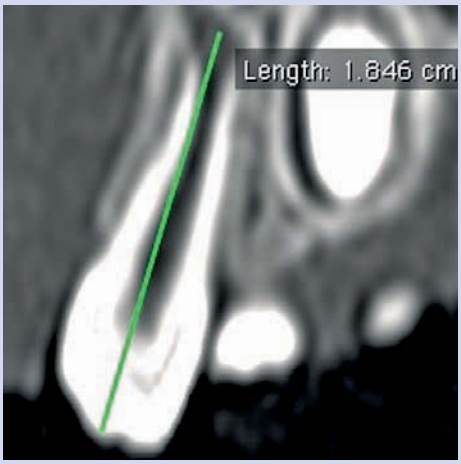

Fig. 45.3 a

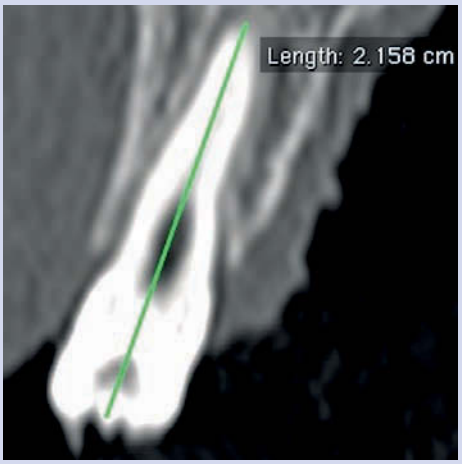

Fig. 45.3 b

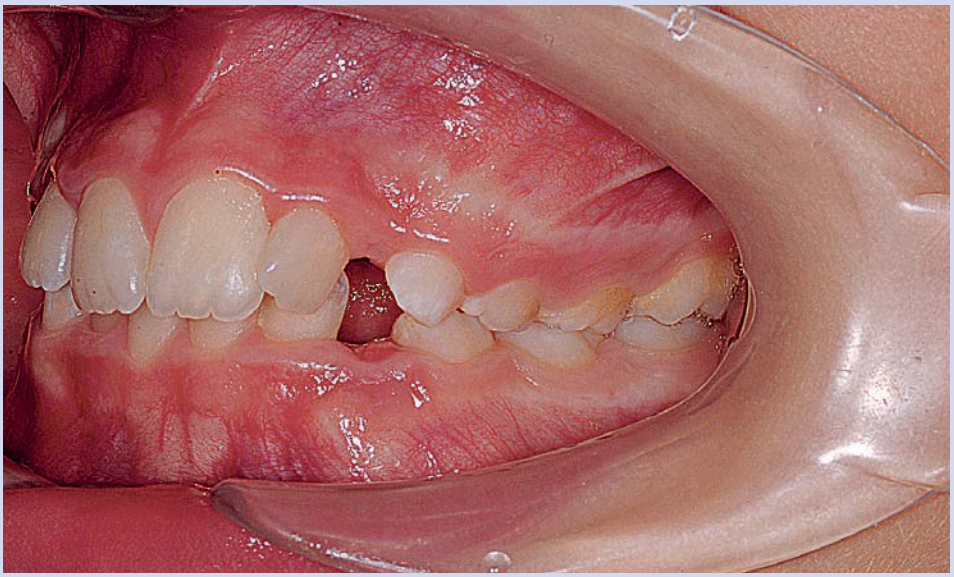

Fig. 45.4

Anomalies in location (Clinical Case 46)

CLINICAL CASE 46

Emanuele Ambu

A forty-year-old female patient came to the practice with a panoramic radiograph showing the abnormal position of her upper right third molar (Fig. 46.1).
The volumetric exam highlighted the strict relationship with the impacted element and the second molar roots (Fig. 46.2).
This finding is completely accidental and the OPG has been required for routine dental checking.

Fig. 46.1

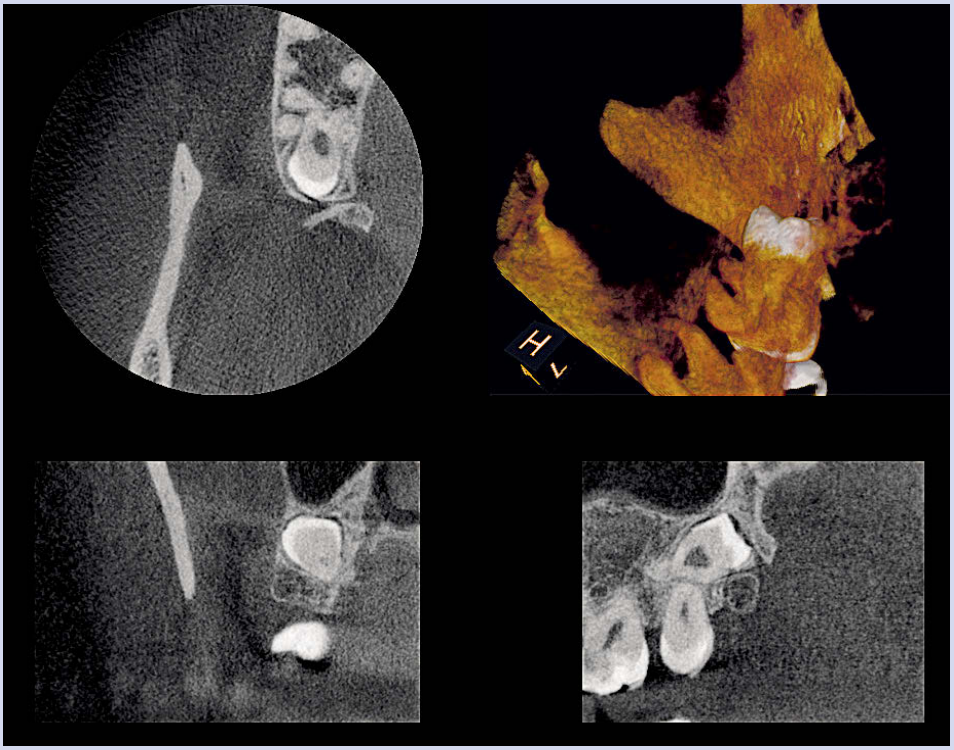

Fig. 46.2

CBCT in maxillofacial surgery

Claudio Marchetti - Achille Tarsitano

Introduction

Radiographic evaluation and diagnosis have undergone enormous changes in the last twenty years. New technologies are being developed and are becoming readily available in the medical and dental fields. The progress made in the hardware and software sectors have led to the development of innovative methods for facial diagnosis, treatment planning, and clinical application.
Cone beam computed tomography is a medical image acquisition technique based on a cone-shaped X-ray beam centered on a two-dimensional detector. The source-detector system performs one rotation around the object producing a series of 2D images. The images are reconstructed in a three-dimensional data set using a modified version of the original cone-beam algorithm developed by Feldkamp in 1984 (Feldkamp et al. 1994).
This technique is widely used in different industrial and biomedical applications, such as micro-CT. Among the first clinical applications were single-photon emission computed tomography (SPECT), angiography, and image-guided radiation therapy (IGRT). Dedicated CBCT scanners for the oral and maxillofacial area were pioneered in the late 1990s separately by Arai in Japan (Arai et al. 1999) and Mozzo in Italy (Mozzo et al. 1998).
Since then, there has been an explosion of interest in this new imaging technique in the oral and maxillofacial region by different research groups. The rapid evolution of the first prototypes into faster and better dedicated scanners has been driven by the development of new detector technology and by the increasing data processing power of common commercially available personal computers. In the last decade, the number of CBCT related papers published each year has also increased. The first systematic review published in literature on CBCT imaging of the oral and maxillofacial region to evaluate data on clinical applications, technical parameters, and radiation dose, was carried out by De Vos in 2009 (De Vos et al. 2009b). According to this review, eighty-six papers dealt with clinical applications of CBCT imaging in the oral maxillofacial region (OMF). All papers in which dedicated OMR CBCT scanners were used on patients in clinical situations were assigned to this group. The group was subdivided into nine clinical subcategories (Tab. 6.2).
One of the major fields of interest in CBCT in the maxillofacial area is the diagnosis and surgical planning of jaw bone lesions. It provides clear images of highly contrasted structures and is extremely useful for evaluating bone (Ziegler et al. 2002).
Although limitations currently exist in the use of this technology for soft tissue imaging, efforts are being directed toward the development of techniques and software algorithms to improve signal-to-noise ratio and increase contrast.

Tab. 6.2 - **Papers related to clinical applications of CBCT imaging of the OMF region (modified from De Vos, Casselman, Swennen 2009).**

Dentoalveolar	25	29%
Maxillofacial surgery	35	41%
Orthodontics	14	16%
Implantology	11	13%
Endodontics	4	5%
Periodontics	3	3%
General dentistry	1	1%
Forensic dentistry	1	1%
Otolaryngology	1	1%
Total	**95**	**110%**

CBCT used for detecting benign lesions of the jaws

Compared with conventional CT, the use of CBCT technology in clinical practice provides a number of potential advantages for the study of cysts of the jaws:

- Reducing the size of the irradiated area by collimation of the primary X-ray beam to the area of interest minimizes the radiation dose. Most CBCT units can be adjusted to scan small regions for specific diagnostic tasks.
- Since CBCT acquires all basis images in a single rotation, the scanning time is rapid (ten to seventy seconds) and comparable to that of medical spiral computed tomography (MDCT) systems. Although faster scanning time usually means fewer basis images from which to reconstruct the volumetric data set, motion artifacts due to subject movement are reduced.

We will show below two different types of benign jaw lesions assessed using CBCT images (Clinical Cases 47 and 48).

CLINICAL CASE 47

Claudio Marchetti and Achille Tarsitano

A thirty-five-year-old Caucasian man affected by a cystic lesion of the left maxilla was assessed using CBCT (Fig. 47.1). An impacted third molar was associated to the lesion. In this case, CBCT gave us good quality images.
The cyst was removed by intra-oral approach. The histological diagnosis was of a keratocystic odontogenic tumor. Besides the benefits for the diagnostic processes, three-dimensional imaging of cysts and tumors of the upper jaw can provide the surgeon with vital information necessary for planning surgery.
In the present case, we would like to emphasize that the CBCT image allowed a three-dimensional visualization showing the real extension of the lesion into the maxillary sinus. It could be useful, from the surgeon's perspective, to evaluate the possible bone erosion and the extension of the lesion to the masticatory space.

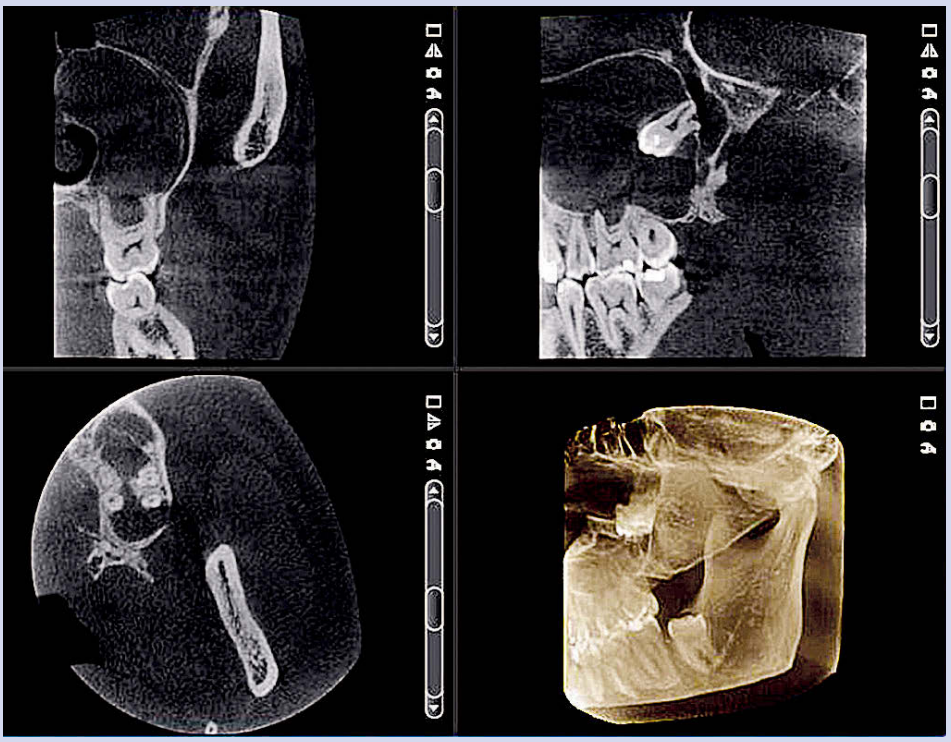

Fig. 47.1

CLINICAL CASE 48

Claudio Marchetti and Achille Tarsitano

A fifty-year-old African female patient affected by a large mandibular bone lesion was scheduled to undergo a full mandibular resection. The patient had both a multi-slice CT (MSCT) scan and CBCT. The MSCT (Fig. 48.1) showed that the large mandible bone erosion involved the entire mandible symphysis associated to the tooth loss. The CBCT was performed to assess the real efficacy of this diagnostic procedure for studying this kind of large bone lesion. The quality of the images was considered satisfactory, even though the dental scan view was not large enough to well depict the entire lesion (Figs. 48.2-48.4).

The histological diagnosis was of ameloblastoma. The patient underwent surgery consisting of a mandibular resection through cervical access. The mandibular reconstruction was performed at the same time, using a microvascular fibula free flap.

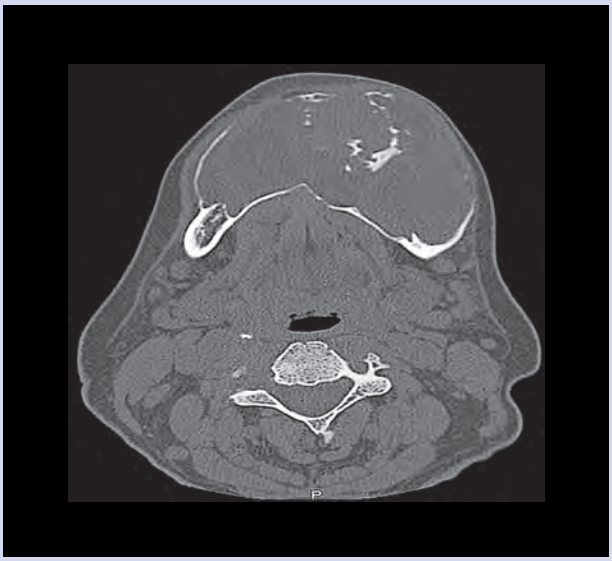

Fig. 48.1

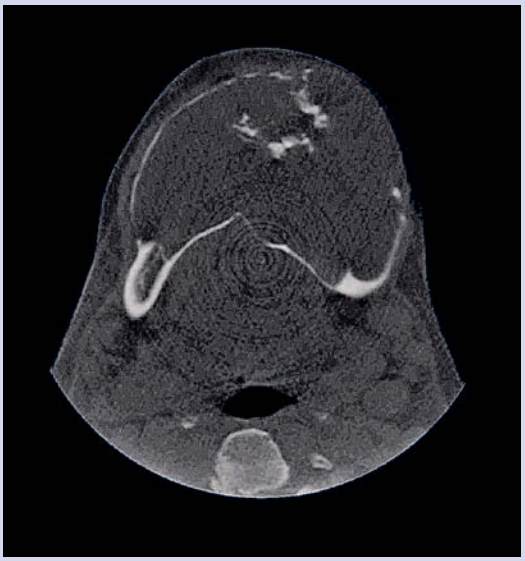

Fig. 48.2

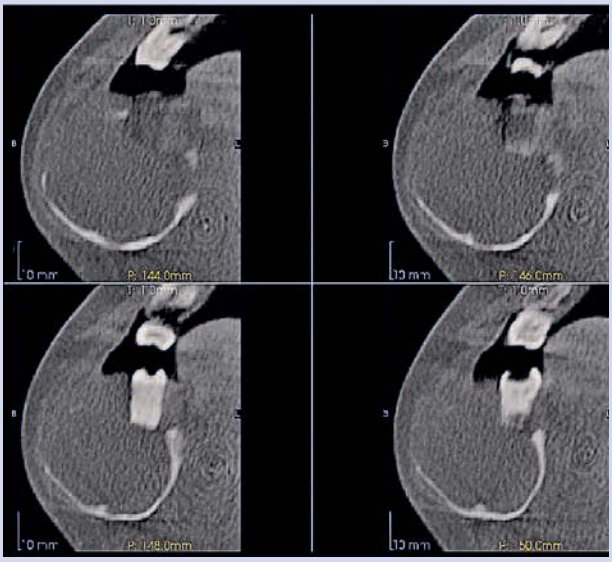

Fig. 48.3

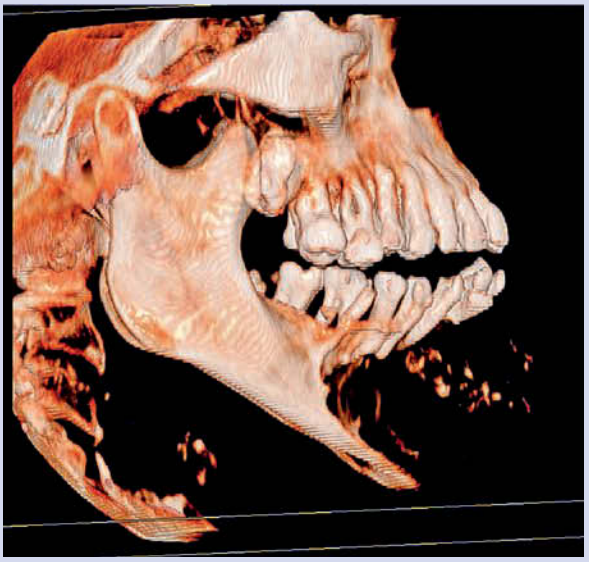

Fig. 48.4

CBCT used for detecting malignant lesions involving the jaws

Squamous cell carcinoma is the most frequent malignant neoplasm of the oral mucosa. Originating from the alveolar gingiva, it easily invades the mandible or maxilla. When the tumor extends to the alveolar bone, marginal or segmental ostectomy is mandatory, depending on the extent of involvement (Brown et al. 2002). Thus, one of the most important roles of imaging for alveolar gingival carcinomas is to evaluate the presence and extent of tumor invasion into the bone.

Various imaging modalities, including plain radiographs, bone scintigraphy, CT, and MRI have been used for this purpose and each modality has its advantages and disadvantages. Panoramic radiography is widely used for initial diagnosis of gingival carcinomas and its diagnostic accuracy has been reported by many authors.

Ord reported that the sensitivity, specificity, and accuracy of panoramic images in evaluating mandibular invasion by oral carcinoma were 87%, 80%, and 82%, respectively (Ord et al. 1997). According to the study, panoramic images failed to show early involvement, although they could show gross bone destruction. Other studies also reported false positive and/or false negative rates of 20-30% (Zupi et al. 1996).

Among these various imaging modalities used for evaluating mandibular invasion by oral carcinoma, helical CT is considered one of the most accurate whenever appropriate CT techniques are used. Goerres used 3-mm-thick bone algorithm axial and coronal CT images, and reported a sensitivity of 100% and specificity of 91% (Goerres et al. 2005). The common results in published studies about this topic were that helical CT causes few false negative results, although it generates some false positive results due to periodontal diseases or secondary changes from tooth extraction.

Recently, CBCT has been widely used in the oral and maxillofacial region (Boeddinghaus and Whyte 2008).

When compared with helical CT, the major advantages of cone beam CT include high spatial resolution and low radiation dose. However, there have been no systematic studies that evaluated its usefulness in the diagnosis of mandibular invasion by oral carcinoma.

Momin, in a study published in 2009 (Momin et al. 2009), made a comparison of CBCT and panoramic radiography for assessment of bone invasion by oral squamous cell carcinoma. According to the author, the cone beam CT showed that there were a large number of false negative results and the mean sensitivity was 89%.

He could not directly compare cone beam CT with helical CT, because the imaging protocol of the latter was not standardized and the number of cases with optimal helical CT images was quite limited. However, combining the results of his study with those of other studies of helical CT (Mukherji et al. 2001), the hypothesis that cone beam CT is more accurate than other imaging modalities, including helical CT, in evaluating mandibular invasion by a tumor may not be correct. Severe dental artifacts and image noise were responsible for the relatively low sensitivity of cone beam CT.

It is well known that dental artifacts can hamper the images in not only cone beam CT but also helical CT. However, in the latter, the amount of streak dental artifacts can effectively be reduced by the technique of angling the gantry to avoid metallic dental restorations.

In conclusion, CBCT, today, cannot be considered the gold standard of imaging techniques in the evaluation of bone involvement by malignant oral lesions.

Periodontics

Massimo Frosecchi

CBCT in periodontics

For quite some time, there have been accurate protocols for making periodontal diagnoses. According to those procedures, all risk factors should be assessed when making a patient's medical history; a clinical exam should be done afterwards, writing down, in a special chart (periodontal chart), data, like probing, gingival recession, tooth mobility, furcation defects, bleeding, and deposits. There are several kinds of periodontal charts with some little differences. All of them, however, are designed to define the type of periodontal disease, the type of treatment to perform, and which prognosis of the elements is to be expected.

Radiographic exams are essential in periodontology, because it is possible to define a number of parameters which are necessary for planning treatment and prognosis. Moreover, since they can be repeated several times, the follow-up exams performed after a lapse of time can show us whether our treatment has been successful. Traditionally this exam, known as "periodontal status," includes a set of fourteen to sixteen intra-oral X-rays with a radiation dose to patients of about 100 microsievert. This status enables us to check such important parameters as dental factors that could worsen the periodontal diseases and the amount of dental root anchorage to the bone below the loss area. It is also possible to examine the bone mineralization around the dental elements, any defects of the bone and their morphology. Both clinical and instrumental parameters, including radiological exams, will lead to diagnosis, treatment, and prognosis.

The use of three-dimensional radiology based on CT Dentascan has been restricted especially because of its high radiation dose to patients, which is contrary to the justification principle. Other negative factors are low definition and high interference of metal artifacts, which are not in compliance with the optimization principle. There exists one more problem with conventional CT that is related to high rates of ionizing radiation: it is not possible to repeat the exam at a subsequent checkup. This problem has been solved with the introduction of CBCT systems, which, especially with small FOV, will supply highly defined images with a low radiation dose, thus avoiding two serious problems of two-dimensional imaging.

Intra-oral X-rays are not able to detect bone lesions in non-proximal areas, like vestibular or lingual/buccal sections. These could only be detected by probing. Furthermore, this exam will not be subject to the malpositioning of film holders, or depend on palatal morphology or crowded teeth, as opposed to conventional two-dimensional exams. Since the CBCT system supplies a low radiation dose to patients, it is therefore safe for subsequent follow-up exams.

The use of CBCT in periodontology has been widely explained by Mohan et al. (2011). They have classified the various uses of CBCT, from pre-surgical diagnosis to follow-up, to bone defect measurements, up to so-called "soft tissue CBCT," to measure gingival tissues and the dental-gingival complex. These authors have stressed the limitations of 2D diagnostics for detecting the bone status in vestibular or lingual/buccal portions. The same has been highlighted by Misch et al. (2006); they have proved that there are no differences in bone defect measurements in interproximal portions, whether though probing, or performing a 2D or 3D radiological exam. However, no intra-oral X-ray can detect vestibular or lingual/buccal defects. According to these authors, CBCT can offer important advantages in detecting and quantifying bone defects, because of its three-dimensional images. According to Vandenberghe et al. (2007), though 2D digital radiology gives better information about the bone quality, CBCT can improve the morphological description of periodontal bone defects, and they anticipate further studies on the use of CBCT for the diagnosis, prognosis, and surgical planning of periodontal defects. Furthermore, thanks to rendering it is possible to recognize clearly and immediately any bone defect morphology, which is very effective when explaining to patients their specific case (Clinical Cases 49 and 50).

CLINICAL CASE 49

Massimo Frosecchi

This forty-eight-year-old male patient had been suffering from diffuse gingivitis. At the periodontal visit, we detected bleeding when probing and periodontal pockets of over 3 mm in several sites. When examining the intraoral X-rays (radiographic status), no serious bone loss was detected in any dental element. After scaling and root planning, the patient was examined again by probing. The periodontal pockets had decreased to a normal range and the bleeding after probing had disappeared everywhere but the palatal site of the upper right central incisor (Fig. 49.1), where a 6-mm pocket was still detected. Thanks to the 3D exam performed with a small FOV CBCT, a three-wall bone defect was detected in the palatal site. This defect could not have been detected by two-dimensional exams because of its palatal position (Figs. 49.2 and 49.3). During the surgical treatment, this defect was clinically confirmed (Fig. 49.4). Periodontal probing was performed after a period of time; a follow-up CBCT exam performed six months after surgery confirmed the healing process of bone tissues (Figs. 49.5 and 49.6).

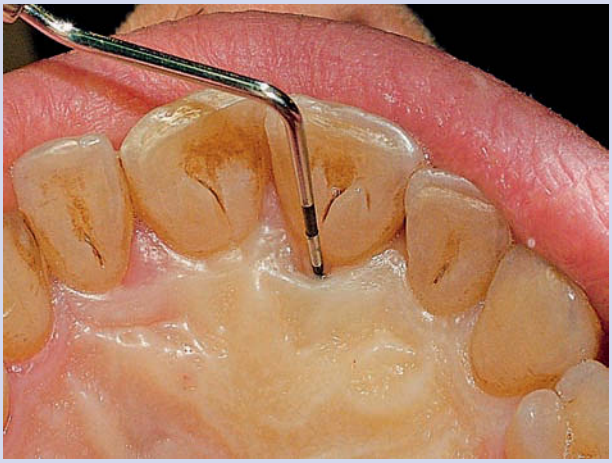

Fig. 49.1

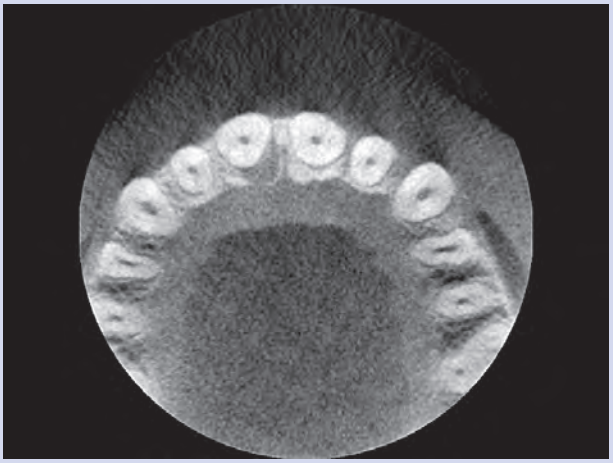

Fig. 49.2

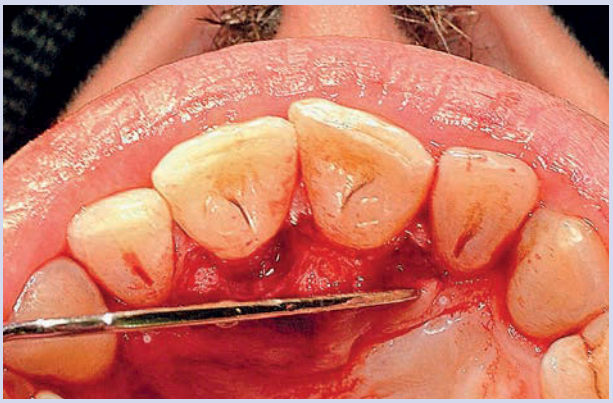

Figs. 49.3 and 49.4

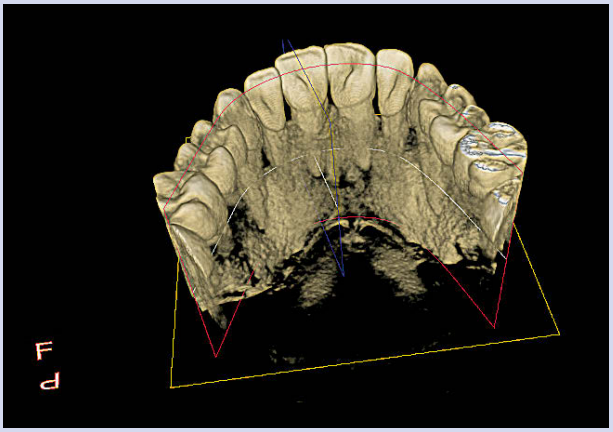

Figs. 49.5 and 49.6

CLINICAL CASE 50

Daniele Cardaropoli

This fifty-six-year-old female patient came to the practice because of migration of teeth with a loss of regular occlusion effects and multiple recessions of the free gingival margin. Some of her teeth were failing in the first quadrant. The initial OPG (Fig. 50.1) showed a diffuse horizontal bone resorption in both arches and high resorption of the crest in the first quadrant. It was possible to make a first diagnosis of chronic periodontitis based on the clinical pattern, the anamnestic datum, periodontal probing, and the 2D radiological exam. Two deep periodontal pockets were detected in the upper front group (Fig. 50.2), where intrabony defects were seen with the intra-oral images (Figs. 50.3 and 50.4). The CBCT exam was designed to supply a three-dimensional image of the actual structure of these intrabony defects, because they were located not only in the intraproximal area but also in the palatal area (Figs. 50.5 and 50.6), which was not detected by the 2D radiographic exam. The images taken during the surgical procedure confirmed the images supplied by the CBCT exam (Fig. 50.7).

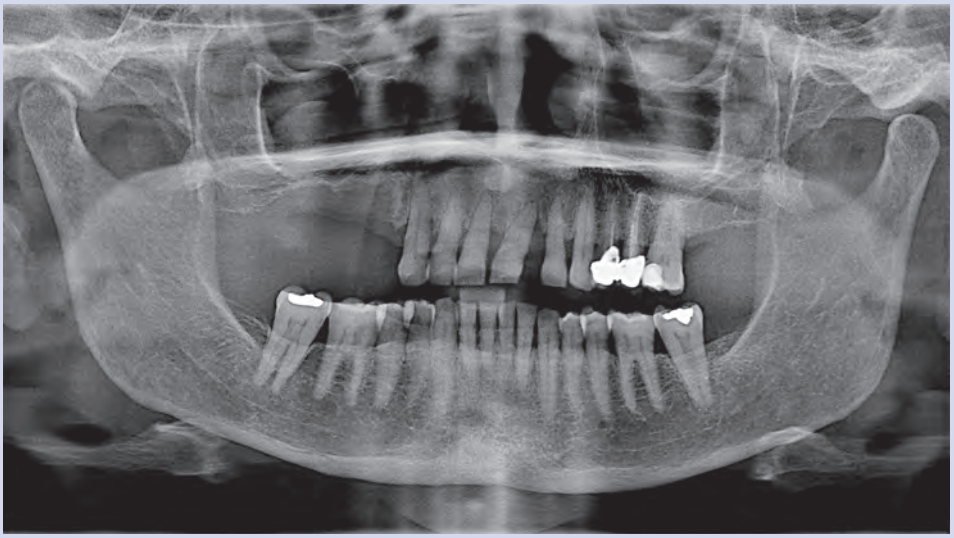

Fig. 50.1

Fig. 50.2

CLINICAL CASE 50 *(cont'd)*

Daniele Cardaropoli

Fig. 50.3

Fig. 50.4

Fig. 50.5

Fig. 50.6

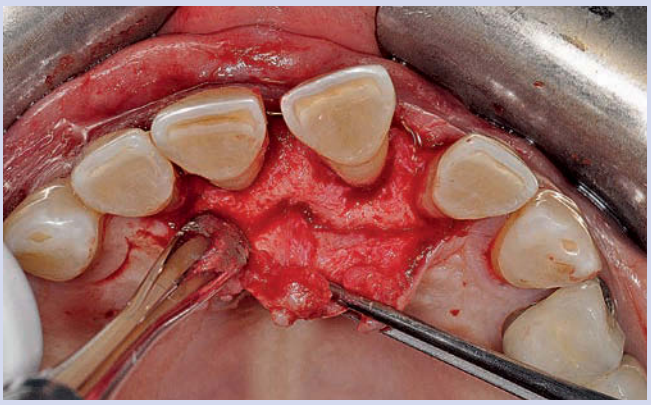

Fig. 50.7

Orthodontics

Andrea Nakhleh - Santiago Isaza Penco

CBCT in orthodontics

During the last century, orthodontists and researchers have used two-dimensional lateral cephalometric analysis to study the growth and development of craniofacial structures, to diagnose orthodontic problems, to plan orthodontic therapies, and to evaluate treatment outcomes (Broadbent 1931 and 1937; Brodie 1941; Salzmann 1948; Downs 1948; Steiner 1953; Sassouni 1955; Tweed 1962; Harvold 1968; Jarabak 1972; Jacobson 1975 and 1976; Burstone et al. 1978; Ricketts 1981; McNamara 1984). Because of the craniofacial structure, which is a three-dimensional object, a traditional lateral cephalometric radiograph provides limited information in terms of results. The advent of cone beam computed tomography technology and 3D software has now made it possible to evaluate all three dimensions of the craniofacial structure. Three-dimensional radiographs provide information not only about the axial plane, but also the intricate interrelationship between the sagittal, frontal, and transverse dimensions. Since CBCT offers high diagnostic value with a relatively low radiation dose, it has become a popular method of evaluation of orthodontic diagnoses and outcomes (Molen 2010). There has been considerable interest in CBCT imaging, with some even suggesting routine use for all patients (Walker et al. 2006; Kau et al. 2005). A preliminary review shows that the current literature does not yet support the universal use of this technology for all patients (Farman and Scarfe 2006). With this in mind, and until the literature has become more encouraging, orthodontists are advised to use CBCT with caution and always ask themselves whether the clinical question can be answered using conventional radiography. Radiographs should be taken only when justified clinically. To summarize the British Orthodontic Society guidelines, there are NO orthodontic indications for the following (Turpin 2008):

- radiographs taken routinely before a clinical examination;
- a set of routine radiographs for all orthodontic patients;
- full-mouth periapical views before treatment;
- a single lateral cephalometric radiograph for the prediction of facial growth;
- radiographs of the hand and wrist to predict the onset of the pubertal growth spurt;
- routine radiographs to investigate TMJ (myofascial) pain dysfunction;
- prospective radiographs for medical legal reasons;
- radiographs after treatment purely for professional examinations or for clinical presentations;
- CBCT taken routinely for all orthodontic patients.

CT or CBCT for orthodontists?

Three-dimensional craniofacial imaging techniques have changed how professionals approach diagnoses in dentistry and orthodontics. Although computed tomography is still used in many clinical situations when 3D information is needed, its use has been limited in dentistry due to its high cost, low vertical resolution, and high dose of radiation. The cone beam CT scanner is intrinsically 3D in its acquisition of images and provides usable images from equipment that is compact and affordable for small diagnostic centers (Arai et al. 1999a; Sukovic 2003). CBCT has been considered the examination of choice in many instances, since it provides high-resolution imaging, diagnostic reliability, and risk-benefit analysis (Mozzo et al. 1998; Yammamoto et al. 2003). Its use is recommended in orthodontic practice for impacted teeth (Nakajima et al. 2005), temporomandibular joint evaluations (Honda et al. 2004), 3D views of the upper airways (Aboudara et al. 2003), assessment of maxillofacial growth and development, and dental age estimation (Yang et al. 2006). CBCT has also demonstrated validity for biomechanical simulations, models for bone remodeling, simulations for orthodontic surgical

planning (Maki et al. 2003), and measurements taken by digitizing points in 3D coordinates (Halazonetis 2005). Because of these advantages and possibilities in orthodontic assessment, treatment, and follow-up, and its relatively low cost, many orthodontists use CBCT routinely for all patients. The main limitations of CBCT compared to conventional CT are the lack of a soft tissue window, higher image noise, and the lack of precise Hounsfield units (Hounsfield 1973; White 2008); this implies that the values assigned to each voxel in a CBCT scan are relative to HU and cannot be used directly to estimate bone density.

The radiation dose to the patient with CBCT is markedly lower than that of multi-slice CT (Nakajima et al. 2005; Swennen and Schutyser 2006); doses are three to seven times more than panoramic doses and forty percent less than those of conventional CT (Frederiksen et al. 1994; Ludlow et al. 2006). However, orthodontic assessment with CBCT should follow the "as low as reasonably achievable" (ALARA) principle. Other studies have shown a dose reduction of fifty percent in orthodontic practice with digital direct (Visser et al. 2001; Gijbels et al. 2004) or indirect cephalometric radiography, or the collimated lateral beam for cephalometric images (Gijbels et al. 2003). From the dose to the patient's point of view, the routine use of CBCT is not recommended in orthodontic procedures because conventional images deliver lower doses to patients. However, when 3D imaging is required in orthodontic practice, CBCT should be preferred over CT (Silva et al. 2008). In this way, "[t]he pendulum of imaging technology is quickly swinging toward 3D CBCT. But as clinicians in private practice who order these scans for our patients, we must first ask this question: will the benefit that I gain from this scan outweigh the potential risk to the patient? The responsibility is ours" (Kokich 2010).

Applications of CBCT in orthodontic practice

Below we will describe some clinical applications of CBCT in orthodontics.

Impacted teeth

Panoramic radiography is a standard diagnostic tool in orthodontics for the pre-operative diagnosis of routine cases. The diagnostic accuracy and validity for localizing impacted teeth and adjacent structures can be underestimated due to deficiencies, such as distortion projection errors, blurred images, and complex maxillofacial structures that are projected onto a 2D plane, thus increasing the risk of misinterpretation (Ericson and Kurol 1987).

Localization of impacted teeth was traditionally done by 2D radiographs using the buccal object rule (SLOB), as well as by taking two radiographic images, a periapical and an occlusal view at right angles to one another (White and Pharoah 2004). Diagnosis and treatment planning often develops a higher degree of complication when dealing with the presence of one or more impacted teeth that may be present in an unusual relationship to the erupted dentition. Studies of patients with impacted canines have demonstrated that root resorption of maxillary lateral incisors is considered a well-known and relatively common phenomenon. Statistically, 35.7% of cases showed a slight level, while 14.2% and 4% showed moderate and severe root resorption of the adjacent lateral incisor (Oberoi and Knueppel 2011).

The introduction of CBCT has recently allowed us to cast a new and much more documented light on diagnostic and therapeutic strategies, focusing on managing such complex cases (Alqerban et al. 2009a; Alqerban et al. 2009b; Curley and Hatcher 2009). Small volume CBCT may be justified as a supplement to a routine panoramic X-ray, especially for patients when (Wriedt et al. 2012):

- canine inclination in the panoramic X-ray exceeds 30°;
- root resorption of adjacent teeth is suspected;
- the canine apex is not clearly discernible in the panoramic X-ray;
- a dilaceration of the canine root might be implied.

Liu et al. demonstrated the efficacy of impacted canine localization using CBCT (Liu et al. 2008). CBCT may be a reliable method for detecting canine impaction and root resorption of adjacent teeth (Alqerban et al. 2011).
Additionally, observers using CBCT images showed a statistically significant increase in diagnostic confidence, and after viewing CBCT images, statistically significant changes were made to twenty-seven percent of treatment plans that were originally based on 2D radiographs (Haney et al. 2010) (Clinical Case 51).

CLINICAL CASE 51

Andrea Nakhleh, Santiago Isaza Penco

A twelve-year-old female was referred to the practice because of the absence of the right second molar in the lower dental arch and an asymmetrical Class II malocclusion (Fig. 51.1 a-c). From the OPG two aspects are visible: tooth 4.7 impacted in the bone and an initial process of extrusion of tooth 1.7 (Fig. 51.2). It was necessary to take a CBCT of this area in order to remove any doubt about some pathologic interference for a forced orthodontic eruption. At the same time, it was helpful in analyzing the proximity to the wisdom tooth and in measuring the space for inserting a mini-screw (Fig. 51.3). Therefore, full-mouth bonding was proposed early on as a treatment. It could have aimed at two objectives: to correct the occlusion and to bring element 4.7 up into the dental arch. In the end, the patient refused this treatment, so we decided only to intercept tooth 4.7 by using the orthodontic segmented arch technique (Burstone 1966) and a mini-screw as a temporary anchorage device (TAD) inserted between the lower right first and second premolars (Fig. 51.4). After the removal of the mini-screw, tooth 4.7 was in the dental arch (Figs. 51.5 and 51.6).

Fig. 51.1 a-c

CLINICAL CASE 51 *(cont'd)*

Andrea Nakhleh, Santiago Isaza Penco

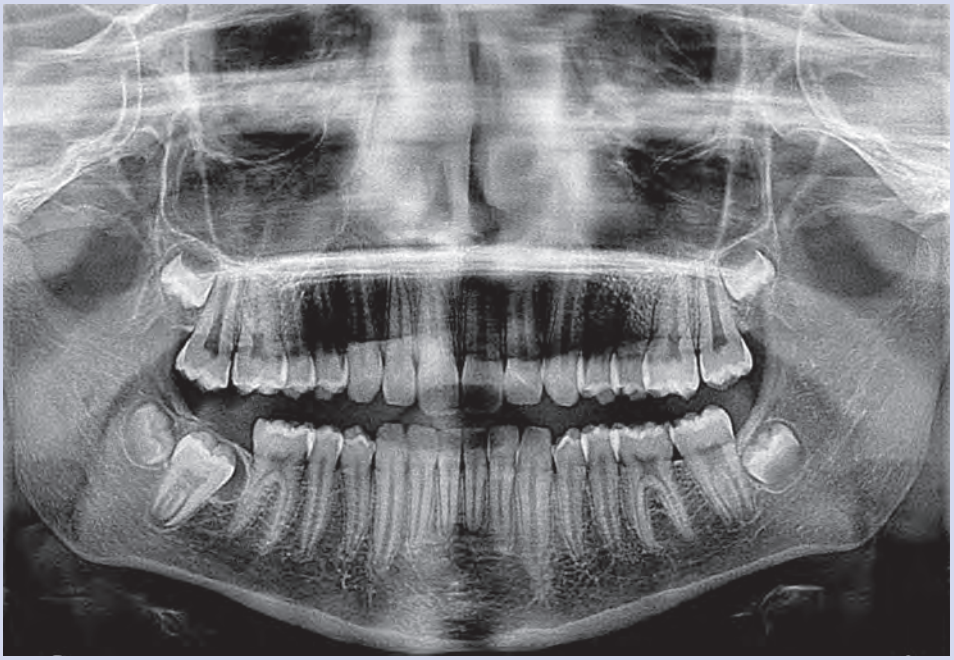

Fig. 51.2

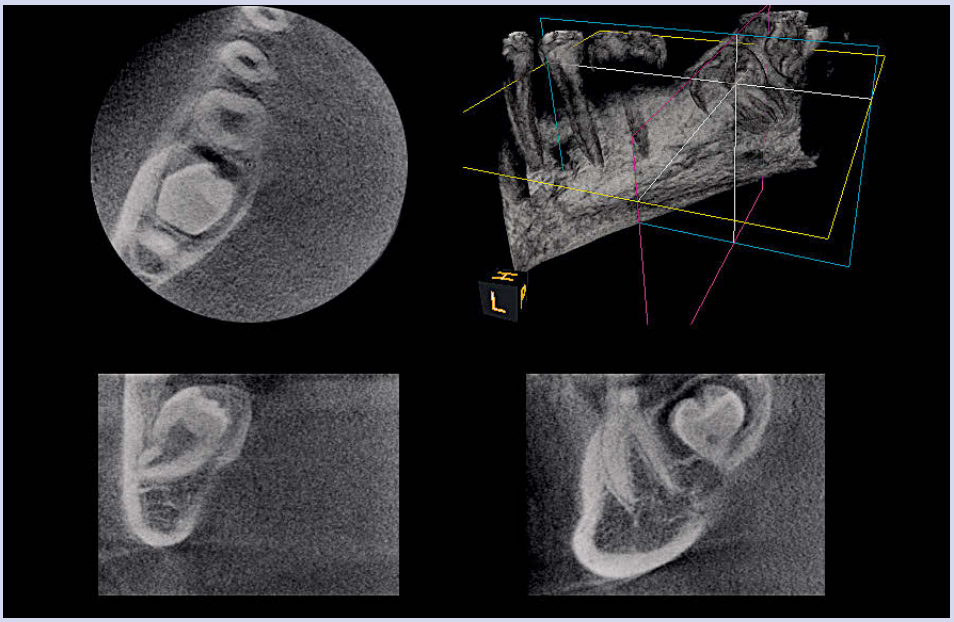

Fig. 51.3

Fig. 51.4

Fig. 51.5

Fig. 51.6

Assessment of crestal bone levels

Cone beam computed tomography is rapidly emerging as an appropriate imaging method for the assessment of crestal bone levels, and might ultimately replace conventional periapical and bitewing radiographs in routine diagnosis of orthodontic patients. In a recent investigation comparing artificially created crestal defects on mandibles of dry skulls, CBCT and conventional periapical images were equally accurate in showing the size and presence of interproximal osseous craters (Misch et al. 2006).

However, CBCT was found to be more reliable than conventional periapical films in documenting buccal and lingual defects because of it unique three-dimensional capability (Misch et al. 2006).

The presence of fenestrations and/or dehiscences decreases the bony support for the teeth. It is well documented that, under certain conditions (e.g. plaque-induced inflammation), a lack of bony support during orthodontic movement can be detrimental to the health of the teeth and the periodontium (Ericsson et al. 1977; Wennstrom et al. 1993; Årtun and Urbye 1988). In addition, orthodontic tooth movement can create alveolar bone defects (Zachrisson and Alnaes 1974a; Wehrbein et al. 1996; Karring et al. 1982; Wainwright 1973; Garib et al. 2006; Zachrisson and Alnaes 1974b; Sarikaya et al. 2002).

Until recently, bony dehiscences and fenestrations could not be visualized by traditional two-dimensional radiography because of the superimposition of contralateral cortical bony or dental structures (Lang and Hill 1977; Rees et al. 1971). The development of CT and especially CBCT has provided the means to visualize these defects three-dimensionally (Mengel et al. 2005; Fuhrmann 1996).

The literature has reported the accuracy of CT and CBCT for measuring and identifying artificially created alveolar bone defects (Misch et al. 2006; Mengel et al. 2005; Pinsky et al. 2006).

An undiagnosed buccal alveolar bone defect could occur in a few patients and cause greater potential for treatment relapse (Rothe et al. 2006; Ericsson and Thilander 1980) or gingival recession resulting in an unaesthetic finish of the orthodontic treatment (Melsen and Allais 2005; Wennstrom 1996; Wennstrom et al. 1987; Yared et al. 2006).

The diagnostic value of CBCT for the detection of buccal defects was high for fenestrations: both sensitivity and specificity scores were about 0.80. While for dehiscences, specificity values were higher (0.95) than those reached for sensitivity (0.40). Positive predictive values were 0.50 for dehiscences and 0.25 for fenestrations, respectively. In other words, when a defect was found in CBCT, it was a true dehiscence about half of the time and a true fenestration about a quarter of the time. The negative predictive values, however, were high for both, at 0.93 for dehiscences and 0.98 for fenestrations. This meant that, when a defect was not found in CBCT, most likely there was no defect at all (Leung et al. 2010) (Clinical Case 52).

CLINICAL CASE 52

Santiago Isaza Penco, Alberto Bianchi

A twenty-nine-year-old woman came to the practice in order to finish the orthodontic treatment she had started abroad. Unfortunately, the presence of a Class III, severe open bite and multiple recessions associated to bilateral crossbite put us on alert (Fig. 52.1).
Comparing the photo with the pre-orthodontic plaster model the patient had given us (Fig. 52.2 a-f), lead us to establish that most of the recessions were caused by excessive buccal movement exerted by the orthodontic braces on the teeth. Observing the OPG (Fig. 52.3) and the clinical condition of element 1.6, we decided to extract this tooth. After taking the cephalometric teleradiography with superimposition of the soft tissue profile (Fig. 52.4) and the CBCT (Fig. 52.5 a, b), we decided to change the orthodontic technique and prepare the patient for orthognathic surgery in order to close the bite and to surgically correct the sagittal discrepancy and the transversal deficiency of the upper maxillary (Fig. 52.6 a-c).
The figures 52.7 a-c display the good healing of the soft tissue and the orthdontic refinement.

Fig. 52.1 a-b

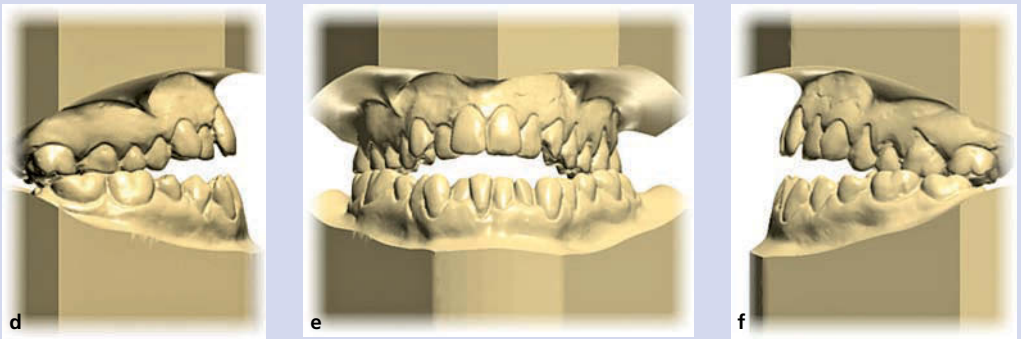

Fig. 52.2 a-f

CLINICAL CASE 52 *(cont'd)*

Santiago Isaza Penco, Alberto Bianchi

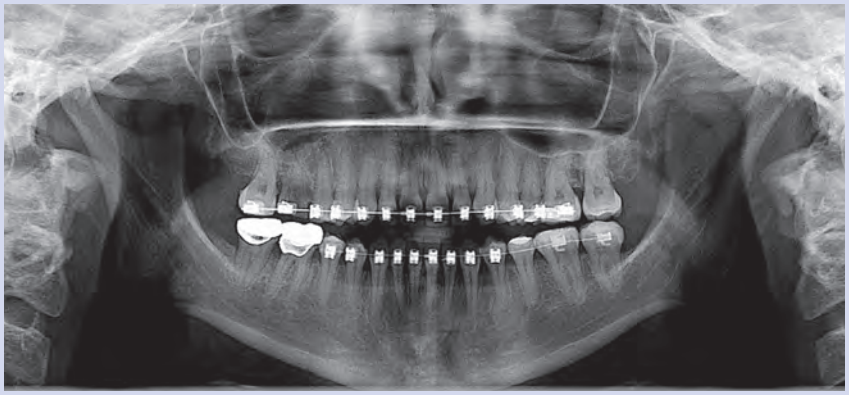

Fig. 52.3

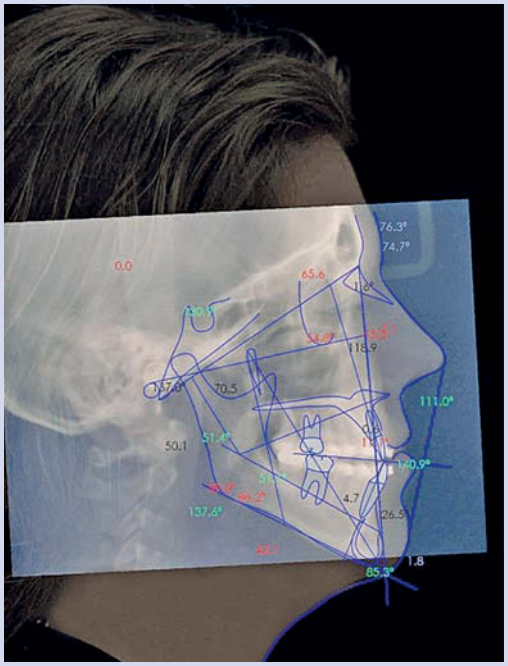

Fig. 52.4

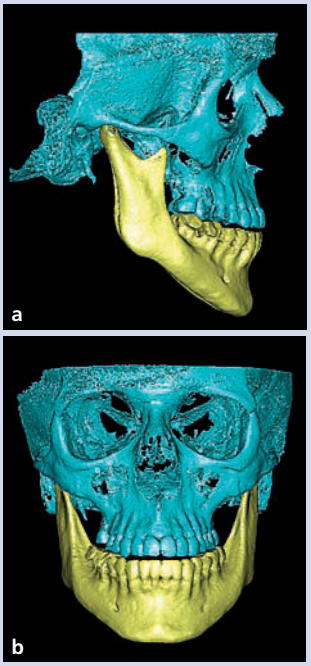

Fig. 52.5 a-b

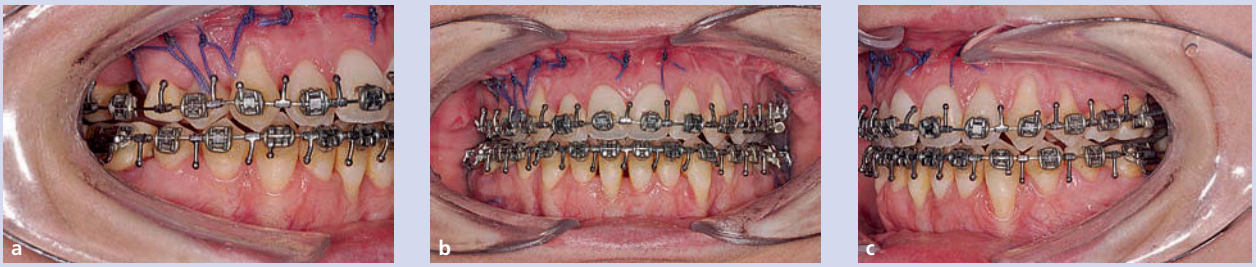

Fig. 52.6 a-c

Fig. 52.7 a-c

Mini-implant placement

Orthodontic mini-implants are reliable anchorage mechanisms for achieving the desired amount of tooth movement without patient compliance (Chen et al. 2008; Antoszewska et al. 2011).

In order to achieve an effective result, it is very important that stability be attained at the initial stage. Accurate interradicular placement and angulation can improve primary stability and decrease TAD failure rates (Kuroda et al. 2007; Wilmes et al. 2008), since root proximity has been defined as a major risk factor of initial stability (Kim et al. 2010). A number of studies have attempted to survey optimal locations for mini-implant placement (Estelita et al. 2006; Kim et al. 2007; Kitai et al. 2002; Baros et al. 2010; Liu et al. 2010). Several methods use periapical radiography, panoramic radiography, computed tomography, and cone beam computed tomography (Kim et al. 2010; Estelita et al. 2006; Kim et al. 2007; Poggio et al. 2006). However, conventional periapical and panoramic imaging techniques combined with visual inspection are insufficient for performing accurate pre-surgical planning (D'haese et al. in press) because of inherent distortions of the radiographic images. CT is isotropically accurate but has been limited in dentistry due to its high cost, lower image resolution, and high radiation dose (Silva et al. 2008).

The recent development of CBCT has overcome many of the limitations of conventional dental radiographic techniques by providing reasonable tissue contrast, minimizing blurring and overlapping of adjacent teeth, and offering orthogonal views by eliminating projection artifacts. Additional advantages of CBCT include reduced cost and significant reduction of radiation exposure, compared with typical medical CT devices (Kwong et al. 2008). In this way, evaluation of cortical bone thickness and quality, interradicular space, and ridge width using CBCT imaging can ensure proper TAD site selection, positioning, and angulation (Park and Cho 2009) (Clinical Case 53).

CLINICAL CASE 53

Santiago Isaza Penco, Matteo Di Lorenzo

A thirty-five-year-old male patient came to the practice who had already been treated orthodontically with extractions of lower second premolars to resolve inferior dental crowding (Fig. 53.1 a-c). The patient reported symptomatic bilateral temporomandibular joint disorder. This was probably due to premature contact of teeth 2.5 and 3.6, which were mesialized due to the previous extraction of 3.5, causing an irregular occlusal plane. Intra-oral photos and OPG (Fig. 53.2) demonstrated the mesialization of 3.6 and the absence of good interproximal contact between 3.6 and 3.4. The proposed treatment plan was the placement of a mini-implant (TOMAS Pin) between teeth 3.4 and 3.3 in order to put element 3.6 upright, and the closure of the interproximal space with an orthodontic segmented arch technique, achieving good occlusal and interproximal contact (Fig. 53.3). CBCT was extremely important in determining the optimal position to insert the mini-screw between the roots of 3.4 and 3.3 (Fig. 53.4).

Fig. 53.1 a-c

CLINICAL CASE 53 *(cont'd)*

Santiago Isaza Penco, Matteo Di Lorenzo

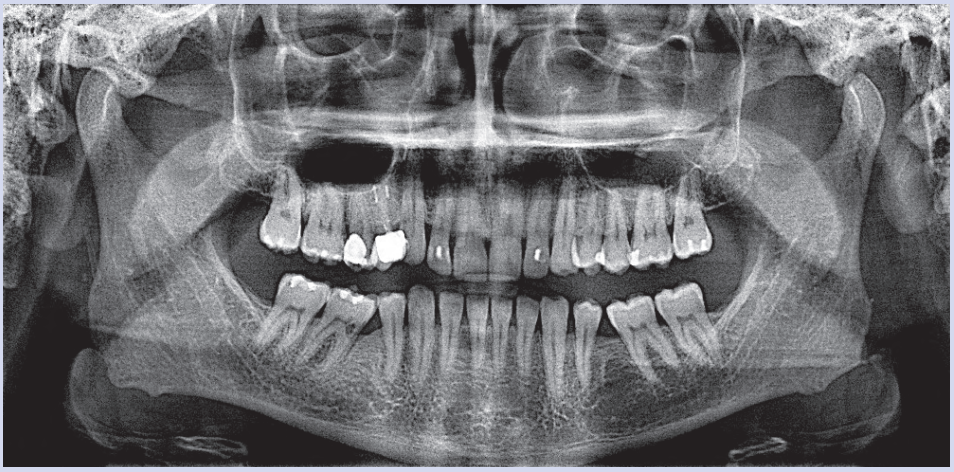

Fig. 53.2

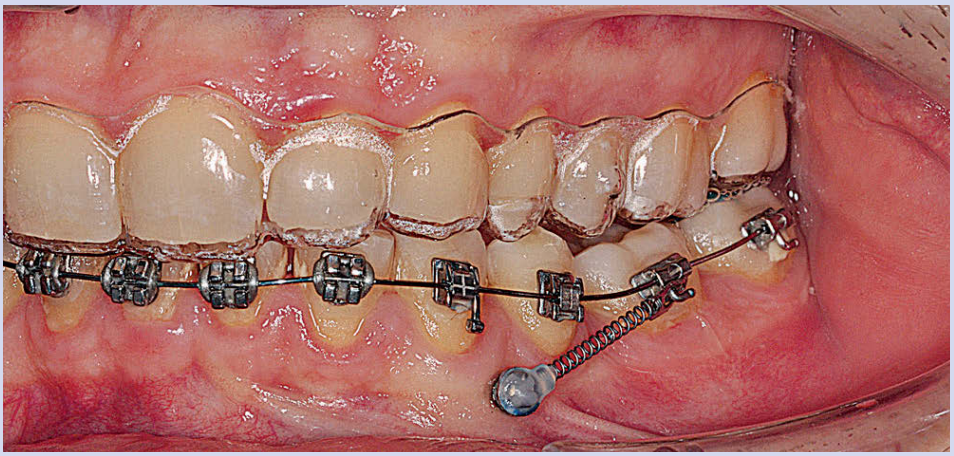

Fig. 53.3

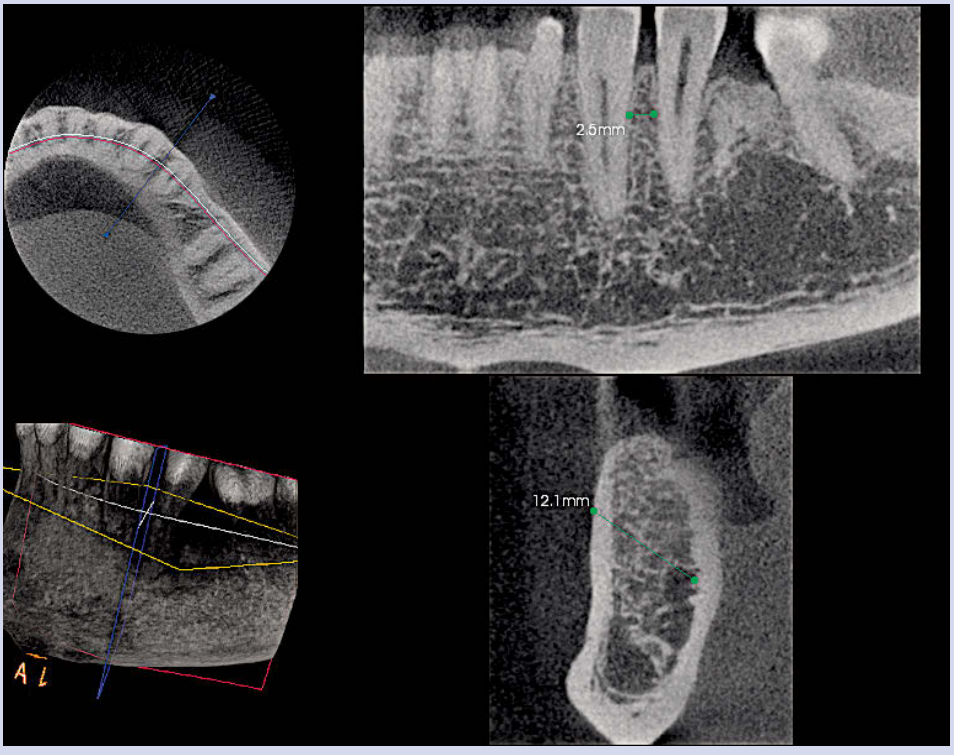

Fig. 53.4

Orthognathic surgery

Advances in the field of medical imaging have led 3D imaging techniques to become readily available in the clinical setting. Hard tissue structures, including the skull, maxilla, mandible, and dentition, can be analyzed in 3D using cone beam computed tomography. Its accessibility, relatively low cost, and decreased radiation dose are all together important features that must be considered when comparing CBCT to conventional medical CT. In addition, CBCT provides the patient with the possibility of being scanned while he is seated vertically with his head in a natural position. All these technical advantages have definitely contributed to making an progress in the field of 3D imaging (Cattaneo and Melsen 2008).

Three-dimensional surface imaging is also available in various forms using the concept of stereophotogrammetry to provide high-resolution reproductions of the facial soft tissue surface (Ayoub et al. 2007) and plaster dental models (Bell et al. 2003). By linking these data sets, a virtual 3D model structure of the patient, including the bony skeleton, the dentition, and the facial soft tissue surface, can be completely created and performed in 3D to allow the assessment, diagnosis, and treatment planning of dentofacial deformities (Xia et al. 2000; Olszewski et al. 2008; Caloss et al. 2007).

Quantitative and qualitative analysis of skeletal displacement, adaptive response, and resorption that could not be attempted with 2D techniques can now be accomplished through three-dimensional CBCT reconstructions and superimpositions (Cevidanes et al. 2005; Cevidanes et al. 2007b; Motta 2007).

The complex movements during surgery for dentofacial deformities clearly need to be assessed in three dimensions to improve the outcome and stability, and to reduce symptoms of temporomandibular joint disorder after surgery (Cevidanes et al. 2007a). In this way, CBCT images can be applied before and after surgery to analyze the condylar position with intercondylar distance and angle after sagittal split osteotomy in mono- and bimaxillary orthognathic surgery (Draenert et al. 2010).

Facial soft tissue prediction in orthognathic surgery could be a valuable aid for previewing results and determining the best surgical treatment: simulations in orthognathic surgery for skull-maxillofacial deformities using CBCT acquisition are reliable, and could become the reference point for planning surgical treatment (Bianchi et al. 2010; Marchetti et al. 2011) (Clinical Case 54).

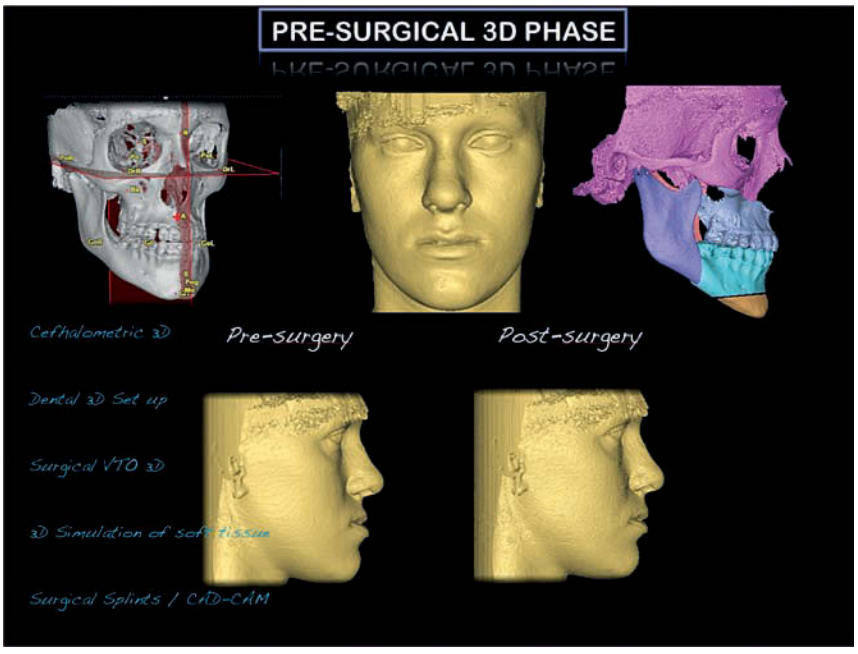

CLINICAL CASE 54

Santiago Isaza Penco, Alberto Bianchi

An eighteen-year-old female patient was referred to the practice. She had had a previous orthodontic treatment that led to a dental compensation with sufficient leveling and alignment of the teeth (Fig. 54.1 a-f). Extremely poor results in terms of facial aesthetics (Fig. 54.2 a, b) had led her to make a decision about her skeletal deformity. A simulation of orthodontic treatment and orthognathic surgery was planned on the lateral cephalometric as follows (Fig. 54.3 a, b):

- the extraction of two upper premolars in order to decrease the inclination of the upper incisors;
- orthodontic leveling, alignment, and space closure, with the creation of an anterior crossbite, and increased incisor mandibular plane angle (IMPA);
- bimaxillary surgery of upper maxillary advancement and mandible sagittal reduction;
- orthodontic finishing and contention.

Then, we started the pre-surgery orthodontics (Fig. 54.4 a-c). A CBCT was taken (Fig. 54.5 a, b) looking to plan the surgery in an accurate way (Fig. 54.6), and to simulate the final soft tissue aesthetics as well (Fig. 54.7).

After undergoing surgery and completing orthodontic therapy, the patient reported being highly satisfied with the new look of her facial features (Figs. 54.8 a-c and 54.9 a, b).

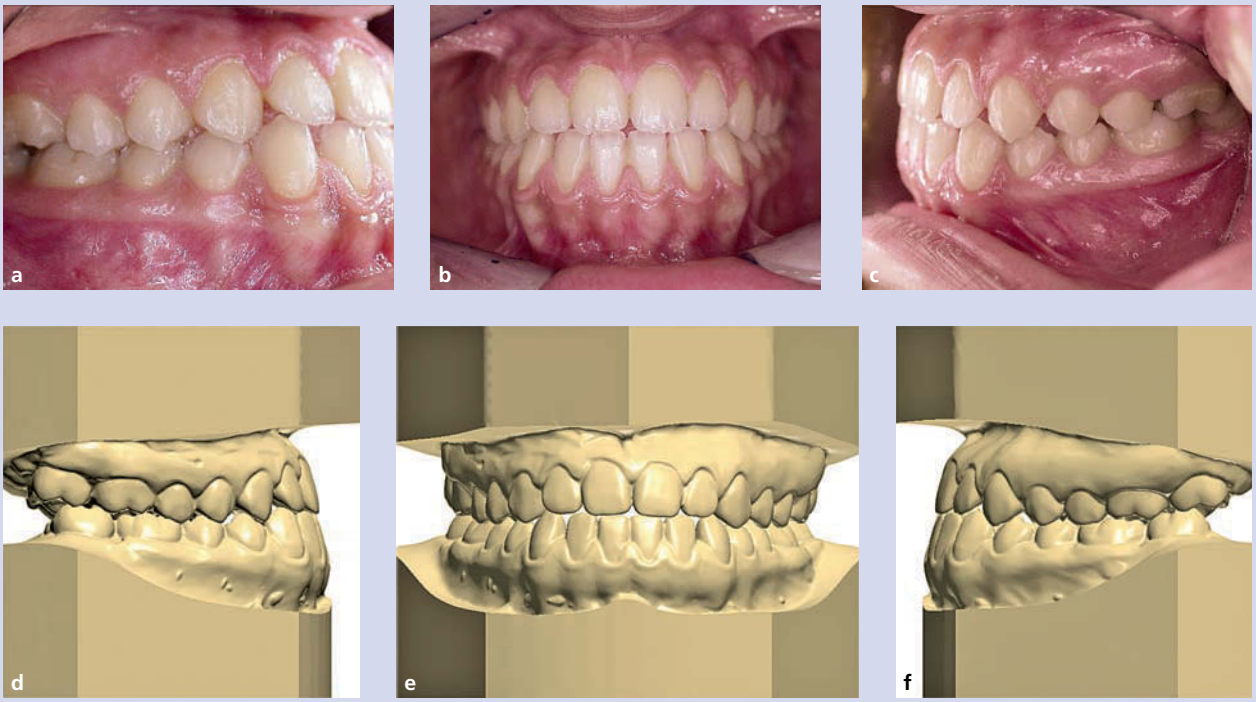

Fig. 54.1 a-f

Fig. 54.2 a

CLINICAL CASE 54 *(cont'd)*

Santiago Isaza Penco, Alberto Bianchi

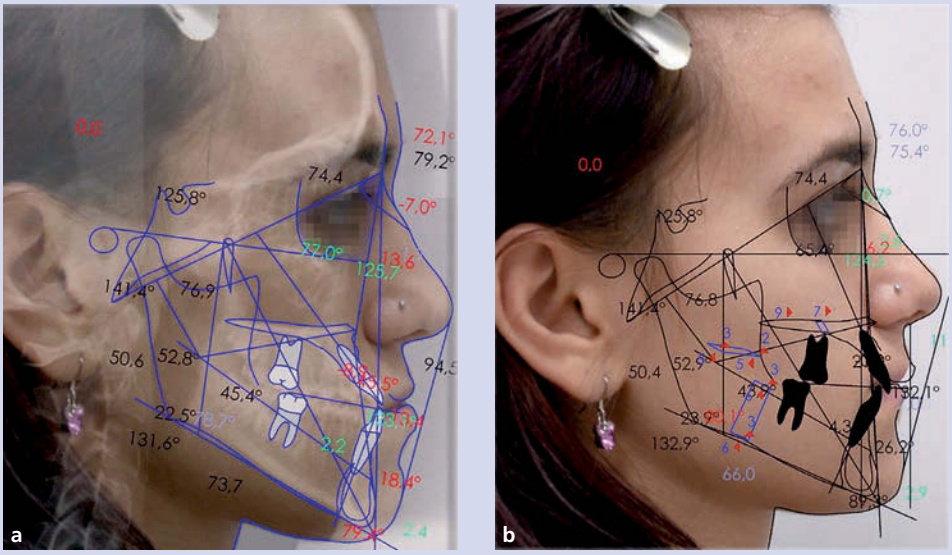

Fig. 54.3 a-b

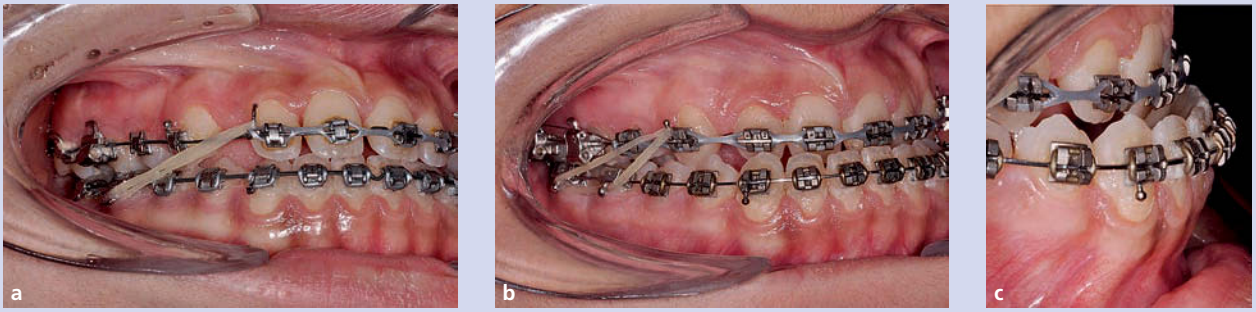

Fig. 54.4 a-c

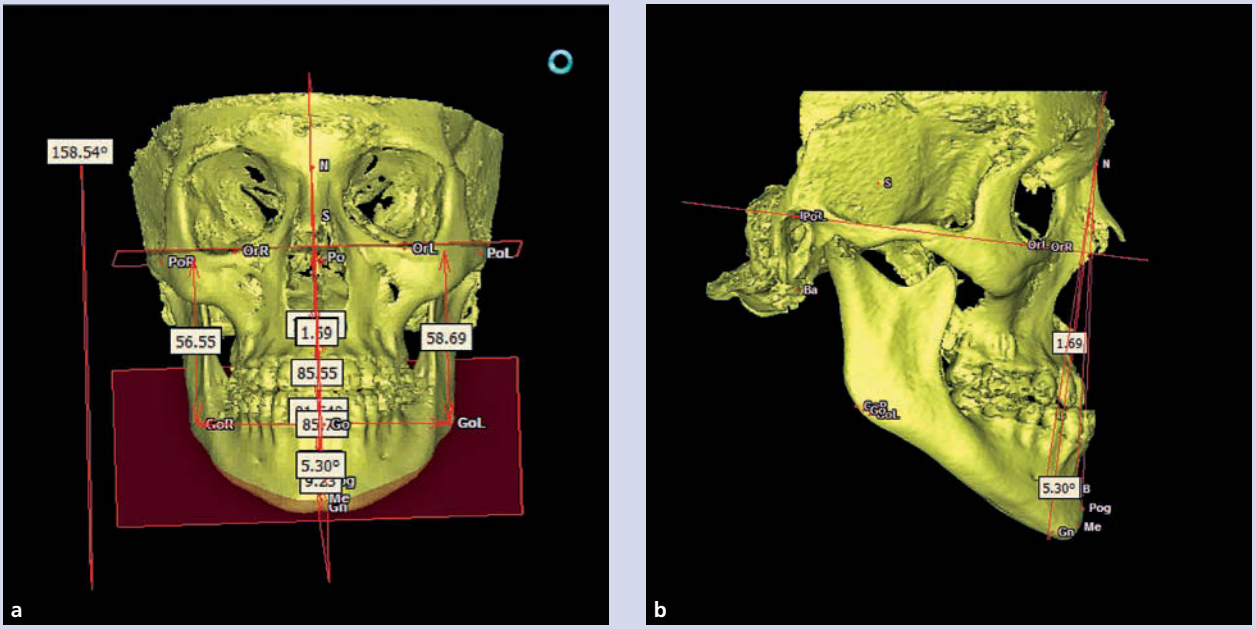

Fig. 54.5 a-b

CLINICAL CASE 54 *(cont'd)*

Santiago Isaza Penco, Alberto Bianchi

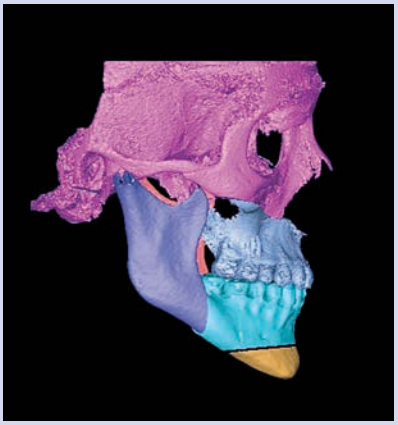

Fig. 54.6

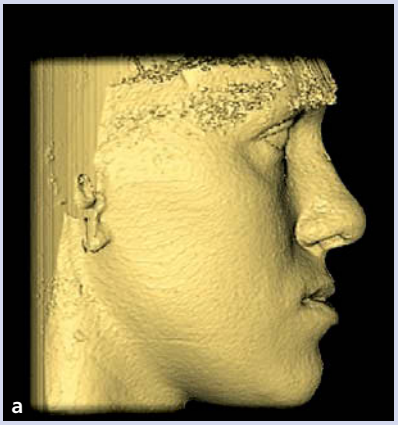

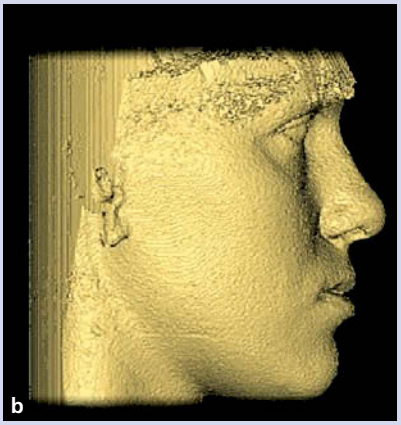

Fig. 54.7 a-b

Fig. 54.8 a-c

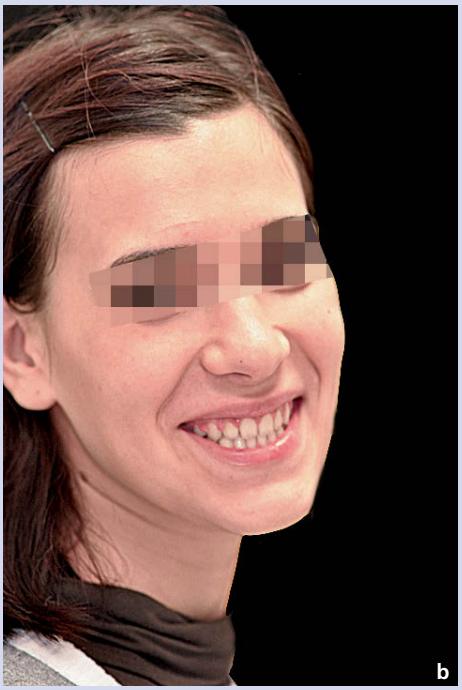

Fig. 54.9 a-b

Condylar fractures

Standard radiographic studies of the temporomandibular joint, such as plain film radiography and panoramic radiography, have little capacity to reveal anything more than gross osseous changes within the joint (Brooks et al. 1997). Within the condyle, there is a variation in bone density and composition. Cortical bone, trabeculae, and intertrabecular tissue have various densities and mechanical properties (Aranyarachkul et al. 2005; Shapurian et al. 2006; Stoppie et al. 2006; Rho et al. 1995; Hatcher et al. 2003). Therefore, in some cases a more comprehensive radiographic study is recommended (Schlueter et al. 2008).

When evaluating linear measurements of the TMJ, Hilgers et al. found that CBCT images were more accurate and reliable than traditional linear cephalometric, posteroanterior, and submentovertex radiographs (Hilgers et al. 2005). Furthermore, when comparing panoramic radiology, linear tomography, and CBCT, Honey et al. found that CBCT images allowed much more accurate and reliable identification of condylar cortical erosion (Honey et al. 2007).

The accuracy of CBCT and that of multidetector computed tomography (MDCT) were similar in detecting surface osseous changes, with comparable intraobserver reliability. However, MDCT is operator-dependent, so CBCT should be encouraged for imaging TMJ surface osseous changes (Zain-Alabdeen and Alsadhan 2011) (Clinical Case 55).

CLINICAL CASE 55

Marcos Gribel, Bruno Frazão Gribel

A five-year-old girl was referred to the practice due to a left deviation of the mandible when opening the mouth. A CBCT made it possible to visualize the left condyle fracture and its displacement forward, downward, and medially following the direction of the lateral pterygoid muscle (Fig. 55.1). The right condyle, on the other hand, was healthy (Fig. 55.2).

The OPG (Fig. 55.3) and the left and right cephalometric radiographs were extrapolated from the CBCT images. The analysis of the temporomandibular articulation (TMA) showed that the articular spaces of the right TMA were decreased in the anterior area and increased in the posterior area (Fig. 55.4). On the left side the condyle was completely dislocated (Fig. 55.5). The treatment plan initially consisted of functional orthopedics with SN1 device in order to sustain the vertical dimension of occlusion in this side and stimulate the growth of the fractured condyle.

After two months of treatment, the CBCT revealed a partial remodeling of the left condyle and changes in the mandibular posture, as shown by the superimpositions (Fig. 55.6 a, b). The articular spaces of the left TMA were increased in the posterior area (Fig. 55.7), while in the right TMA the articular spaces were preserved (Fig. 55.8).

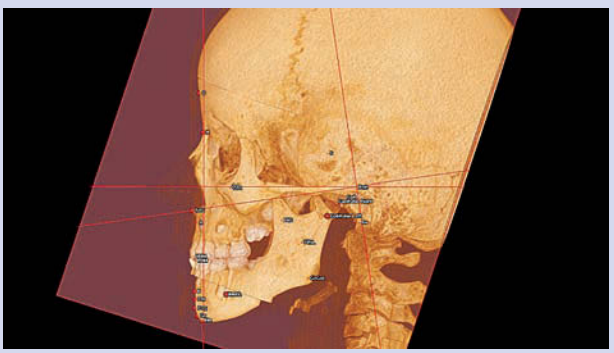

Fig. 55.1

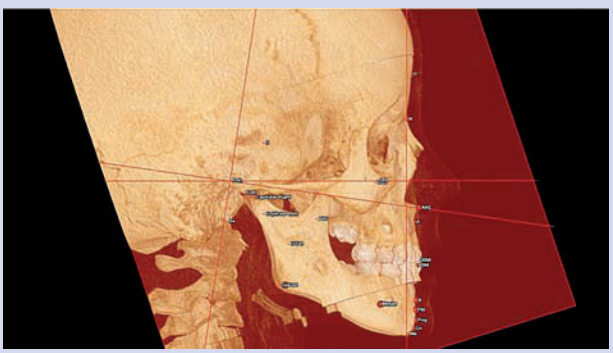

Fig. 55.2

CLINICAL CASE 55 *(cont'd)*

Marcos Gribel, Bruno Frazão Gribel

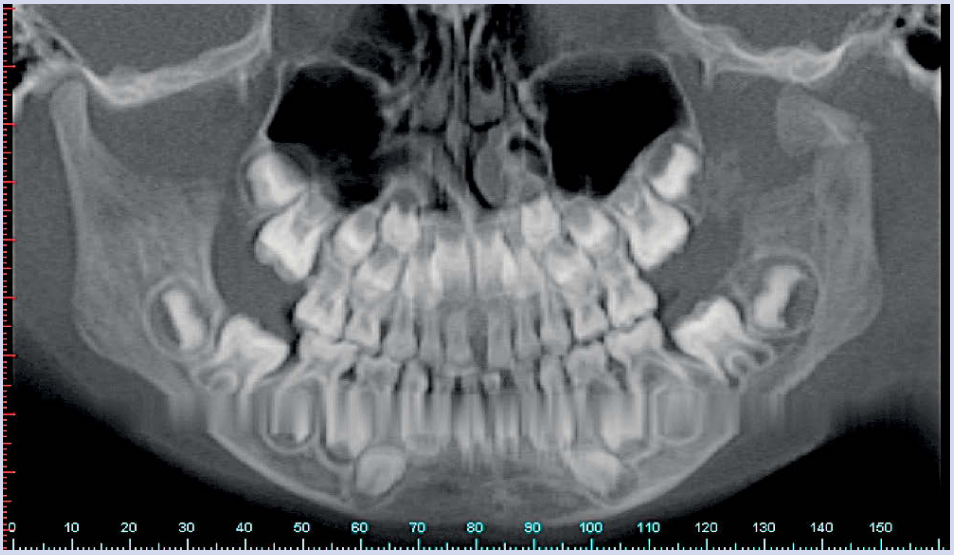

Fig. 55.3

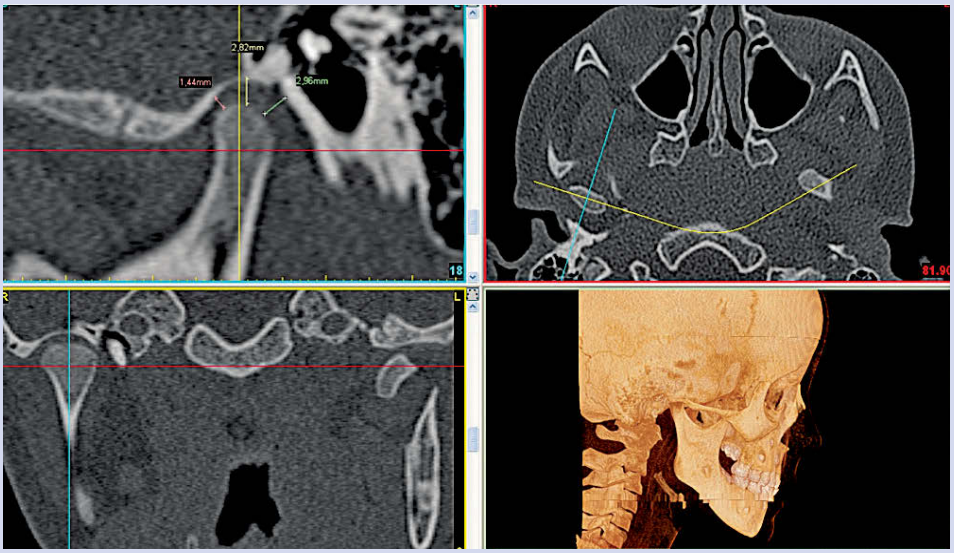

Fig. 55.4

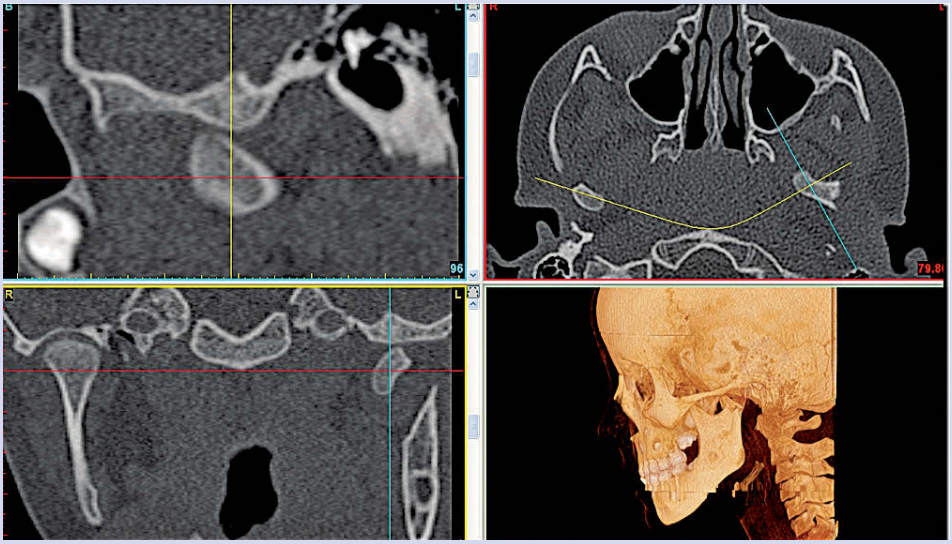

Fig. 55.5

CLINICAL CASE 55 *(cont'd)*

Marcos Gribel, Bruno Frazão Gribel

The treatment started with an SN11 orthodontic device. Then we put on a Gribel modified Planas direct track of composite (Gribel 2002) in the upper left deciduous canine. In this way, the patient was compelled to chew mainly on the right side, in order to asymmetrically enhance the mandible development. The patient was able to open her mouth without deviation and deflection (Fig. 55.9 a, b).

Moreover, she was taught about mouth opening and closing as daily routine exercises. After seven months, the last CBCT taken revealed the normalization of the mandible posture and the remodeling of the anatomy of the left condyle, meaning great potential for adaptation of the condylar cartilage. The right and left TMA articular spaces are now correct and symmetrical (Fig. 55.10 a, b).

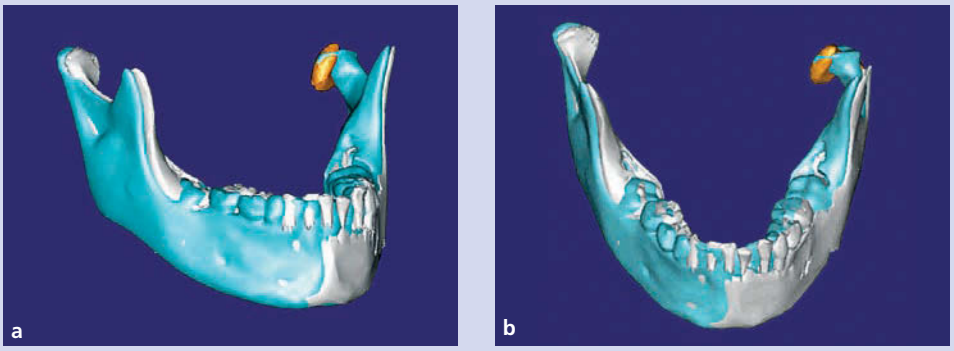

Fig. 55.6 a-b

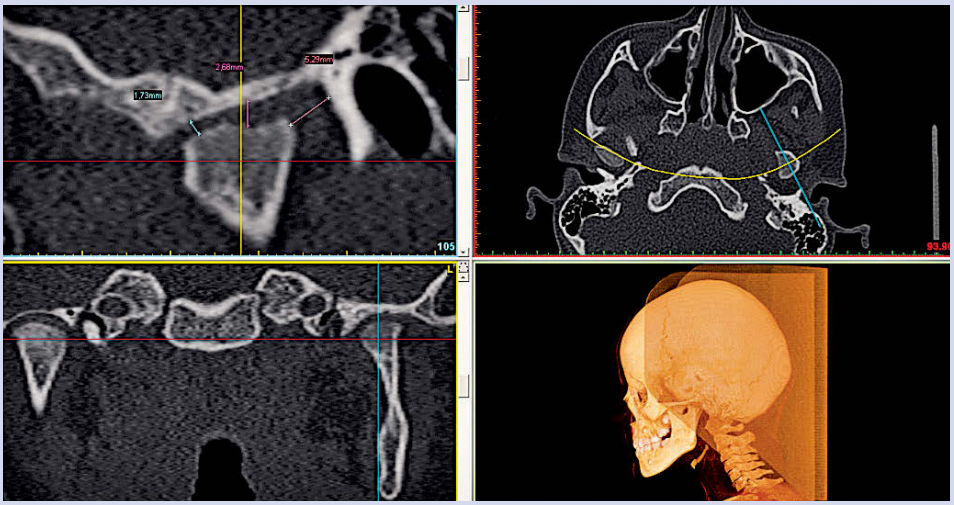

Fig. 55.7

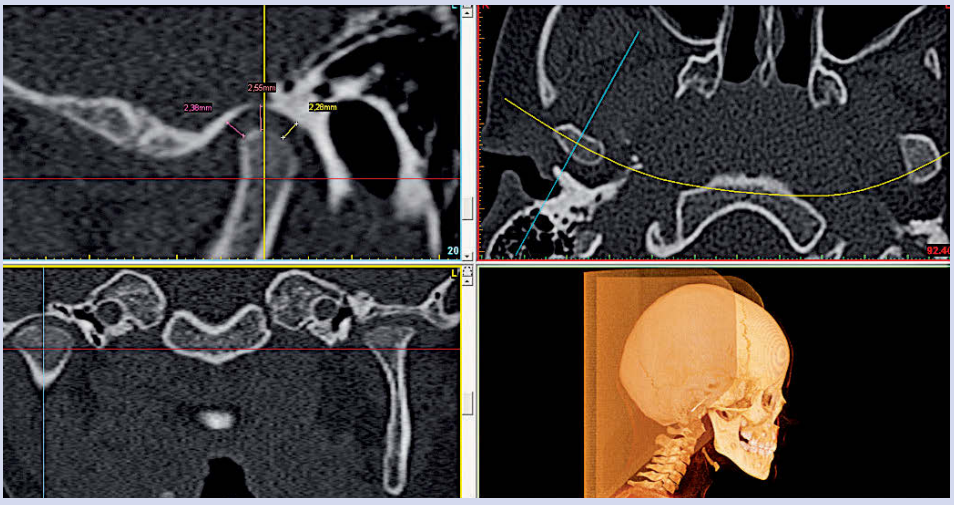

Fig. 55.8

CLINICAL CASE 55 *(cont'd)*

Marcos Gribel, Bruno Frazão Gribel

Fig. 55.9 a-b

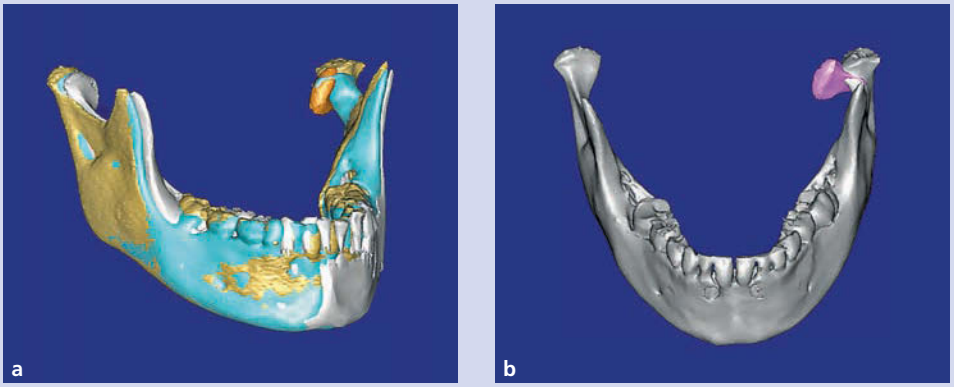

Fig. 55.10 a-b

Functional orthopedics

In young, growing patients with skeletal malocclusions, it is fundamental to stimulate the skeletal growth in order to correct the maxillary discrepancy. Craniofacial development is a process which involves both biochemical and physical stimuli (Riolo et al. 1974). Indeed, its known as a very complex process if we consider that bones are dynamic structures which undergo significant remodeling over their life cycle. This process of remodeling consists of the depositing and resorption of bone through specialized bone cells. Bone growth occurs when the rate of depositing is greater than that of resorption, resulting in a gradual increase in size as time progresses (Martini and Nath 2008).

The masticatory function markedly affects the mandibular condylar cartilage growth and mandibular morphology (Planas 1994; Petrovic et al. 1976; McNamara et al. 1976). The evaluation of mandible growth, either experimentally or theoretically, is very complex due to the geometric shape and significant bone drifting of the mandible (Enlow et al. 1982). Therefore, quantitative and qualitative analysis of skeletal displacement, adaptive response, and resorption that could not at one time be attempted by 2D techniques, can now be accomplished through 3D CBCT reconstructions and superimpositions (Cevidanes et al. 2005; Cevidanes et al. 2007b) (Clinical Case 56).

CLINICAL CASE 56

Marcos Gribel, Bruno Frazão Gribel

A seventeen-year-old girl with a Class II malocclusion and an increased overjet came to the practice in order to be treated with functional orthopedics after an initial pre-surgery orthodontic treatment that she refused to continue (Figs. 56.1 and 56.2). According to Planas philosophy, the patient's gnathostatic models (Fig. 56.3 a-c) were obtained by using the Planas facial arch. In addition, a first CBCT was taken in order to ascertain the absence of pathologic signs in the temporomandibular region (TMJ) and to determine whether the articular spaces had a correct distribution (Fig. 56.4 a, b).

Furthermore, the gnathostatic models were digitized in order to be inserted into the CBCT (Fig. 56.5 a, b). The OPG was extracted from the CBCT, as well as the right and left cephalometric radiographs. These images were significant in recognizing a retrognathic mandible, deviated to the right, and belonging to a favorable auxological category: A1N (Lavergne-Petrovic) (Petrovic 1994).

A volumetric reconstruction was performed (Fig. 56.6 a, b). Treatment started with an orthopedic functional appliance, including "pista indirecta planas composta" in order to move the mandible posture forward.

Fig. 56.1 a-b

Fig. 56.2 a-c

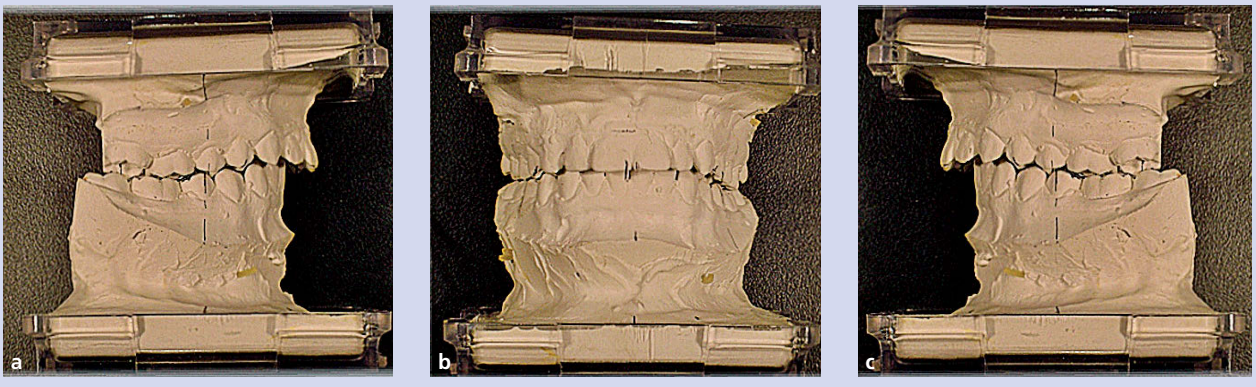

Fig. 56.3 a-c

CLINICAL CASE 56 *(cont'd)*

Marcos Gribel, Bruno Frazão Gribel

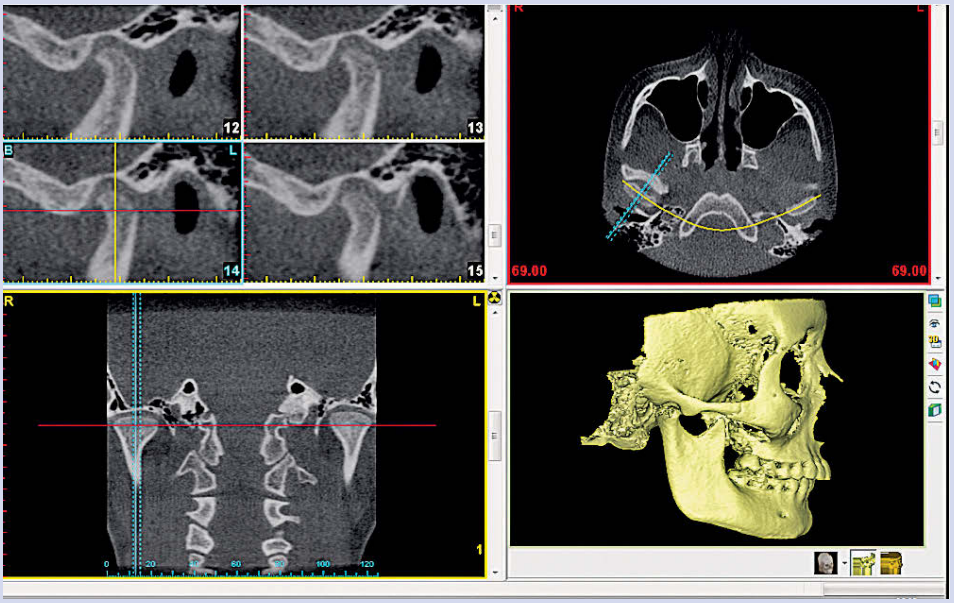

Fig. 56.4 a

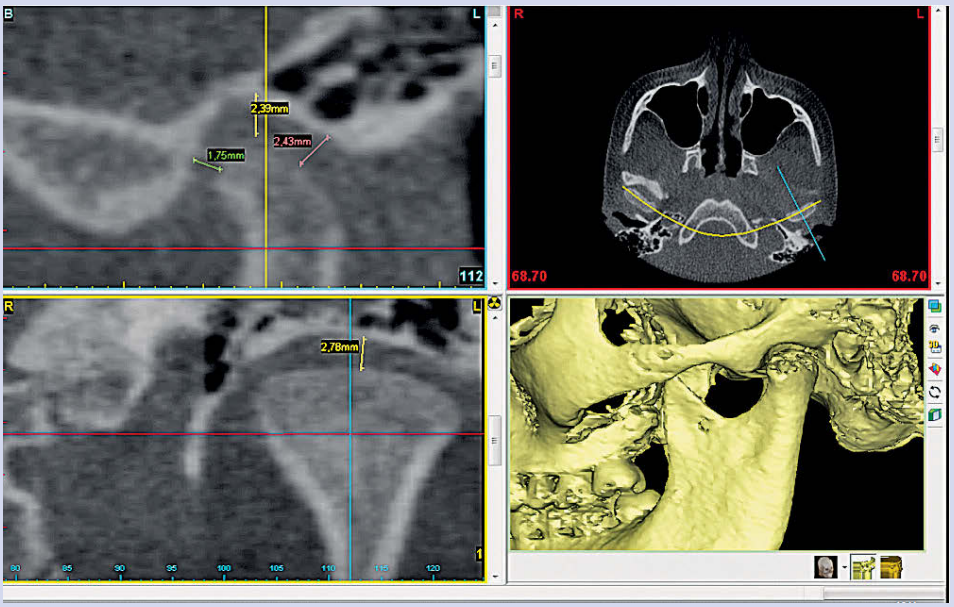

Fig. 56.4 b

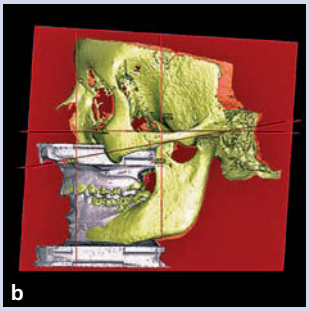

Fig. 56.5 a-b

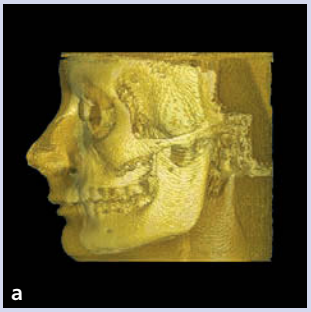

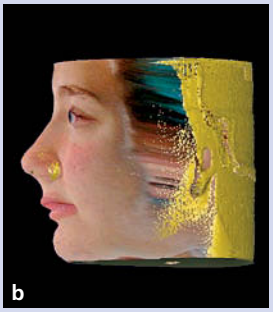

Fig. 56.6 a-b

CLINICAL CASE 56 *(cont'd)*

Marcos Gribel, Bruno Frazão Gribel

After three months, Gribel modified planas direct tracks (Gribel 2002) in composite were applied on the upper and lower first molars to stabilize the new mandible position twenty-four hours a day and to make possible a precise intercuspidation of the premolars and the second molars (Fig. 56.7 a-c). After one year of treatment, the occlusion was Class I, nevertheless the intercuspidation was still not perfect (Fig. 56.8 a-e). Treatment is being carried out with the tracks and an AOF with a metallic equiplan (Fig. 56.9 a-c). A second CBCT was taken in order to exclude anatomical abnormalities at the articular level (Fig. 56.10 a, b). A CBCT was also carried out to highlight the structural changes in the maxillofacial area, supported by cephalometric analysis and 3D superimpositions; the green color means differences in millimeters: yellow is 2 mm and red is 3 mm (Fig. 56.11 a, b).

Fig. 56.7 a-c

Fig. 56.8 a-c

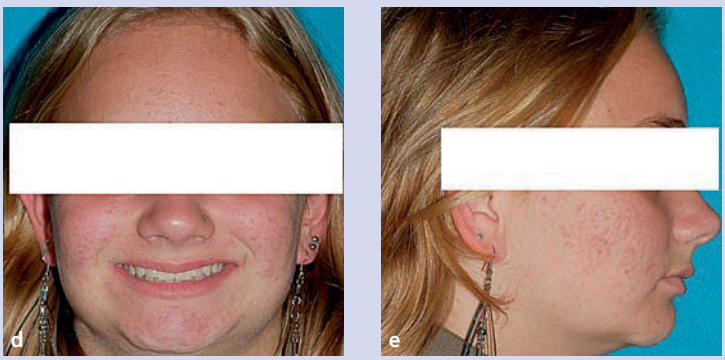

Fig. 56.8 d-e

Fig. 56.9 a-c

CLINICAL CASE 56 *(cont'd)*

Marcos Gribel, Bruno Frazão Gribel

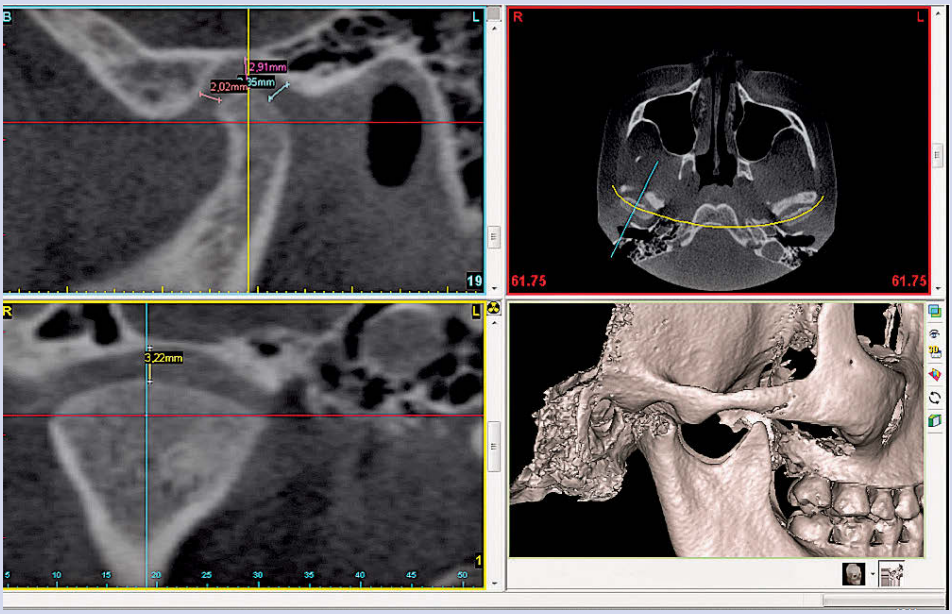

Fig. 56.10 a

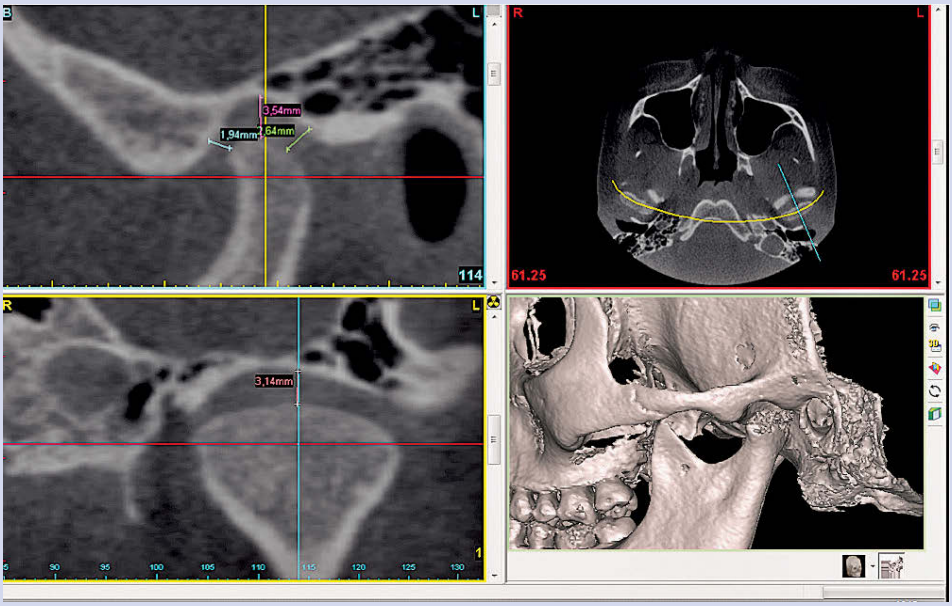

Fig. 56.10 b

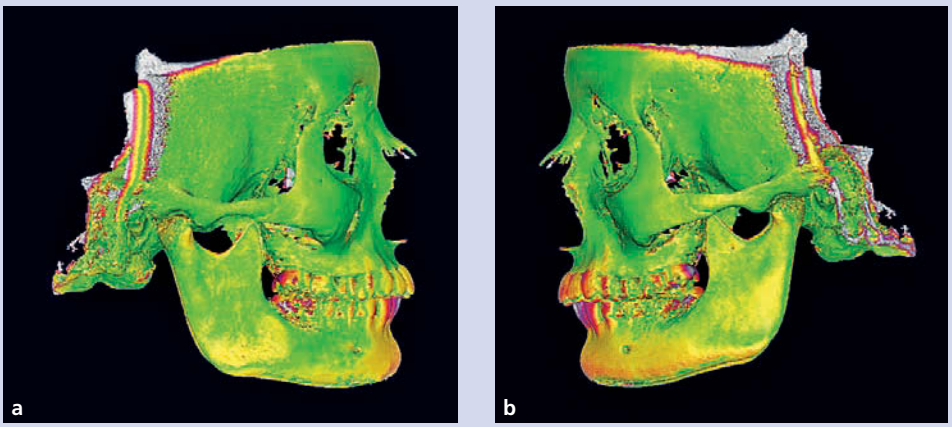

Fig. 56.11 a-b

Odontogenic sinus diseases

Emanuele Ambu - Roberto Ghiretti

CBCT in maxillary sinus diseases

Since the maxillary sinus floor is located in close proximity to the dental apices, it is often difficult to make accurate diagnoses and plan suitable treatments. The shared innervation can sometimes cause dental symptoms (Radman 1983). For example, the acute inflammation of the sinus membrane as a result of a bad cold produces pain when chewing and is experienced by the patient as a dental condition. On the other hand, periapical diseases may extend to the maxillary sinus with acute phases resulting in facial pain or swelling in and around the eyes, nose, and oral cavity.

Before the introduction of CBCT, odontogenic sinusitis was traditionally referred to as acute sinusitis only in ten percent of cases (Mehra and Murad 2004), confirming the assessments made by Maloney and Doku in 1968 (Maloney and Doku 1968). At present, this percentage is deemed much higher, and up to eighty-six percent of cases of mucositis of the maxillary sinus are now considered odontogenic (Bomeli et al. 2009). This is probably due to the fact that CBCT has allowed dental clinicians to perform diagnoses and follow-up of the maxillary sinus lesions associated with endodontic and periodontal problems.

Maillet et al. (2011) have recently suggested new criteria for radiological diagnosis of odontogenic sinusitis, modifying the classification proposed by Abrahams and Glassberg (1996). These authors, medical radiologists, made no evaluation of the endodontic diseases of the teeth involved or detected any decay.

Thanks to the work done by Maillet et al., it was proved that the sinus mucosa is, on average, 7.4 mm thick and that the first and second molars are in most cases responsible for odontogenic sinusitis (eleven times as much as the premolars), and that the bacterial disease affecting the periradicular area up to the maxillary sinus is mostly due to the palatal root of the first molar and the mesiobuccal root of the second molar. In this work, 51.8% of cases proved to be odontogenic, while the sum of sinusitis cases associated with periapical diseases of molars amounted to 65.4%—very close to the 71.3% detected by Obayashi et al. (2004). To this end, it should be underlined that the failure to detect the odontogenic origin often leads to the failure of the treatments. Five patients were examined who had undergone various operations (2.8, on average) and had suffered from sinusitis symptoms for a period of three to fifteen years before the real cause of their problem was found. An early diagnosis of dental origin of sinusitis would reduce the number of interventions, causing less discomfort to patients and reducing the social costs of these treatments, as well. This should suggest to otorhinolaryngologists to ask for dental evaluation when they have to deal with sinusitis which they are unable to solve with a pharmacological approach, before performing surgical interventions (Clinical Case 57).

CLINICAL CASE 57

Emanuele Ambu

This thirty-five-year-old female patient was referred to my office because of a fistula in the buccal area between the second premolar and the first molar in her left upper maxillary bone. The conventional X-ray showed the presence of some endodontic problems in both elements, which had already been treated endodontically. A little periapical radiolucency was detected in the second premolar (Fig. 57.1). During the week after the first endodontic retreatment (of her second premolar), the patient developed a tremendous abscess affecting the entire maxillary sinus. The patient reported that she had previously undergone two surgical operations in her maxillary sinus for otorhinolaryngoiatric problems. Both surgical treatments had failed. The CBCT exams showed a large radiolucency connected to the apices of both treated teeth (Fig. 57.2). In the two-dimensional reconstruction, we can see the area of the cyst and that of the inflamed portion of the sinus mucosa (Fig. 57.3). The 3D reconstruction emphasizes the area of the endodontic lesion, showing it in color (Fig. 57.4). A diagnosis of odontogenic sinusitis was made.

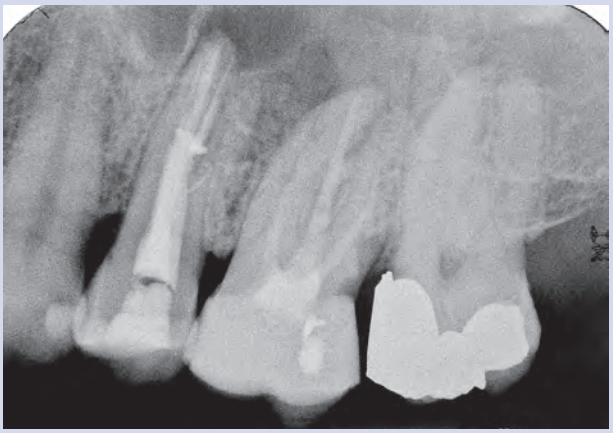

Fig. 57.1

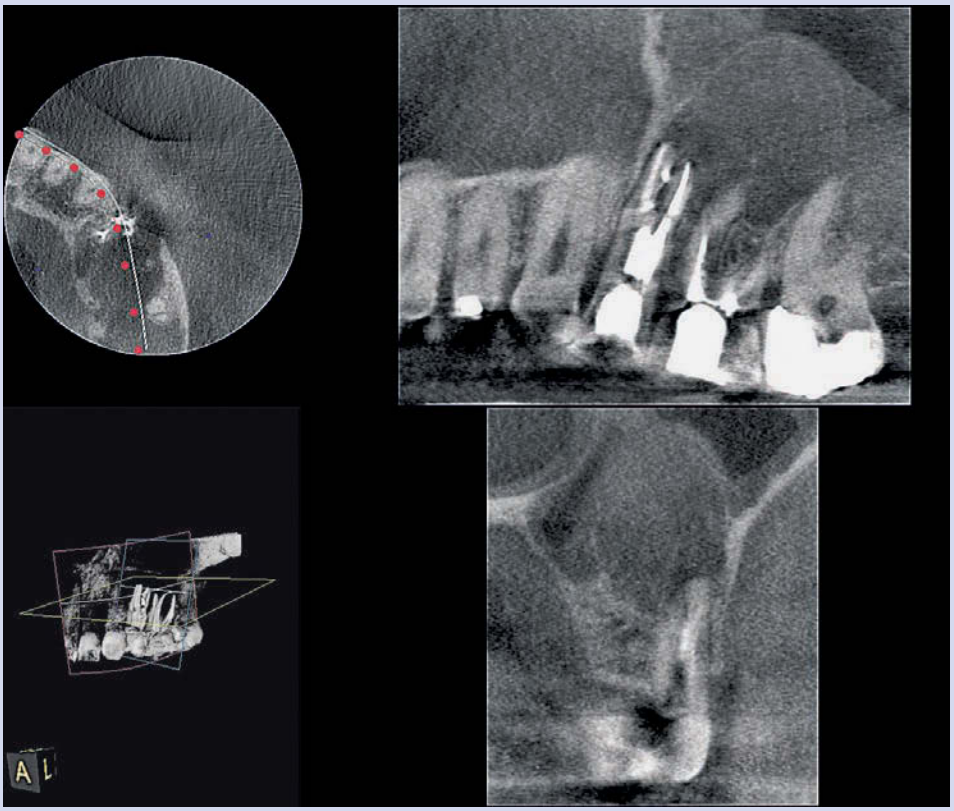

Fig. 57.2

CLINICAL CASE 57 *(cont'd)* **Emanuele Ambu**

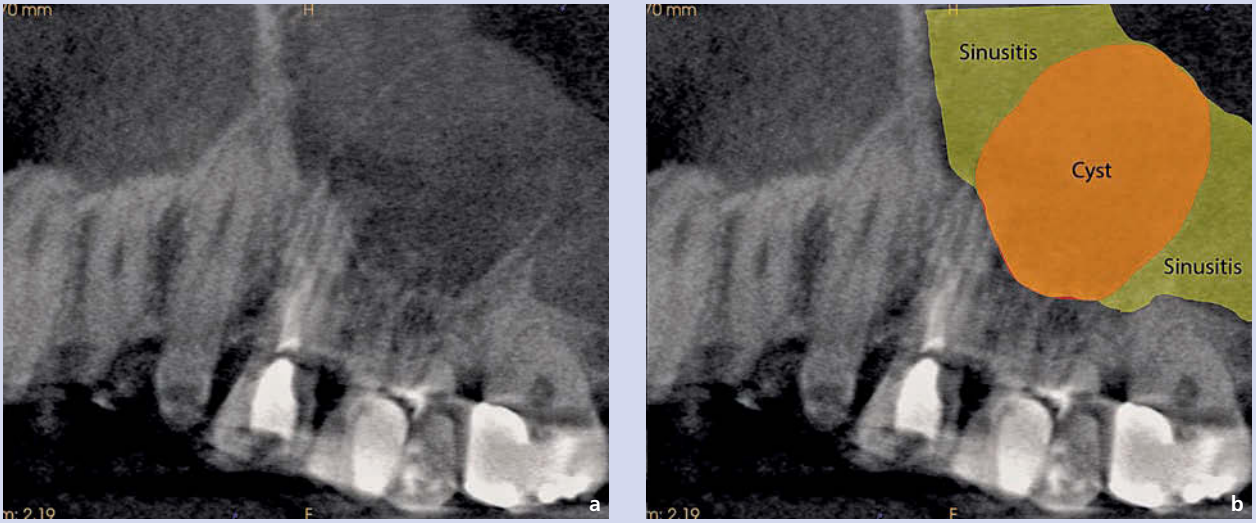

Fig. 57.3 a-b

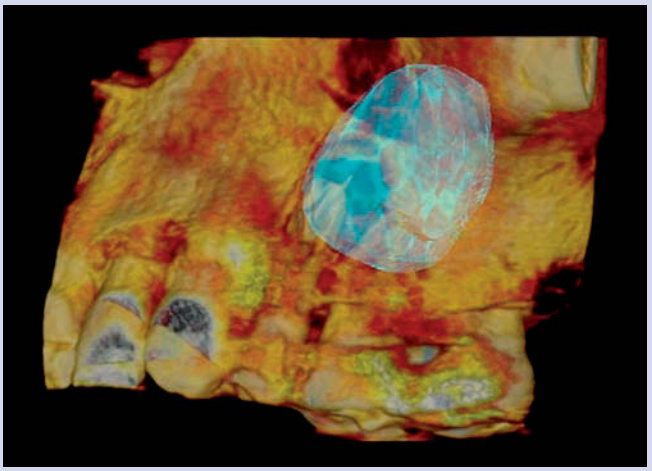

Fig. 57.4

It has been known for quite some time that maxillary sinus mucositis can be healed through proper endodontic treatment removing any intra-root bacteria (Nenzen and Welander 1967), and that inflammatory lesions of the sinus floor, when due to endodontic problems, can be reduced in the first three months in sixty percent of cases (Nurbakhsh et al. 2011). As suggested by Cymerman et al., the volumetric exam performed by the CBCT is very helpful in evaluating patients with concurrent sinus and dental diseases (Cymerman et al. 2011) (Clinical Case 58).

CLINICAL CASE 58

Emanuele Ambu

This female patient came to my practice to have her upper left second molar retreated. The intra-oral X-ray showed a fragment of instrument inside the mesial root of this tooth and a poor endodontic treatment of the first molar (Fig. 58.1). Since the sinus looked rather opaque, a volumetric exam was performed, detecting a large inflamed area of the maxillary sinus mucosa (Fig. 58.2a), which can be seen here colored in blue for the sake of clarity (Fig. 58.2b). Six months after retreating both molars, a second volumetric exam was performed showing a sharp reduction in the inflamed area of the maxillary sinus (Fig. 58.3a), which can be seen colored in red (Fig. 58.3b).

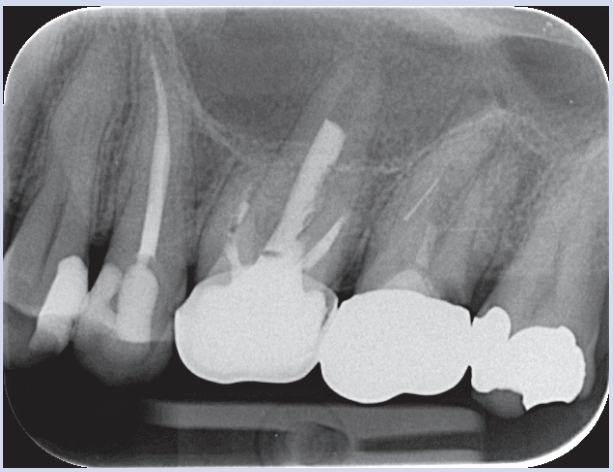

Fig. 58.1

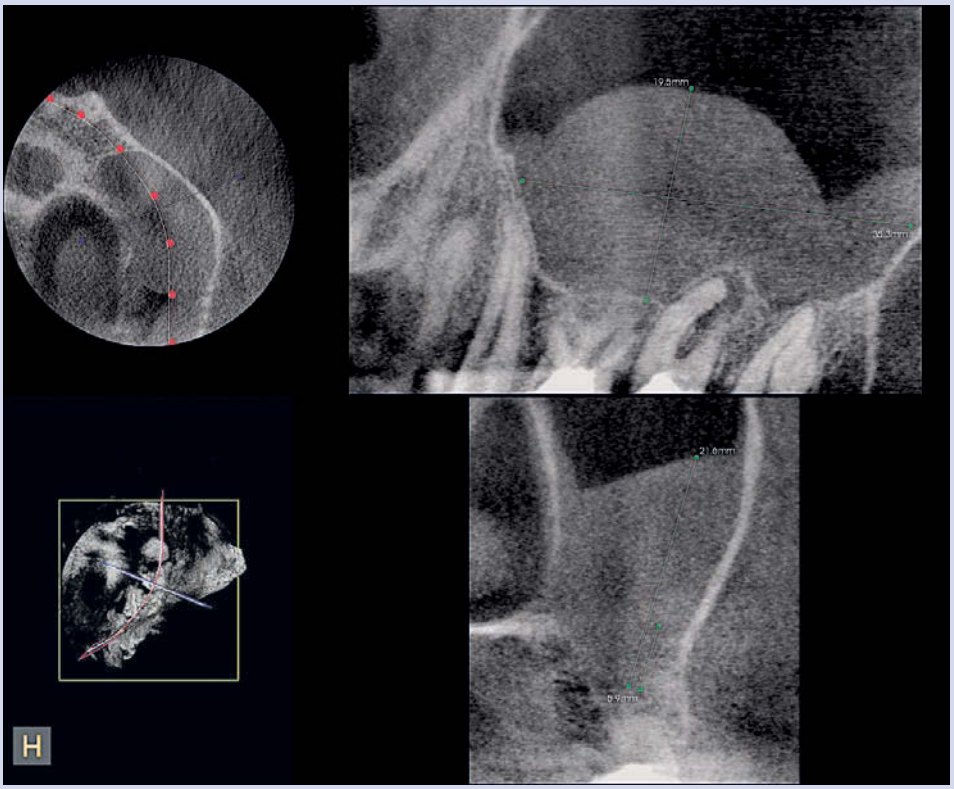

Fig. 58.2 a

CLINICAL CASE 58 *(cont'd)* **Emanuele Ambu**

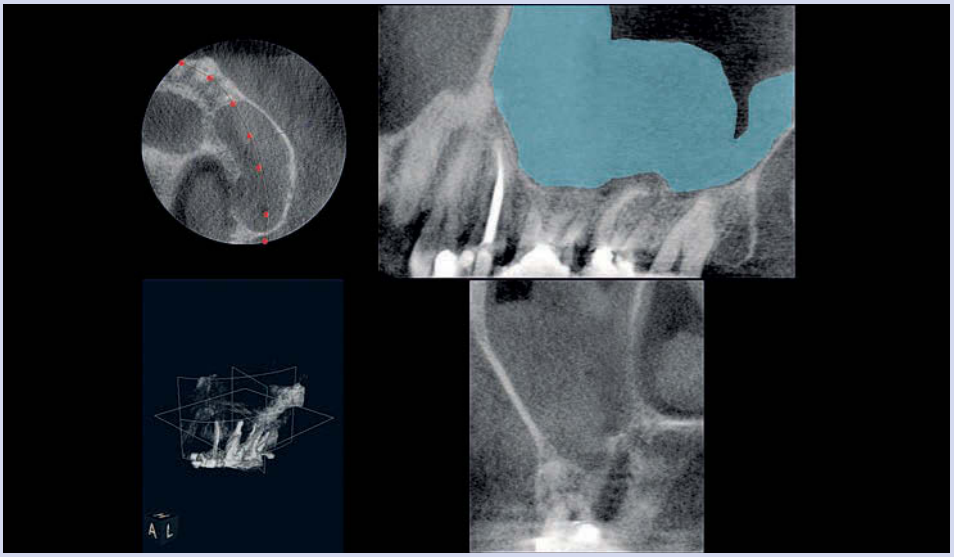

Fig. 58.2 b

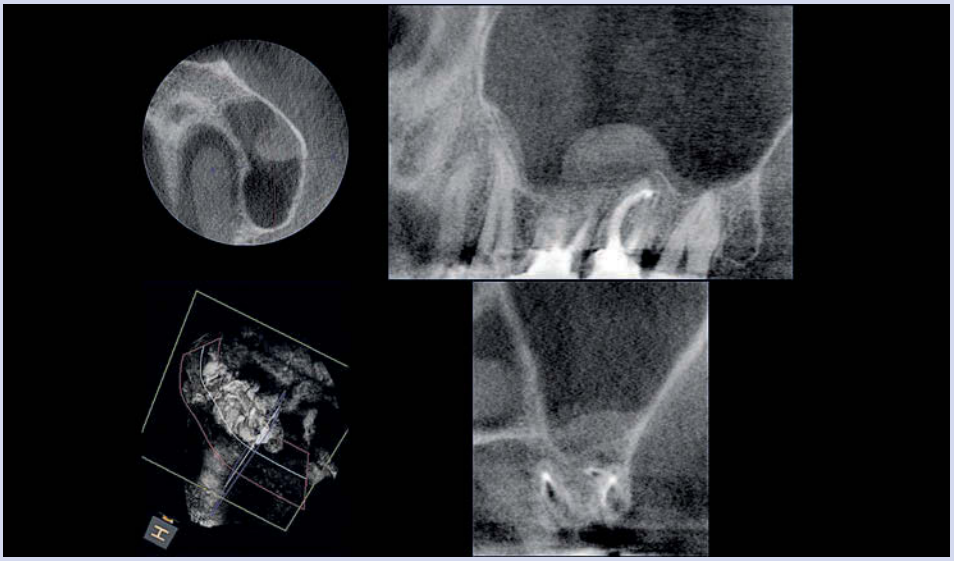

Fig. 58.3 a

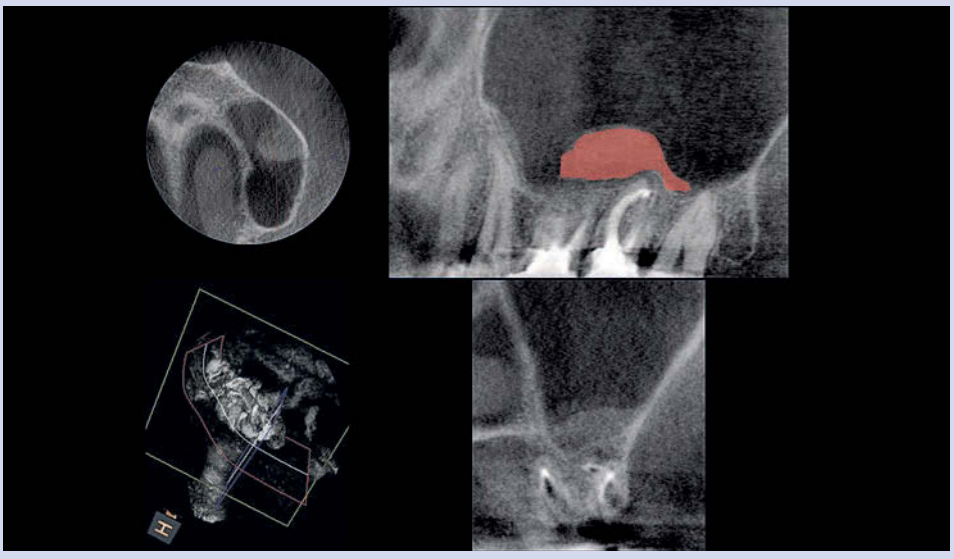

Fig. 58.3 b

In addition to endodontic problems, sinus diseases may be due to implants and periodontal diseases (Costa et al. 2007) (Clinical Case 59).

CLINICAL CASE 59

Emanuele Ambu

This forty-five-year-old female patient underwent a crestal sinus lift and the contextual insertion of an implant in the area of her upper left first molar (Fig. 59.1). Six months later, the follow-up CBCT exam showed maxillary sinus mucositis all around the implant (Fig. 59.2), despite the excellent stability of the implant and the absence of symptoms and clinical signs of failure.

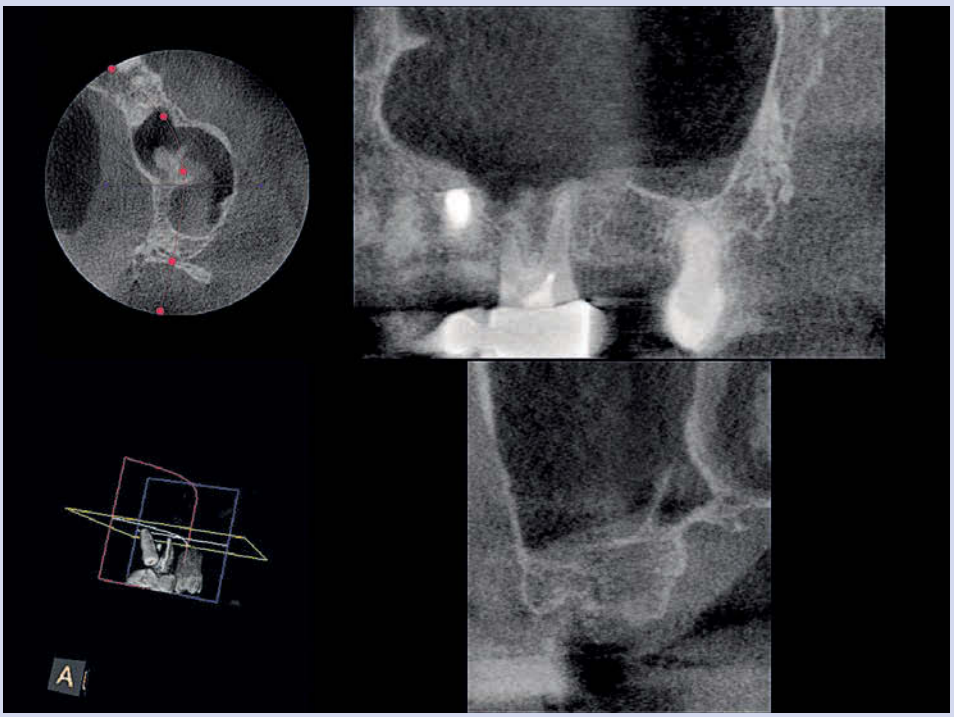

Fig. 59.1

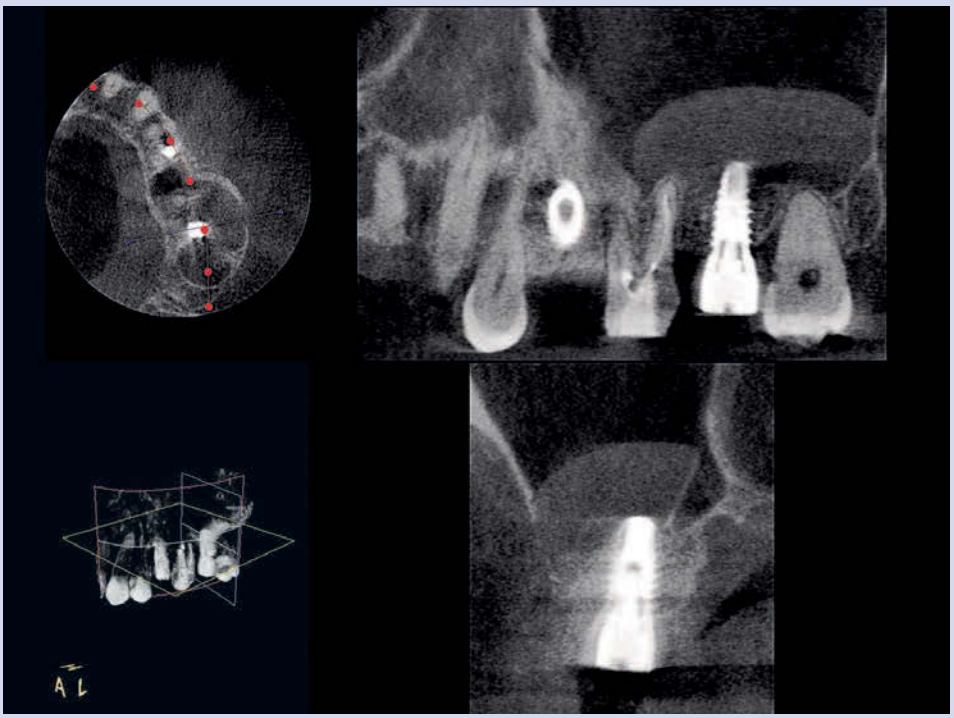

Fig. 59.2

Contrary to conventional radiology, CBCT may be very helpful for the diagnosis and treatment of oro-sinusal communications, as well as for examining foreign bodies in the maxillary sinus (Clinical Cases 60 and 61).

CLINICAL CASE 60

Roberto Ghiretti

A sixty-five-year-old female patient had been examined because of a broken lamina and a fracture in the other bridge abutment (Fig. 60.1). The lamina was removed. The patient reported that in the post-treatment period she felt water going through her nose, when drinking. The OPG was unable to explain the clinical pattern (Fig. 60.2), while the volumetric exam showed the presence of an oro-sinusal fistula (Fig. 60.3). The surgical operation performed to solve this problem proved that the clinical pattern (Fig. 60.4) was exactly that shown in the 3D image (Fig. 60.5).

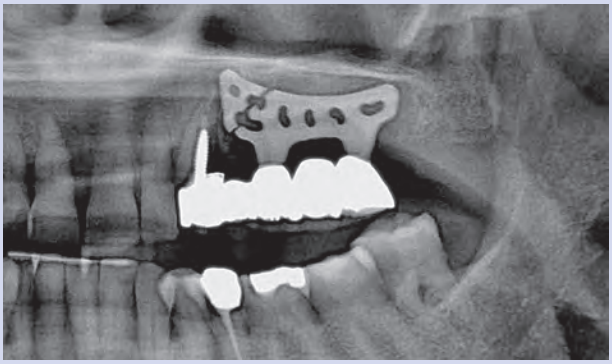

Fig. 60.1

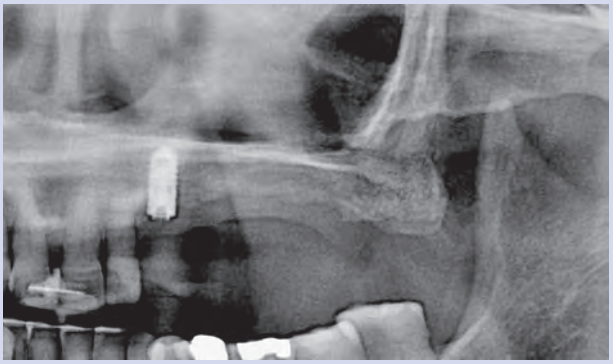

Fig. 60.2

Fig. 60.3

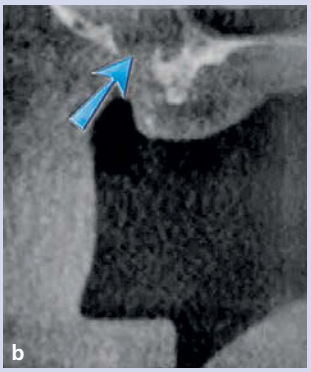

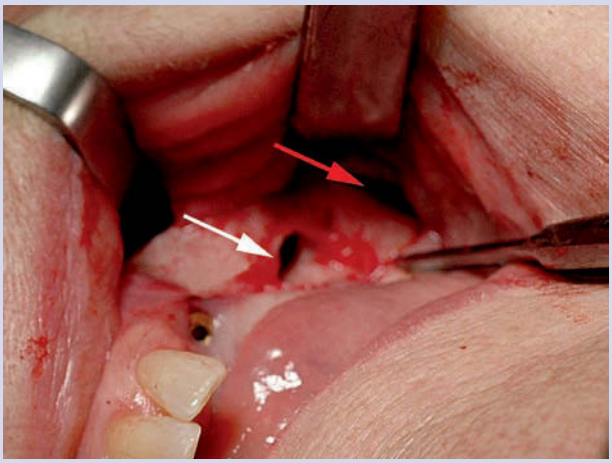

Fig. 60.4

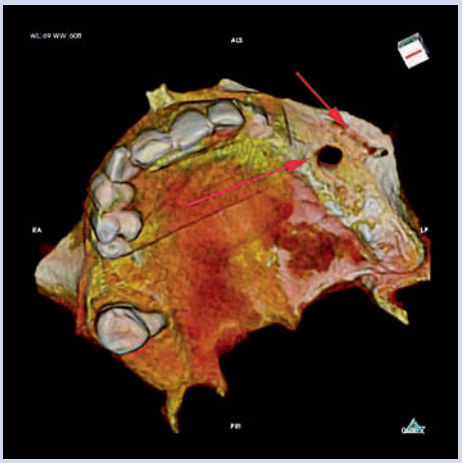

Fig. 60.5

CLINICAL CASE 61

Emanuele Ambu

A twenty-eight-year-old female patient came to my practice because of persistent pain and swelling in her left maxillary sinus area. The volumetric exam showed the presence of a large inflamed sinus area. Several radiopaque foreign bodies were also detected inside the area. These were probably due to endodontic cement which had spilled out of the root canal sealing of the first and second molars. These elements, too, showed periradicular osteolysis (Fig. 61.1). Since this phenomenon is often associated with aspergillosis of the maxillary sinus, it was suggested to the patient to call for an otorhinolaryngologists or a maxillofacial surgeon to solve the problem surgically.

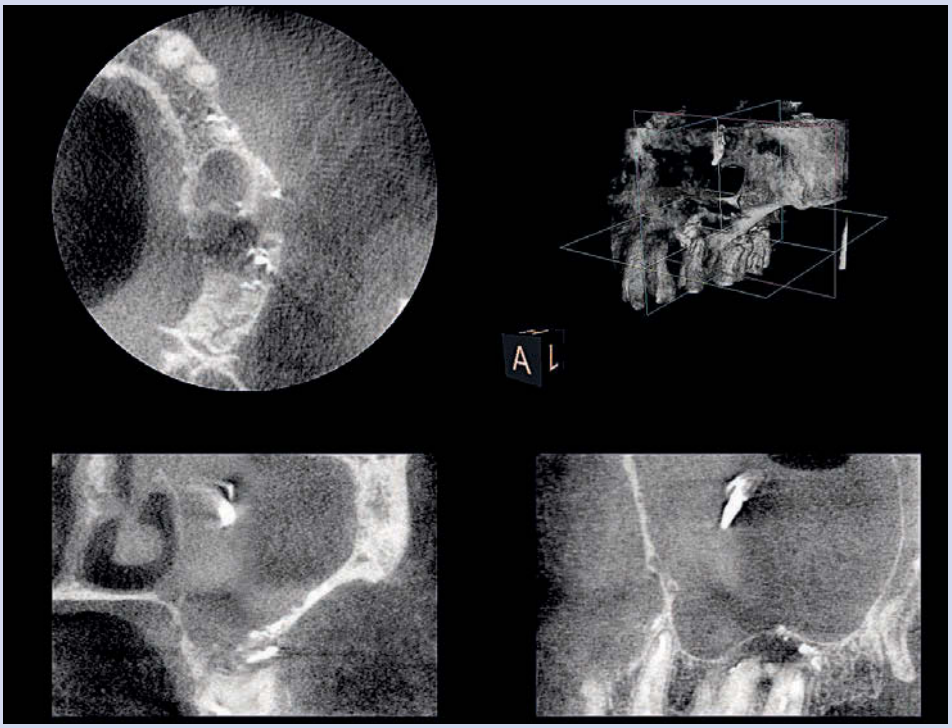

Fig. 61.1

References

Aboudara CA, Hatcher D, Nielsen IL, Miler A. A three-dimensional evaluation of the upper airway in adolescents. Orthod Craniofac Res. 2003; 6 Suppl 1: 173-175.

Abrahams JJ, Glassberg RM. Dental disease: a frequently unrecognized cause of maxillary sinus abnormalities? AJR Am J Roentgenol. 1996 May; 166(5): 1219-1223.

Ahmad M, Jenny J, Downie M. Application of cone beam computed tomography in oral and maxillofacial surgery. Aust Dent J. 2012 Mar; 57 Suppl 1: 82-94.

Alqerban A, Jacobs R, Fieuws S, Willems G. Comparison of two cone beam computed tomographic systems versus panoramic imaging for localization of impacted maxillary canines and detection of root resorption. Eur J Orthod. 2011; 33(1): 93-102.

Alqerban A, Jacobs R, Lambrechts P, Loozen G, Willems G. Root resorption of the maxillary lateral incisor caused by impacted canine: a literature review. Clin Oral Investig. 2009 Sep; 13(3): 247-255.

Alqerban A, Jacobs R, Souza PC, Willems G. In-vitro comparison of 2 cone-beam computed tomography systems and panoramic imaging for detecting simulated canine impaction-induced external root resorption in maxillary lateral incisors. Am J Orthod Dentofacial Orthop. 2009 Dec; 136(6): 764.e1-11; discussion 764-765.

Andreasen JO, Andreasen FM, Andersson L. Classification, etiology, and epidemiology. Textbook and color atlas of traumatic injuries of the teeth, 3rd edition. Munksgaard (Copenhagen) 1994: 151-177.

Andreasen JO, Bakland LK, Flores MT, Andreasen FM, Andersson L. Traumatic Dental Injuries: A Manual. Wiley-Blackwell, Paperback. 3rd Edition; May 2011.

Angelopoulos C, Thomas SL, Hechler S, Parissis N, Hlavacek M. Comparison between digital panoramic radiography and conebeam computed tomography for the identification of the mandibular canal as part of presurgical dental implant assessment. J Oral Maxillofac Surg. 2008; 66(10): 2130-2135.

Antoszewska J, Trzesniewska P, Kawala B, Ludwig B, Park HS. Qualitative and quantitative evaluation of root injury risk potentially burdening insertion of miniscrew implants. Korean J Orthod. 2011 Apr; 41(2): 112-120.

Arai Y, Tammisalo E, Iwai K, Hashimoto K, Shinoda K. Development of a compact computed tomographic apparatus for dental use. Dentomaxillofac Radiol. 1999: 28: 245-248.

Aranyarachkul P, et al. Bone density assessments of dental implant sites: 2. Quantitative cone-beam computerized tomography. Int J Oral Maxillofac Implants. 2005; 20: 416-424.

Årtun J, Smale I, Behbehani F, Doppel D, Van't Hof M, Kuijpers-Jagtman AM. Apical root resorption six and twelve months after initiation of fixed orthodontic appliance therapy. Angle Orthod. 2005; 75: 919-926.

Årtun J, Urbye KS. The effect of orthodontic treatment on periodontal bone support in patients with advanced loss of marginal periodontium. Am J Orthod Dentofacial Orthop. 1988; 93: 143-148.

Ayoub AF, Xiao Y, Khambay B, Siebert JP, Hadley D. Towards building a photo-realistic virtual human face for craniomaxillofacial diagnosis and treatment planning. Int J Oral Maxillofac Surg. 2007; 36: 423-428.

Baratto Filho F, Zaitter S, Haragushiku GA, de Campos EA, Abuabara A, Correr GM. Analysis of the internal anatomy of a maxillary first molar by using different methods. J Endod. 2009; 35(3): 337-342.

Barone A, Covani U, Cornelini R, Gherlone E. Radiographic bone density around immediately loaded oral implants: A case series. Clin Oral Implants Res. 2003; 14: 610-615.

Barone R, Chiapasco M, Clauser C. Chirurgia Orale. Le cisti dei mascellari. Manuale Atlante, Timeo Ed, Bologna. 1999.

Barros SE, Janson G, Chiqueto K, Garib DG. Two-dimensional radiographic and clinical references of the tooth crown for orthodontic mini-implant insertion: a guide-free technique. Oral Surg Oral Med Oral Pathol Oral Radiol Endod. 2010 Nov; 110(5): e8-e16.

Barthel CR, Zimmer S, Trope M. Relationship of radiologic and histologic signs of inflammation in human root-filled teeth. J Endod 2004; 30(2): 75-79.

Bauman M. The effect of CBCT voxel resolution on the detection of canals in the mesiobuccal roots of permanent maxillary first molars. MS Thesis. University of Louisville School of Dentistry Masters in Oral Biology, Louisville, Kentucky, May, 2009.

Becker A, Binstein E, Shteyer A. Interdisciplinary treatment of multiple unerupted supernumerary teeth. Report of a case. Am J Orthod. 1982; 81: 417-422.

Bell A, Ayoub AF, Siebert JP. Assessment of the accuracy of a three-dimensional imaging system for archiving dental study models. J Orthod. 2003 Sep; 30(3): 219-223.

Benavides E, Rios HF, Ganz SD, An CH, Resnik R, Reardon GT, Feldman SJ, Mah JK, Hatcher D, Kim MJ, Sohn DS, Palti A, Perel ML, Judy KW, Misch CE, Wang HL. Use of cone beam computed tomography in implant dentistry: the International Congress of Oral Implantologists Consensus Report. Implant Dent. 2012 Apr; 21(2): 78-86.

Bernardes RA, de Moraes IG, Húngaro Duarte MA, Azevedo BC, de Azevedo RJ, Bramante CM. Use of cone-beam volumetric tomography in the diagnosis of root fractures. Oral Surg Oral Med Oral Pathol Oral Radiol Endod. 2009 Aug; 108(2): 270-277.

Bianchi A, Muyldermans L, Di Martino M, Lancellotti L, Amadori S, Sarti A, Marchetti C. Facial soft tissue esthetic predictions: validation in craniomaxillofacial surgery with cone beam computed tomography data. J Oral Maxillofac Surg. 2010 Jul; 68(7): 1471-1479.

Blattner TC, George N, Lee CC, Kumar V, Yelton CD. Efficacy of cone-beam computed tomography as a modality to accurately identify the presence of second mesiobuccal canals in maxillary first and second molars: a pilot study. J Endod. 2010; 36(5): 867-870.

Boeddinghaus R, Whyte A. Current concepts in maxillofacial imaging. Eur J Radiol. 2008; 66: 396-418.

Bomeli SR, Branstetter BF 4th, Ferguson BJ. Frequency of a dental source for acute maxillary sinusitis. Laryngoscope. 2009 Mar; 119(3): 580-584.

Bornstein MM, Wölner-Hanssen AB, Sendi P, von Arx T. Comparison of intraoral radiography and limited cone beam computed tomography for the assessment of root-fractured permanent teeth. Dental Traumatol. 2009; 25: 571-577.

Broadbent BH. A new X-ray technique and its application to orthodontia. Angle Orthod. 1931; 1: 45-66.

Broadbent BH. The face of the normal child. Angle Orthod. 1937; 7: 183-208.

Brodie AG. On the growth pattern of the human head: From the third month to the eighth year of life. Am J Anat. 1941; 68: 209-262.

Brooks SL, Brand JW, Gibbs SJ, Hollender L, Lurie AG, Omnell KA, Westesson PL, White SC. Imaging of the temporomandibular joint: a position paper of the American Academy of Oral and Maxillofacial Radiology. Oral Surg Oral Med Oral Pathol Oral Radiol Endod. 1997 May; 83(5): 609-618.

Brown JS, Kalavrezos N, D'Souza J, Lowe D, Magennis P, Woolgar JA. Factors that influence the method for mandibular resection in the management of oral squamous cell carcinoma. Br J Oral Maxillofac Surg. 2002 Aug; 40(4): 275-284.

Bueno MR, Estrela C, Figueiredo JAP, Azevedo B. Map-reading strategy to diagnose root perforations near metallic intracanal posts by using cone beam computed tomography. J Endodon. 2011; 37(1): 85-90.

Burstone C. The mechanics of the segmented arch techniques. The Angle Orthod.1966; 36: 99-120.

Burstone C, James RB, Legan H, Murphy GA, Norton LA. Cephalometrics for orthognathic surgery. J Oral Surg. 1978; 36: 269-277.

Caloss R, Atkins K, Stella JP. Three-dimensional imaging for virtual assessment and treatment simulation in orthognathic surgery. Oral Maxillofac Clin North Am. 2007; 19: 287-309.

Cattaneo PM, Melsen B. The use of cone-beam computed tomography in an orthodontic department in between research and daily clinic. World J Orthod. 2008; 9: 269-282.

Cevidanes LH, Bailey LJ, Tucker GR Jr, Styner MA, Mol A, Phillips CL, Proffit WR, Turvey T. Superimposition of 3D cone-beam CT models of orthognathic surgery patients. Dentomaxillofac Radiol. 2005 Nov; 34(6): 369-375.

Cevidanes LH, Bailey LJ, Tucker SF, Styner MA, Mol A, Phillips CL, Proffit WR, Turvey T.Three-dimensional cone-beam computed tomography for assessment of mandibular changes after orthognathic surgery. Am J Orthod Dentofacial Orthop. 2007 Jan; 131(1): 44-50.

Cevidanes LH, Motta A, Styner M, Phillips C. 3D imaging for early diagnosis and assessment of treatment response. In: McNnamara JA, Jr, Kapila SD, editors. Early orthodontic treatment: is the benefit worth the burden? 33rd Annual Moyers Symposium, Ann Arbor. 2007; 305-321.

Chen YJ, Chang HH, Lin HY, Lai E, Hung HC, Yao CC. Stability of miniplates and miniscrews used for orthodontic anchorage: experience with 492 temporary anchorage devices. Clin Oral Implant Res. 2008; 19(11): 1188–1196.

Cohenca N, Simon JH, Roges R, Morag Y, Malfaz JM. Clinical indications for digital imaging in dento-alveolar trauma. Part I: traumatic injuries. Dent Traumatol 2007; 23: 95-104.

Cohenca N, Simon JH, Mathur A, Malfaz JM. Clinical indications for digital imaging in dento-alveolar trauma. Part 2: root resorption. Dental Traumatol 2007; 23(2): 105-113.

Costa F, Emanuelli E, Robiony M, Zerman N, Polini F, Politi M. Endoscopic surgical treatment of chronic maxillary sinusitis of dental origin. J Oral Maxillofac Surg. 2007; 65: 223-228.

Cotton TP, Schindler WG, Schwartz SA, Watson WR, Hargreaves KM. Endodontic applications of cone-beam volumetric tomography. J Endod. 2007; 33(9): 1121-1132.

Curley A, Hatcher DC. Cone beam CT—anatomic assessment and legal issues: the new standards of care. J Calif Dent Assoc. 2009; 37(9): 653-662.

Cymerman JJ, Cymerman DH, O'Dwyer RS. Evaluation of odontogenic maxillary sinusitis using cone-beam computed tomography: three case reports. J Endod 2011; 37(10): 1465-1469.

da Silveira HID, Silveira HED, Liedke GS, Lermen CA, Dos Santos RB, de Figueiredo JAP. Diagnostic ability of computed tomography to evaluate external resorptions in vitro. Dentomaxillofacial Radiology. 2007; 36(7): 393-396.

de Oliveira RC, Leles CR, Normanha LM, Lindh C, Ribeiro-Rotta RF. Assessments of trabecular bone density at implant sites on CT images. Oral Surg Oral Med Oral Pathol Oral Radiol Endod. 2008; 105(2): 231-218.

De Vos W, Casselman J, Swennen GRJ. Cone-beam computerized tomography (CBCT) imaging of the oral and maxillofacial region: A systematic review of the literature. Int J Oral Maxillofac Surg. 2009; 38: 609-625.

D'haese J, Van De Velde T, Komiyama A, Hultin M, De Bruyn H. Accuracy and complications using computer-designed stereolithographic surgical guides for oral rehabilitation by means of dental implants: a review of the literature. Clin Implant Dent Relat Res. Epub May 2010.

Dölekoglu S, Fisekçioglu E, Ilgüy D, Ilgüy M, Bayirli G. Diagnosis of jaw and dentoalveolar fractures in a traumatized patient with cone-beam computed tomography. Dent Traumatol. 2010; 26: 200-203.

dos Santos Neto P, dos Santos L, Coletta RD, Laranjeira AL, de Oliveira Santos CC, Bonan PR, Martelli-Júnior H. Imaging evaluation of the gingival fibromatosis and dental abnormalities syndrome. Dentomaxillofac Radiol. 2011 May; 40(4): 236-243.

Downs, WB. Variations in Facial Relationships: Their Significance in Treatment and Prognosis. Am J Orthod. 1948; 34: 812-840.

Draenert FG, Coppenrath E, Herzog P, Müller S, Mueller-Lisse UG. Beam hardening artefacts occur in dental implant scans with the NewTom cone beam CT but not with the dental 4-row multidetector CT. Dentomaxillofac Radiol. 2007 May; 36(4): 198-203.

Draenert FG, Erbe C, Zenglein V, Kämmerer PW, Wriedt S, Al Nawas B. 3D analysis of condylar position after sagittal split osteotomy of the mandible in mono- and bimaxillary orthognathic surgery—a methodology study in 18 patients. J Orofac Orthop. 2010 Nov; 71(6): 421-429. Epub 17 Nov 2010.

Durack C, Patel S, Davies J, Wilson R, Mannocci F. Diagnostic accuracy of small volume cone beam computed tomography and intraoral periapical radiography to detect the simulated external inflammatory root resorption. Int End J. 2011; 44: 136-147.

Enlow D, Moyers R, Merow W. Handbook of Facial Growth, W.B. Saunders Company. 1982.

Ericson S, Kurol J. Incisor resorption caused by maxillary cuspids. A radiographic study. Angle Orthodontist. 1987; 57: 332-346.

Ericsson I, Thilander B. Orthodontic relapse in dentitions with reduced periodontal support: an experimental study in dogs. Eur J Orthod. 1980; 2: 51-57.

Ericsson I, Thilander B, Lindhe J, Okamoto H. The effect of orthodontic tilting movements on the periodontal tissues of infected and non-infected dentitions in dogs. J Clin Periodontol. 1977; 4: 278-293.

Esposito S, Cardaropoli M, Cotti E A suggested technique for the application of cone beam computed tomography periapical index. Dentomaxillofacial Radiology 2011; 40: 506-512.

Estelita S, Janson G, Chiqueto K, Janson M, Freitas M. Predictable drill-free screw positioning with a graduated 3-dimensional radiographic-surgical guide: a preliminary report. Am J Orthod Dentofacial Orthop. 2006; 136: 722-735.

Estevez R, Aranguren J, Escorial A, de Gregorio C, De La Torre F, Vera J, Cisneros R. Invasive cervical resorption class III in a maxillary central incisor: diagnosis and follow-up by means of cone-beam computed tomography. J Endodon. 2010; 36(12): 2012-2014.

Estrela C, Bueno MR, Azevedo BC, Azevedo JR, Pecora JD. A new periapical index based on cone beam computed tomography. J Endod. 2008; 34(11): 1325-1331.

Estrela C, Bueno MR, Leles CR, Azevedo B, Azevedo JR. Accuracy of cone beam computed tomography and panoramic and periapical radiography for detection of apical periodontitis J Endod 2008; 34(3): 273-279.

Faitaroni LA, Bueno MR, Calvalhosa AA, Mendonça EF, Estrela C. Differential diagnosis of apical periodontitis and nasopalatine duct cyst. J Endod. 2011; 37(3): 403-410.

Farman AG, Scarfe WC. Development of imaging selection criteria and procedures should precede cephalometric assessment with cone-beam tomography. Am J Orthod Dentofacial Orthop. 2006; 130: 257-265.

Feldkamp LA, Davis LC, Kress JW. Practical cone-beam algorithm. J Opt Soc Am. 1994: 1: 612-619.

Ficarra G. Cisti delle ossa mascellari. 2010. http://www.malattieorali.it.

Flores MT, Andersson L, Andreasen JO, Bakland LK, Malmgren B, Barnett F, et al. Guidelines for the management of traumatic dental injuries. I:

Fractures and luxations of permanent teeth. Dental Traumatol. 2007; 23: 66-71.

Fortin T, Bosson JL, Coudert JL, Isidori M. Reliability of preoperative planning of an image-guided system for oral implant placement based on 3-dimensional images: an in vivo study. Int J Oral Maxillofac Implants. 2003; 18: 886-893.

Frain C, Lacroix F. De l'obtention de coupes horizontales. J Radiol Electrol. 1948; 29, n° 5-6: 256-257.

Frank AL, Torabinejad M. Diagnosis and treatment of extracanal invasive resorption. J Endodon. 1998; 24: 500-504.

Frederiksen NL, Benson BW, Sokolowski TW. Effective dose and risk assessment from film tomography used for dental implant diagnostics. Dentomaxillofac Radiol. 1994; 23: 123-127.

Fuhrmann R. Three-dimensional interpretation of alveolar bone dehiscences. An anatomical-radiological study—Part I. J Orofac Orthop. 1996; 57: 62-74.

Ganz SD. Defining new paradigms for assessment of implant receptor sites. Compend Cont Edu Dent. 2008: 29(5): 256-267.

Ganz SD. Use of conventional CT and Cone Beam for improved dental diagnostic and implant planning. AADMRT Newsletter 19-24. Spring 2005.

Garib DG, Henriques JF, Janson G, de Freitas MR, Fernandes AY. Periodontal effects of rapid maxillary expansion with tooth-tissue-borne and tooth-borne expanders: a computed tomography evaluation. Am J Orthod Dentofacial Orthop. 2006; 129: 749-758.

Ghaeminia H, Meijer GJ, Soehardi A, et al. The use of cone beam CT for the removal of wisdom teeth changes the surgical approach compared with panoramic radiography: a pilot study. Int J Oral Maxillofac Surg. 2011; 40: 834-839.

Gijbels F, Sanderink G, Wyatt J, Van Dam J, Nowak B, Jacobs R. Radiation doses of collimated vs non-collimated cephalometric exposures. Dentomaxillofac Radiol. 2003; 32: 128-133.

Gijbels F, Sanderink G, Wyatt J, Van Dam J, Nowak B, Jacobs R. Radiation doses of indirect and direct digital cephalometric radiography. Br Dent J. 2004; 197: 149-152.

Goerres GW, Schmid DT, Schuknecht B, Eyrich GK. Bone invasion in patients with oral cavity cancer: comparison of conventional CT with PET/CT and SPECT/CT. Radiology. 2005; 237: 281-287.

Gribel, MN. Planas direct tracks in the early treatment of unilateral crossbite with mandibular postural deviation: Why worry so soon? World J Orthod. 2002; (3): 239-249.

Guerrero ME, Jacobs R, Loubele M, Schutyser F, Suetens P, van Steenberghe D. State-of-the-art on cone beam CT imaging for preoperative planning of implant placement. Clin Oral Investig. 2006; 10: 1-7.

Haapasalo M, Endal U. Internal inflammatory resorption: an unknown resorption of the tooth. Endodontic Topics. 2006; 14: 60-79.

Halazonetis DJ. From 2-dimensional cephalograms to 3-dimensional computed tomography scans. Am J Orthod Dentofacial Orthop. 2005; 127: 627-637.

Haney E, Gansky SA, Lee JS, Johnson E, Maki K, Miller AJ, Huang JC. Comparative analysis of traditional radiographs and cone-beam computed tomography volumetric images in the diagnosis and treatment planning of maxillary impacted canines. Am J Orthod Dentofacial Orthop. 2010; 137: 590-597.

Harris D, et al. E.A.O. guidelines in the use of diagnostic imaging in implant dentistry. Clin Oral Impl Res. 2002; 13: 566-570.

Harvold EP. The role of function in the etiology and treatment of malocclusion. Am J Orthod. 1968; 54: 883-898.

Hashimoto K, Sawada K, Honda K, Araki M, Iwai K, Shinoda K. Diagnostic efficacy of three-dimensional images by helical CT for lesions in the maxillofacial region. J Oral Sci. 2000; 42: 211-219.

Hassan B, Metska ME, Ozok AR, van der Stelt P, Wesselink PR. Comparison of five cone beam computed tomography systems for the detections of vertical root fractures. J Endod. 2010; 36: 126-129.

Hassan B, Metska ME, Ozok AR, van der Stelt P, Wesselink PR. Detection of vertical root fractures in endodontically treated teeth by a cone beam computed tomography scan. J Endod. 2009; 35: 719-722.

Hatcher DC, Dial C, Mayorga C. Cone beam CT for pre-surgical assessment of implant sites. J Calif Dent Assoc. 2003 Nov; 31(11): 825-833.

Heithersay GS. Clinical, radiologic and histopathologic features of invasive cervical resorption. Quintessence Int. 1999; 30: 27-37.

Hilgers ML, Scarfe WC, Scheetz JP, Farman AG. Accuracy of linear temporomandibular joint measurements with cone beam computed tomography and digital cephalometric radiography. Am J Orthod Dentofacial Orthop. 2005; 128(6): 803-811.

Honda K, Larheim TA, Maruhashi K, Matsumoto K, Iwai K. Osseous abnormalities of the mandibular condyle: diagnostic reliability of cone beam computed tomography compared with helical computed tomography based on an autopsy material. Dentomaxillofac Radiol. 2006; 35: 152-157.

Honey OB, Scarfe WC, Hilgers MJ, Klueber K, Silveira AM, Haskell BS, Farman AG. Accuracy of cone-beam computed tomography imaging of the temporomandibular joint: comparisons with panoramic radiology and linear tomography. Am J Orthod Dentofacial Orthop. 2007; 132: 429-438.

Horner K, Islam M, Flygare L, Tsiklakis K, Whaites E. Basic principles for use of dental cone beam computed tomography: consensus guidelines of the European Academy of Dental and Maxillofacial Radiology. Dentomaxillofacial Radiology. 2009; 38: 187-195.

Hounsfield GN. Computerized transverse axial scanning (tomography). 1. Description of system. Br J Radiol. 1973 Dec; 46(552): 1016-1022.

Ilgüy D, Ilgüy M, Fisekçioglu E, et al. Detection of jaw and root fractures using cone beam computed tomography: a case report. Dentomaxillofac Radiol. 2009; 38(3): 169-173.

Jacobson A. The "Wits" appraisal of jaw disharmony. Am J Orthod. 1975; 67: 125-138.

Jacobson A. Application of the "Wits" appraisal. Am J Orthod. 1976; 70: 179-189.

Jarabak, JR. Diagnostic aids, in Technique and Treatment with LightWire Edgewise Appliances, vol. 1, 2nd ed., ed. JR Jarabak and JA Fizzel, CV Mosby Co., St. Louis. 1972; 128-166.

Kamburoglu K, Cebeci ARI, Gröndahl HG. Effectiveness of limited cone-beam computed tomography in the detection of horizontal root fracture. Dental Traumatol. 2009; 25: 256-261.

Kamel SG, Kau CH, Wong ME, Kennedy JW, English JD. The role of Cone beam CT in the evaluation and management of a family with Gardner's syndrome. J Craniomaxillofac Surg. 2009 Dec; 37(8): 461-468.

Kanagasingam S, Patel S, Chong BS, Mannocci F. Cone beam computed tomography in endodontics: A review. Il Dentista Moderno. 2011 Sept; 146-162. In Italian and English.

Kaneda T, Minami M, Kurabayashi T. Benign odontogenic tumours of the mandible and maxilla. Neuroimaging Clin N Am. 2003; 13: 495-507.

Karring T, Nyman S, Thilander B, Magnusson I. Bone regeneration in orthodontically produced alveolar bone dehiscences. J Periodontal Res. 1982; 17: 309-315.

Kau CH, Richmond S, Palomo JM, Hans MG. Three-dimensional cone beam computerized tomography in orthodontics. J Orthod. 2005; 32: 282-283.

Kaya S, Yavuz I, Uysal I, Akkus Z. Measuring bone density in healing periapical lesions by using Cone Beam Computer Tomography: a clinical investigation. J Endod. 2012; 38(1): 28-31.

Kieffer J. Le laminagraphe et ses variants; applications et indications des principes de planigraphie. Am J Roentgenol. 1938; 39, n° 4: 227-228.

Kim E, Kim KD, Roh BD, Cho YS, Lee SJ. Computer tomography as a diagnostic aid for extracanal invasive resorption. J Endod. 2003; 29 (7): 463-465.

Kim SH, Choi YS, Hwang EH, Chung KR, Kook YA, Nelson G. Surgical positioning of orthodontic mini-implants with guides fabricated on models replicated with cone-beam computed tomography. Am J Orthod Dentofacial Orthop. 2007; 131(suppl): S82-S89.

Kim SH, Kang SM, Choi YS, Kook YA, Chung KR, Huang JC. Cone-beam computed tomography evaluation of mini-implants after placement: is root proximity a major risk factor for failure? Am J Orthod Dentofac Orthop. 2010; 138: 264-276.

Kitai N, Yasuda Y, Takada K. A stent fabricated on a selectively colored stereolithographic model for placement of orthodontic mini-implants. Int J Adult Orthod Orthognath Surg. 2002; 17: 264-266.

Kleoniki ML, Vasiliki ID, Ourania CHP, Theodoros L, Ioannis KP. Internal root resorption studied by radiography, stereomicroscope, scanning electron microscope and computerized 3D reconstructive method. Dental Traumatol. 2002; 18: 148-152.

Koçak-Berberoglu H, et al. Three-dimensional cone-beam computed tomography for diagnosis of keratocyst odontogenic tumors; evaluation of four cases. Med Oral Patol Oral Cir Cucal. 2012; doi: 10.4317/medoral.17629.

Kokich VG. Cone-beam computed tomography: Have we identified the orthodontic benefits? Am J Orthod Dentofacial Orthop. 2010; 137(4Supp): S16.

Kramer IRH, Pindborg JJ, Shear M. Histological typing of odontogenic tumors 2nd ed. WHO, Springer Verlag, Berlin. 1992.

Kumar ND, Sherubin JE, Raman U, Shettar S. Indian Solitary bone cyst. J Dent Res. 2011 Jan-Feb; 22(1): 172-174.

Kuroda S, Yamada K, Deguchi T, Hashimoto T, Kyung HM, Takano-Yamamoto T. Root proximity is a major factor for screw failure in orthodontic anchorage. Am J Orthod Dentofacial Orthop. 2007; 131 (Suppl 4): S68-73.

Kwong J, Paloma J, Landers M, Figueroa A, Hans M. Image quality produced by different cone-beam computed tomography settings. Am J Orthod Dentofacial Orthop. 2008; 133: 317-327.

La SH, Jung DH, Kim EC, Min KS. Identification of independent middle mesial canal in mandibular first molar using cone-beam computed tomography imaging. J Endod. 2010; 36(5): 542-545.

Lang NP, Hill RW. Radiographs in periodontics. J Clin Periodontol. 1977; 4: 16-28.

Lee S, Gantes B, Riggs M, Crigger M. Bone density assessments of dental implant sites: 3. Bone quality evaluation during osteotomy and implant placement. Int J Oral Maxillofac Implants. 2007; 22: 208-212.

Lelli D. Notes of Radiographic Technique. Radiology Museum. http://www.aosp.bo.it/rad2/Rad/Radiolgy_Museum.htm. Last modified 24 Nov 2009.

Leung CC, Palomo L, Griffith R, Hans MG. Accuracy and reliability of cone-beam computed tomography for measuring alveolar bone height and detecting bony dehiscences and fenestrations. Am J Orthod Dentofacial Orthop. 2010 Apr; 137 (4 Suppl): S109-119.

Liedke GS, da Silveira HE, da Silveira HL, Dutra V, de Figueiredo JA. Influence of voxel size in the diagnostic ability of cone beam tomography to evaluate simulated external root resorption. J Endod. 2009; 35(2): 233-235.

Liu D, Zhang W, Zhang Z, Wu Y, Ma X. Localization of impacted maxillary canines and observation of adjacent incisor resorption with cone-beam computed tomography. Oral Surg Oral Med Oral Pathol Oral Radiol Endod. 2008; 105(1): 91-98.

Liu DG, Zhang WL, Zhang ZY, Wu YT, Ma XC. Three-dimensional evaluations of supernumerary teeth using cone-beam computed tomography for 487 cases. Oral Surg Oral Med Oral Pathol Oral Radiol Endod. 2007 Mar; 103(3): 403-411. Epub 4 Aug 2006.

Liu H, Liu DX, Wang G, Wang CL, Zhao Z. Accuracy of surgical positioning of orthodontic miniscrews with a computer-aided design and manufacturing template. Am J Orthod Dentofacial Orthop. 2010; 137: 728.e1-728.e10.

Lofthag-Hansen S, Huumonen S, Grondhal K, Grondhal HG. Limited cone-beam CT and intraoral radiography for the diagnosis of periapical pathology. Oral Surg Oral Med Oral Pathol Oral Radiol Endodon. 2007; 103(1): 114-119.

Longhini AB, Branstetter BF, Ferguson BJ. Unrecognized odontogenic maxillary sinusitis: a cause of endoscopic sinus surgery failure. Am J Rhinol Allergy. 2010; 24: 296-300.

Low KMT, Dula K, Bürgin W, von Arx T. Comparison of periapical radiography and limited cone-beam tomography in posterior maxillary teeth referred for apical surgery. J Endod. 2008; 34(5): 557-562.

Ludlow JB, Davies-Ludlow LE, Brooks SL, Howeerton WB. Dosimetry of 3 CBCT devices for oral and maxillofacial radiology: CB Mercuray, NewTom 3G and i-CAT. Dentomaxillofac Radiol. 2006; 35: 219-226.

Madrigal C, Ortega R, Meniz C, López-Quiles J. Study of available bone for interforaminal implant treatment using cone-beam computed tomography. Med Oral Patol Oral Cir Bucal. 2008; 13(5): E 307-312.

Mailett M, et al. Cone-beam Computed Tomography evaluation of maxillary sinusitis. J Endod. 2011; 37(6): 753-757.

Maki K, Inou N, Takanishi A, Miller AJ. Computer-assisted simulations in orthodontic diagnosis and the application of a new cone beam x-ray computed tomography. Orthod Craniofac Res. 2003: 95-101.

Maloney PL, Doku HC. Maxillary sinusitis of odontogenic origin. J Can Dent Assoc. 1968; 34: 591-603.

Marchetti C, Bianchi A, Muyldermans L, Di Martino M, Lancellotti L, Sarti A. Validation of new soft tissue software in orthognathic surgery planning. Int J Oral Maxillofac Surg. 2011 Jan; 40(1): 26-32. Epub 28 Oct 2010.

Martini F, Nath J. Fundamentals of Anatomy and Physiology. Pearson, Benjamin Cummings, San Francisco. 2008.

Mathew R, Omami G, Gianoli D, Lurie A. Unusual cone-beam computerized tomography presentation of traumatic (simple) bone cyst: case report and radiographic analysis. Oral Surg Oral Med Oral Pathol Oral Radiol 2012 Mar; 113(3):410-413. Epub 2011 Aug 26.

McNamara JA, Jr. A method of cephalometric evaluation. Am. J. Orthod. 1984; 86: 449-469.

McNamara JA, ed. Determinants of mandibular form and growth, Monograph 4, Craniofacial Growth Series. Ann Arbor: Center for Human Growth and Development, University of Michigan, 1976.

Mehra P, Murad H. Maxillary sinus disease of odontogenic origin. Otolaryngol Clin North Am. 2004; 37: 347-364.

Meister F, Lommel TJ, Gerstein H. Diagnosis and possible causes of vertical root fractures. Oral Surg Oral Med Oral Pathol. 1980; 49: 243-253.

Melsen B, Allais D. Factors of importance for the development of dehiscences during labial movement of mandibular incisors: a retrospective study of adult orthodontic patients. Am J Orthod Dentofacial Orthop. 2005; 127: 552-561

Mengel R, Candir M, Shiratori K, Flores-de-Jacoby L. Digital volume tomography in the diagnosis of periodontal defects: an in vitro study on native pig and human mandibles. J Periodontol. 2005; 76: 665-673.

Michetti J, Maret D, Mallet JP, Diemer F. Validation of cone beam computed tomography as a tool to explore root canal anatomy. J Endod. 2010; 36(7): 1187-1190.

Misch KA, Yi ES, Sarment DP. Accuracy of cone beam computed tomography for periodontal defect measurements. J Periodontol. 2006 Jul; 77(7): 1261-1266.

Mischkowski RA, Pulsfort R, Ritter L, Neugebauer J, Brochhagen HG, Keeve E, Zöller JE. Geometric accuracy of a newly developed cone-beam device for maxillofacial imaging. Oral Surg, Oral Med Oral Path Oral Radiol Endod. 2007; 104: 551-559.

Mizbah K, Gerlach N, Maal TJ, Berge SJ, Meijer GJ. The clinical relevance of bifid and trifid mandibular canals. Oral Maxillofac Surg. 2012 Mar; 16(1): 147-151.

Mohan R, Singh A, Gundappa M. Three-dimensional imaging in periodontal diagnosis—Utilization of cone beam computed tomography. J Indian Soc Periodontol. 2011; 15(1): 11-17.

Molen AD. Considerations in the use of cone-beam computed tomography for buccal bone measurements. Am J Orthod Dentofacial Orthop. 2010 Apr; 137(4 Suppl): S130-135.

Momin MA, Okochi K, Watanabe H, Imaizumi A, et al. Diagnostic accuracy of cone-beam CT in the assessment of mandibular invasion of lower gingival carcinoma: Comparison with conventional panoramic radiography. European Journal of Radiology. 2009; 72: 75-81.

Mortman RE. Technologic advances in Endodontics. Dent Clin North Am. 2011; 55: 461-480.

Most DS, Roy EP. A large dentigerous cyst associated with a supernumerary tooth. J Oral Maxillofac Surg. 1982; 40: 119-120.

Motta, AT. Avaliação da cirurgia de avanço mandibular através da superposição de modelos tridimensionais. [Tese]. Universidade do Estado do Rio de Janeiro (RJ), 2007.

Moule AJ, Kahler B. Diagnosis and management of teeth with vertical root fractures. Aust Dent J. 1999; 44: 75-87.

Mozzo P, Procacci C, Tacconi A, Tinazzi Martini P, Bergamo Andreis IA. A new volumetric CT machine for dental imaging based on the cone-beam technique: preliminary results. Eur Radiol. 1998; 8: 1558-1564.

Mukherji SK, Isaacs DL, Creager A, Shockley W, Weissler M, Armao D. CT detection of mandibular invasion by squamous cell carcinoma of the oral cavity. AJR Am J Roentgenol. 2001; 177: 237-243.

Nackaerts O, Maes F, Yan H, Couto Souza P, Pauwels R, Jacobs R. Analysis of intensity variability in multislice and cone beam computed tomography. Clin Oral Implants Res. 2011 Aug; 22(8): 873-879.

Nair PNR. On the causes of persistent apical periodontitis: a review. Int Endod J. 2006; 39: 249-281.

Nakajima A, Sameshima GT, Arai Y, Homme Y, Shimizu N, Dougherty H. Two- and three-dimensional orthodontic imaging using limited cone beam-computed tomography. Angle Orthod. 2005; 75: 895-903.

Nakata K, Niatoh M, Izumi M, Inamoto K, Ariji E, Nakamura H. Effectiveness of dental computed tomography in diagnostic imaging of periradicular lesion of each root of a multirooted tooth: a case report. J Endodon. 2006; 32(6): 583-587.

Neelakantan P, Subbarao C, Ahuja R, Subbarao CV, Gutmann JL. Cone-beam computed tomography study of root and canal morphology of maxillary first and second molars in an Indian population. J Endod. 2010 Oct; 36(10): 1622-1627.

Nenzen B, Welander U. The effects of conservative root canal therapy on local mucosal hyperplasia in the maxillary sinus. Odontol Revy. 1967; 18: 295-302.

Nickenig HJ, Eitner S. An alternative method to match planned and achieved positions of implants, after virtual planning using cone-beam CT data and surgical guide templates—a method reducing patient radiation exposure (part 1). J Craniomaxillofac Surg. 2010; 38: 436-440.

Nomura T, Watanabe H, Honda E, Kurabayashi T. Reliability of voxel values from cone-beam computed tomography for dental use in evaluating bone mineral density. Clin Oral Implants Res. 2010; 21: 558-562.

Nurbakhsh B, et al. Resolution of maxillary sinus mucositis after endodontic treatment of maxillary teeth with apical periodontitis: a cone-beam computed tomography pilot study. J Endod 2011; 37(11): 1504-1511.

Obayashi N, et al. Spread of odontogenic infection originating in the maxillary teeth: computerized tomographic assessment. Oral surg Oral Med Oral Pathol Oral Radiol Endod. 2004; 98: 223-231.

Oberoi S, Knueppel S. Three-dimensional assessment of impacted canines and root resorption using cone beam computed tomography. Oral Surg Oral Med Oral Pathol Oral Radiol Endod. 25 Jun 2011. [Epub ahead of print]

Oehlers FAC. Periapical lesions and residual dental cysts. Brit J Oral Surg. 1970 Nov; 8(2): 103-113.

Oliveira-Santos C, Capelozza AL, Dezzoti MS, Fischer CM, Poleti ML, Rubira-Bullen IR. Visibility of the mandibular canal on CBCT cross-sectional images. J Appl Oral Sci. 2011 May-Jun; 19(3): 240-243.

Olszewski R, Villamil MB, Trevisan DG, et al. Towards an integrated system for planning and assisting maxillofacial orthognathic surgery. Comput Methods Programs Biomed. 2008; 91: 13-21.

Ord RA, Sarmadi M, Papadimitrou J. A comparison of segmental and marginal bony resection for oral squamous cell carcinoma involving the mandible. J Oral Maxillofac Surg. 1997; 55: 470-477.

Özer SY. Detection of vertical root fractures by using cone beam computed tomography with variable voxel sizes in an in vitro model. J Endod. 2011 Jan;37(1):75-79. Epub 2010 Nov 5.

Palomo L, Palomo JM. Cone beam CT for diagnosis and treatment planning in trauma cases. Dent Clin N Am. 2009; 53: 717-727.

Park J, Cho HJ. Three-dimensional evaluation of interradicular spaces and cortical bone thickness for the placement and initial stability of microimplants in adults. Am J Orthod Dentofacial Orthop. 2009; 136 (3): 314.e1-12.

Patel S. The use of cone beam computed tomography in the conservative management of dens invaginatus: a case report. Int Endod J. 2010 Aug; 43(8): 707-713.

Patel S, Dawood A. The use of cone beam computed tomography in the management of external cervical resorption lesions. Int Endod J. 2007; 40: 730-737.

Patel S, Dawood A, Ford TP, Whaites E. The potential applications of cone beam computed tomography in the management of endodontic problems. Int Endod J. 2007; 40(10): 818-830.

Patel S, Dawood A, Wilson R, Horner K, Mannocci F. The detection and management of root resorption lesions using intraoral radiography and cone beam computed tomography—an in vivo investigation. Int End J. 2009; 42(9): 831-838.

Patel S, Horner K. The use of cone beam computed tomography in Endodontics. Int Endod J. 2009; 42(9): 755-756.

Peck JN, Conte GJ. Radiologic techniques using CBCT and 3-D treatment planning for implant placement. J Calif Dent Assoc. 2008; 36: 287-290.

Pelinsari Lana J, Moura Rodrigues Carneiro P, de Carvalho Machado V, Eduardo Alencar de Souza P, Ricardo Manzi F, Campolina Rebello Horta M. Anatomic variations and lesions of the maxillary sinus detected in cone beam computed tomography for dental implants. Clin Oral Implants Res. 3 Oct 2011; doi: 10.1111/j.1600-0501.2011.02321.x. Epub ahead of print.

Petrovic AG, Stutzmann JJ, Oudet CL. Control processes in the postnatal growth of the condylar cartilage in the mandible. In: Determinants of mandibular form and growth. McNamara JA Jr, editor. Monograph 5. In: Craniofacial growth series. Ann Arbor: Centerfor Human Growth and Development, University of Michigan, 1975.

Petrovic A. Auxologic categorization and chronobiologic specification for the choice of appropriate orthodontic treatment. Am J Orthod Dentofacial Orthop. 1994 Feb; 105(2): 192-205.

Pinsky HM, Champleboux G, Sarment PD. Periapical surgery using CAD/CAM guidance: preclinical results. J Endodon. 2007; 33(2): 148-151. Epub ahead of print.

Pinsky HM, Dyda S, Pinsky RW, Misch KA, Sarment DP. Accuracy of three-dimensional measurements using cone-beam CT. Dentomaxillofac Radiol. 2006; 35: 410-416.

Planas P. Riabilitazione Neuro-Occlusale. Masson Salvat, 1994.

Poggio PM, Incorvati C, Velo S, Carano A. "Safe zones": a guide for miniscrew positioning in the maxillary and mandibular arch. Angle Orthod. 2006; 76: 191-197.

Radman WP. The maxillary sinus—revisited by an endodontist. J Endod. 1983; 9: 382-383.

Rees TD, Biggs NL, Collings CK. Radiographic interpretation of periodontal osseous lesions. Oral Surg Oral Med Oral Pathol. 1971; 32: 141-153.

Rho JY, Hobatho MC, Ashman RB. Relations of mechanical properties to density and CT numbers in human bone. Med Eng Phys. 1995; 17: 347-355.

Ricketts, RM. Perspectives in the clinical application of cephalometrics: The first fifty years. Angle Orthod. 1981; 51: 115-150.

Rigolone M, Pasqualini D, Bianchi L, Berutti E, Bianchi D. Vestibular surgical access to the palatine root of the superior first molar: "low-dose cone-beam" CT analysis of the pathway and its anatomic variations. J Endodon. 2003; 39(11): 773-775.

Riolo ML, Moyers RE, McNamara JA, Hunter WS. An atlas of craniofacial growth. In: ed. 7. Monograph 2, Craniofacial Growth Series. Center for Human Growth and Development, University of Michigan, Ann Arbor. 1974.

Rood JP, Shehab BA. The radiological prediction of inferior alveolar nerve injury during third molar surgery. Br J Oral Maxillofac Surg. 1990; 28: 20-25.

Rosenberg PA, et al. Evaluation of pathologists (histopathology) and radiologists (cone beam computed tomography) differentiating radicular cysts from granulomas. J Endod. 2010; 36(3): 423-428.

Rothe LE, Bollen AM, Little RM, Herring SW, Chaison JB, Chen CS, et al. Trabecular and cortical bone as risk factors for orthodontic relapse. Am J Orthod Dentofacial Orthop. 2006; 130: 476-484.

Rud J, Omnell KA. Root fracture due to corrosion. Scand J Dent Res. 1970; 78: 397-403.
Ruprecht A, Batniji S, El-Neweihi E. Incidence of supernumerary teeth. Ann Dent. 1984; 43: 18-21.
Salzmann JA. Review of The Face in Profile: An Anthropological Xray Investigation on Swedish Children and Conscripts by A. Björk, Am J Orthod. 1948; 34: 691-699.
Sameshima GT, Sinclair PM. Predicting and preventing root resorption: part I. Diagnostic factors. Am J Orthod Dentofacial Orthop. 2001; 119: 505-510.
Sarikaya S, Haydar B, Ciger S, Ariyurek M. Changes in alveolar bone thickness due to retraction of anterior teeth. Am J Orthod Dentofacial Orthop. 2002; 122: 15-26.
Sarment DP, Sukovic P, Clinthorne N. Accuracy of implant placement with a stereolithographic surgical guide. Int J Oral Maxillofac Implants. 2003; 18: 571-577.
Sassouni V. A roentgenographic cephalometric analysis of cephalo-facio-dental relationships. Am. J. Orthod. 1955; 41: 735-764.
Scarfe WC, Farman AG. What is cone-beam CT and how does it work? Dent Clin North Am. 2008; 52(4): 707-730.
Scarfe WC, Farman AG, Sukovic P. Clinical applications of cone-beam computed tomography in dental practice. J Can Dent Assoc. 2006; 72(1): 75-80.
Scarfe WC, Levin MD, Gane D, Farman AG. Use of cone beam computed tomography in Endodontics. Int J Dent. 2009;2009:634567. Epub 2010 Mar 31.
Schlueter B, Kim KB, Oliver D, Sortiropoulos G. Cone Beam Computed Tomography 3D Reconstruction of the Mandibular Condyle. Angle Orthod. 2008 Sep; 78(5): 880-888.
SEDENTEXCT. Radiation Protection: Cone Beam CT for Dental and Maxillofacial Radiology. Evidence-based Guidelines. v2.0, May 2011. www.sedentexct.eu.
Shafer WG, Hine MK, Levy BM. A Textbook of Oral Pathology. 4th ed. Philadelphia, Pa: WB Saunders. 1983: 47-50.
Shapurian T, Damoulis PD, Reiser GM, Griffin TJ, Rand WM. Quantitative evaluation of bone density using the Hounsfield index. Int J Oral Maxillofac Implants. 2006; 21: 290-297.
Shemesh H, Cristescu RC, Wesselink PR, Wu MK. The use of cone-beam computed tomography and digital periapical radiographs to diagnose root perforations. J Endodon. 2011; 37(4): 513-516.
Sherrard JF, Rossouw PE, Benson BW, Carrillo R, Buschang PH. Accuracy and reliability of tooth and root length measured on cone beam computed tomographs. Am J Orthod Dentofacial Orthop. 2010; 37(4 Suppl): S100-108.
Shintaku WH, Venturin JS, Azevedo B, Noujeim M. Applications of cone-beam computed tomography in fractures of the maxillofacial complex. Dental Traumatol. 2009; 25: 358-366.
Silva MA, Wolf U, Heinicke F, Bumann A, Visser H, Hirsch E. Cone-beam computed tomography for routine orthodontic treatment planning: a radiation dose evaluation. Am J Orthod Dentofacial Orthop. 2008; 133: 640.e1-640.e5.
Simon JHS, Enciso R, Malfaz JM, Roges R, Balley-Perry M, Patel A. Differential diagnosis of large periapical lesions using cone-beam computed tomography measurements and biopsy. J Endod. 2006; 32(9): 833-837.
Sokhn S, Nasseh I, Noujeim M. Using cone beam computed tomography to determine safe regions for implant placement. Gen Dent. 2011; 59(2): e 72-77.
Stafne EC, Gibilisco JA. Anomalies. In: Stafne EC, Gibilisco JA, eds. Oral Roentgenographic Diagnosis. 4th ed. Philadelphia, Pa: WB Saunders. 1975: 18-21.
Steiner CC. Cephalometrics for you and me. Am J Orthod. 1953; 39: 729-755.
Stoppie N, Pattijn V, Van Cleynenbreugel T, Wevers M, Sloten JV, Ignace N. Structural and radiological parameters for the characterization of jawbone. Clin Oral Implants Res. 2006; 17: 124-133.
Stuebmer C, Essig H, Bormann KH, Majdani O, Gellrich NC, Rücker M. Cone beam CT imaging of airgun injuries to the craniofacial region. Int J Oral Maxillofacial Surg. 2008; 37: 903-906.
Sukovic P. Cone beam computed tomography in craniofacial imaging. Orthod Craniofac Res. 2003; 6(Suppl 1): 31-36.
Swennen GRJ, Schutyser F. Three-dimensional cephalometry: spiral multi-slice vs cone-beam computed tomography. Am J Orthod Dentofacial Orthop. 2006; 130: 410-416.
Tamse A. Iatrogenic vertical root fractures in endodontically treated teeth. Endod Dent Traumatol. 1988; 4: 190-196.
Testori T, Badino M, Castagnola M. Vertical root fractures in endodontically treated teeth: a clinical survey of 36 cases. J Endod. 1993; 19: 87-90.
Tian YY, Guo B, Zhang R, Yu X, Wang H, Hu T, Dummer PM. Root and canal morphology of maxillary first premolar in a Chinese subpopulation evaluated using cone-beam computed tomography. Int Endod J. 2012. Epub May 2012.
Tsurumachi T, Honda K. A new cone-beam computerized tomography system for use in endodontic surgery. Int Endod J. 2007; 40(3): 224-232.
Turpin DL. British Orthodontic Society revises guidelines for clinical radiography. Am J Orthod Dentofacial Orthop. 2008 Nov; 134(5): 597-598.
Tweed CH. Was the development of the diagnostic facial triangle as an accurate analysis based on fact or fancy? Am J Orthod. 1962; 48: 823-840.
Uchida Y, Noguchi N, Goto M, Yamashita Y, Hanihara T, Takamori H, Sato I, Kawai T, Yosue T. Measurement of anterior loop length for the mandibular canal and diameter of the mandibular incisive canal to avoid nerve damage when installing endosseous implants in the interforaminal region: a second attempt introducing cone beam computed tomography. J Oral Maxillofac Surg. 2009; 67: 744-750.
Vandenberghe B, Jacobs R, Yang J. Diagnostic validity (or acuity) of 2D CCD versus 3D CBCT-images for assessing periodontal breakdown. Oral Surg Oral Med Oral Pathol Oral Radiol Endod. 2007; 104(3): 395-401.
Visser H, Rödig T, Hermann KP. Dose reduction by direct-digital cephalometric radiography. Angle Orthod. 2001; 71: 159-63.
von Arx T, Hänni A, Sendi P, Buser D, Bornstein MM. Radiographic study of the mandibular retromolar canal: an anatomic structure with clinical importance. J Endod. 2011 Dec; 37(12): 1630-1635.
Wainwright WM. Faciolingual tooth movement: its influence on the root and cortical plate. Am J Orthod. 1973; 64: 278-302.
Walker L, Enciso R, Mah J. Three-dimensional localization of maxillary canines with cone-beam computed tomography. Am J Orthod Dentofacial Orthop. 2005; 128: 418-425.
Wang P, He W, Sun H, Lu Q, Ni L. Evaluation of horizontal/oblique root fractures in the palatal roots of maxillary first molars using cone-beam computed tomography: a report of three cases. Dental Traumatol. 2011(Dec); 27(6): 464-467.
Wehrbein H, Bauer W, Diedrich P. Mandibular incisors, alveolar bone, and symphysis after orthodontic treatment. A retrospective study. Am J Orthod Dentofacial Orthop. 1996; 110: 239-246.
Wennstrom JL. Mucogingival considerations in orthodontic treatment. Semin Orthod. 1996; 2: 46-54.
Wennstrom JL, Lindhe J, Sinclair F, Thilander B. Some periodontal tissue reactions to orthodontic tooth movement in monkeys. J Clin Periodontol. 1987; 14: 121-129.
Wennstrom JL, Stokland BL, Nyman S, Thilander B. Periodontal tissue response to orthodontic movement of teeth with infrabony pockets. Am J Orthod Dentofacial Orthop. 1993; 103: 313-319.
White SC. Cone-beam imaging in dentistry. Health Phys. 2008; 95: 628-637.
White SC, Pharoah MJ. Oral radiology, principles and interpretation. Philadelphia, Mosby. 2004.
Wilmes B, Su Y, Drescher D. Insertion angle impact on primary stability of orthodontic mini-implants. Angle Orthod. 2008; 78(6): 1065-1070.
Worthington P, Rubenstein J, Hatcher DC. The role of cone-beam computed tomography in the planning and placement of implants. J Am Dent Assoc. 2010; 141: 19S-24S.
Wriedt S, Jaklin J, Al-Nawas B, Wehrbein H. Impacted upper canines: examination and treatment proposal based on 3D versus 2D diagnosis. J Orofac Orthop. 2012 Jan; 73(1): 28-40. Epub 15 Jan 2012.

Wu MK, Shemesh H, Wesselink PR. Limitations of previously published systematic reviews evaluating the outcome of endodontic treatment. Int Endod J. 2009; 42(8): 656-666.

Wu MK, Wesselink PR, Shemesh H, Patel S. Endodontic epidemiologic investigations and clinical outcomes studies with cone-beam computed tomography. J Endod. 2011. PII: S0099-2399(11)00410-9.

Wu MK, Wesselink P, Shemesh H. New terms for categorizing the outcomes of root canal treatment. Int. Endod J. 2011; 44(11): 1079 -1080.

Xia J, Samman N, Yeung RW, et al. Three-dimensional virtual reality surgical planning and simulation workbench for orthognathic surgery. Int J Adult Orthodon Orthognath Surg. 2000; 15: 265-282.

Yamamoto K, Ueno K, Seo K, Shinohara D. Development of dento-maxillofacial cone beam x-ray computed tomography system. Orthod Craniofac Res. 2003; 6(Suppl 1): 160-162.

Yang F, Jacobs R, Willems G. Dental age estimation through volume matching of teeth imaged by cone-beam CT. Forensic Sci Int. 2006; 159(Suppl 1): S78-83.

Yang SF, Rivera EM, Waiton RE. Vertical root fracture in nonendodontically treated teeth. J Endodon. 1995; 21: 337-339.

Yared KFG, Zenobio EG, Pacheco W. Periodontal status of mandibular central incisors after orthodontic proclination in adults. Am J Orthod Dentofacial Orthop. 2006; 130: 6.e1-8.

Young GR. Contemporary management of lateral root perforation diagnosed with the aid of dental computed tomography. Aust Endod J. 2007 Dec; 33(3): 112-118.

Youssefzadeh S, Gahleitner A, Dorffner R, Bernhart T, Kainberger FM. Dental Vertical Root Fractures: value of CT in detection. Radiology. 1999; 210: 545-549.

Yu VSH, Messer HH, Tan KB. Multiple idiopathic cervical resorption: case report and discussion of management options. Int Endod J. 2011; 44(1): 77-85.

Zachrisson BU, Alnaes L. Periodontal condition in orthodontically treated and untreated individuals. I. Loss of attachment, gingival pocket depth and clinical crown height. Angle Orthod. 1974; 43: 402-411.

Zachrisson BU, Alnaes L. Periodontal condition in orthodontically treated and untreated individuals. II. Alveolar bone loss: radiographic findings. Angle Orthod. 1974; 44: 48-55.

Zain-Alabdeen EH, Alsadhan RI. A comparative study of accuracy of detection of surface osseous changes in the temporomandibular joint using multidetector computed tomography and cone beam computed tomography. Dentomaxillofac Radiol. 24 Nov 2011. Epub ahead of print.

Zannos S. Godfrey Hounsfield and the invention of CAT scans. Mitchell Lane Publisher. 2003: 23.

Zhang Y, Zhang L, Zhu XR, et al. Reducing metal artifacts in cone-beam CT images by preprocessing projection data. Int J Radiat Oncol Biol Phys. 2007; 67: 924-932.

Ziegler CM, Woertche R, Brief J, Hassfeld S. Clinical indications for digital volume tomography in oral and maxillofacial surgery. Dentomaxillofac Radiol. 2002; 31(2): 126-130.

Zupi A, Califano L, Maremonti P, Longo F, Ciccarelli R, Soricelli A. Accuracy in the diagnosis of mandibular involvement by oral cancer. J Craniomaxillofac Surg. 1996; 24: 281-284.

Index

H

I

K

L

M

N

O

P

R

S

T

U

V

X